



**HAL**  
open science

# Rapid detection of food antioxidants using electrochemical sensors based on molecularly imprinted polymers

Marie El Hachem

► **To cite this version:**

Marie El Hachem. Rapid detection of food antioxidants using electrochemical sensors based on molecularly imprinted polymers. Chemical Sciences. Université Bourgogne Franche-Comté; Université Saint-Joseph (Beyrouth), 2022. English. NNT : 2022UBFCK093 . tel-04789975

**HAL Id: tel-04789975**

**<https://theses.hal.science/tel-04789975v1>**

Submitted on 19 Nov 2024

**HAL** is a multi-disciplinary open access archive for the deposit and dissemination of scientific research documents, whether they are published or not. The documents may come from teaching and research institutions in France or abroad, or from public or private research centers.

L'archive ouverte pluridisciplinaire **HAL**, est destinée au dépôt et à la diffusion de documents scientifiques de niveau recherche, publiés ou non, émanant des établissements d'enseignement et de recherche français ou étrangers, des laboratoires publics ou privés.

**DOCTORAL DISSERTATION OF THE UNIVERSITY OF BURGUNDY FRANCHE-COMTE**

**Prepared at L'Institut Agro Dijon**

Specialty: Analytical Chemistry

Doctoral School n° 554

« Environnement-Santé » (ES)

**AND SAINT-JOSEPH UNIVERSITY OF BEIRUT**

**Prepared at the Faculty of Sciences**

Specialty: Chemistry

Doctoral School

« École Doctorale de Sciences, d'Ingénierie et de Technologie » (EDSIT)

Presented and supported by

**EL HACHEM Marie**

in Beirut, on the 18th of November 2022

« Rapid detection of food antioxidants using electrochemical sensors based on molecularly imprinted polymers »

**Jury members:**

Mr. PALLAVICINI Piersandro	Professor, University of Pavia	Reviewer
Ms. KHREICH Nathalie	Professor, Lebanese University	Reviewer
Ms. DESPAS Christelle	Associate professor, University of Lorraine	Examiner
Mr. ISMAIL Ali	Professor, Lebanese University	Examiner
Mr. BOU-MAROUN Elias	Associate professor, L'Institut Agro Dijon	Supervisor (France)
Mr. MAROUN Richard	Professor, Saint-Joseph University	Supervisor (Lebanon)
Mr. CAYOT Philippe	Professor, L'Institut Agro Dijon	Co-supervisor (France)
Mr. ABOUD Maher	Professor, Saint-Joseph University of Beirut	Co-supervisor (Lebanon)



## PREFACE

This thesis work was realized in co-supervision between Saint-Joseph University, Faculty of Sciences and University of Burgundy-Franche Comté, L'Institut Agro Dijon under the supervision of Pr. Richard MAROUN and Dr. Elias BOU-MAROUN, and the co-supervision of Pr. Maher ABOUD and Pr. Philippe CAYOT. The laboratory experiments were carried out within the PCAV team (Physical-Chemistry for food and wine) at l'Institut Agro Dijon.

This work was the subject of:

- **Publications in the journal “Antioxidants”:**

Elhachem, M., Bou-Maroun, E., Abboud, M., Maroun, R. G., & Cayot, P. (2022). Combination of Screen-Printed Carbon Electrode and Molecularly Imprinted Polymers for the Selective Determination of Phenolic Compounds in Wine. *Antioxidants*, 11(10). <https://doi.org/10.3390/antiox11102036>

Elhachem, M., Cayot, P., Abboud, M., Louka, N., Maroun, R. G., & Bou-Maroun, E. (2021). The Importance of Developing Electrochemical Sensors Based on Molecularly Imprinted Polymers for a Rapid Detection of Antioxidants. *Antioxidants*, 10(3). <https://doi.org/10.3390/antiox10030382>

- **Poster in the national congress « Forum des Jeunes Chercheurs, FJC »:**

Application of a molecularly imprinted polymer specific to caffeic acid in a hydro-alcoholic medium, June 2021.

- **Poster in the Fifth Edition of the International Conference Series on Wine Active Compounds « WAC 2022 »:**

The development of a simple electrochemical method based on molecularly imprinted polymers for the selective determination of caffeic acid in wine, June 2022.

<https://ives-openscience.eu/14821/>

- **Papers to be submitted:**

- 1) Combination of screen printed carbon electrode and molecularly imprinted polymers for the selective determination of caffeic acid in wine
- 2) Optimization of a molecularly imprinted polymer synthesis for a specific and selective detection of caffeic acid in wine
- 3) Molecularly imprinted electrochemical sensor for a direct caffeic acid detection in wine

# **ACKNOWLEDGEMENTS**

## ABSTRACT

Our work concerns three major scientific topics: the study of antioxidants, molecular imprinting and analysis by electrochemistry. The main objective was to develop a simple and rapid method for the detection of caffeic acid in liquid food media, specifically in a model hydro-alcoholic medium and in wine. To reach this objective, two electrochemical analytical approaches combined to molecular imprinting were adopted: the indirect and the direct method. The indirect method consisted on the preparation of a molecularly imprinted polymer (MIP) and a non-imprinted polymer (NIP) external to the electrode (*ex-situ*) and then the determination of the target molecule by electrochemistry in the presence of the polymer in solution. The direct method involved the electro-polymerization of the polymers (MIP and NIP) straight on the surface of the electrode (*in-situ*) and the application of the sensor directly in the medium of interest. Screen-printed carbon electrodes (SPCE) replaced traditional electrodes since they are compact, disposable and inexpensive. On the other hand, the *in-situ* method was developed after the optimization of the following electro-polymerization parameters and conditions: the choice of the functional monomer using molecular simulation, the ratio of the target molecule to functional monomer concentrations, the number of cycles applied and the immersion time of the sensor in the measurement solution. This sensor was developed and successfully applied in wine, and the results were validated by a liquid chromatography conventional method (HPLC-UV). The results showed that the *in-situ* method was selective and sensitive for CA, with a limit of detection LOD of 0.68  $\mu\text{M}$  and a limit of quantification LOQ of 2.05  $\mu\text{M}$ . This method was as well accurate, precise (recovery between 95 and 110%), robust and fast.

Overall, our results indicate that the methods used in our study could potentially improve antioxidant detection in wine but as well as in other food matrices and during several industrial applications. They are also close to the requirements of green chemistry (limited sample preparation and the use of low volumes of solvent).

**Keywords:** Molecularly Imprinted Polymers (MIP); Antioxidants; Caffeic acid; Electrochemistry; Screen-Printed Electrode (SPE); Electropolymerization; Sensor; Wine.

## RÉSUMÉ

Les travaux de cette thèse concernent trois grands domaines scientifiques : l'étude des antioxydants, l'impression moléculaire et l'analyse par l'électrochimie. L'objectif principal vise à développer une méthode de détection électrochimique simple et rapide de l'acide caféique (CA) dans des milieux liquides alimentaires, plus précisément dans un milieu hydro-alcoolique modèle et son application dans le vin. Pour atteindre cet objectif, deux voies d'analyses par électrochimie combinées à la synthèse de polymères à empreintes moléculaires (MIP) ont été utilisées : la voie indirecte et la voie directe. La voie indirecte consiste à synthétiser un MIP et son polymère non imprimé (NIP) d'une part, puis d'autre part le dosage de la molécule cible par électrochimie en présence du polymère en solution (le polymère est externe à l'électrode ; stratégie *ex-situ*). La voie directe implique l'électropolymérisation à la surface de l'électrode (*in-situ*) et l'application du capteur directement dans le milieu d'intérêt. Les électrodes traditionnelles sont remplacées par des électrodes de carbone sérigraphiques (SPCE) car elles sont compactes, à usage unique et bon marché. Dans la méthode *ex-situ*, un polymère spécifique de l'acide caféique CA-MIP a été synthétisé, puis optimisé pour accroître sa performance. L'optimisation des conditions de synthèse du polymère a été conduite afin d'aboutir à un polymère avec une spécificité plus importante. Les paramètres optimisés sont : le monomère fonctionnel, le solvant et le type d'initiation radicalaire. D'autre part, la méthode *in-situ* a été mise en place à la suite d'un travail d'optimisation des paramètres de d'électropolymérisation suivants: le choix du monomère fonctionnel par modélisation moléculaire, le ratio des concentrations molécule cible-monomère fonctionnel, le nombre de cycles appliqués et le temps d'immersion du capteur dans la solution de mesure. Ce capteur a été développé et appliqué dans le vin et les résultats ont été validés par une méthode conventionnelle, la chromatographie en phase liquide (HPLC-UV). Les résultats montrent que la méthode *in-situ* est sélective pour le CA, sensible avec une limite de détection LOD de 0,68  $\mu\text{M}$  et une limite de quantification LOQ de 2,05  $\mu\text{M}$ , juste, précise (taux de recouvrement compris entre 95 et 110%), robuste et rapide. Tous ces résultats indiquent que les méthodes que nous avons développées dans le cadre de cette thèse pourraient potentiellement améliorer la détection des antioxydants dans le vin ainsi que dans d'autres matrices alimentaires et dans d'autres applications industrielles. Elles sont également proches des exigences de la chimie verte (très peu de préparation de l'échantillon et utilisation de faibles volumes de solvant).

**Mots-clés :** Polymères à empreinte moléculaire (MIP) ; Antioxydants; Acide caféique; électrochimie; Screen-printed electrode (SPE); Electropolymérisation; Capteur; Vin.

# Table of Contents

<b>PREFACE</b> .....	iii
<b>ACKNOWLEDGEMENTS</b> .....	iv
<b>ABSTRACT</b> .....	v
<b>RÉSUMÉ</b> .....	vi
<b>List of figures</b> .....	x
<b>List of tables</b> .....	xiii
<b>List of Abbreviations</b> .....	xiv
<b>General Introduction</b> .....	xvi
<b>Part I</b> .....	1
<b>Literature Review</b> .....	1
<b>1. Introduction</b> .....	2
<b>2. Antioxidants</b> .....	4
<b>2.1. Common types of food oxidation</b> .....	4
<b>2.2. Mechanism of action</b> .....	7
<b>2.3. Main antioxidant families</b> .....	9
<b>2.4. Total antioxidant capacity assays</b> .....	9
<b>2.5. Extraction and detection of antioxidants</b> .....	14
<b>3. Electrochemistry</b> .....	15
<b>4. Molecular imprinting</b> .....	22
<b>4.1. MIP synthesis and applications</b> .....	22
<b>4.2. MIPs-antioxidants</b> .....	26
<b>4.3. MIS-antioxidants</b> .....	28
<b>5. Electrochemistry, molecular imprinting and antioxidants</b> .....	30
<b>5.1. Electrochemistry and antioxidants</b> .....	30
<b>5.2. Electrochemistry and molecular imprinting</b> .....	30
<b>6. Conclusions</b> .....	38
<b>Part II</b> .....	39
<b>Materials and Methods</b> .....	39
❖ <i>Ex-situ</i> polymerization .....	40
<b>1. Parameters of the synthesis of the imprinted (MIP) and non-imprinted (NIP) polymers</b> .....	40
<b>2. Synthesis of of two selected caffeic acid imprinted polymers (CA-MIP) and corresponding non-imprinted polymer (NIP)</b> .....	46
<b>3. Application of the CA-MIP/NIP in a hydro-alcoholic medium</b> .....	47
<b>4. Morphological characterization techniques</b> .....	48

5. Applications of the polymers in wine.....	49
❖ <i>In-situ</i> polymerization: electropolymerization.....	50
1. Choice of the functional monomer (FM): molecular simulation.....	51
2. Electropolymerization steps .....	52
3. Optimization of MIP sensor preparation conditions.....	53
4. Rebinding properties.....	54
5. Sensors response in the presence of interferents .....	54
6. Stability and repeatability of the sensor .....	54
References .....	55
<b>Part III</b> .....	74
<b>Results and discussion</b> .....	74
<b>Chapter 1</b> .....	75
1. Introduction .....	76
2. <b>Article 1: Combination of screen printed carbon electrode and molecularly imprinted polymers for the selective determination of caffeic acid in wine</b> .....	78
2.1. Introduction .....	79
2.2. Material and methods .....	82
2.3. Results and discussion.....	85
2.4. Conclusion.....	91
References.....	92
<b>Chapter 2</b> .....	95
1. Introduction .....	96
2. <b>Article 2: Optimization of a molecularly imprinted polymer synthesis for a specific and selective detection of caffeic acid in wine</b> .....	98
2.1. Introduction .....	99
2.2. Material & methods .....	100
2.3. Results and Discussion .....	105
2.4. Conclusion.....	114
References.....	115
<b>Chapter 3</b> .....	117
1. Introduction .....	118
2. <b>Article 3: Molecularly imprinted electrochemical sensor for a direct caffeic acid detection in wine</b> .....	120
2.1. Introduction .....	121
2.2. Material and methods .....	123
2.3. Results and discussion.....	125
2.4. Conclusions .....	132

<b>References</b> .....	133
<b>Part IV</b> .....	135
<b>Conclusion and perspectives</b> .....	135
<b>Supplementary Material</b> .....	138

## List of figures

Figure 1. The general process of lipid peroxidation [25]. RH: target polyunsaturated fatty acid; R•: fatty acid radical; ROO•: fatty acid peroxy radical; ROOH: lipid hydroperoxides.....	5
Figure 2. Oxidation process of: (I), (II), (III) aromatic amino acids and (IV) aliphatic amino acids [26]. .....	6
Figure 3. Example of stabilization by resonance, with (VII) butylated hydroxytoluene (BHT) and (VIII) ortho-diphenol, and example of BHT polymerization (IX).....	7
Figure 4. Reaction mechanisms of secondary antioxidants: (X) Metal ion ( $\text{Cu}^{2+}$ ) chelating activity of anthocyanidine (cyanidin), from [41] published by The Royal Society of Chemistry; (XI) oxygen scavenging activity of ascorbic acid, reproduced from [42] under Creative Common license; (XII) chemical reaction of quercetin with singlet oxygen, reproduced from [43] with the permission of Elsevier. ....	8
Figure 5. Antioxidant families. TBHQ: tert-Butylhydroquinone; BHA: butylated hydroxyanisole; BHT: butylated hydroxytoluene; GSH: reduced glutathione; SOD: superoxide dismutase; CAT: catalase; GPx: glutathione peroxidase.....	9
Figure 6. General mechanism of direct (competitive) and indirect (noncompetitive) antioxidant assays. (1) HAT-based assays: R•: free radical; Y: probe, AH: antioxidant; A•: oxidized antioxidant; ⚡ : fluorescence, absorption, light emission, oxygen consumption; (2) ET-based assays: Y•: oxidized probe, AH: antioxidant; YH: reduced probe; ⚡ : color modification of reduced probe. ....	10
Figure 7. Voltammetry potential waveforms and basic voltammograms. (a1): CV potential waveform; (a2): basic cyclic voltammogram of reversible system, anodic and cathodic peak potentials ( $E_{pa}$ and $E_{pc}$ respectively) and half-wave potential ( $E_{1/2}$ ); (a3) basic cyclic voltammogram of (1) quasi-reversible and (2) irreversible systems; (b1) DPV potential waveform; (b2) basic differential pulse voltammogram. ....	18
Figure 8. Differential pulse voltammograms recorded at PGE* for $6.00 \times 10^{-5}$ mol/L NGN in different supporting electrolytes. Reproduced from [82] with the permission of Royal Society of Chemistry. NGN: naringenin, KHPT: potassium phthalate monobasic, ABS: acetate buffer solution, BRB: Britton–Robinson buffer.....	20
Figure 9. General principle of molecular imprinting.....	22
Figure 10. Chemical structures of common (a) functional monomers, (b) cross-linkers and (c) initiators used in radical polymerization. ....	25
Figure 11. Hybrid organic-inorganic printing procedure. ....	28
Figure 12. The steps of electropolymerization on the surface of the electrode.....	31
Figure 13. Calibration plots for the different sensors: with PEDOT film, with PEDOT/NIP membrane and with PEDOT/MIP membranes. Concentration range of 4.95–115 $\mu\text{M}$ diphenylamine, reproduced from [251] with the permission of Elsevier.....	32
Figure 14. On the left: schematic representation of MIS/AuE, reproduced from [253] with the permission of Elsevier. On the right: (A) Differential pulse voltammograms for CA electrooxidation at different concentrations: (a) 0, (b) 0.500, (c) 1.00, (d) 2.00, (e) 5.00, (f) 20.0, (g) 35.0, (h) 50.0, (i) 60.0, (j) 70.0 and (k) 80.0 $\mu\text{mol/L}$ . (B) Calibration plot, $I_p/\mu\text{A} = 0.00619 (\pm 1.92 \times 10^{-4}) [\text{CA}]/\mu\text{mol/L} - 0.00125 (\pm 4.36 \times 10^{-4})$ . Incubation time: 25 min. Supporting electrolyte: 0.4 mol/L sulfuric acid. Scan rate: 40 mV/s. Potential pulse amplitude: 70 mV, reproduced from [253] with the permission of Elsevier. ....	33
Figure 15. Current response (DPV) of the modified electrode recovered by siloxane film. Supporting electrolyte: 0.15 mol/L phosphoric acid. Incubation time: 15 min. DPV at 0.02 V/s. Reproduced from [254] with the permission of Elsevier.....	34

Figure 16. Linear relationship between anodic peak currents and the concentration of vitamin C (Vc) for MIPs electrode and NIPs electrode, reproduced from [239] with the permission of Elsevier.	35
Figure 17. (a) Schematic construction of the MIP/G-MWCNTs/GCE electrode, G-MWCNTs: graphene-multiwall carbon nanotubes, GCE: glassy carbon electrode, PY: pyrrole, RT: rutin; (b) variation of DPVs with RT concentration; (c) linear relationship between peak current and RT concentration, reproduced from [255] with the permission of Elsevier.	35
Figure 18. On the left: schematic representation of the applied approach for preparation of RA-MMIP, reproduced from [258] with the permission of Elsevier. On the right: Effect of other compounds on electrochemical determination of RA using MIP-CPE and NIP-CPE [258].	37
Figure 19. Chemical structures of caffeic acid (CA) and 3,4-dimethoxycinnamic acid (DMCA).	41
Figure 20. Thermal decomposition of AIBN and initiation of radical polymerization	43
Figure 21. Functional monomers: N-phenylacrylamide (left) and methacrylic acid (right).	44
Figure 22. Rebinding experiment steps. CA-MIP: molecularly imprinted polymer for caffeic acid, NIP: non-imprinted polymer, Sol CA: caffeic acid solution, Ipa: anodic peak current	47
Figure 23. Proposed chemical reactions and interactions involved in the CA-MIP synthesis.	86
Figure 24. Calibration curves for caffeic acid (CA) in (PBS 0.05 M/ EtOH) (90/10, v/v) solution, at pH 3 (left) and pH 7 (right). Inset: CV for caffeic acid at different concentrations, ranging from 0.06 to 2.78 mM of CA. The critical value of the Pearson's correlation coefficient is 0.974 for 6 points (degree of freedom 4) and a level of significance for a two-tailed test of 0.1 %	87
Figure 25. pH effect on the quantity of caffeic acid adsorbed ( $N_{ads}$ ) by CA-MIP using cyclic voltammetry in a (PBS 0.05 M/EtOH) (90/10, v/v) solution containing 1.11 mM of CA, in the presence 10 mg (left) and 50 mg (right) of CA-MIPCA and NIP.	88
Figure 26. Left: CV for caffeic acid (CA) remaining in the medium after adding different quantities of CA-MIP (0, 10, 20, 30, 40 and 50 mg). Scan rate: 50 mV/s; the arrow shows the reduction of Ipa and the remaining caffeic acid with increasing the content of imprinting polymer CA-MIP. Right: effect of the polymer mass on the amount of adsorbed caffeic acid in a (PBS 0.05 M/EtOH) (90/10, v/v) solution containing 1.11 mM of caffeic acid. The error bar is of 0.15% for all samples	89
Figure 27. Relative amount of caffeic acid and its interferents adsorbed by the CA-MIP and NIP in a (PBS 0.05M/EtOH) (90/10, v/v) solution containing 0.55 mM of each compound, in the presence of 10 mg of MIP or NIP. The selectivity coefficient $\alpha$ is represented in bold above every bar. Interferents: ferulic acid, sinapic acid, gallic acid and p-coumaric acid.	90
Figure 28. Comparison between the rebinding experiments performed by CA-MIP1/NIP1 and CA-MIP6/NIP6, showing the amount of adsorbed caffeic acid by each polymer.	107
Figure 29. FTIR spectra of CA-MIP6 and NIP6.	108
Figure 30. SEM images for CA-MIP6 and NIP6 at different scales	109
Figure 31. (A) Scatchard plots for CA-MIP6 and NIP6, and (B) affinity distributions plotted in log format	111
Figure 32. Relative amount of caffeic acid and its interferents adsorbed by the CA-MIP6 and NIP6, in a PBS/EtOH solution containing 0.55 mM of each compound, in the presence of 10mg of polymer. CA: caffeic acid, p-cA: p-coumaric acid, GA: gallic acid, FA: ferulic acid, SA: sinapic acid. The selectivity coefficient $\alpha$ is calculated and given above MIP bars.	112
Figure 33. Rebinding properties of CA-MIP6 in spiked wine: (A) variation of the amount of CA in the presence of 10 mg of polymer; and (B) variation of polymer mass in the presence of 0.056 mM of caffeic acid in the solution.	113
Figure 34. CA-ABA aggregation	127
Figure 35. Optimization of the polymerization parameters: (a) ratio of the template (T) to functional monomer (FM) concentrations, (b) the number of cycles and (c) the rebinding time.	128
Figure 36. CV signals representing the polymerization of the MIP(a) and the NIP(b) on the surface of the SPCE	129

Figure 37. Rebinding activity of the MIP-sensor and the NIP in the presence of different concentrations of caffeic acid, prepared in a hydro-alcoholic solution .....	129
Figure 38. The MIP-sensor and NIP response represented by % of rebinding in the presence of CA and other interferents: trans-ferulic acid (FA), sinapic acid (SA) gallic acid (G), and p-coumaric acid ( <i>p</i> -CA).....	131

### Supplementary Material:

Figure S1. Remaining template (DMCA, CA) during the washing steps of the polymers. ....	137
Figure S2. Preparation steps of rebinding experiments using CA-MIP/NIP and measured by CV. ...	137
Figure S3. Kinetic study representing the amount of adsorbed caffeic acid from 1 min to 4 hours of stirring, applied with nine samples of 1 mL containing 1.11 mM of caffeic acid in the presence of 20 mg CA-MIP (error bars are smaller than the symbol). ....	137
Figure S4. ATR-FTIR spectra for CA-MIP and NIP. ....	138
Figure S5. SEM images of CA-MIP and NIP at different scales. ....	138
Figure S6. Deprotonation of caffeic acid as a function of increasing pH and the respective pKa values. ....	139
Figure S7. Calibration curve for the determination of CA in red wine using the MIP-CA/CV method. The wine was diluted 10 times in a (PBS 0.05 M/ EtOH) (90/10, v/v, pH 3), and 10 mg of CA-MIP were added to 1 mL of the diluted wine. Cyclic voltammetry parameters: voltage range of -0.4 to 0.8 V at a scan rate of 50 mV/s versus Ag/AgCl. ....	139
Figure S8. Correlation between MIP-CA/Cyclic voltammetry method and HPLC-UV method for the determination of CA in wine. ....	139

## List of tables

Table 1. Amino acids susceptible to oxidation and their respective oxidation products, reproduced from [26] with the permission of Elsevier.....	6
Table 2. Some applications of CV and DPV techniques for the determination of antioxidants and antioxidant capacity in various analyzed media.....	19
Table 3. Some MIPs applications with antioxidants.....	27
Table 4. List of synthesis trials of CA-MIP, DMCA-MIP and NIP.....	42
Table 5. Synthesis of 11 couples of CA-MIP/NIP.....	45
Table 6. Added and recovered concentration of CA from wine samples using the MIP-CA/Cyclic voltammetry and the HPLC-UV methods.....	91
Table 7. Synthesis of 11 couples of CA-MIP/NIP.....	101
Table 8. Resulting polymers characteristics before and after polymerization. $\Delta N_{ads}$ ( $\mu\text{mol}$ ) represents the difference between the adsorbed amount of CA by CA-MIP and NIP in the presence of 10 mg of polymer and % of NIP adsorption represents the amount of caffeic acid retained by the NIP regarding the amount retained by CA-MIP in the presence of 10 mg of polymer.....	106
Table 9. Added and recovered concentration of CA from wine samples using the CA-MIP6/Cyclic voltammetry and the HPLC-UV methods. [CA] values are represented in % of rebinding. .	114
Table 10. Coordination number (CN), total interaction energy ( $E_{int}$ ) for the CA–monomer complexes, as well as the number of hydrogen bonds(nHB) responsible for their stabilization.....	126
Table 11. Determination of CA concentration and recovery values in spiked wine samples with the developed MIP sensor with DPV and HPLC-UV methods.....	132

## List of Abbreviations

ACN	:	Acetonitrile
AIBN	:	Azobisisobutyronitrile
APTES	:	(3-Aminopropyl)-triethoxysilane
CA	:	Caffeic acid
CL	:	Cross-linker
CN	:	Coordination number
CPE	:	Carbon paste electrode
CV	:	Cyclic voltammetry
DM	:	Dichloromethane
DMPAP	:	2,2-Dimethoxy-2-phenylacetophenone
DPV	:	Differential pulse voltammetry
EGDMA	:	Ethylene glycol dimethacrylate
$E_{\text{int}}$	:	Total interaction energy
ET	:	Electron transfer
EtOH	:	Ethanol
FA	:	Ferulic acid
FM	:	Functional monomer
GA	:	Gallic acid
HAT	:	Hydrogen atom transfer
I	:	Initiator
MAA	:	Methacrylic acid
MeOH	:	Methanol
MIP	:	Molecularly imprinted polymer
MIS	:	Molecularly imprinted silica
MMIP	:	Magnetic functionalized molecularly imprinted polymer
nHB	:	Number of hydrogen bonds

NIP	:	Non-imprinted polymer
N-PAA	:	N-phenylacrylamide
(-OH)	:	Hydroxyl group
PBS	:	Phosphate buffer saline
<i>p</i> -CA	:	<i>p</i> -coumaric acid
PTMOS	:	Phenyltrimethoxysilane
SA	:	Sinapic acid
SPCE	:	Screen-printed carbon electrode
SPE	:	Screen-printed electrode
T	:	Template
TBAPF6	:	Tetrabutylammonium hexafluorophosphate

## General Introduction

Eating healthy is key to healthy body.

Food and health have always been connected: “food is your first medicine” (Hippocrate). Healthy food is vital for the body as it protects it against many chronic diseases such as heart disease, type 2 diabetes, obesity, certain cancers, etc.

Antioxidants represent an important category of the essential compounds for the protection of food products, as well as the human body. Their main role *in vivo* is to prevent or slow damage to cells by neutralizing free radicals. This helps break a chain reaction that can affect other molecules in the cell and other organs in the body. In this work, red wine was chosen as a real medium for the detection of natural antioxidants because it is considered as a rich source of a large number of these compounds, namely the phenolic acids and polyphenols that provide it with its protective redox potential. In addition, caffeic acid was selected as the molecule of interest [1,2]. It is among the major hydroxycinnamic acids present in wine and it was identified as one of the most active antioxidant [3].

Numerous techniques have been developed over the years for the evaluation of these compounds. They are classified according to their mechanism of action. There are methods based on hydrogen atom transfer (HAT) and electron transfer (ET), mainly based on chromophore and fluorophore, as well as separation (HPLC, GC) and detection (UV, MS) techniques. In our case, the technique on which we have based all our studies is electrochemistry, coupled with molecular imprinting to enhance the specificity and selectivity of the phenolic compounds identification.

Electrochemistry is fast, accurate and requires simple instruments. Cyclic voltammetry (CV) and differential pulse voltammetry are mainly used for antioxidant detection. In addition, traditional electrodes were replaced with screen-printed carbon electrode (SPCE) that are suitable for working with microvolumes, SPCEs are inexpensive and reliable [4,5].

Molecular imprinting is a technology used to create cavities with artificial recognition sites in polymeric matrices that are complementary to the target molecule (template) in size, shape and structural arrangement of functional groups [6]. In recent years, molecularly imprinted polymers (MIP) and electrochemistry allowed the targeted detection of organic compounds,

metal ions, emerging pollutants and biomolecules [7–10]. The combination of MIPs and electrochemistry constitutes the main topic of our work as it was applied for the detection of our target molecule.

This work consists of a review and three main chapters.

The review constitutes a bibliographical study on each of the three scientific areas: antioxidants, electrochemistry and molecular imprinting, and the importance of combining the three together for the detection of antioxidants in media of interest.

Chapter 1 involves an indirect method where a molecularly imprinted polymer specific for caffeic acid (CA-MIP) and its relative non-imprinted polymer (NIP) were prepared apart from the electrode and applied in a hydro-alcoholic medium and then in wine. CA-MIP showed a good rebinding and selectivity towards CA regarding other interferents with similar structures to CA. However, the only issue with this couple was the lack of specificity defined by the close responses of CA-MIP and NIP. This led us to work on the optimization of the synthesis conditions in order to have a specific polymer with a difference between CA-MIP and NIP performances by maintaining the selectivity and rebinding characteristics.

Chapter 2 is therefore about the optimization of the synthesis conditions: solubility of the template, functional monomer, solvent(s) and type of radical initiation. The results showed that all these factors contribute in the structuring of the polymer and its performance. The optimal couple was chosen based on the difference between CA-MIP and NIP rebinding response and was then applied in wine.

The indirect method applied in chapters 1 and 2 is simple and accurate, but it requires an *ex-situ* synthesis of the polymers and their applications in the solution before deposition on the electrode. In this case, electropolymerization technique could be used where the polymers are directly polymerized on the surface of the SPCE. The polymerization, the washing and the rebinding steps are simple and fast. This technique allows a superior adhesion of the polymer on the surface of the electrode and the MIPs could be obtained in a few minutes with a certain thickness by controlling the number of cycles or the current that is applied to the electrode [11].

In chapter 3, a CA-MIP sensor was developed for the selective detection of caffeic acid. Electropolymerization becomes fast and simple once the optimal parameters and conditions are selected. First, the choice of functional monomer was done using molecular simulation. Second, the ratio of template to functional monomer concentrations, the number of cycles and the time

of rebinding were tested. After the optimization, the polymerization was done on the surface of the SPCE followed by the washing and the rebinding tests in hydro-alcoholic medium, and then the sensor was successfully applied in wine.

In summary, these three chapters complement each other and the work deserves to be developed in a way to evolve the rebinding by modifying the electrodes and to be applied in other food matrices such as vegetable extracts to produce natural food additives (natural antioxidants).

**Part I**  
**Literature Review**

## 1. Introduction

The world of antioxidants has always interested researchers because of its importance in many sectors: medicine, pharmacy, cosmetic, food, painting, etc. Their main role is to retard oxidation and protect against oxidation caused by free radicals, through different mechanisms of action, presented in the following [12]. Antioxidants are very numerous, they exist in both natural and synthetic forms. There are many conventional and unconventional methods developed for their extraction and characterization. Their detection and the evaluation of their antioxidant capacity constitute a key point for their uses. Several methods exist but each has its advantages and disadvantages [13,14]. Electrochemistry, voltammetry in particular, is suggested as a solution capable of overcoming the obstacles imposed by these techniques, they are based on fast, easy and very affordable techniques. In voltammetry, the current is measured by varying the potential applied to the electrode. Cyclic voltammetry (CV) and differential pulse voltammetry (DPV) are discussed in this review, being the most commonly used in the determination of antioxidants [4]. A large number of applications of these techniques have been carried out, with antioxidant and other compounds, and in several complex matrices. In addition, screen printed electrodes have been able to replace conventional electrodes, reducing the volume of solvents used and eliminating the problem of cleaning and reproducibility of the electrode [16,17]. A good application depends on a good choice of factors. The type of electrode, the solvent, the supporting electrolytes, the method parameters and many others, contribute significantly to the efficiency of the technique.

In order to optimize selectivity, an innovative technique can be added to the antioxidant-electrochemistry couple, which can be used to transfer a signal to a specific antioxidant or family of antioxidants, which is molecular imprinting. It is a technique that consists of creating complementary images in terms of structure and functionality to a target molecule. This happens by creating within a synthetic polymer recognition sites specific to this molecule, in order to enhance its selectivity in the medium. There are different techniques and approaches used for molecular imprinting: radical polymerization and sol-gel process, where molecularly imprinted polymers (MIPs) and molecularly imprinted silica (MIS) are respectively obtained. Each has a large selection of reagents, the most important factor is to choose the appropriate reagents and conditions required for polymer synthesis. At the end of the synthesis, the washing step leaves cavities for recapturing the target molecule in a simple or complex medium [18].

MIPs and MIS have been extensively used in a wide range of applications, some of which are presented in this review. Their application with antioxidants for extraction, quantification, or purification purposes is large, as well as with electrochemistry alone to capture other molecules.

This literature review highlights the importance of combining these three fields: the study of antioxidants, analysis by electrochemistry, and molecular imprinting, in order to create a rapid and specific method for one antioxidant detection, involving the use of electrochemistry and molecular imprinting.

## 2. Antioxidants

Antioxidants, a subject that has always been a major attraction to the researchers, exist in natural and synthetic forms. However, since the consumer has become more concerned regarding his safety, the importance is being attributed to naturally occurring antioxidants in foods, cosmetics, pharmaceuticals, nutraceuticals, etc.

Natural antioxidants are widely used to protect oxidizable species commonly found in pharmaceuticals, paramedical products, cosmetics and foods. They were firstly used as food preservative, to extend the shelf life of food products and preserve their nutritional and organoleptic qualities. Antioxidants play a key role in wine maturing. In addition, they protect human metabolism and prevent many health diseases such as colon and breast cancer, cardiovascular diseases, neurodegenerative diseases, chronic inflammatory diseases, osteoporosis, and others as a result of their anti-proliferative, pro-apoptotic, anti-inflammatory, neuroprotective, neuromodulator, antiviral and many other effects [19–24].

The main targets of antioxidants are reactive oxygen species, such as free radicals mainly derived from oxidation reactions that target different structures (lipids, proteins and carbohydrates) and that can affect foods and health [24].

### 2.1. Common types of food oxidation

Lipid peroxidation is a very common type of oxidation that occurs in foods rich in unsaturated fatty acids and cholesterol. The free radical mechanism of lipid oxidation is usually divided into three stages : initiation, propagation, and termination (Figure 1) [25]. In the initiation stage, different factors can lead to free radical formation, such as temperature, light, heavy metals or other free radicals. During the propagation stage, lipid radicals react with oxygen to form peroxy radicals. Formed at this stage, peroxy radicals react with another molecule of lipid, forming a lipid radical and a hydroperoxide that is not stable and decomposes easily to form primary then secondary products. All these products affect the quality and the taste of the food product. Secondary products are responsible of off-flavor. The latter is one of the main cause of oxidized food rejection by consumers. During the termination stage, radicals react with each other and form nonradical products. Any reaction that prevents the propagation of peroxidation

or removes free radicals from the system plays a key role in the termination mechanism. This is where the importance of antioxidants comes in.

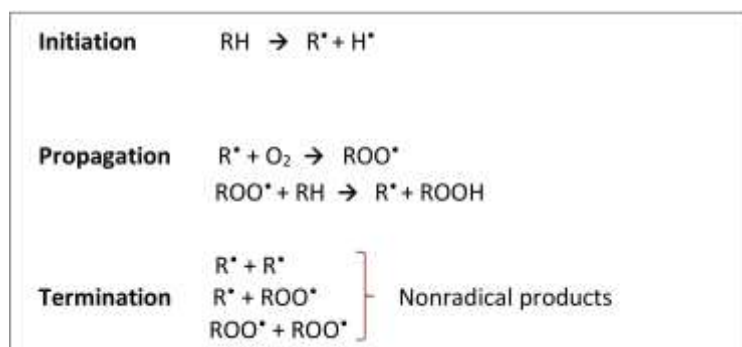
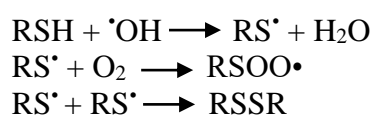


**Figure 1.** The general process of lipid peroxidation [25]. RH: target polyunsaturated fatty acid; R<sup>•</sup>: fatty acid radical; ROO<sup>•</sup>: fatty acid peroxy radical; ROOH: lipid hydroperoxides.

Similarly to lipid peroxidation, protein oxidation has an important impact on food quality, although it is less explored.

Protein oxidation mainly depends on its amino acids composition or the primary structure, and thus their chemical structure. Table 1 shows the most reactive amino acids and their oxidation products. There are sulfur-containing amino acids, such as cysteine, that once oxidized, leads to thiyl radicals (RS<sup>•</sup>) and then generates a thiylperoxy radical (RSOO<sup>•</sup>) or disulfide bond (RSSR) [26] according to the following reactions:



Aromatic amino acids, such as tyrosine, tryptophan, histidine, and phenylalanine, are susceptible to oxygenation of their ring. For example, phenylalanine may generate *ortho*-tyrosine (Figure 2.I) meta-tyrosine (Figure 2.II), and 4-hydroxyphenylalanine (para-tyrosine) (Figure 2.III) during oxidation. Aliphatic amino acids are oxidized by hydrogen abstraction at the alpha carbon and give a carbon-centered radical (Figure 2.IV).

Besides controlling food processing conditions, feeding regime of the animal, and food storage, adding antioxidant to the product can also prevent food oxidation. Antioxidants may have close (ex: hydrophilic) or different (ex: lipophilic) effects on protein than those on lipids, and inhibition of protein oxidation can sometimes present a protective effect on the lipid fraction [27], and *vice versa*. Moreover, many proteins such as bovine serum albumin (BSA), β-lactoglobulin, lactoferrin [28–30], and protein hydrolysates from whey, casein, soy and egg

yolk [31–34] were found to have antioxidant effects themselves, by scavenging free radicals, chelating metals, reducing lipid hydroperoxides and interacting with aldehydes [35].

**Table 1.** Amino acids susceptible to oxidation and their respective oxidation products, reproduced from [26] with the permission of Elsevier.

Amino acid	Oxidation products
<b>Cysteine</b>	Disulfide, cystine
<b>Methionine</b>	Methione sulfoxide/sulphone
<b>Tyrosine</b>	Dityrosine, 3,4-dihydrophenylalanine (DOPA)
<b>Tryptophan</b>	Hydroxytryptophan, <i>N</i> -kynurenine, <i>N</i> -formylkynurenine, 3 hydroxylkynurenine
<b>Phenylalanine</b>	Hydroxyphenylalanine, <i>o</i> -tyrosine, <i>m</i> -tyrosine
<b>Valine, leucine</b>	Hydroxyperoxides
<b>Histidine</b>	2-oxohistidine
<b>Proline</b>	Hydroxyproline, glutamic semialdehyde pyrrolidinone
<b>Threonine</b>	2-amino-3-ketobutyric acid
<b>Arginine</b>	Glutamic semialdehyde
<b>Lysine</b>	Hydroxylysine, 2-aminoadipic semialdehyde

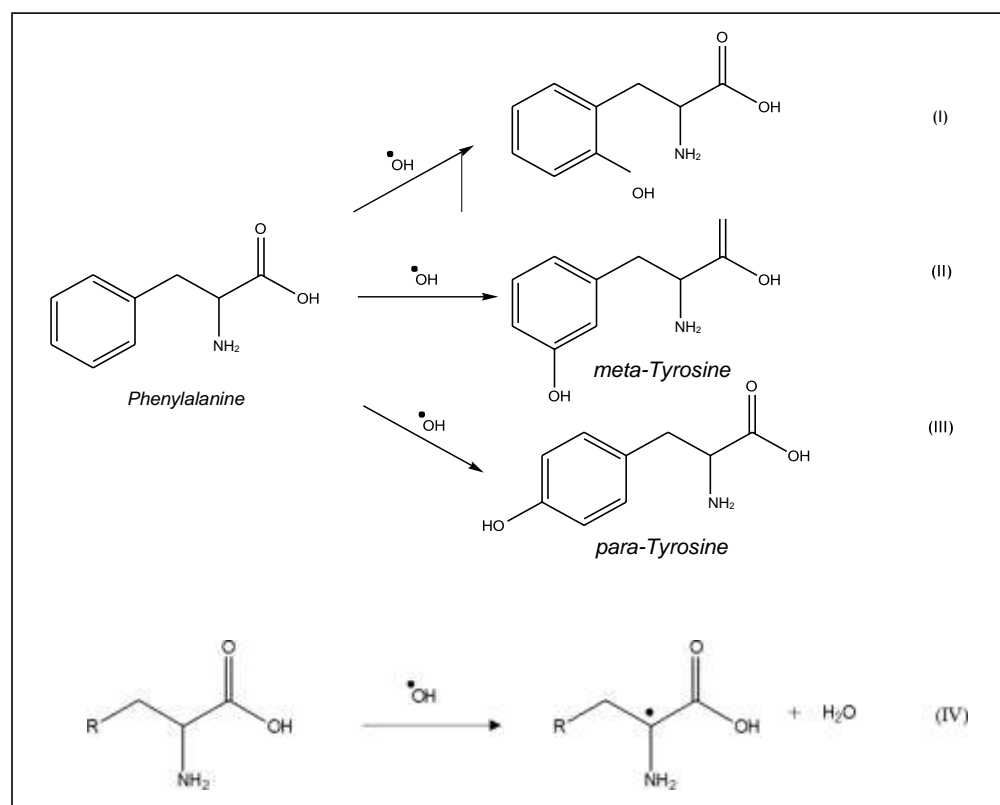
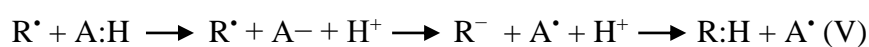


**Figure 2.** Oxidation process of: (I), (II), (III) aromatic amino acids and (IV) aliphatic amino acids [26].

## 2.2. Mechanism of action

In general, the principle of antioxidants is based on avoiding radical initiation or propagation of radical state, through several mechanisms. Antioxidants can be classified as primary or secondary antioxidants according to their mechanism of action. The primary or chain-breaking antioxidants (A:H in the following equations) are able to give a hydrogen atom (Equation V) and a single electron (Equation VI) to a radical and thereby neutralizing it, such as phenolic compounds with one or more hydroxyl group (-OH). This mechanism is known for “radical scavenging,” although this term is not fully adapted to the reality of the mechanism. It should be qualified as “single electron giver”.



Monophenols create unreactive phenoxyl radicals due to resonance stabilization (Figure 3.VII), while diphenols, when oxidized, produce quinones (Figure 3.VIII)). Some of the monophenols (in a radical state and stabilized by resonance) can be polymerized, for example a natural antioxidant gamma-tocopherol or a synthetic antioxidant butylated hydroxytoluene (BHT), and give a non-radical dimer (Figure 3.IX). These reactions disrupt the free radical chain propagation.

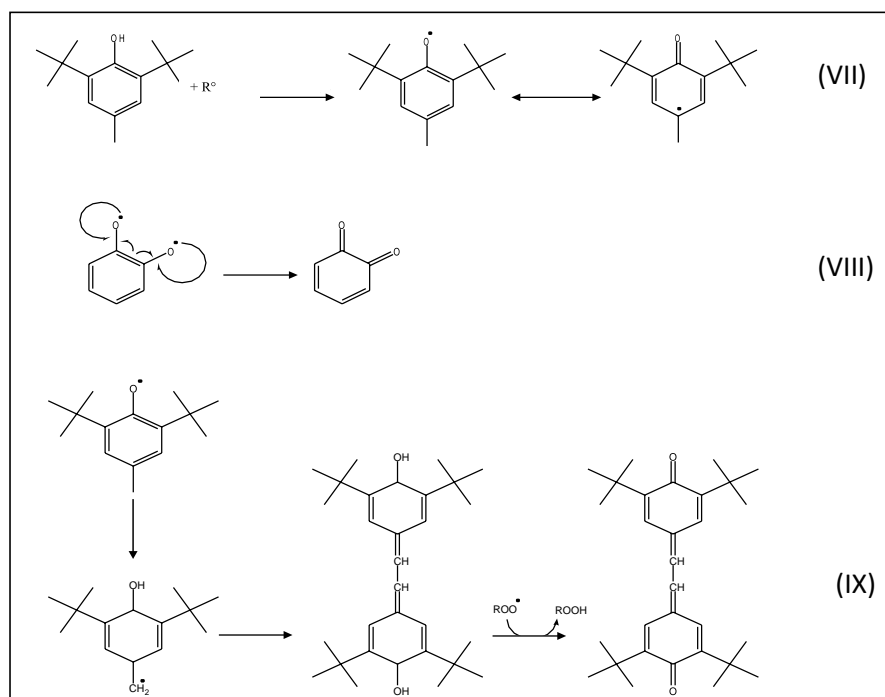


**Figure 3.** Example of stabilization by resonance, with (VII) butylated hydroxytoluene (BHT) and (VIII) ortho-diphenol, and example of BHT polymerization (IX).

The secondary, or preventive antioxidants, are substances able to inhibit or delay chain initiation. Several mechanisms such as chelation of transition metals, oxygen scavenging and quenching of singlet oxygen can be exhibited by these secondary antioxidants (Figure 4) [12,36–40].

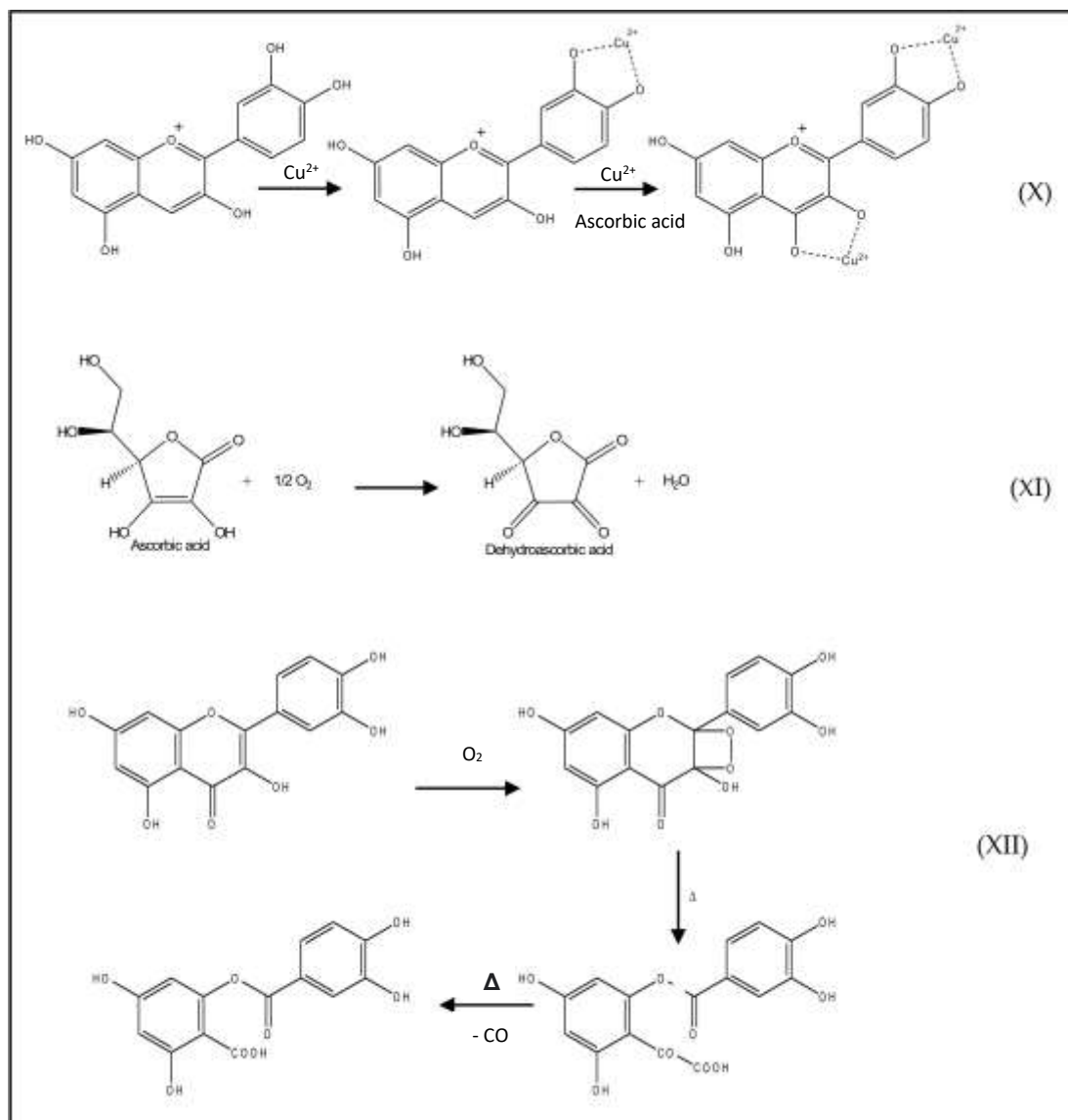


**Figure 4.** Reaction mechanisms of secondary antioxidants: (X) Metal ion ( $\text{Cu}^{2+}$ ) chelating activity of anthocyanidine (cyanidin), from [41] published by The Royal Society of Chemistry; (XI) oxygen scavenging activity of ascorbic acid, reproduced from [42] under Creative Common license; (XII) chemical reaction of quercetin with singlet oxygen, reproduced from [43] with the permission of Elsevier.

### 2.3. Main antioxidant families

Antioxidants are divided between endogenous and exogenous (Figure 5). One of the most interesting families of natural antioxidants is phenolic compounds. They are frequently found in food, such as anthocyanins and monomeric flavanols in red wine and berries, hydroxycinnamic and hydroxybenzoic acids in fruits and vegetables, ferulic acid in cereals, flavonols in tea, secoiridoids in olive oil, etc. [12,25,44–52].

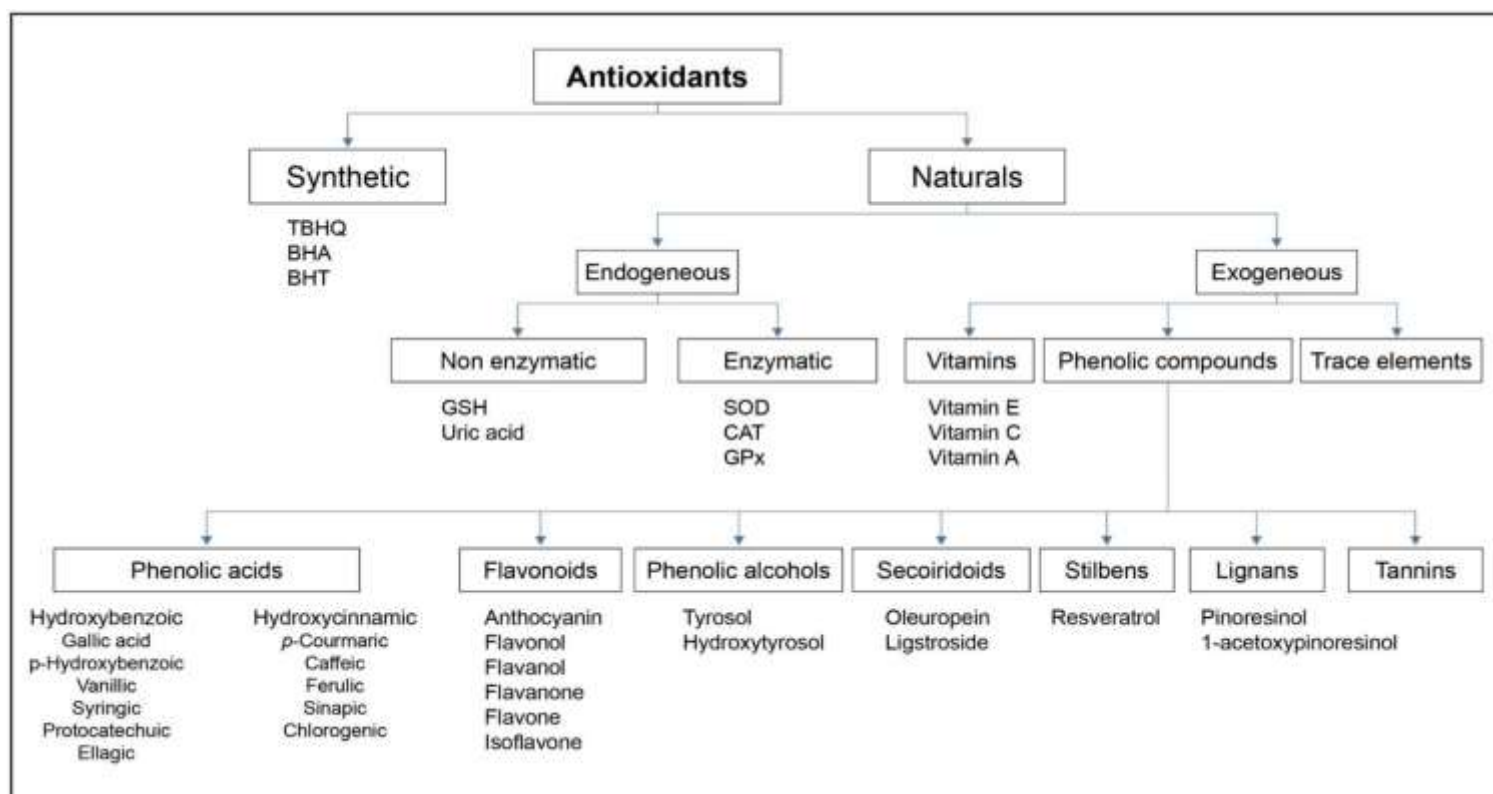


**Figure 5.** Antioxidant families. TBHQ: tert-Butylhydroquinone; BHA: butylated hydroxyanisole; BHT: butylated hydroxytoluene; GSH: reduced glutathione; SOD: superoxide dismutase; CAT: catalase; GPx: glutathione peroxidase.

### 2.4. Total antioxidant capacity assays

Basically, to verify the efficiency of an antioxidant, the most convenient method is to compare a medium with and without added antioxidant and to record for several hours or weeks the content of the molecule of interest to protect. For example, to evaluate the potential of an antioxidant for the preservation of fish oil, recording the oxidation of the oil (using peroxide value (PV), conjugated dienes (CD), thiobarbituric acid reacting substances (TBARS) methods) and comparing the blank (without antioxidants) and samples (oil added with different antioxidants at the same concentration) is the most accurate method to evaluate the efficiency

of an antioxidant against the oxidation of the oil. The weakness of this strategy is the time required to obtain an evaluation of antioxidant efficiency.

Several methods have been used to apply rapid evaluation of the total antioxidant capacity (TAC) of complex samples (food extracts, beverages, biological fluids...), and they are classified into two categories, according to their mechanism of action : hydrogen atom transfer (HAT) and electron transfer mechanisms (ET) (Figure 6).

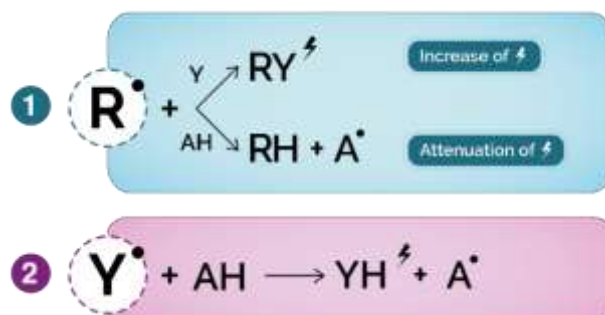


**Figure 6.** General mechanism of direct (competitive) and indirect (noncompetitive) antioxidant assays. (1) HAT-based assays:  $R^\bullet$ : free radical;  $Y$ : probe,  $AH$ : antioxidant;  $A^\bullet$ : oxidized antioxidant;  $\bullet$ : fluorescence, absorption, light emission, oxygen consumption; (2) ET-based assays:  $Y^\bullet$ : oxidized probe,  $AH$ : antioxidant;  $YH^\bullet$ : reduced probe;  $\bullet$ : color modification of reduced probe.

The HAT-based assays are usually based on competitive reactions between the antioxidant and a suitable probe (fluorescent, UV-vis, oxygen, or chemiluminescent reagent) that reacts with the oxidant leading to changes in its measurable properties. The antioxidant capacity is calculated by measuring the fluorescence, absorbance, oxygen consumption or chemiluminescence decay curve of the probe and then integrating the area under the curve (AUC). These assays include total radical-trapping antioxidant parameter (TRAP), oxygen radical absorbance capacity (ORAC), and crocin-bleaching assays (CBAs) [30], [32], [40], [41].

Oxygen radical absorbance capacity (ORAC) monitors the inhibition of peroxy-radical induced oxidation by measuring the fluorescence decay of  $\beta$ -phycoerythrin or fluorescein as probe kinetically in the presence of antioxidants and an oxidizing agent generated by commonly used azo compounds (lipophilic AIBN, ABAP, and AMVN or hydrophilic AAPH). The greater the delay of fluorescence decay, the stronger the antioxidant capacity (AOC). In reality, ORAC is calculated with the area between the decay curve of blank and the curve with the sample containing an antioxidant. ORAC assay is supposed to measure lipophilic as

---

well as hydrophilic antioxidants because it uses a mixed solvent of 50% acetone/50% water (v/v) containing 7% methylated beta-cyclodextrin to solubilize antioxidants [56].

Total radical-trapping antioxidant parameter (TRAP) monitors antioxidant capability to interfere with the reaction between oxygen or fluorescent ( $\beta$ -phycoerythrin) probe and  $\text{ROO}\cdot$  generated by an azo compound in aqueous medium. The method determines oxygen consumption or the fluorescence decay of  $\beta$ -phycoerythrin during oxidation inhibition. Ferric ion reducing antioxidant power (FRAP) and trolox equivalent antioxidant capacity (TEAC) are specific TRAP methods (see further in the ET-based assays) using water solvent but there are other different FRAP techniques using other solvents and probes, such as diphenyl-1-pyrenylphosphine (DPPP) or coumarin-triarylphosphin soluble in organic solvent [57] and could be adapted to evaluate liposoluble antioxidant.

Crocin-bleaching assays (CBAs) monitors the inhibition of crocin-bleaching, based on competitive reaction of an antioxidant and UV-vis probe (crocin) with  $\text{ROO}\cdot$  generated by thermolysis of AAPH in the presence of  $\text{O}_2$ ; determines the absorption decay. This method concerns only water-soluble antioxidants (solvent: a 9:1 water-ethanol mixture) [58]. This method is not suitable to evaluate the radical scavenge capacity of liposoluble antioxidant.

Chemiluminescence measures antioxidant capacity in quenching several ROS, other than  $\text{ROO}\cdot$ , such as hydrogen peroxide. It can be direct or indirect. It is based on the competition between antioxidants and chemiluminescent reagent (ex: luminol) for hydrogen peroxide; and monitors the decrease in light emission intensity caused by the antioxidant. Luminol is dissolved in aqueous borate buffer [59] with a small amount of ethanol to dissolve the standard, Trolox. This method is not suitable to evaluate the radical scavenge capacity of liposoluble antioxidant.

The ET-based assays are based on noncompetitive reactions, they measure the capacity of an antioxidant to reduce an oxidant probe and convert it to a colored, fluorescent or chemiluminescent species. The degree of color change or fluorescence decay is proportional to the antioxidant capacity. These assays include 2,2-diphenyl-1-picrylhydrazyl assay (DPPH), trolox equivalent antioxidant capacity (TEAC), ferric ion reducing antioxidant power (FRAP), cupric ion reducing antioxidant capacity (CUPRAC) assays and the Folin-Ciocalteu assay [30], [34], [40], [41]. Not to mention that some assays, such as DPPH and TEAC can be considered

as mixed-mode methods (ET and HAT) because their radicals may be deactivated via HAT mechanisms, but studies showed better results via ET mechanisms [13,53,54,60,61].

Inhibition of 2,2-diphenyl-1-picrylhydrazyl radical (DPPH•), a colorimetric method based on the capacity of antioxidants to neutralize DPPH• radical, accompanied with absorbance decrease at 517 nm due to its decolorization is widely used as indicator of the antioxidant efficacy. The DPPH method is performed generally in methanol, ethanol or alcohol. This method is not suitable to evaluate the radical scavenge capacity of liposoluble antioxidant. DPPH was also used with a non protic solvent, ethylacetate [62] and even in an aprotic apolar solvent, toluene [63], in order to evaluate AOC of lipophilic antioxidant.

Trolox equivalent antioxidant capacity (TEAC), a colorimetric method based on the capacity of antioxidants to reduce 2,2'-azino-bis(3-ethylbenzothiazoline-6-sulphonique) (ABTS•+) radical, accompanied with absorbance decrease at maximum 734 nm, due to its decolorization. ABTS is soluble in water and is used for example for AOC assays with molecules extracted from plant with supercritical water [64]. This method is not suitable to evaluate the radical scavenge capacity of liposoluble antioxidant.

Ferric-reducing antioxidant power (FRAP), a colorimetric method based on the reduction of ferric ion  $\text{Fe}^{3+}$ -tripirydyltriazine complex ( $\text{Fe}^{3+}$ -TPTZ) to its blue coloured ferrous form ( $\text{Fe}^{2+}$ -TPTZ) by antioxidants, accompanied with absorbance increase at 593 nm. FRAP is a method working in aqueous buffer [64]. This method is not suitable to evaluate the radical scavenge capacity of liposoluble antioxidant.

Cupric reducing antioxidant capacity (CUPRAC), similar to FRAP, this method is based on the reduction of cupric ion  $\text{Cu}^{2+}$ -neocuproine ( $\text{Cu}^{2+}$ -Nc) to cuprous ion ( $\text{Cu}^{+}$ -Nc) by antioxidants, accompanied with absorbance increase at maximum 450 nm. CUPRAC works in water, possibly with a small amount of ethanol [65]. This method is not suitable to evaluate the radical scavenge capacity of liposoluble antioxidant.

Folin-Ciocalteu reducing capacity, a colorimetric method based on the reduction of the Folin-Ciocalteu reagent (phosphomolybdic/phosphotungstic acid complexes) to a blue-coloured chromophore by phenolic compounds, with maximum absorption at 765 nm. This method uses aqueous buffer [64] or in 1:1 methanol-water buffer [66]. This method is not suitable to evaluate the radical scavenge capacity of liposoluble antioxidant.

Despite the evolution and development of these techniques throughout the years, and all the

advantages that they had presented to research in the field of antioxidants, they nevertheless involve limitations and disadvantages that push researchers to seek alternatives in order to improve their studies. Most of them are costly, not sufficiently rapid and present lack of specificity. Although some of the assays were adapted to measure lipophilic as well as hydrophilic antioxidants, they still present an irrelevant classification. Different explanations can be given. The chemical reaction mechanisms and kinetics do not mimic the mechanism of antioxidant in situ as protector of molecules of interests. All these methods require standardization because results can differ between reactions due to several factors, such as type and amount of solvent, pH, presence of metal ions and antioxidant reaction, even with the same sample. For example, hydrophobic antioxidants, soluble in oil and efficient to protect oil against its oxidation, cannot be dissolved in acetone or alcohol with DPPH methods. In addition, the same antioxidant evaluated by different assays or by the same assay in different laboratories may give rise to serious differences in results. Actually these differences in antioxidant capacity or rank lead to a lack of correlation between activities [30], [55].

HAT-based methods suffer from different limitations. A common one is that antioxidant extracts may naturally contain pigments and fluorophores that can interfere with absorbance and fluorescence affecting the results. Moreover,  $\beta$ -phycoerythrin probe used in ORAC and TRAP can interact with phenolic compounds by nonspecific protein binding and cause underestimation of antioxidant capacity, not to mention that its reactivity toward peroxy radicals can vary each time. When oxygen is used as a detection probe, it can affect the results because of its instability. Oxygen pressure cannot be controlled, which makes it impossible to control the peroxide content. In addition, many methods require automated systems that cannot be found in all laboratories, similarly for reagents not easily available commercially, such as crocin. On the other hand, these methods have a lag-phase that is not the same for all antioxidants, and they present ambiguity in end-point determination, which makes data comparison between laboratories more difficult [55].

ET-based methods have been criticized mainly because they ignore the reaction kinetics, and many probes used as oxidant are non-physiological radicals (ABTS $\bullet$ + and DPPH $\bullet$ ) which makes the results incomparable to the real-life antioxidant action [13,53–55,60].

## 2.5. Extraction and detection of antioxidants

A wide range of analytical methods were developed for the extraction of antioxidants from food and their by-products, conventional (Soxhlet extraction, liquid–liquid extraction, solid phase extraction) and non-conventional or emergent techniques (ultrasound, microwave, pulsed electric fields (PEFs), high-voltage electrical discharges, ultrasounds, infrared, supercritical and subcritical fluid extraction, instant controlled pressure drop (DIC), and intensification of vaporization by decompression to the vacuum (IVDV), Infrared), and for their content detection (HPLC with UV, fluorescence or photodiode array detector, thin layer chromatography, capillary electrophoresis, supercritical fluid chromatography, GC-MS, LC-MS) [67,68]. However, there are several limitations in using most of them. For example, conventional extraction techniques are time, solvent, and energy consuming, in addition to the fact that antioxidants are strongly influenced by many important parameters such as the type of solvent used, pH, temperature, etc. [69–72]. Non-conventional techniques presented serious advantages but they also hold some disadvantages that should not be underestimated when choosing the technique. Ultrasound and pressure assisted extractions are expensive, microwave assisted extraction involves quick heating, which risks burning the sample and breakdown of antioxidant compounds, not to mention that solubility should be considered [73]. Moreover, further studies are needed to highlight the energy consumption of these technologies and their environmental impact.

Moving on to detection techniques that are time consuming, they require sample preparation and pre-treatment. Moreover, interfering substances affect the extract purity, and the presence of structurally similar compounds to antioxidants that belong to the same of different families makes selective extraction difficult where many components can be determined simultaneously.

To avoid these problems or at least attenuate them, researchers attributed a special interest to electrochemistry, an alternative method that has been widely used and developed due to its ability to overcome all the obstacles mentioned above in order to enhance the evaluation of antioxidant activities [74–76].

### 3. Electrochemistry

Why electrochemistry? Electrochemistry has numerous advantages. It is fast, sensitive enough for physiological determinations of antioxidants at low limits, affordable, easily accessible in the market, involves simple analytical procedures that does not require complicated and time-consuming sample pre-treatment or any addition of reactive species, etc. Additionally, electrochemical methods may determine several parameters that help understanding antioxidants reaction mechanism, such as redox potential, electrons number, electron transfer, etc.

Electrochemistry works usually with aqueous but can use non-aqueous electrolyte solutions, with a large range of solvent having a high value of permittivity (e.g., formamide,  $\epsilon=111$ ,  $\mu=3.73$  D) but also with low permittivity value and a low dipole moment (e.g., 1,4-dioxane,  $\epsilon=2.3$ ,  $\mu=0.45$ D). Except full apolar solvent (dipolar moment close to zero,  $\mu \rightarrow 0$ ) and very viscous solvent, it is possible to use solvent suitable for lipophilic antioxidant, using surfactant [77] or complex support electrolytes, such as tetrabutylammonium hexafluorophosphate (TBAPF<sub>6</sub>), dissolved in a mixture organic solvents, dichloromethane and acetonitrile [78], or in acetonitrile alone [79].

Electrochemistry has given rise to several electroanalytical methods that have grown greatly in application and importance to offer high sensitivity and precision and allow quantitative evaluations to be made on a variety of samples with relatively low-cost instrumentations. These methods are classified based on the measured signal: (1) amperometry measures the current resulting from a constant potential at different times, (2) voltammetry, a subclass of amperometry, measures the current by varying the potential applied to the electrode, and (3) potentiometry measures the potential of a solution between two electrodes. Electrochemical methods showed viable results in many applications such as food, clinical and pharmaceutical analysis [15].

These electroanalytical techniques, especially voltammetry, have received a special interest in the world of natural antioxidants that are usually known to be electroactive or redox active compounds. In voltammetry, a variation of potential is applied to the electrochemical cell, between a reference electrode (e.g. Ag/AgCl (3M KCl)) and an indicator electrode, often referred as the working electrode (e.g. glassy carbon, silver, gold, platinum...). A third

electrode, the auxiliary electrode (e.g. carbon or platinum), also named counter-electrode, conducts the flow during the redox reaction at the working electrode. The performance of voltammetric techniques is highly influenced by the material of the working electrode. Glassy carbon used the most, but as mentioned, other commonly used materials are platinum, gold, silver, graphite, and carbon paste. The field of modified electrodes has been one of the most active areas of research interest with a large number of applications, where a thin film is coated on the surface of the electrode leading to changing the functionality of its material and enhancing its electronic and structural properties. Moreover, a very well established approach used for the development of electrochemical sensors is the screen-printed electrodes (SPE). They are small, fast, inexpensive, reliable and easy to use. They allow performing a large number of experiments with small volumes of sample and the fact that they are single use sensors eliminates pre-treatment and maintenance procedures. Not to mention that electrode cleaning is a critical step, as it could alter the performance of the electrode, as demonstrated by Lima et al. [80], where the cleaning of the GCE involves its polishing on alumina slurry, leaving alumina residues that affect the electrochemical parameters of the antioxidants. Alternatives have been proposed, in order to avoid these disadvantages. Pencil graphite electrodes (PGE) were fabricated; they are simple, disposable, cheap, and widely commercially available. Their electrochemical performance was well demonstrated [81–84]. Moreover, a very well established approach used for the development of electrochemical sensors is the screen-printed electrodes (SPE). They are small, fast, inexpensive, reliable, and easy to use. They allow performing a large number of experiments with small volumes of sample and the fact that they are single use sensors eliminates pre-treatment and maintenance procedures. They are versatile and customizable, a large variety of materials and configurations of working electrode are available, and even modified electrodes [16,17,74].

Cyclic voltammetry (CV) and differential pulse voltammetry (DPV), provided with several types of working electrodes, are among the most extensively used electroanalytical techniques for studying redox reactions and for evaluating qualitative and quantitative aspects of antioxidants [75,85–92]. Voltammograms profiles are determined by the variation of applied potential.

CV method is based on a controlled potential variation. The potential waveform is usually of the form of an isosceles triangle in cyclical phases (Figure 7.a1), described by its initial, high,

final potentials and scan rate. CV voltammogram is usually represented by an electrochemically reversible reaction showing only one anodic peak ( $E_{pa}$ ) and one cathodic peak ( $E_{pc}$ ) resulting from the redox potential of the studied antioxidant in a specific medium, which provides information about the integrated antioxidant capacity (Figure 7.a2). The more susceptible the compounds are to oxidation, or in other terms the greater their antioxidant capacity, the sooner they will reach the anodic peak potential [93]. Such reversible systems are generated by ortho-diphenols, whereas for quasi-reversible (moderate-sized cathodic peak) and irreversible systems (absence of cathodic peak), where electron transfer is progressively slower, the peaks are separated and reduced in size (Figure 7.a3). A quantitative relationship exists between the reduction potential and concentration of the redox couple, according to Nernst equation (1):

$$E = E^0 + \frac{RT}{nF} \ln \left( \frac{[Ox]}{[Red]} \right) \quad (1)$$

where  $E^0$  is the formal reduction potential, R is the gas constant, T is the temperature, n is the number of electrons transferred in the redox event, F is Faraday's constant, and [Ox] and [Red] are the interfacial concentrations of the oxidised and reduced species respectively [94].

The potential is measured between the working electrode and the reference electrode, while the current is measured between the working electrode and the counter electrode [95,96].

DPV method involves two measurements of the current for each potential pulse : before ( $I_1$ ) and at the end ( $I_2$ ) of the application of the pulse (Figure 7.b1), which makes DPV techniques much more sensitive than CV (cyclic voltammetry) [85], and the difference ( $\Delta I = I_2 - I_1$ ) is plotted according to the potential applied. The voltammogram (Figure 7.b2) has a differential shape that presents a current peak, its height is directly proportional to the concentration of the studied antioxidant. The electrochemical cell is similar to that of CV, in which the potential is measured between the working electrode and the reference electrode and the current is measured between the working electrode and the counter electrode [74,96].

Some of the experiments using CV and DPV techniques for the determination of several compounds with different types of electrode materials are respectively listed in Table 2.

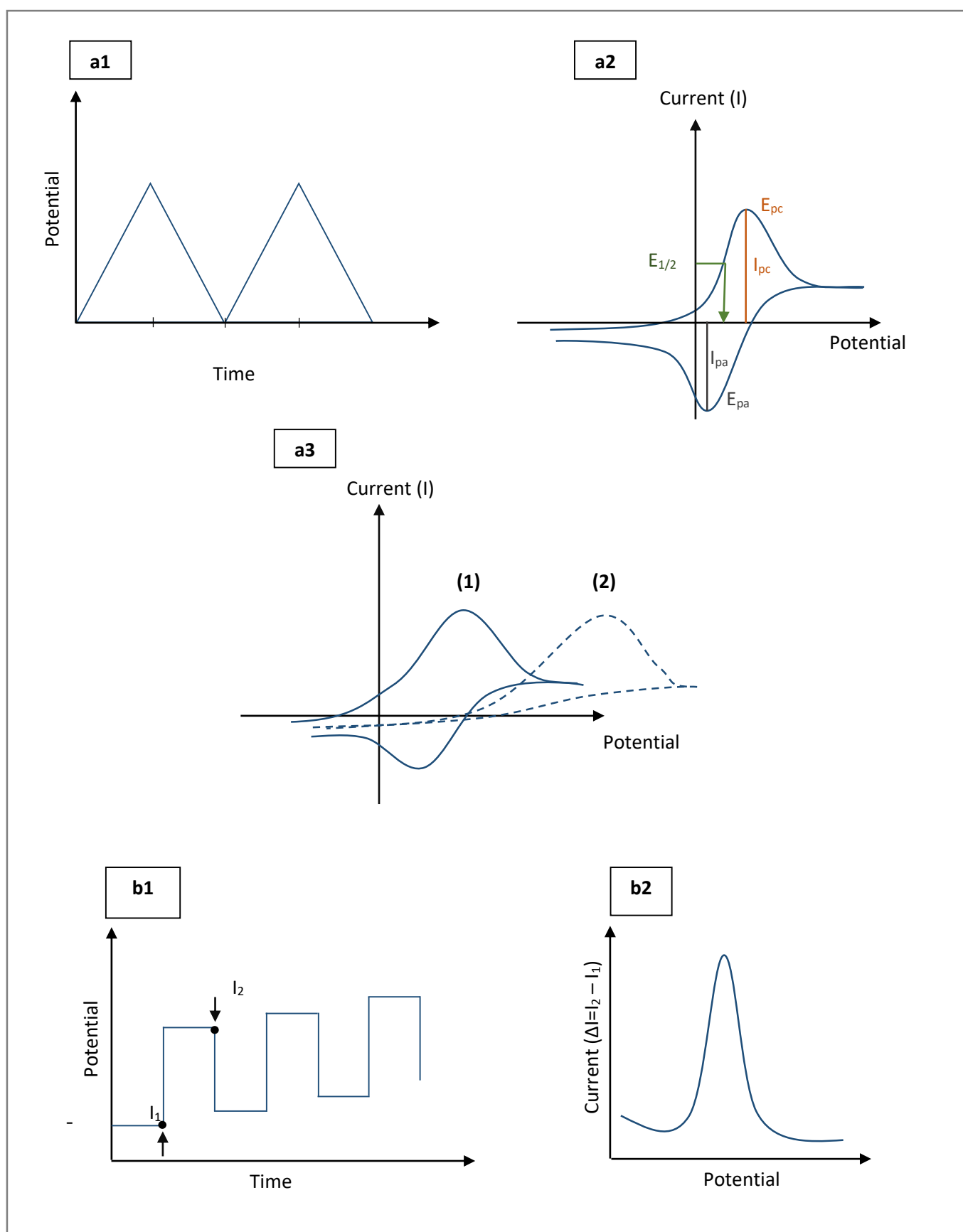


**Figure 7.** Voltammetry potential waveforms and basic voltammograms. (a1): CV potential waveform; (a2): basic cyclic voltammogram of reversible system, anodic and cathodic peak potentials ( $E_{pa}$  and  $E_{pc}$  respectively) and half-wave potential ( $E_{1/2}$ ); (a3) basic cyclic voltammogram of (1) quasi-reversible and (2) irreversible systems; (b1) DPV potential waveform; (b2) basic differential pulse voltammogram.

**Table 2.** Some applications of CV and DPV techniques for the determination of antioxidants and antioxidant capacity in various analyzed media.

Antioxidants	Application Media	Working Electrode	Method	Linear Range ( $\mu\text{M}$ )	Detection Limit ( $\mu\text{M}$ )	References
<b>Polyphenols</b>	Black tea infusion	CNT electrode	CV	0.23–94	0.11	[97]
	Red wine	SnO <sub>2</sub> -RGO/GCE	DPV	0.15–25	80×10 <sup>-3</sup>	[98]
	Coffee	Au@ $\alpha$ -Fe <sub>2</sub> O <sub>3</sub> @RGO/GCE	CV	19–1869	0.098	[99]
<b>Caffeic acid</b>	Wine	F-GO/GCE	DPV	0.5–100	0.018	[100]
	Wine	Au/PdNPs-GRF	DPV	0.03–938.97	6×10 <sup>-3</sup>	[101]
	Wine	RGO@PDA/GCE	DPV	5×10 <sup>-3</sup> –450.55	1.2×10 <sup>-3</sup>	[102]
<b>Gallic acid</b>	Tap water, tea and orange juice	SiO <sub>2</sub> nanoparticles/CPE	DPV	8.0×10 <sup>-1</sup> –1.0×10 <sup>-2</sup>	2.5×10 <sup>-1</sup>	[103]
	Wine	CS–fFe <sub>2</sub> O <sub>3</sub> –ERGO/GCE	DPV	1.0–1.0×10 <sup>6</sup>	1.5×10 <sup>-1</sup>	[104]
	Phosphate buffer solution	Zn-Al-NO <sub>3</sub> layered double hydroxide film/GCE	DPV	4–600	1.6	[105]
<b>Gallic acid and total polyphenols</b>	Red and white wines	CNT modified carbon paste electrode	DPV	5.0×10 <sup>-1</sup> –15	3.0×10 <sup>-1</sup>	[106]
	Mixture of ascorbic acid, dopamine and uric acid	PG/GCE	CV	9.00–2314	6.45	[107]
<b>Ascorbic acid</b>	Aqueous solution	2,7-BFEFO/CPE	CV; DPV	50–2.65×10 <sup>3</sup> ; 9–3.5×10 <sup>3</sup>	18; 4.2	[108]
	Fruit juices and wines	CPE; Pt strip electrode	DPV	70–20×10 <sup>3</sup> ; 310–20×10 <sup>3</sup>	20; 87	[109]
	Flavored beverages	DNA/CPE	DPV	0.05–1.00	5×10 <sup>-4</sup>	[110]
<b>Curcumin</b>	Human blood serum	NiCl <sub>2</sub> /GCE	DPV	10–600	0.109	[111]
	Spices	GCE	CV	9.9–1.07×10 <sup>2</sup>	41	[112]
<b>Vanillic acid</b>	Artificial wine solutions	Graphite; carbon microspheres and CNT CPE	CV	10–400	2.85; 3.82; 4.13	[113]
<b><math>\alpha</math>-tocopherol; <math>\gamma</math>-tocopherol and <math>\delta</math>-tocopherol</b>	Non-aqueous media	Pt electrode	DPV	2×10 <sup>-2</sup> –10; 2.2×10 <sup>-2</sup> –1.4; 2.21×10 <sup>-2</sup> – 31.1	1×10 <sup>-2</sup>	[114]
<b>Quercetin</b>	<i>Rhizoma kaempferiae</i> and buds of <i>Styphnolobium japonicum</i> (L.) Schott	CTAB-cMWCNTs/MWCPE	CV	0.01–20	5.3×10 <sup>-3</sup>	[115]

GCE: glassy carbon electrode, CNT: carbon nanotubes, SnO<sub>2</sub>-RGO: Tin(IV) oxide-reduced graphene oxide composite, F-GO: fluorine-doped graphene oxide, RGO@PDA: reduced graphene oxide and polydopamine composite, SiO<sub>2</sub>: silicon dioxide, CS: chitosan, fFe<sub>2</sub>O<sub>3</sub>: fishbone-shaped Fe<sub>2</sub>O<sub>3</sub>, ERGO: electrochemically reduced graphene oxide, BFEFO: 2,7-bis (ferrocenyl ethynyl) fluoren-9-one, Pt: platinum, CPE: carbon paste electrode, SPCE: screen-printed carbon electrode, PG: pristine graphene, NiCl<sub>2</sub>: nickel chloride, CTAB-cMWCNTs: cetyltrimethyl ammonium bromide-carboxylic multi-walled carbon nanotubes composite, MWCPE: multi-walled carbon paste electrode, CV: cyclic voltammetry, DPV: differential pulse voltammetry.

The choice of electrodes is a key point in electrochemical analysis, but the solvent used and the supporting electrolytes are also important in electrochemistry.

The solvent used in electroorganic reactions must fulfill several specifications: (i) good solubility of the supporting electrolytes and substrates to the solvent, (ii) high electroconductivity, (iii) high electrochemical stability, and (iv) suitable chemical reactivity [100].

The supporting electrolytes have to be non-electroactive in the range of applied potentials [116,117], and they can be different according to the species analyzed and their oxidation and reduction potential : LiCl or KCl; tetrabutylammonium salts with different counter-ions such as acetate, benzoate, bromide, chloride, hexafluorophosphate, tetraphenylborate, tetrafluoroborate, perchlorate. The selection of supporting electrolytes should take into consideration several points: (i) solubility to the solvent used, (ii) electrochemical stability, (iii) interaction with reaction intermediate, and (iv) relative difficulty of preparation.

A very specific and recent study used a disposable electroactivated PGE (PGE\*) to investigate the electrochemical behavior of the flavonoid naringenin (NGN). In this study, several supporting electrolytes were tested with low pH values. Differential pulse voltammograms recorded at PGE for  $6.00 \times 10^{-5}$  mol/L NGN showed the highest signal of NGN oxidation peak obtained at 0.05 mol/L potassium phthalate monobasic (KHPT) pH 4.0 (Figure 8) [82].

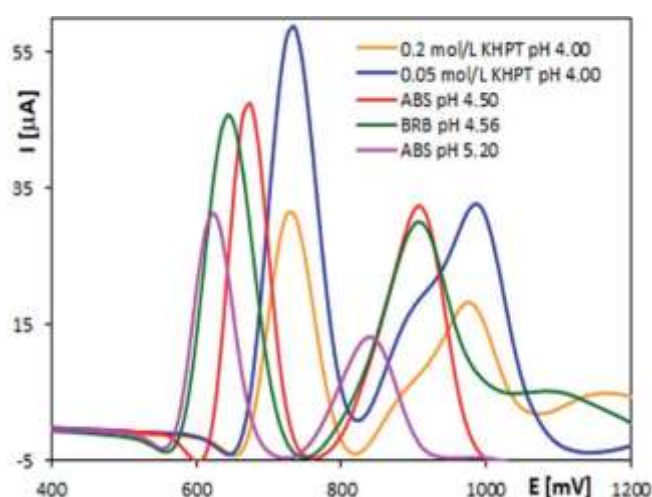


**Figure 8.** Differential pulse voltammograms recorded at PGE\* for  $6.00 \times 10^{-5}$  mol/L NGN in different supporting electrolytes. Reproduced from [82] with the permission of Royal Society of Chemistry. NGN: naringenin, KHPT: potassium phthalate monobasic, ABS: acetate buffer solution, BRB: Britton–Robinson buffer.

Other studies proved several adequate solvent/electrolyte systems, such as : tetra-n-butyl ammonium tetrafluoroborate ( $\text{BF}_4\text{N}$ ) in dichloromethane for electrochemical evaluation of lipophilic antioxidants [118]; or tetrabutylammonium hexafluorophosphate ( $\text{Bu}_4\text{NPF}_6$ ) in oxygen saturated acetonitrile solution [119] using glassy carbon electrode and CV. The combination of these solvents and support electrolyte system was used in different applications. For phenol acids or polyphenols, simple solutions have been used, as following with few examples. A caffeic acid solution in sulfuric acid ( $\text{H}_2\text{SO}_4$ ) was used for voltammetric determination of caffeic acid in red wines, using nitrogen doped carbon/glassy carbon electrode and DPV [120]. A simple phosphate buffer solution was preferred for determination of gallic Acid and total polyphenols in wine samples using carbon paste electrode modified with carbon nanotubes under differential pulse voltammetry conditions [106]. As a last example of diluted sulphuric acid solution as solvent,  $\text{H}_2\text{SO}_4$  in 1:2 (v/v) benzene/ethanol have been used for electrochemical evaluation of tocopherols behaviour, using solid platinum electrodes and pulse voltammetry, cyclic voltammetry and linear sweep voltammetry [74].

Electroanalytical experiments applied for the determination of antioxidants concentrations and/or antioxidant capacity have led to reliable results with a large number of perspectives and suggestions in order to allow researchers improve their studies and better understand the activity of antioxidants and their effects in different media. However, this complementary couple, electrochemistry-antioxidants, also had some limitations, one of which is the lack of specificity.

Given the instability of antioxidants, their high reactivity, their abundance and their structural similarity, it is often difficult to report the results to a specific antioxidant. One solution is a rapidly growing technique, which has yielded very promising results in term of specificity and selectivity, it is molecular imprinting technology. The use of electrode containing molecularly imprinted polymers has improved antioxidant studies and enhanced the selectivity of the results [121,122].

## 4. Molecular imprinting

### 4.1. MIP synthesis and applications

Molecular imprinting technology is a technique that has been attracting the interest of the scientific community for more than 20 years, due to its simplicity, low cost, easy preparation, high selectivity and simplicity, resulting in a great increase in the literature in this field. This technique consists of creating complementary images in terms of structure and chemical functionalities of a target molecule within a synthetic polymer (Figure 9) by creating recognition sites within a polymer with a complementary geometrical and chemical fitting structure, which presents high affinity and selectivity towards the target molecule.

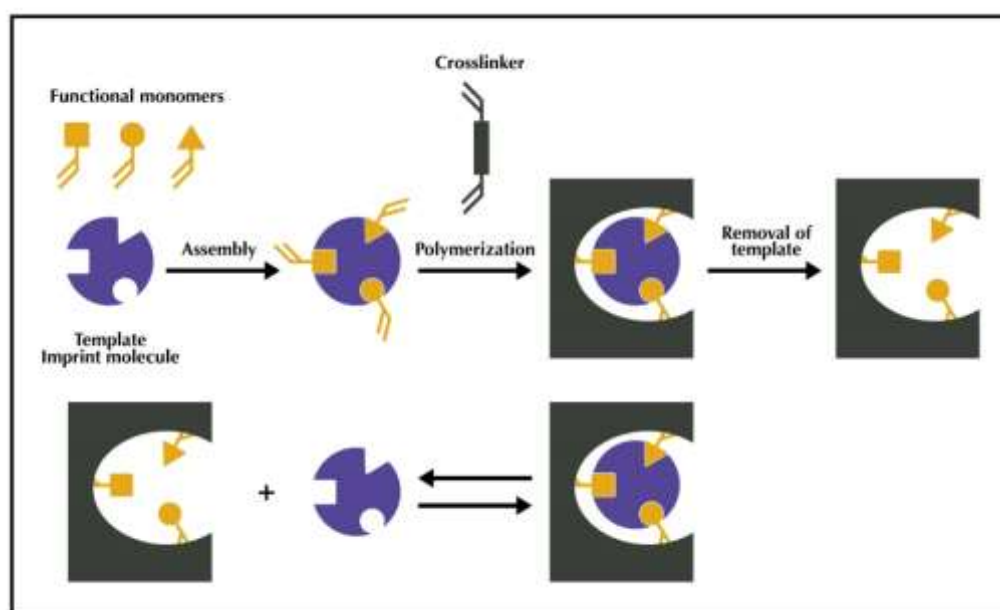


**Figure 9.** General principle of molecular imprinting

The synthesis of MIPs requires the following reagents: (1) the template or target molecule to be imprinted, (2) functional monomers, (3) cross-linking agent, (4) polymerization initiator and (5) porogenic solvent. Several options of each reagent exist, their choice affects the resulting polymer selectivity and depends on their ability to interact with the functional groups of the target molecule, and the synthesis approach used (radical polymerization or sol-gel process).

The main phases of the synthesis process are the following: (1) complexation between functional monomers and template molecules, through different interactions (covalent, semi-covalent, or non-covalent<sup>1</sup>) to form the pre-polymerization complex, (2) polymerization of the pre-polymerization complex with the cross-linkers and initiators under thermal or UV conditions. It involves the bulk, precipitation, suspension, core-shell emulsion, surface imprinting and multi-step polymerizations, and finally, (3) removal of the template which will reveal a well-defined cavity in the polymer characterized by having a complementary structure to that of the target.

A great majority of molecularly imprinted polymers (MIPs) has been synthesized by radical polymerization, they are also called acrylate based MIPs due to the structures of functional monomers that are usually organic. In this type of polymerization, the template molecule chosen should be stable and must not participate in the reaction mechanism or inhibit polymerization. Therefore it is necessary to make sure that it only contains functional groups that are inert during polymerization [123], otherwise it would be necessary to look for alternative printing strategies, such as sol-gel process or the protection of the function responsible for the antioxidant effect. Functional monomers are directly responsible for the structure of the recognition site in the resulting polymer. Some typical monomers are methacrylic acid, acrylic acid, itaconic acid, 2-(trifluoromethyl)acrylic acid, 4-vinylpyridine, acrylamide, methacrylamid, and 2-hydroxyethyl (Figure 10.a). Molecular modelling can be used for the selection of the functional monomer and for the evaluation of the stability of the pre-polymerization complex [124–126]. It can also be used to study the effect of the porogenic solvent on the selectivity of MIPs [127]. Porogenic solvent acts as pore-forming agent and primarily affects the imprinting efficiency, the most frequently used solvents are toluene, dichloromethane, methanol, acetonitrile, etc.). The choice of the solvent depends on the solubility of the chosen reagents [128].

Cross-linkers control the morphology of the polymer, stabilize the binding site and give the polymer its mechanical stability [123]. The most commonly used cross-linkers are divinylbenzene, ethylene glycol dimethacrylate, and trimethylolpropane trimethacrylate

---

<sup>1</sup> Covalent is a term usually used in MIP-synthesis. To be formal in chemistry, “covalent interaction” means chemical reaction et “non-covalent interaction” mean physicochemical interactions such as dipole-dipole interactions. “Semi-covalent interaction” means charge-charge interactions.

(Figure 10.b). In most cases, polymerization is initiated by thermal or UV radiation (radical initiation). Many initiators can be used as a source of radicals during radical polymerization. Generally, initiators of the azo compound (-N=N-) type are used. By the fact that their radical cleavage is easy ( $R_3C-N=N-CR'_3 \rightarrow N_2 + R_3C^\circ + ^\circ CR'_3$ ), producing radical initiator, they are able to initiate a large number of monomers, in particular thermal initiation. The most commonly used is azo bis(isobutyronitrile) or 2,2'-azobis(2-methylpropionitrile) (known by the abbreviation AIBN, fairly soluble in water or toluene and especially very soluble in dichloromethane), mostly used for thermal initiation, and 2,2-dimethoxy-2-phenylacetophenone (DMPAP) is a commonly used photoinitiator (Figure 10.c).

Molecularly imprinted polymers (MIPs) have been developed and applied for several purposes. Initially, they were used to enhance the extraction selectivity of target analytes in solid-phase extraction techniques (SPE), so-called molecularly imprinted SPE (MISPE) as alternatives to immunosorbents (time-consuming and expensive technique) [129,130] and aptamers (availability of a limited number of sequences) [131–133] for their cheap, easy and rapid preparation, high thermal and chemical stability. The first application was carried out by Sellergren in 1994 [134] for the direct extraction of pentamidine, a drug used to treat AIDS-related pneumonia, from diluted human urine samples. MISPE allowed the detection or the clean-up of many target analytes (Sudan I [135], caffeine [136] from food matrices, 17 $\beta$ -estradiol from fishery samples [137], etc.). Moreover, it was recently applied to the trace analysis of pesticides [138,139], industrial contaminants [140,141] and drugs [142,143] from environmental waters, and natural products from food or plants [144–149]. MISPE is usually coupled with high performance liquid chromatography (HPLC) [129,130,150,151], and MIPs can even be integrated and used as the stationary phase in liquid chromatographic columns [150–154], capillary electrophoresis (CE) and electrochromatography (CEC) [155,156]. Then, notable attention has been directed to MIPs for sensing applications, where they are integrated with several transduction platforms in order to create a chemical or biochemical sensor. The adhesion of the MIP on the transducer is a major factor in the sensor response, and it was developed over time. The evaluation of binding properties has advanced from absorbance measurements [157] to HPLC [158]. This approach was firstly used with acoustic [159] and optical transducers [160], then with electrochemical sensors [161].

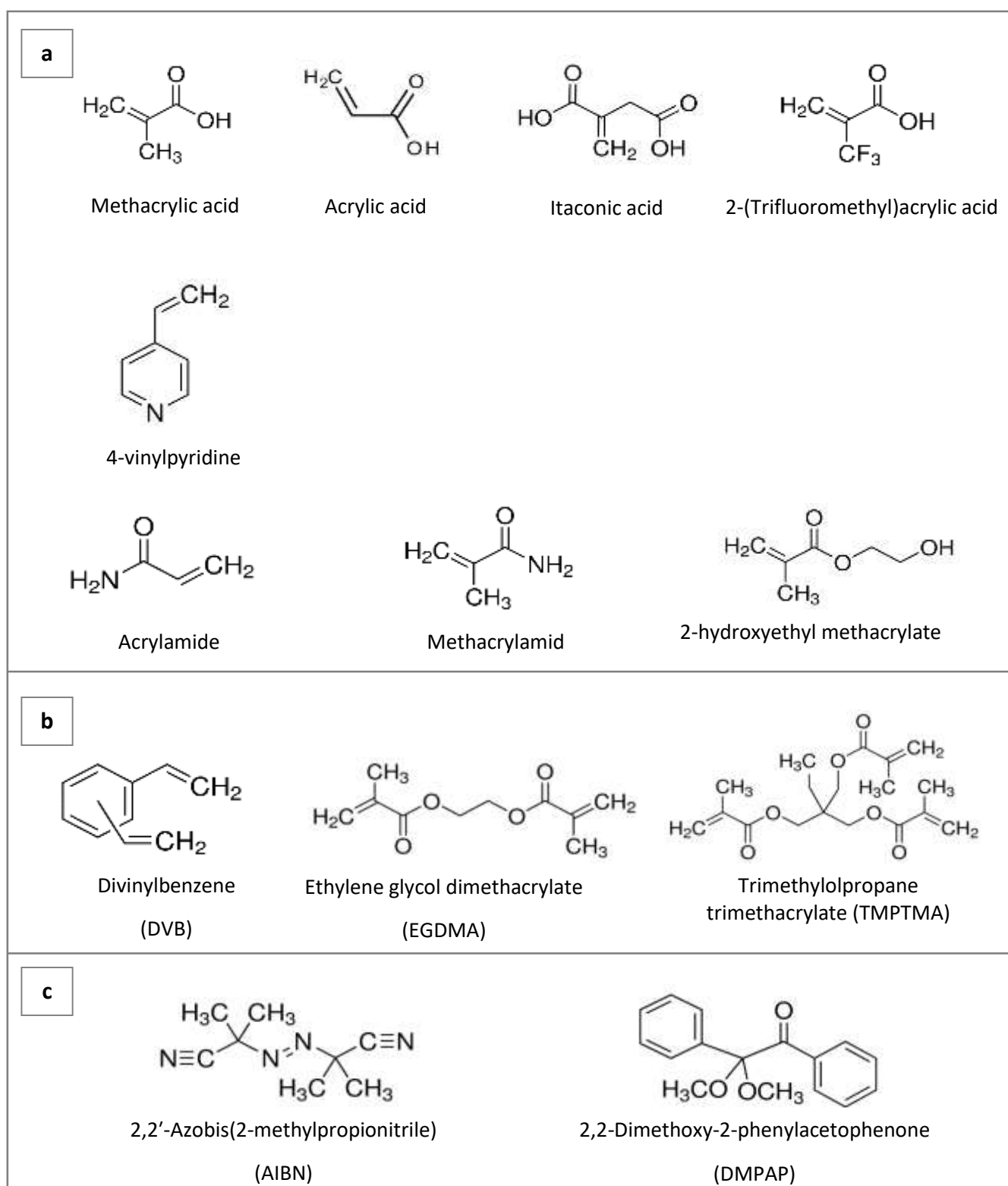


**Figure 10.** Chemical structures of common (a) functional monomers, (b) cross-linkers and (c) initiators used in radical polymerization.

#### 4.2. MIPs-antioxidants

MIPs have allowed a huge number of studies to achieve results that helped researchers to move forward and seek out further perspectives. One of the most important domains is antioxidant detection where a wide range of polymers was developed and designed for their recognition. Several antioxidant components are known for their structural similarity within the same or different families, the fact that made molecular imprinting technique of great interest in order to discriminate them. Some of the applications are listed in Table 3.

Molecular imprinting has even been incorporated into biomedical applications of antioxidants, such as the preparation of a controlled drug delivery device for  $\alpha$ -tocopherol oral supplementation, where polymers were synthesized using methacrylic acid (MAA) as functional monomer and ethylene glycol dimethacrylate (EGDMA) as cross-linker, they showed a sustained drug release capacity in gastrointestinal simulating fluids [162]. The same complex was used in the synthesis of a selective developed for tocopherol recognition, which has proved to be suitable for the separation and extraction of tocopherols from biological media [163].

Some applications require the template to be imprinted in order to recognize a structurally similar molecule. For example, a MIP has been synthesized using quercetin as template, 4-vinylpyridine as functional monomer, and ethylene glycol dimethacrylate as cross-linker and was successfully applied to the clean-up and preconcentration of catechins from several natural samples [164].

Caffeic acid is a very common antioxidant. A molecularly imprinted polymer mono-lithic stationary phase was prepared in the chromatographic column using caffeic acid as template, MAA and EGDMA as functional monomer and cross-linker, respectively, was successfully applied to the separation and purification of chlorogenic acid from *Eucommia ulmodies* leaves by absorbing the impurities that co-existed in the extract [154].

**Table 3.** Some MIPs applications with antioxidants.

Template	Application	Reference
<b>Tocopherols</b>	$\alpha$ -tocopherol delivery in gastrointestinal simulating fluids.	[162]
	Tocopherol recognition	[163]
<b>Quercetin</b>	Pre-concentration and clean-up of catechins	[164]
	Extraction of anthocyanin from mangosteen pericarp	[165]
	Extraction of quercetin and kaempferol from the hydrolyzate of ginkgo leaves	[166]
	Separation of active inhibitors of epidermal growth factor receptor (EGFR) from <i>Caragana Jubata</i>	[167]
	Solid-phase extraction for the sample pretreatment of natural products prior to HPLC analysis	[168]
<b>(+)-Catechin</b>	Extraction of catechins from tea extracts	[169]
	Retention of catechin	[170]
<b>Caffeic acid</b>	Separation and purification of chlorogenic acid	[154]
	Extraction of CA in commercial apple juice samples	[171]
	Selective extraction of polyphenols from olive mill waste waters	[172]
	Extraction of CA from fruits	[173]
	Separation and purification of the antioxidant compounds from mushrooms	[174]
<b><i>p</i>-hydroxybenzoic acid</b>	Selective extraction of polyphenols from olive mill waste waters	[172]
<b>Resveratrol</b>	Selective recognition of resveratrol	[175]

As previously mentioned, one of the essential steps to verify when initiating the synthesis of a MIP is the inert state of the template. However, antioxidants are active compounds susceptible to react with free radicals. To be on the safe side of these issues, a convenient alternative to acrylic-based MIP is the sol-gel molecularly imprinted silicas (MIS) [176–178].

### 4.3. MIS-antioxidants

The sol-gel process is based on two main steps: hydrolysis (acid or basic) and condensation. The most used functional monomers are alkoxy silane molecules, such as (3-Aminopropyl) triethoxysilane (APTES), phenyltrimethoxysilane (PTMOS), N-[3-(Trimethoxysilyl)propyl] aniline (TMSPA), and phenyl trimethoxysilane. A very important point is that the solvent used is a hydro-alcoholic solution, which means that, contrary to the organic solvents used in the synthesis of MIP, it respects the principles of green chemistry. Water:ethanol or water:methanol ratio varies according to the solubility of the template. The most commonly used cross-linker is tetraethoxysilane (TEOS) [177,179–181]. Figure 9 represents a hybrid organic-inorganic printing procedure.

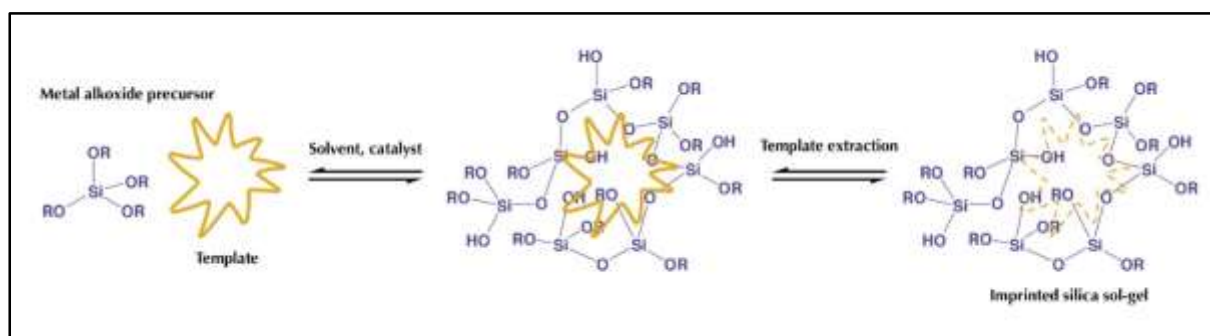


**Figure 11.** Hybrid organic-inorganic printing procedure.

MIS are more specific towards the target species than MIP, and they allow faster diffusion of analytes [177,182]. The silica-based materials allow the use of high temperature for template removal from the polymer network, a step that has always been challenging in MIP synthesis, and they provide products of high thermal and mechanical stability with longer lifetime [181,183]. L. Wang et al. established a comparative study between three different molecularly imprinted polymers for gossypol, which showed that MIP prepared by bulk polymerization had a high adsorption capacity (564 mg/g) but MIS showed faster adsorption kinetics (40 min) [179].

Some of the applications of MIS in analytical and bioanalytical fields are solid-phase extraction of enrofloxacin from fish and chips samples [185], methyl-3-quinoxaline-2-carboxylic acid and quinoxaline-2-carboxylic acid from pork muscle [186], florfenicol from meat samples [187], polar organophosphorus pesticides from almond oil [188], iprodione fungicide from wine

samples [178], methylxanthines natural water and human urine [183], patulin from apple juice samples [189], vitamin D3 from aqueous samples [190], phenobarbital in human plasma [176], solid-phase microextraction of fentanyl [191] and bilirubin [192] from urine and plasma samples, etc.

As for antioxidants, MIS applications are not as extensive as those of MIPs, but they have however achieved satisfactory results. Many studies combined both approaches, they prepared acrylate based MIPs followed by sol-gel process [193]. MIS monolith was developed in SPME for the separation and determination of gallic acid in orange juice samples [194], MIS microspheres were prepared for quercetin recognition [195], MIS mediated by aluminum ions was prepared for SPE of quercetin from Ginkgo biloba L. [196], carbon dots coated with MIS was successfully developed for caffeic acid detection [197], others were prepared for the recognition of caffeine [198,199].

## 5. Electrochemistry, molecular imprinting and antioxidants

Given the importance of electrochemistry, the usefulness of molecular imprinting, and the plethora of research on antioxidants, few studies have combined all three elements.

### 5.1. Electrochemistry and antioxidants

Electrochemistry, especially cyclic voltammetry and differential pulse voltammetry, has been widely used in the detection of antioxidants, using conventional or screen-printed electrodes, with or without surface modification. For example, several studies used modified electrodes for caffeic acid determination in wine samples by electrochemical methods, such as a (poly(3,4-ethylenedioxy)thiophene) modified electrode prepared using water-soluble polyelectrolyte poly(styrene-4-sulfonate) (PEDOT:PSS) [200], a screen printed carbon electrode modified with electrochemically reduced graphene oxide (ERGO/SPCE) [201], a nitrogen doped carbon modified glassy carbon electrode (NDC/GCE). Other nanomaterial based approaches represented valid alternatives to conventional methods for polyphenols analysis (antioxidant capacity evaluation [104,106,202–208], total phenols estimation [209,210], o-diphenol evaluation [211,212], polyphenols studies [213–215], etc.). When compared to pulse techniques, cyclic voltammetry suffer from restricted limits of detection ( $10^{-5}$  M), and therefore from poor sensitivity and selectivity at the analysis of samples rich in different types of antioxidant that are oxidized at potentials greater than 500 mV [216].

### 5.2. Electrochemistry and molecular imprinting

On the other hand, electrochemical biosensors based on molecularly imprinted polymers have been extensively designed for sensing applications of various biomolecules using modified electrodes, such as hormones [217–220], proteins [221–226], antibiotics [227–233], pesticides [234–238], neurotransmitters [239–242], etc.

One of the most challenging steps in the development of these sensors is the polymer deposition on the electrode, especially when screen-printed electrodes are used. Among these methods are dip coating, spin coating, drop casting, etc. [243–246].

In addition, the synthesis can be performed *in situ*, by electropolymerization. It is a fast and straightforward means of obtaining a sensor where polymer films are directly polymerized on the surface of the electrode (Figure 12), by applying a range of potentials to a solution containing the pre-polymerization complex in presence of the template molecule. The most important part of electropolymerization is the optimization of the conditions: choice of the functional monomer, ratio of template to functional monomer concentrations, number of cycles and time of immersion of the sensor in the rebinding solution. The advantages of this approach are the thickness control of the polymer related to the number of cycles applied for the polymerization that influences the sensitivity of the imprinted electrochemical sensor, and the ability to attach the film to electrode surfaces of any shape or size [247–250].

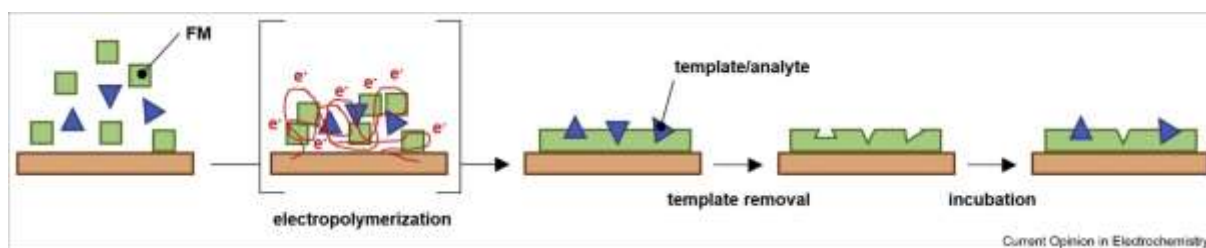


**Figure 12.** The steps of electropolymerization on the surface of the electrode.

Few electrochemical sensors based on molecular imprinting (MIP or MIS) for determination of antioxidants are developed.

A thin-film electrochemical sensor based on MIPs was prepared for diphenylamine detection. For MIP synthesis, MAA was used as functional monomer, trimethylolpropane trimethacrylate (TRIM) as cross-linker, 2,2,4,4-tetraazobis(2-methylpropionitrile) as catalyst and acetonitrile as solvent. Microfabricated gold electrodes were cleaned, electrochemically activated, and well coated with electropolymerized poly(3,4-ethylenedioxythiophene) (PEDOT) membrane. The optimum membrane thickness of about 50 nm. Then, the prepared MIP was immobilized on the surface of the electrodes. Electrochemical responses of three electrodes with PEDOT

membranes, containing the MIP, the NIP, and no particles (blank) have been investigated. Calibration of the three sensors showed that PEDOT/MIP electrodes displayed higher sensitivity compared to the electrodes with PEDOT and PEDOT/NIP (Figure 13). The response characteristics of PEDOT/MIP sensor were a sensitivity of  $1.74 \times 10^{-3} \mu\text{C}/\mu\text{M}$  in a linear range of 4.95–115  $\mu\text{M}$ , a limit of detection of 5.4  $\mu\text{M}$ , and a good selectivity in the presence of structurally similar compounds. The sensor was then applied to the quantification of diphenylamine in spiked apple juice samples [251].

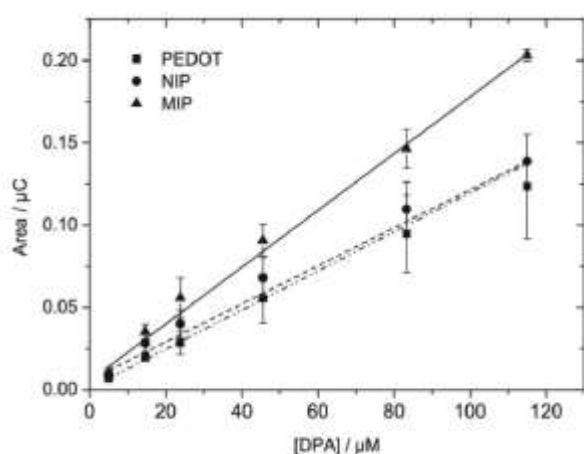


**Figure 13.** Calibration plots for the different sensors: with PEDOT film, with PEDOT/NIP membrane and with PEDOT/MIP membranes. Concentration range of 4.95–115  $\mu\text{M}$  diphenylamine, reproduced from [251] with the permission of Elsevier.

A carbon entrapped molecularly imprinted polymer (CEMIP) electrode, made from scratch, was designed for electrochemical detection of resveratrol in wine using DPV, where carbon was tightly packed in a poly(MAA-co-EGDMA) polymer monolith fritted micropipette tip, then the MIP/NIP pre-polymer solution mixture, consisting of MAA as monomer, EGDMA as cross-linker, 4,40-azobis(4- cyanovaleric acid) (ACVA) as initiator, and acetonitrile as solvent, was infused on the carbon packed micropipette tip. A platinum wire was immersed, and the polymerization was initiated and kept overnight at 70 °C. The polymer was then washed and the CEMIP was exposed for chemical sensing. The CEMIP was 12 times more sensitive for the detection of resveratrol than the carbon entrapped non-imprinted polymer (CENIP). It had a detection limit of 20  $\mu\text{g}/\text{L}$  with good linear standard addition calibrations with  $R^2 = 0.99$  for concentrations between 0.1 and 5  $\text{mg}/\text{L}$ . Compared to the conventional carbon MIP composite

electrode, the CEMIP was found to be more sensitive due to the accessibility of the resveratrol cavities with a more efficient electron transfer due to their thin layer design [252].

An electrochemical sensor using a gold electrode pre-modified with 3-mercaptopropyltrimethoxysilane and based on molecularly imprinted siloxanes was prepared for selective determination of caffeic acid in wines. The MIS film was prepared by sol-gel process, using the acid catalyzed hydrolysis and condensation of tetraethoxysilane (TEOS), phenyltriethoxysilane (PTEOS), and 3-aminopropyltrimethoxysilane (3-APTMS) in presence of caffeic acid as template molecule, then it was immobilized onto the modified electrode surface. DPV for CA oxidation were carried out at different concentrations. According to the author, the sensor was found to be highly selective toward the template, stable and repeatable. The sensor showed a linear current response to the target caffeic acid concentration in the range from 0.500 to 60.0  $\mu\text{mol/L}$ , with a detection limit of 0.15  $\mu\text{mol/L}$  (Figure 14) [253].

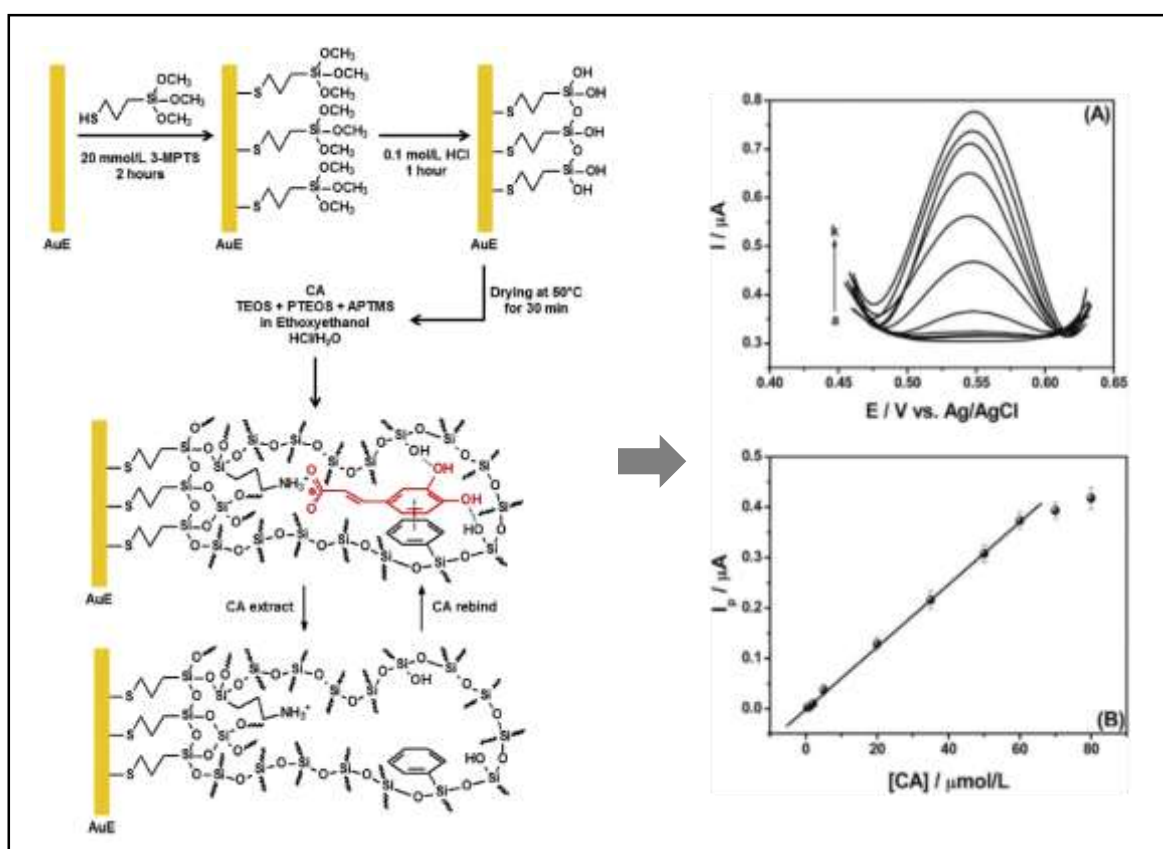


**Figure 14.** On the left: schematic representation of MIS/AuE, reproduced from [253] with the permission of Elsevier. On the right: (A) Differential pulse voltammograms for CA electrooxidation at different concentrations: (a) 0, (b) 0.500, (c) 1.00, (d) 2.00, (e) 5.00, (f) 20.0, (g) 35.0, (h) 50.0, (i) 60.0,

(j) 70.0 and (k) 80.0  $\mu\text{mol/L}$ . (B) Calibration plot,  $I_p/\mu\text{A} = 0.00619 (\pm 1.92 \times 10^{-4}) [\text{CA}]/\mu\text{mol/L} - 0.00125 (\pm 4.36 \times 10^{-4})$ . Incubation time: 25 min. Supporting electrolyte: 0.4 mol/L sulfuric acid. Scan rate: 40 mV/s. Potential pulse amplitude: 70 mV, reproduced from [253] with the permission of Elsevier.

3-MPTS: (3-mercaptopropyl)trimethoxysilane, CA: caffeic acid, TEOS: tetraethoxysilane, PTEOS: phenyltriethoxysilane, APTMS: aminopropyltrimethoxysilane.

A glassy carbon electrode modified with multiwall carbon nanotubes/vinyltrimethoxysilane recovered by siloxane film was developed for caffeine determination using DPV. Figure 15 shows a linear anodic peak current for caffeine concentration from 0.75 to 40  $\mu\text{mol/L}$  with high selectivity and sensitivity. The linear regression equation was  $\Delta I/\mu\text{A} = 0.39 (\pm 0.04) + 0.07 (\pm 0.002) [\text{caffeine}]/\mu\text{mol/L}$ ,  $R^2 = 0.998$ . The detection limit was estimated to be 0.22  $\mu\text{mol/L}$  [254].

A molecularly imprinted electrochemical sensor based on polypyrrole (PPy) decorated with black phosphorene quantum dots (BPQDs) was prepared by electropolymerization onto poly 3,4 ethylenedioxythiophene (PEDOTNRs) for voltametric sensing of vitamin C. The peak currents recorded by DPV showed a linear proportionality on vitamin C concentrations ranging from 0.01 to 4 mM with a detection limit of 0.0033 mM (Figure 16). The prepared sensor demonstrated a good reproducibility, repeatability, stability, and selectivity for the electrochemical analysis of vitamin C [250].

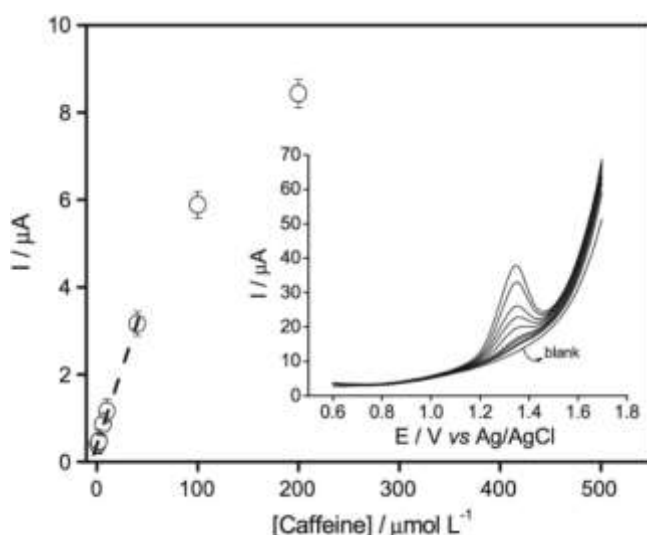


**Figure 15.** Current response (DPV) of the modified electrode recovered by siloxane film. Supporting electrolyte: 0.15 mol/L phosphoric acid. Incubation time: 15 min. DPV at 0.02 V/s. Reproduced from [254] with the permission of Elsevier.

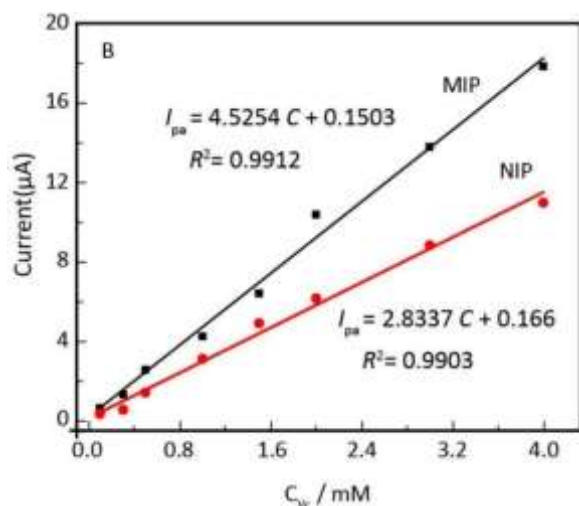


**Figure 16.** Linear relationship between anodic peak currents and the concentration of vitamin C ( $V_c$ ) for MIPs electrode and NIPs electrode, reproduced from [239] with the permission of Elsevier.

Furthermore, a glassy carbon electrode was modified with molecularly imprinted polypyrrole-graphene-multiwalled carbon nanotubes composite film and used for rutin sensing (Figure 17.a) and showed a proper increase of the peak current with increasing rutin concentrations (Figure 17.b,c) where a linear relationship in the range of 0.01–1.0  $\mu\text{mol/L}$  with a regression equation of  $I_p(\mu\text{A}) = 26.18.C(\mu\text{mol/L}) + 0.6308$  ( $R^2=0.997$ ) was obtained [255].

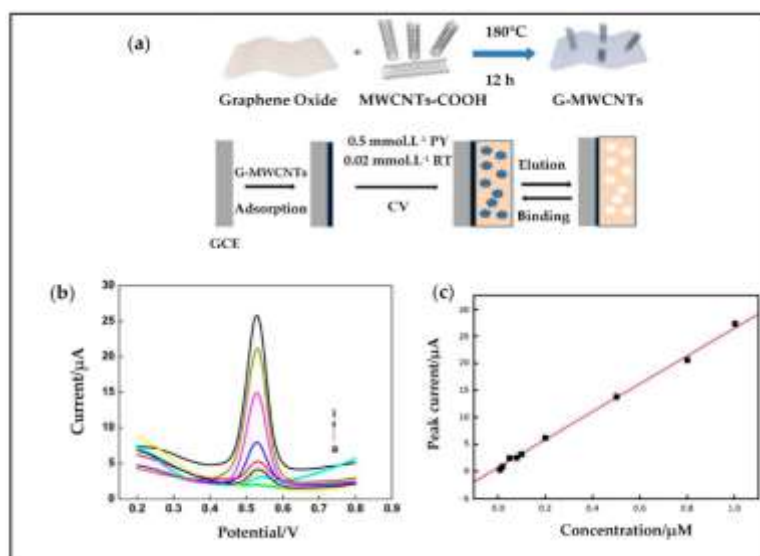


**Figure 17.** (a) Schematic construction of the MIP/G-MWCNTs/GCE electrode, G-MWCNTs: graphene-multiwall carbon nanotubes, GCE: glassy carbon electrode, PY: pyrrole, RT: rutin; (b) variation of DPVs with RT concentration; (c) linear relationship between peak current and RT concentration, reproduced from [255] with the permission of Elsevier.

A glassy carbon electrode was modified with molecularly imprinted polymer based on polypyrrole incorporated graphene oxide for electrochemical determination of quercetin. Once the graphene oxide/glassy carbon was fabricated, an electropolymerization was carried out in a solution containing pyrrole, quercetin, and H<sub>2</sub>SO<sub>4</sub>. Cyclic voltammetric experiments were performed on the modified electrode and oxidation peak current of quercetin was regressed with the concentration in the range from 6.0x10<sup>-7</sup> to 1.5x10<sup>-5</sup> mol/L (R<sup>2</sup> = 0.997) with a detection limit of 4.8x10<sup>-8</sup> mol/L. This electrode showed good stability and reproducibility [256].

Although we are actually more interested in natural antioxidants, an electrochemical sensor was prepared for tert-butylhydroquinone (TBHQ) recognition, a synthetic phenolic antioxidant that is extensively applied in food samples for its chemical stability, low cost, and availability; TBHQ-imprinted core-shell nanoparticles (TICSNs). TICSNs were fabricated in several steps. Silica spheres were synthesized and modified by (3-chloropropyl) trimethoxysilane then by polyethylenimine, and polymerized to form the TICNs and polymerized to form the TICSNs with ethylene glycol dimethacrylate as the cross-linker. The resulting sensor was highly specific and selective. The linear range of the calibration curve was 0.1–50.0 mg/kg with the detection limit of 0.27 mg/kg [257].

In addition, a modified carbon paste electrode (CPE) was designed based on magnetic functionalized molecularly imprinted polymer (MMIP) nanostructure for selective determination of rosmarinic acid (RA) in some plant extracts (*Salvia officinalis*, *Zataria multiflora*, *Mentha longifolia*, and *Rosmarinus officinalis*). The synthesis of MMIP was performed in four steps: (1) Iron oxide magnetite nanoparticles (Fe<sub>3</sub>O<sub>4</sub> MNPs) were synthesized; (2) silica functionalized Fe<sub>3</sub>O<sub>4</sub> MNPs (Fe<sub>3</sub>O<sub>4</sub>@SiO<sub>2</sub>) were synthesized and collected by a magnet, then washed and dried; (3) the surface of Fe<sub>3</sub>O<sub>4</sub>@SiO<sub>2</sub> sample was modified using 3-amino propyltriethoxysilane (APTES); and (4) magnetic Fe<sub>3</sub>O<sub>4</sub>@SiO<sub>2</sub>@NH<sub>2</sub> decorated with MIP was synthesized by surface polymerization. The CPE was modified with MMIP by mixing graphite powder, MMIP, and paraffin oil. All the steps are provided in Figure 17. The electrode behavior was studied with CV and DPV techniques. Two linear concentration ranges (0.1–100 μM and 100–500 μM) with a low detection limit (0.085 μM), and a good

precision were obtained. The modified sensor showed good sensitivity and selectivity for the rosmarinic acid in the presence of other compounds (Figure 18) [258].

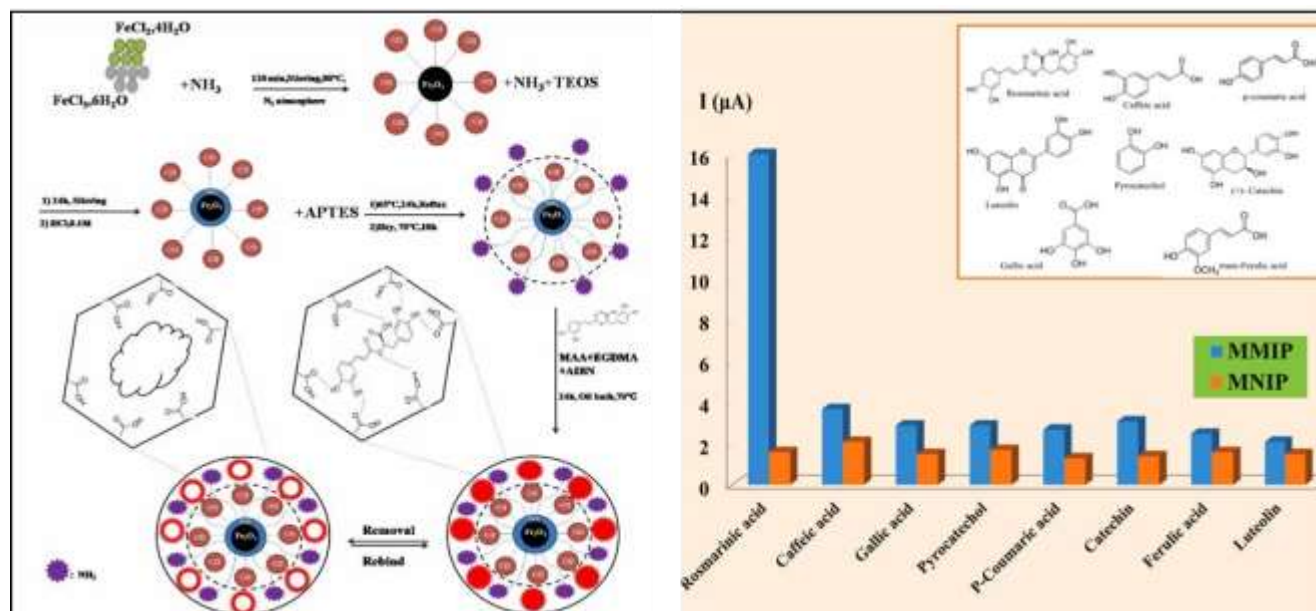


**Figure 18.** On the left: schematic representation of the applied approach for preparation of RA-MMIP, reproduced from [258] with the permission of Elsevier. On the right: Effect of other compounds on electrochemical determination of RA using MIP-CPE and NIP-CPE [258].

## 6. Conclusions

Given the major importance of antioxidants in the food industry, it would be always interesting to improve the evaluation methods of their content and their radical scavenging capacity.

While it is true that numerous techniques exist and have recently evolved, it should be noted that most of the classical methods suffer from a lack of selectivity, and among them methods that are time consuming and costly, others require large volumes of solvents. Consequently, it would be necessary to develop a method that is fast, inexpensive and has a good selectivity towards the desired compound. Therefore, to extend the applications some strategies combine molecular imprinting with analytical methods, for example electrochemistry using MIP or MIS, with electrochemistry, for the determination of antioxidants. This combination could lead to the development of an electrochemical sensor, consisting of an electrode on which a specific polymer will be deposited or directly synthesized on its surface, taking into consideration every critical step during the procedure, such as the choice of reagents for polymer synthesis, the synthesis methods, electrochemical methods and equipment, the choice of electrode, its modification, polymer deposition on the electrode, etc. Given the advantages of both methods, this sensor could be very promising especially with the growing importance accorded to imprinted polymers with antioxidants, helping researchers and manufacturers to identify and detect one antioxidant at a time or a family of antioxidants, with high selectivity and specificity compared to other techniques, in different media. Wine for example, which is known to be very rich in antioxidants, or even olive oil, fruit juices, and many other food or cosmetic products, where this sensor would be useful to identify the type and amount of antioxidants present in these products.

**Part II**  
**Materials and Methods**

The series of experiments performed are divided into two main categories based on the strategy of incorporation of the MIP: *ex-situ* polymerization where the synthesis of the polymer is done separately from the electrode and *in-situ* polymerization or electropolymerization where the polymer is directly synthesized on the surface of the electrode.

### ❖ *Ex-situ* polymerization

Decoupling the synthesis from the electrode facilitates the optimization of the synthesis parameters before proceeding to the application of the polymers, it makes the morphological characterization of the polymers simpler, and even allows the addition of materials that could enhance the electrochemical signal [259]. The following experiments consist on the synthesis of a polymer using radical polymerization with the precipitation approach under thermal conditions, and its application in model and real wine. Based on the results, an optimization of the synthesis was done to improve the performance of the polymers in terms of specificity and then the optimal polymer chosen between several others was applied in the same way as the first one.

## 1. Parameters of the synthesis of the imprinted (MIP) and non-imprinted (NIP) polymers

### 1.1. Choice of the template

Caffeic acid was chosen to be the target molecule for multiple reasons. During wine aging, several compounds can be considered as markers of aging and can provide an idea of the quality of the wine. The content of caffeic acid increases during aging, it is mainly due to the hydrolysis of cafeoyl tartaric acid, known as caftaric acid (ester of caffeic acid formed with tartaric acid), which generates caffeic acid in the medium [260–264].

In addition to this, caffeic acid is a very common polyphenol, known for its antioxidant, inflammatory, anti-AIDS and anticarcinogenic activity. It belongs to the class of phenolic acids, specifically hydroxycinnamic acids. It is widespread in plants and foods such as rosemary, fruits such wild blueberries, blackcurrant, artichokes, black beans, but also coproducts of already prepared plants and fruits such as potatoes peels or fruits peels that can be valorized by antioxidant extraction, and drinks such as ginko infusion, tea, wine etc. [265,266].

## 1.2. CA-MIP vs DMCA-MIP: molecularly imprinted polymer for caffeic acid and for 3,4-dimethoxycinnamic acid

A very important condition for the choice of the template is that it must be appropriate for radical polymerization and must not participate in the reaction mechanism or inhibit the polymerization. Since caffeic acid has hydroxyl functional groups (OH), it was important to verify this hypothesis.

For this purpose, two polymerizations have been proposed, a molecularly imprinted polymer for caffeic acid (CA-MIP), and another one for 3,4-dimethoxycinnamic acid (DMCA-MIP). DMCA is a molecule with a similar structure to caffeic acid but in which the hydroxyl groups (R-OH) are methylated (R-O-CH<sub>3</sub>) (Figure 19). Several syntheses were done in order to determine adequate reagents for the polymerization of CA-MIP and DMCA-MIP. First, the templates should be soluble in the solvent. Secondly, MIP and NIP should polymerize, and that is why we needed several trials of polymerizations (

Table 4).

To demonstrate that caffeic acid does not participate in free radical polymerization, it was necessary that the two compounds were extracted in the same way from their polymer. The washing was verified by HPLC-UV. In our case, both compounds were similarly washed (figure S1), and this shows that caffeic acid is a convenient template for the next experiments.

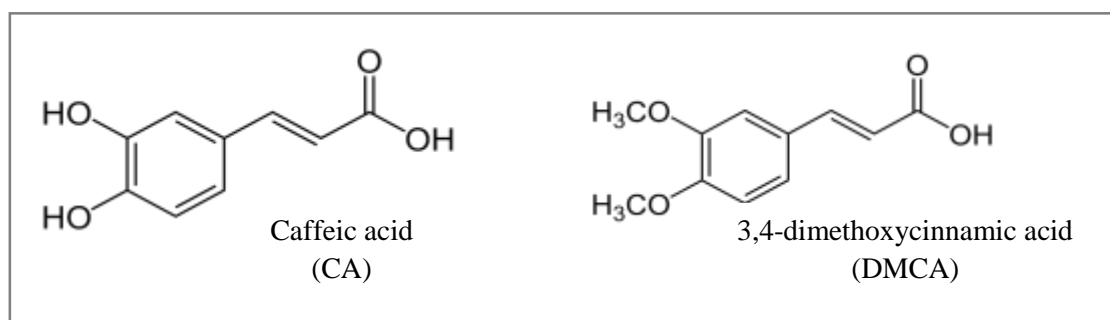


**Figure 19.** Chemical structures of caffeic acid (CA) and 3,4-dimethoxycinnamic acid (DMCA).

**Table 4.** List of synthesis trials of CA-MIP, DMCA-MIP and NIP.

FM: functional monomer, CL: cross-linker, I: initiator, pol: polymerization, CA: caffeic acid, DMCA: 3,4-dimethoxycinnamic acid, ACN: acetonitrile, MeOH: methanol, DM: dichloromethane, 4-VP: 4-vinylpyridine, N-PAA: N-phenylacrylamide, EGDMA: ethylene glycol dimethacrylate, DMPAP: 2,2-dimethoxy-2-phenylacetophenone, AIBN: azobisisobutyronitrile.

Polymer	Solvent(s)	Template	FM	CL	I	Molar ratio	Type of radical initiation
CA-MIP1	ACN	CA	X	X	X	X	X
CA-MIP2	ACN/MeOH; 3:1, 30ml	CA	4-VP	EGDMA	DMPAP	1:2:6	UV
<b>DMCA-MIP</b>	ACN/MeOH; 3:1, 30ml	DMCA	4-VP	EGDMA	DMPAP	1:2:6	UV
<b>NIP1</b>	ACN/MeOH; 3:1, 30ml	X	4-VP	EGDMA 2%	DMPAP	2:6	UV
<b>NIP2</b>	ACN/MeOH; 3:1, 30ml	X	N-PAA	EGDMA	DMPAP	2:6	UV
<b>NIP3</b>	ACN/toluene; 3:1, 30ml	X	4-VP	EGDMA	DMPAP	2:6	UV
<b>NIP4</b>	ACN/MeOH; 4:1, 30ml	X	4-VP	EGDMA	DMPAP	2:6	UV
<b>NIP5</b>	ACN/ toluene; 3:1, 75ml	X	4-VP	EGDMA	AIBN	4:20	thermal, 60°C
<b>NIP6</b>	ACN/MeOH; 4:1, 75ml	X	4-VP	EGDMA	AIBN	4:20	thermal, 60°C
<b>NIP7</b>	DM, 30ml	X	4-VP	EGDMA	DMPAP	2:6	UV
<b>NIP8</b>	DM, 75ml	X	4-VP	EGDMA	AIBN	4:20	thermal, 40°C
<b>NIP9</b>	ACN/toluene 3:1, 75ml	X	N-PAA	EGDMA	DMPAP	4:20	UV
<b>NIP10</b>	ACN/toluene 3:1, 75ml	X	N-PAA	EGDMA	AIBN	4:20	thermal, 60°C
<b>NIP11</b>	ACN/MeOH 4:1, 75ml	X	N-PAA	EGDMA	AIBN	4:20	thermal, 60°C

### 1.3. Choice of the reagents

#### 1.3.1. Synthesis of the first polymer

As shown in Table S2, and after several trials, the best selection of reagents for CA-MIP1 and NIP1 included:

- Acetonitrile-methanol mixture, ACN/MeOH 4:1, as solvents,
- N-phenylacrylamide (N-PAA) as functional monomer,
- Ethylene glycol dimethacrylate (EGDMA) as cross-linker,
- Azobisisobutyronitrile (AIBN) as an initiator with a thermal polymerization at 60°C.

The choice of the functional monomer has a major importance regarding the resultant selectivity of the MIP. The ideal monomer should develop strong interactions with the template. N-PAA was proposed among the series of experiments because of the possible interactions that can be made with CA, whether hydrogen bonds or  $\pi$ - $\pi$  stacking at the aromatic rings. The cross-linking is ensured by the EGDMA, and the initiation of the reaction was carried out thermally by placing the mixture (T, FM, CL) added with AIBN as initiator, in the incubator at 60°C for 24 hours. Under the effect of heat, AIBN decomposes and generates two radical compounds (Figure 20).

The alkyl radicals produced initiate the polymerization of monomers. This polymerization in presence of a template allows the synthesis of a specific MIP.

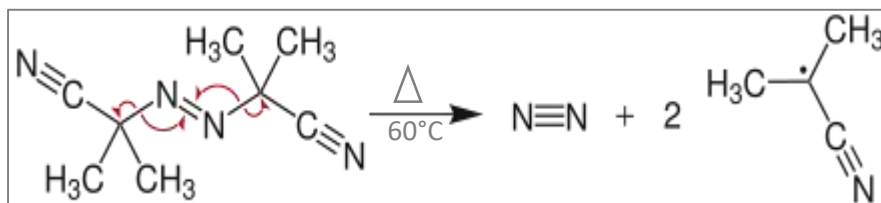


**Figure 20.** Thermal decomposition of AIBN and initiation of radical polymerization

### 1.3.2. Optimization of the synthesis

The application of the CA-MIP1 and NIP1 brought us to optimize the synthesis in order to improve the specificity and the performance of the polymers. The main objective was to increase the difference between the CA-MIP and NIP regarding their rebinding properties.

A series of synthesis was done by changing one parameter at a time. The parameters that were varied were:

- Functional monomer:

N-PAA and methacrylic acid (MAA) were used. MAA was suggested because of its extensive applications in radical polymerization experiments. Its structure gives an idea about its ability to form strong electrostatic interactions with CA. Figure 21 shows the chemical structures of both functional monomers.

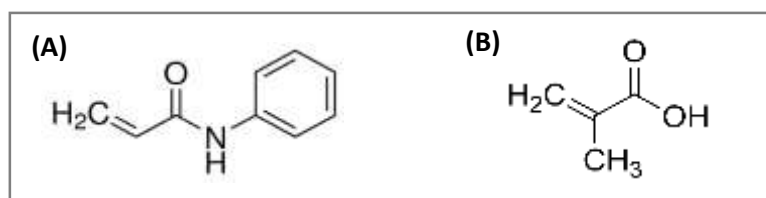


**Figure 21.** Functional monomers: N-phenylacrylamide (A) and methacrylic acid (B).

- Method of polymerization initiation

Thermal (24h, 60°C), with AIBN as initiator and UV irradiation (24h, 365nm), with DMPAP as initiator were applied.

Thermal heating is a widely used conventional technique to prepare MIPs and MIP composites; it is simple and does not require advanced instrumentation. However, the main drawback of this technique is related to the heterogeneity of binding sites due to conformational entropy gains caused by the increase of the internal energy of the system that affects the monomer-template complex formed during the self-assembly step [267].

UV irradiation requires simple equipment and is eco-friendly. It was shown that the imprinting process is more efficient at lower temperatures; it increases the concentration of the monomer-template complexes formed prior and during polymerization and therefore, increases the number of specific binding sites in the cavity after removing the template. A major disadvantage of this process is the non-uniform transfer and low penetration of light during polymerization [267].

- Solvent

Several solvents were used, simple and mixtures: acetonitrile, toluene, acetonitrile/toluene (80/20 v/v), and acetonitrile/methanol (80/20, v/v). The choice of the solvent is also important because the solubility of the reagents must be taken into account.

- The list of syntheses without adding the templates without adding the template.

Table 5 represents the several mixtures prepared for each couple, in order to choose the optimal polymer at the end. NIPs are synthesized with the same reagents without adding the template.

**Table 5.** Synthesis of 11 couples of CA-MIP/NIP

MIP: molecularly imprinted polymer, NIP: non imprinted polymer, T: template, FM: functional monomer, CL: cross-linker, I: initiator, S: solvent, CA: caffeic acid, N-PAA: N-phenylacrylamide, EGDMA: ethylene glycol dimethacrylate, AIBN: azobisisobutyronitrile, DMPAP: 2,2-dimethoxy-2-phenylacetophenone, ACN: acetonitrile. UV at 365 nm for 24 hours, thermal at 60°C for 24 hours.

CA-MIP/NIP	T	FM	CL	I	S (80/20)	Method of radical initiation
1	CA	N-PAA	EGDMA	AIBN	ACN/MeOH	Thermal
2	CA	N-PAA	EGDMA	DMPAP	ACN/MeOH	UV
3	CA	N-PAA	EGDMA	DMPAP	ACN/Toluene	UV
4	CA	N-PAA	EGDMA	AIBN	ACN/Toluene	Thermal
5	CA	MAA	EGDMA	AIBN	ACN/MeOH	Thermal
6	CA	MAA	EGDMA	DMPAP	ACN/MeOH	UV
7	CA	MAA	EGDMA	AIBN	ACN/Toluene	Thermal
8	CA	MAA	EGDMA	DMPAP	ACN/Toluene	UV
9	CA	N-PAA	EGDMA	AIBN	ACN	Thermal
10	CA	N-PAA	EGDMA	AIBN	Toluene	Thermal
11	CA	MAA	EGDMA	AIBN	Toluene	Thermal

After all the rebinding tests done with these associations, CA-MIP6/NIP6 was chosen as optimal polymer for the following experiments.

## 2. Synthesis of two selected caffeic acid imprinted polymers (CA-MIP) and corresponding non-imprinted polymer (NIP)

For CA-MIP1/NIP1, the synthesis was done using the molar ratio 1/4/20 CA/N-PAA/EGDMA with 0.09 g of CA for 50 mL of solvent ACN/MeOH 80/20 v/v. The reagents were progressively added while stirring the mixture with a bar and a magnetic stirrer. After ultrasonic degassing for 10 min, and nitrogen degassing for 15min, the flasks were placed in the incubator (60°C) for 24 hours. The obtained polymers are left at room temperature for about an hour to cool down before proceeding with the template removal.

For CA-MIP6/NIP6, the synthesis was done using the molar ratio 1/4/20 CA/MAA/EGDMA with 0.06 g of CA for 33.3 mL of solvent ACN/MeOH 80/20 v/v. The reagents were progressively added, while stirring the mixture with a bar and a magnetic stirrer then transferred into tubes of 17 mm internal diameter and 50 mL volume, and then exposed in front of a UV lamp at 10 cm away for 24 hours.

### 2.1. Template removal

Several washing steps were done in order to extract all the caffeic acid from the cavities.

As a washing solution, a mixture of ethanol/acetic acid 90/10 v/v was prepared using the following ratio: EtOH/Ac 90/10 v/v. The presence of the acid accelerates the extraction due to the competition by acetic acid and CA, but at the end, it was followed by at least three washes with pure ethanol to remove the acetic acid. Although NIP does not contain templates, they were also washed to stay in the same experimental conditions.

Before proceeding with the washing, the polymers and their solvents were transferred into centrifuge tubes. They were first centrifuged for 10 min, at 20°C and 11,872 g to separate the polymer from the solvent. Then, the supernatant was removed and 10 mL of washing solution was added into the tubes, followed by a 10 min agitation, 10 min of ultrasonication and finally centrifugation. The first supernatant was diluted 10 times in a graduated flask, filtered, and injected in HPLC-UV, in order to verify the decrease of the CA peak. This cycle of washing, centrifugation and HPLC-UV injection was repeated until total disappearance of CA peak. Once the template was totally removed, the supernatant was also removed and the polymers

were transferred into flasks and placed in the incubator at 60°C, for one night, until dry. Then, polymers are ground into homogeneous powder in a mortar.

## 2.2. Effect of pH on electrochemical detection of CA in a hydro-alcoholic medium

The electrochemical technique used in these experiments is voltammetry. All the measurements were carried out using a portable  $\mu$ Stat-I 400 potentiostat and screen-printed carbon electrodes.

The analyses were performed between -0.4 and +0.8 V, at a scan rate of 50 mV/s. Three scans were applied for each sample.

In order to choose the adequate pH, two calibration curves were constructed over the range of 0.06 mM to 2.78 mM of caffeic acid, meaning 10.8 mg/L and 500.8 mg/L. Six standards were prepared in a mixture phosphate buffer saline and ethanol: PBS 0.05M/EtOH 90/10, v/v, at pH 3 and pH 7. Then, cyclic voltammetric measurements were applied.

## 3. Application of the CA-MIP/NIP in a hydro-alcoholic medium

The following experiments were applied with CA-MIP1/NIP1 and CA-MIP6/NIP6

### 3.1. Rebinding properties

Rebinding experiments were done following the same technique; the steps are presented in Figure 22.

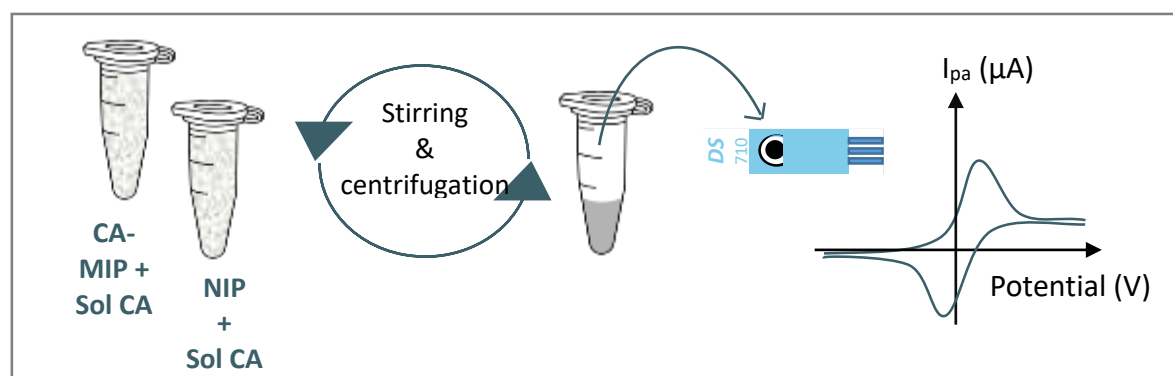


**Figure 22.** Rebinding experiment steps. CA-MIP: molecularly imprinted polymer for caffeic acid, NIP: non-imprinted polymer, Sol CA: caffeic acid solution,  $I_{pa}$ : anodic peak current

In the Eppendorf tubes, 1 mL of PBS/EtOH containing 1.11 mM of caffeic acid solution were added to the polymer with a variation of the polymer mass. For CA-MIP1/NIP1, this experiment was tested at pH 3 and pH 7 in the presence of 10 mg and 50 mg of polymers, in order to confirm

the choice of our experimental pH. The Eppendorf tubes were stirred for 2 hours, followed by centrifugation at 10,640 *g* for 10 min, then the supernatant was deposited on the surface of the electrode by drop-casting and the electrochemical measurements were initiated. In our case, pH 3 was chosen for the following experiments.

The time of stirring was chosen based on a kinetic study in which the rebinding properties of one sample were tested at various times of stirring, ranging from 5 min. to 4 hours.

### 3.2. Behavior of the polymers in the presence of interferents

The rebinding properties of the polymers were also tested when applied not only with caffeic acid, but with other interferents with close chemical structures to caffeic acid, such as ferulic acid, sinapic acid, gallic acid and *p*-coumaric acid. This experiment determines the selectivity of the polymer towards its template.

10 mg of polymer were added to 1 mL of PBS/EtOH containing 0.55 mM of each compound. The samples were then stirred and centrifuged, and the supernatants were deposited on the SPCE and CV measurements were applied.

## 4. Morphological characterization techniques

### 4.1. Fourier transform infrared spectroscopy (FTIR)

FTIR spectrophotometry is a widely used analytical technique for the spectrometric identification of organic compounds, often in combination with other techniques such as UV-Visible spectrometry, nuclear magnetic resonance and mass spectrometry. Its main applications include quality control of raw materials, intermediates and finished products. Although this type of spectrometry is mainly used for qualitative analysis, several quantitative applications are beginning to emerge. The infrared (IR) range extends from 0.78 to 1000  $\mu\text{m}$ , and is itself subdivided into three regions:

- the near IR: from 0.77 to 2.5  $\mu\text{m}$ , mainly exploited for the quantitative analysis of food products;
- the mid IR from 2.5 to 50  $\mu\text{m}$  (or 4000 to 200  $\text{cm}^{-1}$ ), mainly for organic qualitative analysis as well as for structure determination;
- and the far IR from 50 to 1000  $\mu\text{m}$  particularly useful for the study of inorganic species.

In mid-infrared spectroscopy (MIR), IR radiation is not energetic enough to induce electronic transitions; it can only affect the different vibrational and rotational energy levels. When IR radiation encounters this molecule, the photon field of the wave can interact with the molecule and cause a change in the amplitude of one of these motions and therefore the absorption of the wave.

The infrared spectra of our samples were plotted on the Perkin Elmer spectrum 65 FT-IR spectrometer. Acquisitions were performed over a wavelength range from 4000  $\text{cm}^{-1}$  to 600  $\text{cm}^{-1}$ . The resolution was 4  $\text{cm}^{-1}$  and the number of accumulations for each experiment was 64.

#### **4.2. BET surface area analysis**

When synthesizing solid materials such as polymers (MIPs and NIPs), volumetric analyses are interesting. They allow sometimes to establish a relation between the binding properties of the target molecule and the structure of the polymers.

BET analysis was performed on our polymers by nitrogen adsorption-desorption at a temperature of 77 K using an ASAP 2020 instrument. Prior to analysis, 50 mg of sample were outgassed for 14 h at room temperature.

#### **4.3. Scanning Electron Microscope (SEM)**

The surface morphological characterization was evaluated with SEM. This technique generates high-resolution images of the shapes of the objects and shows the spatial variations by using a focused beam of electrons.

SEM was applied to our polymers using a Zeiss Gemini SEM 500 apparatus. A SE2 Everhart-Thornley was used as a detector.

### **5. Applications of the polymers in wine**

#### **5.1. Preparation of wine samples and electrochemical analysis**

A Burgundy red wine (Pinot Noir, 2018) was purchased at a local supermarket in order to apply the tests. The wine was diluted 10 times in a PBS 0.05 M (pH3)/EtOH (90/10, v/v) solution and

then spiked with caffeic acid at different concentrations. A calibration curve was constructed over the range 0.06 mM to 1.67 mM of caffeic acid in the diluted wine.

### 5.2. Rebinding properties in wine

The rebinding properties are done following the same procedure used in hydro-alcoholic medium (paragraph 4). 10 mg of CA-MIP or NIP were added to 1 mL of the diluted and spiked wine. Analytical recovery experiments were also performed after spiking four different samples with 0.17, 0.22, 0.28 and 0.42 mM of caffeic acid. Voltammograms were extracted in order to determine the rebinding properties and the efficiency of the method in our real matrix.

### 5.3. HPLC determination of CA in wine samples

HPLC-UV was used as a reference method to validate the results obtained with electrochemistry. A C18-column on a Shimadzu LC equipped with a UV visible absorbance detector were used. The determination was performed using a gradient of two solvents: (solvent A 0.1 % v/v acetic acid in water, solvent B 0.1 % v/v acetic acid in acetonitrile) 7.5 % of B from 0 to 8 min, 95 % from 8 to 10 min and 7.5 % from 10 to 12 min. Flow rate was 1.0 mL.min<sup>-1</sup> and detection was performed at 325 nm.

For this experiment, the same supernatant that was drop casted on the surface of the electrode, was filtrated and injected in HPLC-UV. The recovery was then calculated in order to compare both techniques.

### ❖ *In-situ* polymerization: electropolymerization

Electropolymerization is carried out on the surface of the electrode, and it is a process that can be observed on the computer screen. Besides how fast and simple it is, it holds an amazing advantage in terms of controlling the thickness of the polymer by managing the administered current.

The main difficulties of this process are the choice of the functional monomer, optimization of the conditions (monomer to template concentration ratio, number of cycles, rebinding time), template removal, selectivity and specificity. Once these difficulties are overcome, the sensor may succeed.

## 1. Choice of the functional monomer (FM): molecular simulation

The prepolymerization mixtures (caffeic acid - functional monomers) were simulated at pH 3 and pH 7 by molecular dynamics in order to choose the functional monomer forming the most stable interaction with caffeic acid. These mixtures are composed of caffeic acid and 10 functional monomers among the most used in the literature (4-aminobenzoic acid, o-phenylenediamine, p-phenylenediamine, pyrrole, thiophene, aniline, phenol, carbazole, scopoletin, and mercaptobenzimidazole). These 10 functional monomers were previously selected by examining their structure, which suggests that they are likely to interact favorably, non-covalently, with caffeic acid. To conduct this study, the program GROMACS [268,269] was used with the OPLS-AA force field parameters [270,271] to represent caffeic acid, functional monomers, and ethanol. These parameters were automatically generated by the LigParGen server [272], available at <http://zarbi.chem.yale.edu/ligpargen/>. No further optimization of these parameters was performed. Water molecules were represented by the TIP4P/2005 model [273]. The LINCS algorithm [274] was used to fix the length of all bonds involving a hydrogen atom and the equations of motion were integrated with the Verlet leapfrog algorithm using a time step of 2 fs. The van der Waals interaction forces were cancelled by a "switch" function between 10 and 12 Å (the energy of the van der Waals forces is represented by a Lennard-Jones potential  $V_{LJ} = 4\varepsilon \left[ \left(\frac{\sigma}{r}\right)^{12} - \left(\frac{\sigma}{r}\right)^6 \right]$ , where  $\varepsilon$  is the minimum energy of the potential,  $\sigma$  is the distance for which the potential is 0, and  $r$  represents the interatomic distance; if  $r > \sigma$ , the energy of the van der Waals forces is proportional to the inverse of the interatomic distance to the power of 6. The Lorentz - Berthelot mixing rules were used to define the crossed van der Waals interactions. The "particle mesh Ewald" method [275] was considered to calculate the electrostatic interactions, with a mesh spacing of 1 Å for the calculation of the fast Fourier transform.

An ethanol/water mixture (10/90 v/v) was used as the solvent for the polymerization tests. The mixtures were prepared with the PACKMOL program [276] (<http://leandro.iqm.unicamp.br/m3g/packmol/home.shtml>). Each mixture consisted of 1 molecule of caffeic acid, 4 molecules of functional monomer, 113 molecules of ethanol, and 3327 molecules of water in a cubic simulation box with an initial side length of 48 Å, which corresponds to a caffeic acid concentration of approximately 15 mM. At pH 7, the deprotonated forms of caffeic acid and 4-aminobenzoic acid were considered. A sodium ion was therefore added for each acid molecule in the mixtures at pH 7 to maintain the neutrality of the simulated systems. For each mixture, 3 independent random configurations were generated. The energy of

these configurations was minimized using the steepest slope algorithm in four successive steps: (i) constraining the atomic positions of the caffeic acid, monomers, and ethanol with a harmonic potential of stiffness constant  $106 \text{ kJ.mol}^{-1}.\text{nm}^{-2}$  (60 iterations), (ii) constraining the atomic positions of the heavy atoms of the caffeic acid, monomers, and ethanol with a harmonic potential of stiffness constant of  $106 \text{ kJ.mol}^{-1}.\text{nm}^{-2}$  (2000 iterations), (iii) constraining the atomic positions of the heavy atoms of caffeic acid, monomers, and ethanol with a harmonic potential of stiffness constant of  $103 \text{ kJ.mol}^{-1}.\text{nm}^{-2}$  (2000 iterations), and (iv) without any constraint on any atom in the simulation box (10000 iterations).

A 200 ps molecular dynamics simulation in the canonical set (N, V, T) was then performed to heat the system from 10 K to 298 K. Finally, a 200 ns molecular dynamics simulation in the isothermal-isobaric ensemble (N, P, T) with  $T = 298 \text{ K}$  and  $P = 1 \text{ atm}$  was performed, recording atomic coordinates every 2 ps. The interactions between caffeic acid and functional monomers were analyzed over the second half of each simulation ( $t = [100 \text{ ns}-200 \text{ ns}]$ ), determining the average values of the following three parameters: (i) the number of functional monomers in contact with caffeic acid (coordination number), (ii) the number of hydrogen bonds formed between caffeic acid and functional monomers, and (iii) the interaction energy between caffeic acid and functional monomers.

The following experiments were done with 4-aminobenzoic acid as functional monomer.

## 2. Electropolymerization steps

Electropolymerization is an easy and simple process. The steps are close to the *ex-situ* ones, in terms of order and objective, but it requires smaller volumes and less time. The solutions to prepare are:

- S1: template solution (CA in PBS 0.05M pH3/EtOH; 90/10 v/v)
- S2: FM solution (4-ABA in PBS/EtOH), also used for the NIP synthesis
- S3: polymerization solution (MIP) containing template and functional monomer solutions
- S4: rebinding solution (50  $\mu\text{M}$  of CA in PBS/EtOH)
- WS: washing solutions (a) EtOH/acetic acid (90/10 v/v) and (b) EtOH

Electrochemical parameters were:

For CV: -0.2 to 1 V, scan rate 100 mV/s

For DPV: 0.1 to 0.8 V,  $E_{\text{step}}$ : 0.004 V,  $E_{\text{pulse}}$ : 0.08 V,  $t_{\text{pulse}}$ : 200 ms and  $S_{\text{rate}}$ : 0.04 V.

Once the solutions were prepared, 50  $\mu\text{L}$  of S3 were deposited on the surface of the screen-printed carbon electrode (SPCE) and CV cycles were applied in order to polymerize the MIP. The same was done with S2 for the NIP. At the end of the CV cycles, a DPV was applied on the same electrode.

The SPCE was removed and rinsed with water, then dipped in the WS (a) for 10 min (except the connectors part), and in WS (b) for 10 min to remove the acid. The SPCE was dried, connected again to the device, 50  $\mu\text{L}$  of PBS 0.05 M pH 3 were drop casted on the surface of the electrode, and another DPV is applied, in order to make sure that the washing was completely done.

After the extraction of CA, the SPCE was dipped in S4 for rebinding tests. Then the SPCE is rinsed, dried and connected again with 50  $\mu\text{L}$  of PBS on its surface, and a DPV is applied, for the rebinding evaluation.

For the reuse of the electrode, it should be washed again prior to each rebinding experiment.

### **3. Optimization of MIP sensor preparation conditions**

#### **3.1. Functional monomer to template concentration ratio (FM/T)**

FM/T ratio in the pre-polymerization mixtures influence the number of imprinted cavities in the polymer, which affects the rebinding and recognition capability of the sensor [277]. In order to evaluate the effect of 4-ABA concentration on the performance of the sensor towards CA, several solutions of pre-polymerization composed of different 4-ABA/CA (50  $\mu\text{M}$ ) ratios were prepared: 1:2, 1:4, 1:10, 1:40 and 1:100, and electrochemically polymerized on SPCEs as described in paragraph 2. The rebinding properties were tested with each ratio.

#### **3.2. Number of cycles**

The number of cycles used in electropolymerization impacts the thickness of the polymer layer, thereby the sensor's performance and its capability to form accessible cavities.

For this reason, several MIP-SPCEs were prepared, with the same pre-polymerization solution composed of 0.05 mM of caffeic acid and 0.5 mM of 4-ABA (ratio 1:10) with electropolymerization cycles ranging from 5 to 40, and then the rebinding properties were tested after template removal.

### **3.3. Incubation time for rebinding tests**

The relationship between the sensor's response and the incubation time was also studied by incubating the sensors in S4, after template removal, between 1 and 60 min.

In the following experiments, the conditions that were chosen: 1:10 as T:FM, 10 cycles and 20 min of incubation.

## **4. Rebinding properties**

After setting all the conditions, rebinding tests were tested using the sensor prepared with 0.05 mM of CA, 0.5 mM of 4-ABA.

The polymers (MIP and NIP) were electropolymerized on the surface of the SPCEs and then washed as described in paragraph 2. Incubation solutions were prepared at concentrations of CA ranging between 2  $\mu$ M and 40  $\mu$ M, then rebinding properties were studied in order to evaluate the performance of the MIP while increasing the concentration, and its specificity by comparing it to that of the NIP.

## **5. Sensors response in the presence of interferents**

The selectivity of the sensor towards CA against interferents with similar structures: gallic acid (GA), sinapic acid (SA), ferulic acid (FA) and *p*-coumaric acid (*p*-CA) was evaluated by preparing 50  $\mu$ M of each solution separately, and using them as incubation solutions to the sensor.

## **6. Stability and repeatability of the sensor**

To examine the stability of the imprinted electrode, 2 MIP-SPCEs were prepared (MIPa and MIPb). MIPa was stored at room temperature, and MIPb was stored in PBS 0.05M pH3 for a period of time (10 days) before the second use. Sensor's performance repeatability was also evaluated by detecting CA consecutively with the same sensor and in the same CA concentration, until decrease of the current.

---

**References**

1. Rice-evans, C.A.; Miller, N.J.; Bolwell, P.G.; Bramley, P.M.; Pridham, J.B. The Relative Antioxidant Activities of Plant-Derived Polyphenolic Flavonoids. *Free Radic. Res.* **1995**, *22*, 375–383, doi:10.3109/10715769509145649.
2. German, J.B.; Walzem, R.L. THE HEALTH BENEFITS OF WINE. *Annu. Rev. Nutr.* **2000**, *20*, 561–593, doi:10.1146/annurev.nutr.20.1.561.
3. Ilhami, G. Antioxidant Activity of Caffeic Acid ( 3 , 4-Dihydroxycinnamic Acid ). *Toxicology* **2006**, *217*, 213–220, doi:10.1016/j.tox.2005.09.011.
4. Torres-rivero, K.; Florido, A.; Bastos-arrieta, J. Recent Trends in the Improvement of the Electrochemical Response of Screen-Printed Electrodes by Their Modification with Shaped Metal Nanoparticles. **2021**.
5. Mincu, N.-B.; Lazar, V.; Stan, D.; Mihailescu, C.M.; Iosub, R.; Mateescu, A.L. Screen-Printed Electrodes (SPE) for In Vitro Diagnostic Purpose. *Diagnostics (Basel, Switzerland)* **2020**, *10*, doi:10.3390/diagnostics10080517.
6. Ertürk, G.; Mattiasson, B. Molecular Imprinting Techniques Used for the Preparation of Biosensors. *Sensors (Basel)*. **2017**, *17*, doi:10.3390/s17020288.
7. Cui, B.; Liu, P.; Liu, X.; Liu, S.; Zhang, Z. Molecularly Imprinted Polymers for Electrochemical Detection and Analysis: Progress and Perspectives. *J. Mater. Res. Technol.* **2020**, *9*, 12568–12584, doi:https://doi.org/10.1016/j.jmrt.2020.08.052.
8. Oneide, M.; Moraes, S. De; Assis, I.M.; Passos, R.R.; Casarini, J.R.; Masso, D.W.; Galante, D.; Garcia-, Y.; Luiza, M.; Rocco, M.; et al. Electrochemical Sensor Based on Molecularly Imprinted Polymer ( MIP ) for Detection of Gallic Acid. **2015**, *30*, 697–698.
9. Mucio, M.; Vinicius, M.; Helena, D.; Silva, S.; Taboada, P.; Yamanaka, H. Sensors and Actuators B : Chemical Electrochemical Sensor for Dodecyl Gallate Determination Based on Electropolymerized Molecularly Imprinted Polymer. *Sensors Actuators B. Chem.* **2017**, *253*, 180–186, doi:10.1016/j.snb.2017.06.127.
10. Elhachem, M.; Cayot, P.; Abboud, M.; Louka, N.; Maroun, R.G.; Bou-maroun, E. *The Importance of Developing Electrochemical Sensors Based on Molecularly Imprinted Polymers for a Rapid Detection of Antioxidants*; antioxidants, 2021; ISBN 3338077408.
11. Antuña-Jiménez, D.; Díaz-Díaz, G.; Blanco-López, M.C.; Lobo-Castañón, M.J.; Miranda-Ordieres, A.J.; Tuñón-Blanco, P. Chapter 1 - Molecularly Imprinted Electrochemical Sensors: Past, Present, and Future. In; Li, S., Ge, Y., Piletsky, S.A., Lunec, J.B.T.-M.I.S., Eds.; Elsevier: Amsterdam, 2012; pp. 1–34 ISBN 978-0-444-56331-6.
12. Brewer, M.S. Natural Antioxidants : Sources , Compounds , Mechanisms of Action , and Potential Applications. *Compr. Rev. food Sci. food Saf.* **2011**, *10*, 221–247, doi:10.1111/j.1541-4337.2011.00156.x.
13. Shahidi, F.; Zhong, Y. Measurement of Antioxidant Activity. *J. Funct. Foods* **2015**, *18*, 757–781, doi:10.1016/j.jff.2015.01.047.
14. Apak, R.; Özyürek, M.; Güçlü, K.; Çapanoğlu, E. Antioxidant Activity/Capacity Measurement. 3. Reactive Oxygen and Nitrogen Species (ROS/RNS) Scavenging Assays, Oxidative Stress Biomarkers, and Chromatographic/Chemometric Assays. *J. Agric. Food Chem.* **2016**, *64*, 1046–1070, doi:10.1021/acs.jafc.5b04744.
15. Taylor, P.; Uslu, B.; Ozkan, S.A. Electroanalytical Methods for the Determination of Pharmaceuticals: A Review of Recent Trends and Developments. **2011**, 37–41, doi:10.1080/00032719.2011.553010.
16. Li, M.; Li, D.W.; Xiu, G.; Long, Y.T. Applications of Screen-Printed Electrodes in Current Environmental Analysis. *Curr. Opin. Electrochem.* **2017**, *3*, 137–143, doi:10.1016/j.coelec.2017.08.016.

17. Giné Bordonaba, J.; Terry, L.A. Electrochemical Behaviour of Polyphenol Rich Fruit Juices Using Disposable Screen-Printed Carbon Electrodes: Towards a Rapid Sensor for Antioxidant Capacity and Individual Antioxidants. *Talanta* **2012**, *90*, 38–45, doi:10.1016/j.talanta.2011.12.058.
18. Lingxin, S. As Featured in: Molecular Imprinting: Perspectives and Applications. *Chem. Soc. Rev.* **2016**, *45*, 2137–2211, doi:10.1039/C6CS00061D.
19. Garcia-Martinez, O.; Ruiz, C.; Gutierrez-Ibanez, A.; Illescas-Montes, R.; Melguizo-Rodriguez, L. Benefits of Olive Oil Phenolic Compounds in Disease Prevention. *Endocrine, Metab. Immune Disord. - Drug Targets* **2018**, *18*, 333–340, doi:10.2174/1871530318666180213113211.
20. Parkinson, L.; Cicerale, S. The Health Benefiting Mechanisms of Virgin Olive Oil Phenolic Compounds. *Molecules* **2016**, *21*, 1–12, doi:10.3390/molecules21121734.
21. Boronat, A.; Mateus, J.; Soldevila-Domenech, N.; Guerra, M.; Rodríguez-Morató, J.; Varon, C.; Muñoz, D.; Barbosa, F.; Morales, J.C.; Gaedigk, A.; et al. Cardiovascular Benefits of Tyrosol and Its Endogenous Conversion into Hydroxytyrosol in Humans. A Randomized, Controlled Trial. *Free Radic. Biol. Med.* **2019**, *143*, 471–481, doi:10.1016/j.freeradbiomed.2019.08.032.
22. Mazué, F.; Delmas, D.; Murillo, G.; Saleiro, D.; Limagne, E.; Latruffe, N. Differential Protective Effects of Red Wine Polyphenol Extracts (RWEs) on Colon Carcinogenesis. *Food Funct.* **2014**, *5*, 663–670, doi:10.1039/c3fo60417a.
23. Kurin, E.; Atanasov, A.G.; Donath, O.; Heiss, E.H.; Dirsch, V.M.; Nagy, M. Synergy Study of the Inhibitory Potential of Red Wine Polyphenols on Vascular Smooth Muscle Cell Proliferation. *Planta Med.* **2012**, *78*, 772–778, doi:10.1055/s-0031-1298440.
24. Basli, A.; Soulet, S.; Chaher, N.; Mérillon, J.M.; Chibane, M.; Monti, J.P.; Richard, T. Wine Polyphenols: Potential Agents in Neuroprotection. *Oxid. Med. Cell. Longev.* **2012**, *2012*, doi:10.1155/2012/805762.
25. Shahidi, F.; Ambigaipalan, P. Phenolics and Polyphenolics in Foods, Beverages and Spices: Antioxidant Activity and Health Effects - A Review. *J. Funct. Foods* **2015**, *18*, 820–897, doi:10.1016/j.jff.2015.06.018.
26. Lund, M.N.; Baron, C.P. *Protein Oxidation in Foods and Food Quality*; Woodhead Publishing Limited;
27. Baron, C.P.; Berner, L.; Skibsted, L.H.; Refsgaard, H.H.F. Evaluation of Activity of Selected Antioxidants on Proteins in Solution and in Emulsions. *Free Radic. Res.* **2005**, *39*, 777–785, doi:10.1080/10715760500043199.
28. Jacobsen, C.; Let, M.B.; Nielsen, N.S.; Meyer, A.S. Antioxidant Strategies for Preventing Oxidative Flavour Deterioration of Foods Enriched with N-3 Polyunsaturated Lipids: A Comparative Evaluation. *Trends Food Sci. Technol.* **2008**, *19*, 76–93, doi:https://doi.org/10.1016/j.tifs.2007.08.001.
29. Liu, H.C.; Chen, W.L.; Mao, S.J.T. Antioxidant Nature of Bovine Milk  $\beta$ -Lactoglobulin. *J. Dairy Sci.* **2007**, *90*, 547–555, doi:10.3168/jds.S0022-0302(07)71538-2.
30. Refsgaard, H.H.F.; Tsai, L.; Stadtman, E.R. Modifications of Proteins by Polyunsaturated Fatty Acid Peroxidation Products. **2000**, 97.
31. Díaz, M.; Decker, E.A. Antioxidant Mechanisms of Caseinophosphopeptides and Casein Hydrolysates and Their Application in Ground Beef. *J. Agric. Food Chem.* **2004**, *52*, 8208–8213, doi:10.1021/jf048869e.
32. Peña-Ramos, E.A.; Xiong, Y.L. Whey and Soy Protein Hydrolysates Inhibit Lipid Oxidation in Cooked Pork Patties. *Meat Sci.* **2003**, *64*, 259–263, doi:10.1016/S0309-1740(02)00187-0.
33. Sakanaka, S.; Tachibana, Y. Active Oxygen Scavenging Activity of Egg-Yolk Protein

- Hydrolysates and Their Effects on Lipid Oxidation in Beef and Tuna Homogenates. *Food Chem.* **2006**, *95*, 243–249, doi:https://doi.org/10.1016/j.foodchem.2004.11.056.
34. Sakanaka, S.; Tachibana, Y.; Ishihara, N.; Juneja, L.R. Antioxidant Properties of Casein Calcium Peptides and Their Effects on Lipid Oxidation in Beef Homogenates. *J. Agric. Food Chem.* **2005**, *53*, 464–468, doi:10.1021/jf0487699.
  35. Elias, R.J.; Kellerby, S.S.; Decker, E.A. Antioxidant Activity of Proteins and Peptides. *Crit. Rev. Food Sci. Nutr.* **2008**, *48*, 430–441, doi:10.1080/10408390701425615.
  36. Pietta, P.-G. Flavonoids as Antioxidants. *J. Nat. Prod.* **2000**, *63*, 1035–1042, doi:10.1021/np9904509.
  37. Young, I.S.; Woodside, J. V Antioxidants in Health and Disease Antioxidants in Health and Disease. *J. Clin. Pathol.* **2001**, *54*, 176–186, doi:10.1136/jcp.54.3.176.
  38. Tsao, R. Chemistry and Biochemistry of Dietary Polyphenols. *Nutrients* **2010**, *2*, 1231–1246, doi:10.3390/nu2121231.
  39. Horton, W.; Török, M. *Natural and Nature-Inspired Synthetic Small Molecule Antioxidants in the Context of Green Chemistry*; Elsevier Inc., 2018; ISBN 9780128095492.
  40. Shahidi, F.; Janitha, P.K.; Wanasundara, P.D. Phenolic Antioxidants. *Crit. Rev. Food Sci. Nutr.* **1992**, *32*, 67–103, doi:10.1080/10408399209527581.
  41. Balasaheb, S.; Pal, D. RSC Advances. **2015**, 27986–28006, doi:10.1039/c4ra13315c.
  42. Avdeeva, L. V; Gvozdev, R.I. Oxidation of L-Ascorbic Acid in the Presence of the Copper-Binding Compound from Methanotrophic Bacteria *Methylococcus Capsulatus* ( M ). **2020**.
  43. Croux, S.; Beck, I.; Hocquaux, M.; Braun, M.; Oliveros, E. Antioxidant Quenching Activity of Flavonoids : Efficiency of Singlet Oxygen ( ‘ A , ). **1993**, *19*, 205–215.
  44. Herrero, M.; Ibáñez, E.; Cifuentes, A. Analysis of Natural Antioxidants by Capillary Electromigration Methods. *J. Sep. Sci.* **2005**, *28*, 883–897, doi:10.1002/jssc.200400104.
  45. Shahidi, F. Antioxidants in Food and Food Antioxidants. *Food/Nahrung* **2000**, *44*, 158–163, doi:10.1002/1521-3803(20000501)44:3<158::AID-FOOD158>3.0.CO;2-L.
  46. Manach, C.; Scalbert, A.; Morand, C.; Rémésy, C.; Jiménez, L. Polyphenols: Food Sources and Bioavailability. *Am. J. Clin. Nutr.* **2004**, *79*, 727–747, doi:10.1093/ajcn/79.5.727.
  47. Robbins, R.J. Phenolic Acids in Foods: An Overview of Analytical Methodology. *J. Agric. Food Chem.* **2003**, *51*, 2866–2887, doi:10.1021/jf026182t.
  48. King, A.; Young, G. Characteristics and Occurrence of Phenolic Phytochemicals. *J. Am. Diet. Assoc.* 1999, *99*, 213–218.
  49. Boskou, D.; Blekas, G.; Tsimidou, M. Olive Oil Composition. In *Olive Oil: Chemistry and Technology: Second Edition*; Elsevier Inc., 2006; pp. 41–72 ISBN 9780128043547.
  50. Rice-Evans, C.A.; Miller, N.J.; Paganga, G. Antioxidant Properties of Phenolic Compounds. *Trends Plant Sci.* **1997**, *2*, 152–159, doi:10.1016/S1360-1385(97)01018-2.
  51. Debelo, H.; Li, M.; Ferruzzi, M.G. Processing Influences on Food Polyphenol Profiles and Biological Activity. *Curr. Opin. Food Sci.* **2020**, doi:10.1016/j.cofs.2020.03.001.
  52. Drahansky, M.; Paridah, M.; Moradbak, A.; Mohamed, A.; Owolabi, F. Abdulwahab taiwo; Asniza, M.; Abdul Khalid, S.H.. We Are IntechOpen , the World ’ s Leading Publisher of Open Access Books Built by Scientists , for Scientists TOP 1 % . *Intech* **2016**, *i*, 13, doi:http://dx.doi.org/10.5772/57353.
  53. Apak, R.; Özyürek, M.; Güçlü, K.; Çapanoğlu, E. Antioxidant Activity/Capacity Measurement. 1. Classification, Physicochemical Principles, Mechanisms, and Electron Transfer (ET)-Based Assays. *J. Agric. Food Chem.* **2016**, *64*, 997–1027, doi:10.1021/acs.jafc.5b04739.

54. Apak, R.; Özyürek, M.; Güçlü, K.; Çapanoğlu, E. Antioxidant Activity/Capacity Measurement. 2. Hydrogen Atom Transfer (HAT)-Based, Mixed-Mode (Electron Transfer (ET)/HAT), and Lipid Peroxidation Assays. *J. Agric. Food Chem.* **2016**, *64*, 1028–1045, doi:10.1021/acs.jafc.5b04743.
55. Rock, L.; Brunswick, N. Standardized Methods for the Determination of Antioxidant Capacity and Phenolics in Foods and Dietary Supplements. **2005**, 4290–4302, doi:10.1021/jf0502698.
56. Niki, E. Free Radical Biology & Medicine Assessment of Antioxidant Capacity in Vitro and in Vivo. *Free Radic. Biol. Med.* **2010**, *49*, 503–515, doi:10.1016/j.freeradbiomed.2010.04.016.
57. Li, B.; Pratt, D.A. Author's Accepted Manuscript. **2015**, doi:10.1016/j.freeradbiomed.2015.01.020.
58. Prieto, M.A.; Vázquez, J.A.; Murado, M.A. Crocin Bleaching Antioxidant Assay Revisited: Application to Microplate to Analyze Antioxidant and pro-Oxidant Activities. *FOOD Chem.* **2014**, doi:10.1016/j.foodchem.2014.06.114.
59. Nagatani, N.; Inoue, Y.; Araki, A.; Ushijima, H.; Hattori, G.; Sakurai, Y.; Ogidou, Y.; Saito, M.; Tamiya, E. Rapid Sensing of Antioxidant Capacity Based on Electrochemiluminescence Induced by Electrochemically Generated Reactive Oxygen Species. *Electrochim. Acta* **2016**, doi:10.1016/j.electacta.2016.11.012.
60. Do, E.; Gökmen, V. Evolution of Food Antioxidants as a Core Topic of Food Science for a Century. **2018**, *105*, 76–93, doi:10.1016/j.foodres.2017.10.056.
61. Dai, J.; Mumper, R.J. Plant Phenolics: Extraction, Analysis and Their Antioxidant and Anticancer Properties. *Molecules* **2010**, *15*, 7313–7352, doi:10.3390/molecules15107313.
62. Faculty, B. Talanta DPPH Assay of Vegetable Oils and Model Antioxidants in Protic and Aprotic Solvents. **2013**, *109*, 13–19, doi:10.1016/j.talanta.2013.03.046.
63. Marteau, C.; Guitard, R.; Penverne, C.; Favier, D.; Nardello-rataj, V.; Aubry, J. Boosting Effect of Ortho- Propenyl Substituent on the Antioxidant Activity of Natural Phenols. **2016**, *196*, 418–427, doi:10.1016/j.foodchem.2015.09.007.
64. Pinto, D.; Vieira, E.F.; Peixoto, A.F.; Freire, C.; Freitas, V.; Costa, P.; Delerue-matos, C.; Rodrigues, F. Optimizing the Extraction of Phenolic Antioxidants from Chestnut Shells by Subcritical Water Extraction Using Response Surface Methodology. *Food Chem.* **2021**, *334*, 127521, doi:10.1016/j.foodchem.2020.127521.
65. Krylova, E.; Gavrilenko, N.; Saranchina, N.; Gavrilenko, M. Novel Colorimetric Sensor for Cupric Reducing Antioxidant Capacity ( CUPRAC ) Measurement. *Procedia Eng.* **2016**, *168*, 355–358, doi:10.1016/j.proeng.2016.11.120.
66. Cicco, N.; Lanorte, M.T.; Paraggio, M.; Viggiano, M.; Lattanzio, V. A Reproducible , Rapid and Inexpensive Folin – Ciocalteu Micro-Method in Determining Phenolics of Plant Methanol Extracts. *Microchem. J.* **2009**, *91*, doi:10.1016/j.microc.2008.08.011.
67. Pardeshi, S.; Kumar, A.; Dhodapkar, R. Molecular Imprinting: Mimicking Molecular Receptors for Antioxidants. *Mater. Sci. Forum* **2011**, *675–677*, 515–520, doi:10.4028/www.scientific.net/MSF.675-677.515.
68. Maroun, R.G.; Rajha, H.N.; Darra, N. El; Kantar, S. El; Chacar, S.; Debs, E.; Vorobiev, E.; Louka, N. *8 - Emerging Technologies for the Extraction of Polyphenols from Natural Sources*; Woodhead Publishing: United Kingdom, 2018; ISBN 9780128135723.
69. Mayachiew, P.; Devahastin, S. Antimicrobial and Antioxidant Activities of Indian Gooseberry and Galangal Extracts. *LWT - Food Sci. Technol.* **2008**, *41*, 1153–1159, doi:https://doi.org/10.1016/j.lwt.2007.07.019.
70. Zuo, Y.; Chen, H.; Deng, Y. Simultaneous Determination of Catechins, Caffeine and

- Gallic Acids in Green, Oolong, Black and Pu-Erh Teas Using HPLC with a Photodiode Array Detector. *Talanta* **2002**, *57*, 307–316, doi:https://doi.org/10.1016/S0039-9140(02)00030-9.
71. Chirinos, R.; Rogez, H.; Campos, D.; Pedreschi, R.; Larondelle, Y. Optimization of Extraction Conditions of Antioxidant Phenolic Compounds from Mashua (*Tropaeolum Tuberosum* Ruiz & Pavon) Tubers. *Sep. Purif. Technol.* **2007**, *55*, 217–225, doi:10.1016/j.seppur.2006.12.005.
  72. Spigno, G.; Tramelli, L.; De Faveri, D.M. Effects of Extraction Time, Temperature and Solvent on Concentration and Antioxidant Activity of Grape Marc Phenolics. *J. Food Eng.* **2007**, *81*, 200–208, doi:https://doi.org/10.1016/j.jfoodeng.2006.10.021.
  73. Hidalgo, G.I.; Almajano, M.P. Red Fruits: Extraction of Antioxidants, Phenolic Content, and Radical Scavenging Determination: A Review. *Antioxidants* **2017**, *6*, doi:10.3390/antiox6010007.
  74. Pisoschi, A.M.; Cimpeanu, C.; Predoi, G. Electrochemical Methods for Total Antioxidant Capacity and Its Main Contributors Determination: A Review. **2015**, 824–856, doi:10.1515/chem-2015-0099.
  75. Blasco, A.J.; Crevillén, A.G.; González, M.C.; Escarpa, A. Direct Electrochemical Sensing and Detection of Natural Antioxidants and Antioxidant Capacity in Vitro Systems. *Electroanalysis* **2007**, *19*, 2275–2286, doi:10.1002/elan.200704004.
  76. Valek, L.; Stipc, T. Electrochemical Determination of Antioxidant Capacity of Fruit Tea Infusions. **2010**, *121*, 820–825, doi:10.1016/j.foodchem.2009.12.090.
  77. Lyklema, J. Current Opinion in Colloid & Interface Science Principles of Interactions in Non-Aqueous Electrolyte Solutions. *Curr. Opin. Colloid Interface Sci.* **2013**, *18*, 116–128, doi:10.1016/j.cocis.2013.02.002.
  78. Lucas, D.; Devillers, C.H.; Lucas, D. Journal Pre-Proof. **2020**, doi:10.1016/j.molstruc.2020.129321.
  79. Rolle, S.D.; Konev, D. V; Devillers, C.H.; Lizgina, K. V; Lucas, D.; Stern, C.; Herbst, F.; Heintz, O.; Vorotyntsev, M.A. Electrochimica Acta Ef Fi Cient Synthesis of a New Electroactive Polymer of Co ( II ) Porphine by in - Situ Replacement of Mg ( II ) inside Mg ( II ) Polyporphine Fi Lm. **2016**, *204*, 276–286, doi:10.1016/j.electacta.2016.03.039.
  80. Lima, A.P.; Wallans, T.P.; Nossol, E.; Richter, E.M.; Munoz, R.A.A. Electrochimica Acta Critical Evaluation of Voltammetric Techniques for Antioxidant Capacity and Activity: Presence of Alumina on Glassy-Carbon Electrodes Alters the Results. **2020**, *358*, doi:10.1016/j.electacta.2020.136925.
  81. David, I.G.; Buleandr, M.; Popa, D.E.; Bizgan, A.C.; Moldovan, Z.; Badea, I.; Iorgulescu, E.E.; Basaga, H. Voltammetric Determination of Polyphenolic Content as Rosmarinic Acid Equivalent in Tea Samples Using Pencil Graphite Electrodes. **2016**, doi:10.1007/s13197-016-2223-y.
  82. David, I.G.; Litescu, C.; Popa, E.; Buleandra, M.; Iordache, L.; Albu, C.; Alecu, A. Analytical Methods Pencil Graphite Electrode – Application to Polyphenol Content Determination in Citrus Juice †. **2018**, 5763–5772, doi:10.1039/c8ay02281j.
  83. Kariuki, J.; Ervin, E.; Olafson, C. Development of a Novel, Low-Cost, Disposable Wooden Pencil Graphite Electrode for Use in the Determination of Antioxidants and Other Biological Compounds. **2015**, 18887–18900, doi:10.3390/s150818887.
  84. Rezaei, B.; Boroujeni, M.K.; Ensa, A.A. Biosensors and Bioelectronics Caffeine Electrochemical Sensor Using Imprinted Fi Lm as Recognition Element Based on Polypyrrole , Sol-Gel , and Gold Nanoparticles Hybrid Nanocomposite Modi Fi Ed Pencil Graphite Electrode. **2014**, *60*, 77–83, doi:10.1016/j.bios.2014.03.028.
  85. Głód, B.K.; Kiersztyn, I.; Piszcz, P. Total Antioxidant Potential Assay with Cyclic

- Voltammetry and/or Differential Pulse Voltammetry Measurements. *J. Electroanal. Chem.* **2014**, *719*, 24–29, doi:10.1016/j.jelechem.2014.02.004.
86. Maji, P.; Basu, S.; Banik, B.K.; Ganguly, J. Antioxidant Edible Mushrooms: A Green and Rapid Electrochemical Study with the Aqueous Extracts. *Mod. Chem. Appl.* **2018**, *06*, 1–7, doi:10.4172/2329-6798.1000247.
87. Suliborska, K.; Baranowska, M.; Bartoszek, A.; Chrzanowski, W.; Namieśnik, J. Determination of Antioxidant Activity of Vitamin C by Voltammetric Methods. *Proceedings* **2019**, *11*, 23, doi:10.3390/proceedings2019011023.
88. Teixeira, J.; Gaspar, A.; Garrido, E.M.; Garrido, J.; Borges, F. Hydroxycinnamic Acid Antioxidants: An Electrochemical Overview. *Biomed Res. Int.* **2013**, *2013*, doi:10.1155/2013/251754.
89. Vilas-Boas, Â.; Valderrama, P.; Fontes, N.; Geraldo, D.; Bento, F. Evaluation of Total Polyphenol Content of Wines by Means of Voltammetric Techniques: Cyclic Voltammetry vs Differential Pulse Voltammetry. *Food Chem.* **2019**, *276*, 719–725, doi:10.1016/j.foodchem.2018.10.078.
90. José Jara-Palacios, M.; Hernanz, D.; Luisa Escudero-Gilete, M.; Heredia, F.J. Antioxidant Potential of White Grape Pomaces: Phenolic Composition and Antioxidant Capacity Measured by Spectrophotometric and Cyclic Voltammetry Methods. *Food Res. Int.* **2014**, *66*, 150–157, doi:https://doi.org/10.1016/j.foodres.2014.09.009.
91. José Jara-Palacios, M.; Luisa Escudero-Gilete, M.; Miguel Hernández-Hierro, J.; Heredia, F.J.; Hernanz, D. Cyclic Voltammetry to Evaluate the Antioxidant Potential in Winemaking By-Products. *Talanta* **2017**, *165*, 211–215, doi:https://doi.org/10.1016/j.talanta.2016.12.058.
92. Szczepaniak, O.M.; Ligaj, M.; Kobus-Cisowska, J.; Maciejewska, P.; Tichoniuk, M.; Szulc, P. Application for Novel Electrochemical Screening of Antioxidant Potential and Phytochemicals in Cornus Mas Extracts. *CyTA - J. Food* **2019**, *17*, 781–789, doi:10.1080/19476337.2019.1653378.
93. Amidi, S.; Mojab, F.; Bayandori, A. A Simple Electrochemical Method for the Rapid Estimation of Antioxidant Potentials of Some Selected Medicinal Plants. **2012**, *11*, 117–121.
94. Kissinger, P.T.; Lafayette, W.; Heineman, W.R. Cyclic Voltammetry. 702–706, doi:10.1021/ed060p702.
95. Chevion, S.; Roberts, M.A.; Chevion, M. The Use of Cyclic Voltammetry for the Evaluation of Antioxidant Capacity. *Free Radic. Biol. Med.* **2000**, *28*, 860–870, doi:https://doi.org/10.1016/S0891-5849(00)00178-7.
96. Hoyos-arbeláez, J.; Vázquez, M.; Contreras-calderón, J. Electrochemical Methods as a Tool for Determining the Antioxidant Capacity of Food and Beverages : A Review. **2017**, *221*, 1371–1381, doi:10.1016/j.foodchem.2016.11.017.
97. Sciences, A. Polyphenol Analysis in Black Tea with Carbon Nanotube Electrode. **2019**, 1–5, doi:10.2116/analsci.18P516.
98. Zhang, J.-W.; Wang, K.-P.; Zhang, X. Fabrication of SnO<sub>2</sub> Decorated Graphene Composite Material and Its Application in Electrochemical Detection of Caffeic Acid in Red Wine. *Mater. Res. Bull.* **2020**, *126*, 110820, doi:https://doi.org/10.1016/j.materresbull.2020.110820.
99. Bharath, G.; Alhseinat, E.; Madhu, R.; Mugo, S.M.; Alwasel, S.; Halim, A. Facile Synthesis of Au @ a -Fe<sub>2</sub>O<sub>3</sub> @ RGO Ternary Nanocomposites for Enhanced Electrochemical Sensing of Caffeic Acid toward Biomedical Applications. *J. Alloys Compd.* **2018**, *750*, 819–827, doi:10.1016/j.jallcom.2018.04.052.
100. Manikandan, V.S.; Sidhureddy, B.; Thirupathi, A.R.; Chen, A. Sensitive

- Electrochemical Detection of Caffeic Acid in Wine Based on Fluorine-Doped Graphene Oxide. **2019**, doi:10.3390/s19071604.
101. Kokulnathan, T.; Raja, N.; Chen, S.; Liao, W. Journal of Colloid and Interface Science Nanomolar Electrochemical Detection of Caffeic Acid in Fortified Wine Samples Based on Gold / Palladium Nanoparticles Decorated Graphene Flakes. *J. Colloid Interface Sci.* **2017**, *501*, 77–85, doi:10.1016/j.jcis.2017.04.042.
  102. Palanisamy, S.; Chen, S.-M.; Velusamy, V.; Chen, T.-W.; Ramaraj, S.K. Electrochemical Determination of Caffeic Acid in Wine Samples Using Reduced Graphene Oxide/Polydopamine Composite. *J. Electrochem. Soc.* **2016**, *163*, B726–B731, doi:10.1149/2.1231614jes.
  103. Tashkhourian, J.; Nami-ana, S.F. A Sensitive Electrochemical Sensor for Determination of Gallic Acid Based on SiO<sub>2</sub> Nanoparticle Modified Carbon Paste Electrode. *Mater. Sci. Eng. C* **2015**, *52*, 103–110, doi:10.1016/j.msec.2015.03.017.
  104. Gao, F.; Zheng, D.; Tanaka, H.; Zhan, F.; Yuan, X.; Gao, F.; Wang, Q. An Electrochemical Sensor for Gallic Acid Based on Fe<sub>2</sub>O<sub>3</sub>/Electro-Reduced Graphene Oxide Composite: Estimation for the Antioxidant Capacity Index of Wines. *Mater. Sci. Eng. C. Mater. Biol. Appl.* **2015**, *57*, 279–287, doi:10.1016/j.msec.2015.07.025.
  105. Kahl, M.; Golden, T. Electrochemical Determination of Phenolic Acids at a Zn/Al Layered Double Hydroxide Film Modified Glassy Carbon Electrode. *Electroanalysis* **2014**, *26*, doi:10.1002/elan.201400156.
  106. Souza, L.P.; Calegari, F.; Zarbin, A.J.G.; Marcolino-Júnior, L.H.; Bergamini, M.F. Voltammetric Determination of the Antioxidant Capacity in Wine Samples Using a Carbon Nanotube Modified Electrode. *J. Agric. Food Chem.* **2011**, *59*, 7620–7625, doi:10.1021/jf2005589.
  107. Qi, S.; Zhao, B.; Tang, H.; Jiang, X. Electrochimica Acta Determination of Ascorbic Acid, Dopamine, and Uric Acid by a Novel Electrochemical Sensor Based on Pristine Graphene. *Electrochim. Acta* **2015**, *161*, 395–402, doi:10.1016/j.electacta.2015.02.116.
  108. Raouf, J.B.; Ojani, R.; Beitollahi, H.; Hossienzadeh, R. Electrocatalytic Determination of Ascorbic Acid at the Surface of 2,7-Bis(Ferrocenyl Ethyl)Fluoren-9-one Modified Carbon Paste Electrode. *Electroanalysis* **2006**, *18*, 1193–1201, doi:10.1002/elan.200503516.
  109. Pisoschi, A.M.; Pop, A.; Negulescu, G.P.; Pisoschi, A. Determination of Ascorbic Acid Content of Some Fruit Juices and Wine by Voltammetry Performed at Pt and Carbon Paste Electrodes. *Molecules* **2011**, *16*, 1349–1365, doi:10.3390/molecules16021349.
  110. Barroso, M.F.; de-los-Santos-Álvarez, N.; Lobo-Castañón, M.J.; Miranda-Ordieres, A.J.; Delerue-Matos, C.; Oliveira, M.B.P.P.; Tuñón-Blanco, P. DNA-Based Biosensor for the Electrocatalytic Determination of Antioxidant Capacity in Beverages. *Biosens. Bioelectron.* **2011**, *26*, 2396–2401, doi:https://doi.org/10.1016/j.bios.2010.10.019.
  111. Zokhtareh, R.; Rahimnejad, M. A Novel Sensitive Electrochemical Sensor Based on Nickel Chloride Solution Modified Glassy Carbon Electrode for Curcumin Determination. *Electroanalysis* **2018**, *30*, 921–927, doi:https://doi.org/10.1002/elan.201700770.
  112. Ziyatdinova, G.K.; Nizamova, A.M.; Budnikov, H.C. Voltammetric Determination of Curcumin in Spices. *J. Anal. Chem.* **2012**, *67*, 591–594, doi:10.1134/S1061934812040132.
  113. Apetrei, C.; Apetrei, I.M.; De Saja, J.A.; Rodriguez-Mendez, M.L. Carbon Paste Electrodes Made from Different Carbonaceous Materials: Application in the Study of Antioxidants. *Sensors (Basel)*. **2011**, *11*, 1328–1344, doi:10.3390/s110201328.
  114. Litescu, S.-C.; Radu, G.-L. Estimation of the Antioxidative Properties of Tocopherols –

- an Electrochemical Approach. *Eur. Food Res. Technol.* **2000**, *211*, 218–221, doi:10.1007/s002170050027.
115. Liang, Z.; Zhai, H.; Chen, Z.; Wang, S.; Wang, H.; Wang, S. Sensors and Actuators B : Chemical A Sensitive Electrochemical Sensor for Flavonoids Based on a Multi-Walled Carbon Paste Electrode Modified by Cetyltrimethyl Ammonium Bromide-Carboxylic Multi-Walled Carbon Nanotubes. *Sensors Actuators B. Chem.* **2017**, *244*, 897–906, doi:10.1016/j.snb.2016.12.108.
116. Shono, T. Oxidation by Electrochemical Methods.
117. Union, I.; Pure, O.F.; Chemistry, A. INTERNATIONAL UNION OF PURE AND APPLIED CHEMISTRY COMMISSION ON ELECTROANALYTICAL CHEMISTRY \* RECOMMENDED TERMS , SYMBOLS , AND DEFINITIONS FOR. **1985**, *57*, 1491–1505.
118. Silva, D.H.S.; Pereira, F.C.; Yoshida, M.; Zanoni, M.V.B. Electrochemical Evaluation of Lipophilic Antioxidants from Iryanthera Juruensis Fruits ( Myristicaceae ). **2005**, *30*, 15–21.
119. Taylor, P.; Bertolino, F.A.; Stege, P.W.; Salinas, E. Electrochemical Study of the Antioxidant Activity and the Synergic Effect of Selenium with Natural and Synthetic Antioxidants. 37–41, doi:10.1080/00032711003687088.
120. Karikalan, N.; Karthik, R.; Chen, S.M.; Chen, H.A. A Voltammetric Determination of Caffeic Acid in Red Wines Based on the Nitrogen Doped Carbon Modified Glassy Carbon Electrode. *Sci. Rep.* **2017**, *7*, 1–10, doi:10.1038/srep45924.
121. Cormack, P.A.G.; Elorza, A.Z. Molecularly Imprinted Polymers: Synthesis and Characterisation. *J. Chromatogr. B* **2004**, *804*, 173–182, doi:https://doi.org/10.1016/j.jchromb.2004.02.013.
122. Shi, Y.; Zhang, J.-H.; Shi, D.; Jiang, M.; Zhu, Y.-X.; Mei, S.-R.; Zhou, Y.-K.; Dai, K.; Lu, B. Selective Solid-Phase Extraction of Cholesterol Using Molecularly Imprinted Polymers and Its Application in Different Biological Samples. *J. Pharm. Biomed. Anal.* **2006**, *42*, 549–555, doi:https://doi.org/10.1016/j.jpba.2006.05.022.
123. Włoch, M.; Datta, J. Synthesis and Polymerisation Techniques of Molecularly Imprinted Polymers. *Compr. Anal. Chem.* **2019**, *86*, 17–40, doi:10.1016/bs.coac.2019.05.011.
124. Baggiani, C.; Biagioli, F.; Anfossi, L.; Giovannoli, C.; Passini, C.; Giraudi, G. Effect of the Mimic Structure on the Molecular Recognition Properties of Molecularly Imprinted Polymers for Ochratoxin A Prepared by a Fragmental Approach. *React. Funct. Polym.* **2013**, *73*, 833–837, doi:https://doi.org/10.1016/j.reactfunctpolym.2013.03.018.
125. Gómez-Pineda, L.E.; Pina-Luis, G.E.; Cuán, Á.; García-Calzón, J.A.; Díaz-García, M.E. Physico-Chemical Characterization of Flavonol Molecularly Imprinted Polymers. *React. Funct. Polym.* **2011**, *71*, 402–408, doi:https://doi.org/10.1016/j.reactfunctpolym.2010.12.013.
126. Sergeeva, T.A.; Gorbach, L.A.; Piletska, E. V; Piletsky, S.A.; Brovko, O.O.; Honcharova, L.A.; Lutsyk, O.D.; Sergeeva, L.M.; Zinchenko, O.A.; El'skaya, A. V Colorimetric Test-Systems for Creatinine Detection Based on Composite Molecularly Imprinted Polymer Membranes. *Anal. Chim. Acta* **2013**, *770*, 161–168, doi:https://doi.org/10.1016/j.aca.2013.01.048.
127. Meier, F.; Schott, B.; Riedel, D.; Mizaikoff, B. Computational and Experimental Study on the Influence of the Porogen on the Selectivity of 4-Nitrophenol Molecularly Imprinted Polymers. *Anal. Chim. Acta* **2012**, *744*, 68–74, doi:https://doi.org/10.1016/j.aca.2012.07.020.
128. Nomachi, M.; Kubo, T.; Hosoya, K.; Kaya, K. Solvent Effects in the Preparation of Molecularly Imprinted Polymers for Melatonin Using N-Propionyl-5-

- Methoxytryptamine as the Pseudo Template. *Anal. Bioanal. Chem.* **2006**, *384*, 1291–1296, doi:10.1007/s00216-006-0310-z.
129. Turiel, E.; Martín-Esteban, A. Molecularly Imprinted Polymers for Sample Preparation: A Review. *Anal. Chim. Acta* **2010**, *668*, 87–99, doi:10.1016/j.aca.2010.04.019.
130. Pichon, V. Selective Sample Treatment Using Molecularly Imprinted Polymers. *J. Chromatogr. A* **2007**, *1152*, 41–53, doi:10.1016/j.chroma.2007.02.109.
131. Pichon, V. *Aptamer-Based and Immunosorbents*; Elsevier Inc.: Amsterdam, Netherlands, 2019; ISBN 9780128169063.
132. Acquah, C.; Danquah, M.K.; Yon, J.L.S.; Sidhu, A.; Ongkudon, C.M. A Review on Immobilised Aptamers for High Throughput Biomolecular Detection and Screening. *Anal. Chim. Acta* **2015**, *888*, 10–18, doi:https://doi.org/10.1016/j.aca.2015.05.050.
133. Du, F.; Guo, L.; Qin, Q.; Zheng, X.; Ruan, G.; Li, J.; Li, G. Recent Advances in Aptamer-Functionalized Materials in Sample Preparation. *TrAC Trends Anal. Chem.* **2015**, *67*, 134–146, doi:https://doi.org/10.1016/j.trac.2015.01.007.
134. Sellergren, B. Direct Drug Determination by Selective Sample Enrichment on an Imprinted Polymer. *Anal. Chem.* **1994**, *66*, 1578–1582, doi:10.1021/ac00081a036.
135. Puoci, F.; Garreffa, C.; Iemma, F.; Muzzalupo, R.; Spizzirri, U.G.; Picci, N. Molecularly Imprinted Solid Phase Extraction for Detection of Sudan I in Food Matrices. *Food Chem.* **2005**, *93*, 349–353, doi:https://doi.org/10.1016/j.foodchem.2004.11.014.
136. Farrington, K.; Magner, E.; Regan, F. Predicting the Performance of Molecularly Imprinted Polymers: Selective Extraction of Caffeine by Molecularly Imprinted Solid Phase Extraction. *Anal. Chim. Acta* **2006**, *566*, 60–68, doi:https://doi.org/10.1016/j.aca.2006.02.057.
137. Jiang, T.; Zhao, L.; Chu, B.; Feng, Q.; Yan, W.; Lin, J.-M. Molecularly Imprinted Solid-Phase Extraction for the Selective Determination of 17 $\beta$ -Estradiol in Fishery Samples with High Performance Liquid Chromatography. *Talanta* **2009**, *78*, 442–447, doi:https://doi.org/10.1016/j.talanta.2008.11.047.
138. Sun, X.; Wang, M.; Peng, J.; Yang, L.; Wang, X.; Wang, F.; Zhang, X.; Wu, Q.; Chen, R.; Chen, J. Dummy Molecularly Imprinted Solid Phase Extraction of Climbazole from Environmental Water Samples. *Talanta* **2019**, *196*, 47–53, doi:https://doi.org/10.1016/j.talanta.2018.12.017.
139. Sun, X.; Wang, M.; Yang, L.; Wen, H.; Wang, L.; Li, T.; Tang, C.; Yang, J. Preparation and Evaluation of Dummy-Template Molecularly Imprinted Polymer as a Potential Sorbent for Solid Phase Extraction of Imidazole Fungicides from River Water. *J. Chromatogr. A* **2019**, *1586*, 1–8, doi:https://doi.org/10.1016/j.chroma.2018.11.077.
140. Li, Z.; Qian, Z.; Hu, S.; Gong, T.; Xian, Q. Molecularly Imprinted Solid Phase Extraction Coupled with Gas Chromatography-Mass Spectrometry for Determination of N-Nitrosodiphenylamine in Water Samples. *Chemosphere* **2018**, *212*, 872–880, doi:https://doi.org/10.1016/j.chemosphere.2018.08.159.
141. Wang, C.; Cheng, L.; Zhang, L.; Zuo, Y. Graphene Oxide Based Molecularly Imprinted Polymers Modified with  $\beta$ -Cyclodextrin for Selective Extraction of Di(2-Ethylhexyl) Phthalate in Environmental Waters. *J. Sep. Sci.* **2019**, *42*, 1248–1256, doi:10.1002/jssc.201801171.
142. Zhu, G.; Cheng, G.; Wang, P.; Li, W.; Wang, Y.; Fan, J. Water Compatible Imprinted Polymer Prepared in Water for Selective Solid Phase Extraction and Determination of Ciprofloxacin in Real Samples. *Talanta* **2019**, *200*, 307–315, doi:https://doi.org/10.1016/j.talanta.2019.03.070.
143. Kadirvel, P.; Combès, A.; Bordron, L.; Pichon, V. Development and Application of Water-Compatible Molecularly Imprinted Polymers for the Selective Extraction of

- Carbamazepine from Environmental Waters. *Anal. Bioanal. Chem.* **2019**, *411*, 1525–1536, doi:10.1007/s00216-019-01586-8.
144. Wang, M.; Chang, X.; Wu, X.; Yan, H.; Qiao, F. Water-Compatible Dummy Molecularly Imprinted Resin Prepared in Aqueous Solution for Green Miniaturized Solid-Phase Extraction of Plant Growth Regulators. *J. Chromatogr. A* **2016**, *1458*, 9–17, doi:https://doi.org/10.1016/j.chroma.2016.06.047.
145. Wang, M.; Liang, S.; Bai, L.; Qiao, F.; Yan, H. Green Protocol for the Preparation of Hydrophilic Molecularly Imprinted Resin in Water for the Efficient Selective Extraction and Determination of Plant Hormones from Bean Sprouts. *Anal. Chim. Acta* **2019**, *1064*, 47–55, doi:https://doi.org/10.1016/j.aca.2019.03.025.
146. Wan, Y.; Wang, M.; Fu, Q.; Wang, L.; Wang, D.; Zhang, K.; Xia, Z.; Gao, D. Novel Dual Functional Monomers Based Molecularly Imprinted Polymers for Selective Extraction of Myricetin from Herbal Medicines. *J. Chromatogr. B* **2018**, *1097–1098*, 1–9, doi:https://doi.org/10.1016/j.jchromb.2018.08.033.
147. Mansour, M.S.M.; Abdel-Shafy, H.I.; Mehaya, F.M.S. Valorization of Food Solid Waste by Recovery of Polyphenols Using Hybrid Molecular Imprinted Membrane. *J. Environ. Chem. Eng.* **2018**, *6*, 4160–4170, doi:https://doi.org/10.1016/j.jece.2018.06.019.
148. Rui, C.; He, J.; Li, Y.; Liang, Y.; You, L.; He, L.; Li, K.; Zhang, S. Selective Extraction and Enrichment of Aflatoxins from Food Samples by Mesoporous Silica FDU-12 Supported Aflatoxins Imprinted Polymers Based on Surface Molecularly Imprinting Technique. *Talanta* **2019**, *201*, 342–349, doi:https://doi.org/10.1016/j.talanta.2019.04.019.
149. Yu, H.; He, Y.; She, Y.; Wang, M.; Yan, Z.; Ren, J.H.; Cao, Z.; Shao, Y.; Wang, S.; Abd El-Aty, A.M.; et al. Preparation of Molecularly Imprinted Polymers Coupled with High-Performance Liquid Chromatography for the Selective Extraction of Salidroside from *Rhodiola Crenulata*. *J. Chromatogr. B* **2019**, *1118–1119*, 180–186, doi:https://doi.org/10.1016/j.jchromb.2019.04.004.
150. Balamurugan, K.; Gokulakrishnan, K.; Prakasam, T. Preparation and Evaluation of Molecularly Imprinted Polymer Liquid Chromatography Column for the Separation of Cathine Enantiomers. *Saudi Pharm. J. SPJ Off. Publ. Saudi Pharm. Soc.* **2012**, *20*, 53–61, doi:10.1016/j.jsps.2011.06.004.
151. Yang, S.; Wang, Y.; Jiang, Y.; Li, S.; Liu, W. Molecularly Imprinted Polymers for the Identification and Separation of Chiral Drugs and Biomolecules. *Polymers (Basel)*. **2016**, *8*, doi:10.3390/polym8060216.
152. Remcho, V.T.; Tan, Z.J. MIPs as Chromatographic Stationary. *Anal. Chem.* **1999**, *71*, doi:10.1021/ac990292q.
153. Zander, Å.; Findlay, P.; Renner, T.; Sellergren, B.; Swietlow, A. Analysis of Nicotine and Its Oxidation Products in Nicotine Chewing Gum by a Molecularly Imprinted Solid-Phase Extraction. *Anal. Chem.* **1998**, *70*, 3304–3314, doi:10.1021/ac971272w.
154. Li, H.; Liu, Y.; Zhang, Z.; Liao, H.; Nie, L.; Yao, S. Separation and Purification of Chlorogenic Acid by Molecularly Imprinted Polymer Monolithic Stationary Phase. *J. Chromatogr. A* **2005**, *1098*, 66–74, doi:10.1016/j.chroma.2005.08.046.
155. Alexander, C.; Andersson, H.S.; Andersson, L.I.; Ansell, R.J.; Kirsch, N.; Nicholls, I.A.; O'Mahony, J.; Whitcombe, M.J. Molecular Imprinting Science and Technology: A Survey of the Literature for the Years up to and Including 2003. *J. Mol. Recognit.* **2006**, *19*, 106–180, doi:10.1002/jmr.760.
156. Huang, X.; Zou, H.; Chen, X.; Luo, Q.; Kong, L. Molecularly Imprinted Monolithic Stationary Phases for Liquid Chromatographic Separation of Enantiomers and Diastereomers. *J. Chromatogr. A* **2003**, *984*, 273–282,

- doi:[https://doi.org/10.1016/S0021-9673\(02\)01768-5](https://doi.org/10.1016/S0021-9673(02)01768-5).
157. Kriz, D.; Kempe, M.; Mosbach, K. Introduction of Molecularly Imprinted Polymers as Recognition Elements in Conductometric Chemical Sensors. *Sensors Actuators, B Chem.* **1996**, *33*, 178–181, doi:10.1016/0925-4005(96)80094-3.
  158. Ansell, R.J. Characterization of the Binding Properties of Molecularly Imprinted Polymers. *Adv. Biochem. Eng. Biotechnol.* **2015**, *150*, 51–93, doi:10.1007/10\_2015\_316.
  159. Dickert, F.L.; Forth, P.; Lieberzeit, P.; Tortschanoff, M. Molecular Imprinting in Chemical Sensing – Detection of Aromatic and Halogenated Hydrocarbons as Well as Polar Solvent Vapors. *Fresenius. J. Anal. Chem.* **1998**, *360*, 759–762, doi:10.1007/s002160050801.
  160. Jakusch, M.; Janotta, M.; Mizaikoff, B.; Mosbach, K.; Haupt, K. Molecularly Imprinted Polymers and Infrared Evanescent Wave Spectroscopy. A Chemical Sensors Approach. *Anal. Chem.* **1999**, *71*, 4786–4791, doi:10.1021/ac990050q.
  161. Gui, R.; Jin, H.; Guo, H.; Wang, Z. Biosensors and Bioelectronics Recent Advances and Future Prospects in Molecularly Imprinted Polymers-Based Electrochemical Biosensors. **2018**, *100*, 56–70.
  162. Puoci, F.; Cirillo, G.; Curcio, M.; Iemma, F.; Parisi, O.I.; Castiglione, M.; Picci, N.; Puoci, F.; Cirillo, G.; Curcio, M.; et al. Molecularly Imprinted Polymers for  $\alpha$  - Tocopherol Delivery Molecularly Imprinted Polymers for  $\alpha$  -Tocopherol Delivery. **2008**, *7544*, doi:10.1080/10717540802006724.
  163. Piacham, T.; Nantasenamat, C.; Suksrichavalit, T.; Puttipanyalears, C.; Pissawong, T.; Maneewas, S.; Isarankura-Na-Ayudhya, C.; Prachayasittikul, V. Synthesis and Theoretical Study of Molecularly Imprinted Nanospheres for Recognition of Tocopherols. *Molecules* **2009**, *14*, 2985–3002, doi:10.3390/molecules14082985.
  164. Castro López, M. del M.; Cela Pérez, M.C.; Dopico García, M.S.; López Vilariño, J.M.; González Rodríguez, M.V.; Barral Losada, L.F. Preparation, Evaluation and Characterization of Quercetin-Molecularly Imprinted Polymer for Preconcentration and Clean-up of Catechins. *Anal. Chim. Acta* **2012**, *721*, 68–78, doi:10.1016/j.aca.2012.01.049.
  165. Piacham, T.; Isarankura-Na-Ayudhya, C.; Prachayasittikul, V. Quercetin-Imprinted Polymer for Anthocyanin Extraction from Mangosteen Pericarp. *Mater. Sci. Eng. C* **2015**, *51*, 127–131, doi:10.1016/j.msec.2015.02.051.
  166. Xie, J.; Zhu, L.; Luo, H.; Zhou, L.; Li, C.; Xu, X. Direct Extraction of Specific Pharmacophoric Flavonoids from Gingko Leaves Using a Molecularly Imprinted Polymer for Quercetin. *J. Chromatogr. A* **2001**, *934*, 1–11, doi:[https://doi.org/10.1016/S0021-9673\(01\)01294-8](https://doi.org/10.1016/S0021-9673(01)01294-8).
  167. Zhu, L.; Xu, X. Selective Separation of Active Inhibitors of Epidermal Growth Factor Receptor from Caragana Jubata by Molecularly Imprinted Solid-Phase Extraction. *J. Chromatogr. A* **2003**, *991*, 151–158, doi:[https://doi.org/10.1016/S0021-9673\(03\)00207-3](https://doi.org/10.1016/S0021-9673(03)00207-3).
  168. Theodoridis, G.; Tegou, A.; Giantsiou, N.; Jandera, P. Original Paper Molecular Imprinting of Natural Flavonoid Antioxidants : Application in Solid-Phase Extraction for the Sample Pretreatment of Natural Products Prior to HPLC Analysis. **2006**, 2310–2321, doi:10.1002/jssc.200500492.
  169. Blahová, E.; Lehotay, J.; Skačáni, I. The Use of Molecularly Imprinted Polymer for Selective Extraction of (+)-Catechin. *J. Liq. Chromatogr. Relat. Technol.* **2004**, *27*, 2715–2731, doi:10.1081/JLC-200029276.
  170. Triadhi, U.; Zulfikar, M.A.; Setiyanto, H.; Amran, M.B. Effects of (Monomer - Crosslinker - Initiator) Composition during Non Imprinted Polymers Synthesis for

- Catechin Retention. *J. Phys. Conf. Ser.* **2018**, *1013*, doi:10.1088/1742-6596/1013/1/012192.
171. Valero-Navarro, Á.; Gómez-Romero, M.; Fernández-Sánchez, J.F.; Cormack, P.A.G.; Segura-Carretero, A.; Fernández-Gutiérrez, A. Synthesis of Caffeic Acid Molecularly Imprinted Polymer Microspheres and High-Performance Liquid Chromatography Evaluation of Their Sorption Properties. *J. Chromatogr. A* **2011**, *1218*, 7289–7296, doi:10.1016/j.chroma.2011.08.043.
172. Michailof, C.; Manesiotis, P.; Panayiotou, C. Synthesis of Caffeic Acid and P-Hydroxybenzoic Acid Molecularly Imprinted Polymers and Their Application for the Selective Extraction of Polyphenols from Olive Mill Waste Waters. *J. Chromatogr. A* **2008**, *1182*, 25–33, doi:10.1016/j.chroma.2008.01.001.
173. Fan, D.; Jia, L.; Xiang, H.; Peng, M.; Li, H.; Shi, S. Synthesis and Characterization of Hollow Porous Molecular Imprinted Polymers for the Selective Extraction and Determination of Caffeic Acid in Fruit Samples. *Food Chem.* **2017**, *224*, 32–36, doi:10.1016/j.foodchem.2016.12.042.
174. Li, N.; Bun, T.; Ho, J.; Xuan, J.; Ni, Y.; Zhou, R.; Rong, R. Separation and Purification of the Antioxidant Compounds, Caffeic Acid Phenethyl Ester and Caffeic Acid from Mushrooms by Molecularly Imprinted Polymer. *Food Chem.* **2013**, *139*, 1161–1167, doi:10.1016/j.foodchem.2013.01.084.
175. Schwarz, L.J.; Danylec, B.; Harris, S.J.; Boysen, R.I.; Hearn, M.T.W. Preparation of Molecularly Imprinted Polymers for the Selective Recognition of the Bioactive Polyphenol, (E)-Resveratrol. *J. Chromatogr. A* **2011**, *1218*, 2189–2195, doi:10.1016/j.chroma.2011.02.043.
176. Pilau, E.J.; Silva, R.G.C.; Jardim, I.C.F.S.; Augusto, F. Molecularly Imprinted Sol-Gel Silica for Solid Phase Extraction of Phenobarbital. *J. Braz. Chem. Soc.* **2008**, *19*, 1136–1143, doi:10.1590/S0103-50532008000600013.
177. Cummins, W.; Duggan, P.; McLoughlin, P. A Comparative Study of the Potential of Acrylic and Sol-Gel Polymers for Molecular Imprinting. *Anal. Chim. Acta* **2005**, *542*, 52–60, doi:10.1016/j.aca.2005.01.042.
178. Bitar, M.; Lafarge, C.; Sok, N.; Cayot, P.; Bou-Maroun, E. Molecularly Imprinted Sol-Gel Polymers for the Analysis of Iprodione Fungicide in Wine: Synthesis in Green Solvent. *Food Chem.* **2019**, *293*, 226–232, doi:10.1016/j.foodchem.2019.04.108.
179. Lafarge, C.; Bitar, M.; El Hosry, L.; Cayot, P.; Bou-Maroun, E. Comparison of Molecularly Imprinted Polymers (MIP) and Sol-Gel Molecularly Imprinted Silica (MIS) for Fungicide in a Hydro Alcoholic Solution. *Mater. Today Commun.* **2020**, *24*, 101157, doi:10.1016/j.mtcomm.2020.101157.
180. Díaz-García, M.E.; Laíño, R.B. Molecular Imprinting in Sol-Gel Materials: Recent Developments and Applications. *Microchim. Acta* **2005**, *149*, 19–36, doi:10.1007/s00604-004-0274-7.
181. Moein, M.M.; Abdel-Rehim, A.; Abdel-Rehim, M. Recent Applications of Molecularly Imprinted Sol-Gel Methodology in Sample Preparation. *Molecules* **2019**, *24*, 1–12, doi:10.3390/molecules24162889.
182. Marx, S.; Liron, Z. Molecular Imprinting in Thin Films of Organic-Inorganic Hybrid Sol-Gel and Acrylic Polymers. *Chem. Mater.* **2001**, *13*, 3624–3630, doi:10.1021/cm000983z.
183. da Costa Silva, R.G.; Augusto, F. Sol-Gel Molecular Imprinted Ormosil for Solid-Phase Extraction of Methylxanthines. *J. Chromatogr. A* **2006**, *1114*, 216–223, doi:https://doi.org/10.1016/j.chroma.2006.03.073.
184. Wang, L.; Zhi, K.; Zhang, Y.; Liu, Y.; Zhang, L.; Yasin, A.; Lin, Q. Molecularly

- Imprinted Polymers for Gossypol via Sol-Gel, Bulk, and Surface Layer Imprinting-A Comparative Study. *Polymers (Basel)*. **2019**, *11*, doi:10.3390/polym11040602.
185. Junping, W.; Mingfei, P.; Guozhen, F.; Shuo, W. Preparation of a Novel Molecularly Imprinted Polymer by a Sol-Gel Process for on-Line Solid-Phase Extraction Coupled with High Performance Liquid Chromatography to Detect Trace Enrofloxacin in Fish and Chicken Samples. *Microchim. Acta* **2009**, *166*, 295–302, doi:10.1007/s00604-009-0205-8.
186. Duan, Z.-J.; Fan, L.-P.; Fang, G.-Z.; Yi, J.-H.; Wang, S. Novel Surface Molecularly Imprinted Sol-Gel Polymer Applied to the Online Solid Phase Extraction of Methyl-3-Quinoxaline-2-Carboxylic Acid and Quinoxaline-2-Carboxylic Acid from Pork Muscle. *Anal. Bioanal. Chem.* **2011**, *401*, 2291–2299, doi:10.1007/s00216-011-5329-0.
187. Sadeghi, S.; Jahani, M. Solid-Phase Extraction of Florfenicol from Meat Samples by a Newly Synthesized Surface Molecularly Imprinted Sol-Gel Polymer. *Food Anal. Methods* **2014**, *7*, 2084–2094, doi:10.1007/s12161-014-9849-z.
188. Boulanouar, S.; Combès, A.; Mezzache, S.; Pichon, V. Synthesis and Application of Molecularly Imprinted Silica for the Selective Extraction of Some Polar Organophosphorus Pesticides from Almond Oil. *Anal. Chim. Acta* **2018**, *1018*, 35–44, doi:10.1016/j.aca.2018.02.069.
189. Rajabi Khorrami, A.; Pasandideh, Y. Preparation of a Novel Sol-Gel Molecularly Imprinted Polymer with Dummy Template for On-Line Solid-Phase Extraction of Patulin from Apple Juice Samples. *Int. J. Anal. Tech.* **2016**, *2*, 1–7, doi:10.15226/2471-3627/2/1/00106.
190. Kia, S.; Fazilati, M.; Salavati, H.; Bohlooli, S. Preparation of a Novel Molecularly Imprinted Polymer by the Sol-Gel Process for Solid Phase Extraction of Vitamin D3. *RSC Adv.* **2016**, *6*, 31906–31914, doi:10.1039/C6RA04627D.
191. Bagheri, H.; Piri-Moghadam, H.; Bayat, P.; Balalaie, S. Application of Sol-Gel Based Molecularly Imprinted Xerogel for on-Line Capillary Microextraction of Fentanyl from Urine and Plasma Samples. *Anal. Methods* **2013**, *5*, doi:10.1039/c3ay41559g.
192. Moein, M.M.; Jabbar, D.; Colmsjö, A.; Abdel-Rehim, M. A Needle Extraction Utilizing a Molecularly Imprinted-Sol-Gel Xerogel for on-Line Microextraction of the Lung Cancer Biomarker Bilirubin from Plasma and Urine Samples. *J. Chromatogr. A* **2014**, *1366*, 15–23, doi:10.1016/j.chroma.2014.09.012.
193. Lin, C.I.; Joseph, A.K.; Chang, C.K.; Wang, Y.C.; Lee, Y. Der Synthesis of Molecular Imprinted Organic-Inorganic Hybrid Polymer Binding Caffeine. *Anal. Chim. Acta* **2003**, *481*, 175–180, doi:https://doi.org/10.1016/S0003-2670(03)00095-3.
194. Arabi, M.; Ghaedi, M.; Ostovan, A. Synthesis and Application of In-Situ Molecularly Imprinted Silica Monolithic in Pipette-Tip Solid-Phase Microextraction for the Separation and Determination of Gallic Acid in Orange Juice Samples. *J. Chromatogr. B Anal. Technol. Biomed. Life Sci.* **2017**, *1048*, 102–110, doi:10.1016/j.jchromb.2017.02.016.
195. Yang, P.; Hou, W.D.; Qiu, H.D.; Liu, X.; Jiang, S.X. Preparation of Quercetin Imprinted Core-Shell Organosilicate Microspheres Using Surface Imprinting Technique. *Chinese Chem. Lett.* **2012**, *23*, 615–618, doi:https://doi.org/10.1016/j.ccllet.2012.02.002.
196. Braga, L.R.; Rosa, A.A.; Dias, A.C.B. Synthesis and Characterization of Molecularly Imprinted Silica Mediated by Al for Solid Phase Extraction of Quercetin in Ginkgo Biloba L. *Anal. Methods* **2014**, *6*, 4029–4037, doi:10.1039/c4ay00471j.
197. Xu, X.; Xu, G.; Wei, F.; Cen, Y.; Shi, M.; Cheng, X.; Chai, Y.; Sohail, M.; Hu, Q. Carbon Dots Coated with Molecularly Imprinted Polymers: A Facile Bioprobe for Fluorescent Determination of Caffeic Acid. *J. Colloid Interface Sci.* **2018**, *529*, 568–574,

- doi:<https://doi.org/10.1016/j.jcis.2018.06.050>.
198. Wei, H.-S.; Tsai, Y.-L.; Wu, J.-Y.; Chen, H. Preparation of Inorganic Molecularly Imprinted Polymers with Higher Adsorption and Selectivity by Sol-Gel Method. *J. Chromatogr. B. Analyt. Technol. Biomed. Life Sci.* **2006**, *836*, 57–62, doi:10.1016/j.jchromb.2006.03.047.
  199. Shin, M. Inorganic Molecularly Imprinted Polymer by Sol-Gel Process for Recognition of Caffeine. *Open J. Org. Polym. Mater.* **2013**, *03*, 1–5, doi:10.4236/ojopm.2013.31001.
  200. Bianchini, C.; Curulli, A.; Pasquali, M.; Zane, D. Determination of Caffeic Acid in Wine Using PEDOT Film Modified Electrode. *Food Chem.* **2014**, *156*, 81–86, doi:10.1016/j.foodchem.2014.01.074.
  201. Velmurugan, M.; Balasubramanian, P.; Chen, S.M. Determination of Caffeic Acid in Wine Samples Based on the Electrochemical Reduction of Graphene Oxide Modified Screen Printed Carbon Electrode. *Int. J. Electrochem. Sci.* **2017**, *12*, 4173–4182, doi:10.20964/2017.05.01.
  202. Ziyatdinova, G.; Salikhova, I.; Budnikov, H. Chronoamperometric Estimation of Cognac and Brandy Antioxidant Capacity Using MWNT Modified Glassy Carbon Electrode. *Talanta* **2014**, *125*, 378–384, doi:10.1016/j.talanta.2014.03.039.
  203. Ziyatdinova, G.; Aytuganova, I.; Nizamova, A.; Budnikov, H. Differential Pulse Voltammetric Assay of Coffee Antioxidant Capacity with MWNT-Modified Electrode. *Food Anal. Methods* **2013**, *6*, 1629–1638, doi:10.1007/s12161-013-9591-y.
  204. Ziyatdinova, G.; Kozlova, E.; Budnikov, H. Chronocoulometry of Wine on Multi-Walled Carbon Nanotube Modified Electrode: Antioxidant Capacity Assay. *Food Chem.* **2016**, *196*, 405–410, doi:10.1016/j.foodchem.2015.09.075.
  205. Raymundo-Pereira, P.A.; Campos, A.M.; Prado, T.M.; Furini, L.N.; Boas, N. V.; Calegario, M.L.; Machado, S.A.S. Synergy between Printex Nano-Carbons and Silver Nanoparticles for Sensitive Estimation of Antioxidant Activity. *Anal. Chim. Acta* **2016**, *926*, 88–98, doi:10.1016/j.aca.2016.04.036.
  206. Hui, K.H.; Ambrosi, A.; Pumera, M.; Bonanni, A. Improving the Analytical Performance of Graphene Oxide towards the Assessment of Polyphenols. *Chemistry* **2016**, *22*, 3830–3834, doi:10.1002/chem.201503852.
  207. Chng, C.; Sofer, Z.; Pumera, M.; Bonanni, A. Doped and Undoped Graphene Platforms: The Influence of Structural Properties on the Detection of Polyphenols. *Sci. Rep.* **2016**, *6*, 20673, doi:10.1038/srep20673.
  208. Tirawattanakoson, R.; Rattanarat, P.; Ngamrojanavanich, N.; Rodthongkum, N.; Chailapakul, O. Free Radical Scavenger Screening of Total Antioxidant Capacity in Herb and Beverage Using Graphene/PEDOT: PSS-Modified Electrochemical Sensor. *J. Electroanal. Chem.* **2016**, *767*, 68–75, doi:<https://doi.org/10.1016/j.jelechem.2015.11.037>.
  209. Arribas, A.S.; Martínez-Fernández, M.; Moreno, M.; Bermejo, E.; Zapardiel, A.; Chicharro, M. Analysis of Total Polyphenols in Wines by FIA with Highly Stable Amperometric Detection Using Carbon Nanotube-Modified Electrodes. *Food Chem.* **2013**, *136*, 1183–1192, doi:10.1016/j.foodchem.2012.09.027.
  210. Eguílaz, M.; Gutiérrez, A.; Gutierrez, F.; González-Domínguez, J.M.; Ansón-Casaos, A.; Hernández-Ferrer, J.; Ferreyra, N.F.; Martínez, M.T.; Rivas, G. Covalent Functionalization of Single-Walled Carbon Nanotubes with Polytyrosine: Characterization and Analytical Applications for the Sensitive Quantification of Polyphenols. *Anal. Chim. Acta* **2016**, *909*, 51–59, doi:10.1016/j.aca.2015.12.031.
  211. Del Carlo, M.; Amine, A.; Haddam, M.; della Pelle, F.; Fusella, G.C.; Compagnone, D. Selective Voltammetric Analysis of O-Diphenols from Olive Oil Using Na<sub>2</sub>MoO<sub>4</sub> as

- Electrochemical Mediator. *Electroanalysis* **2012**, *24*, 889–896, doi:doi:10.1002/elan.201100603.
212. Andrei, V.; Sharpe, E.; Vasilescu, A.; Andreescu, S. A Single Use Electrochemical Sensor Based on Biomimetic Nanoceria for the Detection of Wine Antioxidants. *Talanta* **2016**, *156–157*, 112–118, doi:10.1016/j.talanta.2016.04.067.
213. Cetó, X.; Céspedes, F.; Pividori, M.I.; Gutiérrez, J.M.; del Valle, M. Resolution of Phenolic Antioxidant Mixtures Employing a Voltammetric Bio-Electronic Tongue. *Analyst* **2012**, *137*, 349–356, doi:10.1039/c1an15456g.
214. Kumar, A.S.; Shanmugam, R.; Nellaiappan, S.; Thangaraj, R. Tea Quality Assessment by Analyzing Key Polyphenolic Functional Groups Using Flow Injection Analysis Coupled with a Dual Electrochemical Detector. *Sensors Actuators B Chem.* **2016**, *227*, 352–361, doi:https://doi.org/10.1016/j.snb.2015.12.072.
215. Magro, M.; Bonaiuto, E.; Baratella, D.; de Almeida Roger, J.; Jakubec, P.; Corraducci, V.; Tuček, J.; Malina, O.; Zbořil, R.; Vianello, F. Electrocatalytic Nanostructured Ferric Tannates: Characterization and Application of a Polyphenol Nanosensor. *Chemphyschem* **2016**, *17*, 3196–3203, doi:10.1002/cphc.201600718.
216. De Beer, D.; Harbertson, J.; Kilmartin, P.A.; V, R.; T, B.; Adams, D.O.; Waterhouse, A. Phenolics: A Comparison of Diverse Analytical Methods. *Am. J. Enol. Vitic.* **2004**, *55*, 389–400.
217. Florea, A.; Cristea, C.; Vocanson, F.; Săndulescu, R.; Jaffrezic-Renault, N. Electrochemical Sensor for the Detection of Estradiol Based on Electropolymerized Molecularly Imprinted Polythioaniline Film with Signal Amplification Using Gold Nanoparticles. *Electrochem. commun.* **2015**, *59*, 36–39, doi:10.1016/j.elecom.2015.06.021.
218. Han, Q.; Shen, X.; Zhu, W.; Zhu, C.; Zhou, X.; Jiang, H. Magnetic Sensing Film Based on Fe<sub>3</sub>O<sub>4</sub>@Au-GSH Molecularly Imprinted Polymers for the Electrochemical Detection of Estradiol. *Biosens. Bioelectron.* **2016**, *79*, 180–186, doi:10.1016/j.bios.2015.12.017.
219. Liu, W.; Ma, Y.; Sun, G.; Wang, S.; Deng, J.; Wei, H. Molecularly Imprinted Polymers on Graphene Oxide Surface for EIS Sensing of Testosterone. *Biosens. Bioelectron.* **2017**, *92*, 305–312, doi:10.1016/j.bios.2016.11.007.
220. Wang, Y.; Cao, Y.; Fang, C.; Gong, Q. Electrochemical Sensor for Parabens Based on Molecular Imprinting Polymers with Dual-Templates. *Anal. Chim. Acta* **2010**, *673*, 145–150, doi:10.1016/j.aca.2010.05.039.
221. Jolly, P.; Tamboli, V.; Harniman, R.L.; Estrela, P.; Allender, C.J.; Bowen, J.L. Aptamer-MIP Hybrid Receptor for Highly Sensitive Electrochemical Detection of Prostate Specific Antigen. *Biosens. Bioelectron.* **2016**, *75*, 188–195, doi:10.1016/j.bios.2015.08.043.
222. Silva, B.V.M.; Rodríguez, B.A.G.; Sales, G.F.; Sotomayor, M.D.P.T.; Dutra, R.F. An Ultrasensitive Human Cardiac Troponin T Graphene Screen-Printed Electrode Based on Electropolymerized-Molecularly Imprinted Conducting Polymer. *Biosens. Bioelectron.* **2016**, *77*, 978–985, doi:10.1016/j.bios.2015.10.068.
223. Wang, Y.; Han, M.; Liu, G.; Hou, X.; Huang, Y.; Wu, K.; Li, C. Molecularly Imprinted Electrochemical Sensing Interface Based on In-Situ-Polymerization of Amino-Functionalized Ionic Liquid for Specific Recognition of Bovine Serum Albumin. *Biosens. Bioelectron.* **2015**, *74*, 792–798, doi:10.1016/j.bios.2015.07.046.
224. Chen, H.J.; Zhang, Z.H.; Luo, L.J.; Yao, S.Z. Surface-Imprinted Chitosan-Coated Magnetic Nanoparticles Modified Multi-Walled Carbon Nanotubes Biosensor for Detection of Bovine Serum Albumin. *Sensors Actuators, B Chem.* **2012**, *163*, 76–83, doi:10.1016/j.snb.2012.01.010.

225. Cieplak, M.; Szwabinska, K.; Sosnowska, M.; Chandra, B.K.C.; Borowicz, P.; Noworyta, K.; D'Souza, F.; Kutner, W. Selective Electrochemical Sensing of Human Serum Albumin by Semi-Covalent Molecular Imprinting. *Biosens. Bioelectron.* **2015**, *74*, 960–966, doi:10.1016/j.bios.2015.07.061.
226. Moreira, F.T.C.; Sharma, S.; Dutra, R.A.F.; Noronha, J.P.C.; Cass, A.E.G.; Sales, M.G.F. Smart Plastic Antibody Material (SPAM) Tailored on Disposable Screen Printed Electrodes for Protein Recognition: Application to Myoglobin Detection. *Biosens. Bioelectron.* **2013**, *45*, 237–244, doi:10.1016/j.bios.2013.02.012.
227. Karaseva, N.; Ermolaeva, T.; Mizaikoff, B. Piezoelectric Sensors Using Molecularly Imprinted Nanospheres for the Detection of Antibiotics. *Sensors Actuators, B Chem.* **2016**, *225*, 199–208, doi:10.1016/j.snb.2015.11.045.
228. Turco, A.; Corvaglia, S.; Mazzotta, E. Electrochemical Sensor for Sulfadimethoxine Based on Molecularly Imprinted Polypyrrole: Study of Imprinting Parameters. *Biosens. Bioelectron.* **2015**, *63*, 240–247, doi:10.1016/j.bios.2014.07.045.
229. Singh, P.; Kim, Y.-J.; Hoang, V.-A.; Farh, M.E.-A.; Yang, D.-C. *Sphingomonas Panacis* Sp. Nov., Isolated from Rhizosphere of Rusty Ginseng. *Antonie Van Leeuwenhoek* **2015**, *108*, 711–720, doi:10.1007/s10482-015-0527-y.
230. Lopes, F.; Pacheco, J.G.; Rebelo, P.; Delerue-Matos, C. Molecularly Imprinted Electrochemical Sensor Prepared on a Screen Printed Carbon Electrode for Naloxone Detection. *Sensors Actuators, B Chem.* **2017**, *243*, 745–752, doi:10.1016/j.snb.2016.12.031.
231. Huang, B.; Xiao, L.; Dong, H.; Zhang, X.; Gan, W.; Mahboob, S.; Al-Ghanim, K.A.; Yuan, Q.; Li, Y. Electrochemical Sensing Platform Based on Molecularly Imprinted Polymer Decorated N,S Co-Doped Activated Graphene for Ultrasensitive and Selective Determination of Cyclophosphamide. *Talanta* **2017**, *164*, 601–607, doi:10.1016/j.talanta.2016.11.009.
232. Long, F.; Zhang, Z.; Yang, Z.; Zeng, J.; Jiang, Y. Imprinted Electrochemical Sensor Based on Magnetic Multi-Walled Carbon Nanotube for Sensitive Determination of Kanamycin. *J. Electroanal. Chem.* **2015**, *755*, 7–14, doi:10.1016/j.jelechem.2015.07.018.
233. Teng, Y.; Fan, L.; Dai, Y.; Zhong, M.; Lu, X.; Kan, X. Electrochemical Sensor for Paracetamol Recognition and Detection Based on Catalytic and Imprinted Composite Film. *Biosens. Bioelectron.* **2015**, *71*, 137–142, doi:10.1016/j.bios.2015.04.037.
234. Prasad, B.B.; Jauhari, D. A Dual-Template Biomimetic Molecularly Imprinted Dendrimer-Based Piezoelectric Sensor for Ultratrace Analysis of Organochlorine Pesticides. *Sensors Actuators, B Chem.* **2015**, *207*, 542–551, doi:10.1016/j.snb.2014.10.115.
235. Bakas, I.; Hayat, A.; Piletsky, S.; Piletska, E.; Chehimi, M.M.; Noguer, T.; Rouillon, R. Electrochemical Impedimetric Sensor Based on Molecularly Imprinted Polymers/Sol-Gel Chemistry for Methidathion Organophosphorous Insecticide Recognition. *Talanta* **2014**, *130*, 294–298, doi:10.1016/j.talanta.2014.07.012.
236. Gu, Y.; Yan, X.; Li, C.; Zheng, B.; Li, Y.; Liu, W.; Zhang, Z.; Yang, M. Biomimetic Sensor Based on Molecularly Imprinted Polymer with Nitroreductase-like Activity for Metronidazole Detection. *Biosens. Bioelectron.* **2016**, *77*, 393–399, doi:10.1016/j.bios.2015.09.060.
237. Yang, Y.; Cao, Y.; Wang, X.; Fang, G.; Wang, S. Prussian Blue Mediated Amplification Combined with Signal Enhancement of Ordered Mesoporous Carbon for Ultrasensitive and Specific Quantification of Metolcarb by a Three-Dimensional Molecularly Imprinted Electrochemical Sensor. *Biosens. Bioelectron.* **2015**, *64*, 247–254,

- doi:10.1016/j.bios.2014.09.009.
238. Zhao, L.; Zhao, F.; Zeng, B. Synthesis of Water-Compatible Surface-Imprinted Polymer via Click Chemistry and RAFT Precipitation Polymerization for Highly Selective and Sensitive Electrochemical Assay of Fenitrothion. *Biosens. Bioelectron.* **2014**, *62*, 19–24, doi:10.1016/j.bios.2014.06.022.
239. Li, Y.; Song, H.; Zhang, L.; Zuo, P.; Ye, B. ce; Yao, J.; Chen, W. Supportless Electrochemical Sensor Based on Molecularly Imprinted Polymer Modified Nanoporous Microrod for Determination of Dopamine at Trace Level. *Biosens. Bioelectron.* **2016**, *78*, 308–314, doi:10.1016/j.bios.2015.11.063.
240. Yao, T.; Gu, X.; Li, T.; Li, J.; Li, J.; Zhao, Z.; Wang, J.; Qin, Y.; She, Y. Enhancement of Surface Plasmon Resonance Signals Using a MIP/GNPs/RGO Nano-Hybrid Film for the Rapid Detection of Ractopamine. *Biosens. Bioelectron.* **2016**, *75*, 96–100, doi:10.1016/j.bios.2015.08.027.
241. Zhong, M.; Chen, W.; Su, X. A Comparison of One and Two-Dimensional S-Transform in Fringe Pattern Demodulation. *Opt. Lasers Eng.* **2014**, *55*, 212–220, doi:10.1016/j.optlaseng.2013.11.008.
242. Li, B.; Zhou, Y.; Wu, W.; Liu, M.; Mei, S.; Zhou, Y.; Jing, T. Highly Selective and Sensitive Determination of Dopamine by the Novel Molecularly Imprinted Poly(Nicotinamide)/CuO Nanoparticles Modified Electrode. *Biosens. Bioelectron.* **2015**, *67*, 121–128, doi:10.1016/j.bios.2014.07.053.
243. Afsarimanesh, N.; Mukhopadhyay, S.C.; Kruger, M. MIP-based sensor for CTx-I detection. In *Smart Sensors, Measurement and Instrumentation*; Springer: Cham, Switzerland, 2019; pp. 59–91 ISBN 978-3-030-03705-5.
244. Zhao, J.I.E. *Solution-Processable Conductive Graphene-Based Materials for Flexible Electronics*; Acta Universitatis Upsaliensis: Uppsala, Sweden, 2019; ISBN 9789151306360.
245. Dechtrirat, D.; Sookcharoenpinyo, B.; Prajongtat, P.; Sriprachuabwong, C.; Sanguankiat, A.; Tuantranont, A.; Hannongbua, S. An Electrochemical MIP Sensor for Selective Detection of Salbutamol Based on a Graphene/PEDOT:PSS Modified Screen Printed Carbon Electrode. *RSC Adv.* **2018**, *8*, 206–212, doi:10.1039/c7ra09601a.
246. Dechtrirat, D.; Yingyuad, P.; Prajongtat, P.; Chuenchom, L.; Sriprachuabwong, C.; Tuantranont, A.; Tang, I.M. A Screen-Printed Carbon Electrode Modified with Gold Nanoparticles, Poly(3,4-Ethylenedioxythiophene), Poly(Styrene Sulfonate) and a Molecular Imprint for Voltammetric Determination of Nitrofurantoin. *Microchim. Acta* **2018**, *185*, 1–9, doi:10.1007/s00604-018-2797-3.
247. Lahcen, A.A.; Amine, A. Recent Advances in Electrochemical Sensors Based on Molecularly Imprinted Polymers and Nanomaterials. *Electroanalysis* **2019**, *31*, 188–201, doi:10.1002/elan.201800623.
248. Pernites, R.; Ponnappati, R.; Felipe, M.J.; Advincula, R. Biosensors and Bioelectronics Electropolymerization Molecularly Imprinted Polymer ( E-MIP ) SPR Sensing of Drug Molecules : Pre-Polymerization Complexed Terthiophene and Carbazole Electroactive Monomers. *Biosens. Bioelectron.* **2011**, *26*, 2766–2771, doi:10.1016/j.bios.2010.10.027.
249. Zhang, X.; Peng, Y.; Bai, J.; Ning, B.; Sun, S.; Hong, X.; Liu, Y.; Liu, Y.; Gao, Z. Sensors and Actuators B: Chemical A Novel Electrochemical Sensor Based on Electropolymerized Molecularly Imprinted Polymer and Gold Nanomaterials Amplification for Estradiol Detection. *Sensors Actuators B. Chem.* **2014**, *200*, 69–75, doi:10.1016/j.snb.2014.04.028.
250. Zhang, Z.; Li, Y.; Xu, J.; Wen, Y. Electropolymerized Molecularly Imprinted Polypyrrole Decorated with Black Phosphorene Quantum Dots onto Poly(3,4-

- Ethylenedioxythiophene) Nanorods and Its Voltammetric Sensing of Vitamin C. *J. Electroanal. Chem.* **2018**, *814*, 153–160, doi:10.1016/j.jelechem.2018.02.059.
251. Granado, V.L. V; Gutiérrez-capitán, M.; Fernández-sánchez, C.; Gomes, M.T.S.R.; Rudnitskaya, A.; Jimenez-jorquera, C. Thin-Film Electrochemical Sensor for Diphenylamine Detection Using Molecularly Imprinted Polymers. *Anal. Chim. Acta* **2013**, doi:10.1016/j.aca.2013.11.038.
252. Mugo, S.M.; Edmunds, B.J.; Berg, D.J.; Gill, N.K. Analytical Methods An Integrated Carbon Entrapped Molecularly Imprinted Polymer ( MIP ) Electrode for Voltammetric Detection of Resveratrol in Wine. *Anal. Methods* **2015**, *7*, 9092–9099, doi:10.1039/C5AY01799H.
253. Roberto, F.; Leite, F.; Jesus, W. De; Santos, R.; Tatsuo, L. Sensors and Actuators B : Chemical Selective Determination of Caffeic Acid in Wines with Electrochemical Sensor Based on Molecularly Imprinted Siloxanes. **2014**, *193*, 238–246.
254. Santos, W.D.J.R.; Santhiago, M.; Yoshida, I.V.P.; Kubota, L.T. Electrochemical Sensor Based on Imprinted Sol-Gel and Nanomaterial for Determination of Caffeine. *Sensors Actuators, B Chem.* **2012**, *166–167*, 739–745, doi:10.1016/j.snb.2012.03.051.
255. Yang, L.; Yang, J.; Xu, B.; Zhao, F.; Zeng, B. Facile Preparation of Molecularly Imprinted Polypyrrole-Graphene-Multiwalled Carbon Nanotubes Composite Film Modified Electrode for Rutin Sensing. *Talanta* **2016**, *161*, 413–418, doi:10.1016/j.talanta.2016.08.080.
256. Sun, S.; Zhang, M.; Li, Y.; He, X. A Molecularly Imprinted Polymer with Incorporated Graphene Oxide for Electrochemical Determination of Quercetin. *Sensors (Switzerland)* **2013**, *13*, 5493–5506, doi:10.3390/s130505493.
257. Zhao, P.; Hao, J. Tert-Butylhydroquinone Recognition of Molecular Imprinting Electrochemical Sensor Based on Core–Shell Nanoparticles. *Food Chem.* **2013**, *139*, 1001–1007, doi:https://doi.org/10.1016/j.foodchem.2013.01.035.
258. Alipour, S.; Aberoomand, P.; Waqif, S.; Reza, H. Sensors and Actuators : B . Chemical Determination of Rosmarinic Acid in Plant Extracts Using a Modified Sensor Based on Magnetic Imprinted Polymeric Nanostructures. *Sensors Actuators B. Chem.* **2020**, *323*, 128668, doi:https://doi.org/10.1016/j.snb.2020.128668.
259. Herrera-Chacón, A.; Cetó, X.; del Valle, M. Molecularly Imprinted Polymers - towards Electrochemical Sensors and Electronic Tongues. *Anal. Bioanal. Chem.* **2021**, *413*, 6117–6140, doi:10.1007/s00216-021-03313-8.
260. Zafrilla, P.; Morillas, J.; Mulero, J.; Cayuela, J.M.; Martínez-Cachá, A.; Pardo, F.; López Nicolás, J.M. Changes during Storage in Conventional and Ecological Wine: Phenolic Content and Antioxidant Activity. *J. Agric. Food Chem.* **2003**, *51*, 4694–4700, doi:10.1021/jf021251p.
261. Pati, S.; Crupi, P.; Savastano, M.L.; Benucci, I.; Esti, M. Evolution of Phenolic and Volatile Compounds during Bottle Storage of a White Wine without Added Sulfite. *J. Sci. Food Agric.* **2020**, *100*, 775–784, doi:10.1002/jsfa.10084.
262. Monagas, M.; Bartolomé, B.; Gómez-Cordovés, C. Evolution of Polyphenols in Red Wines from *Vitis Vinifera* L. during Aging in the Bottle : III. Non-Anthocyanin Phenolic Compounds. *Eur. Food Res. Technol.* **2005**, *220*, 331–340, doi:10.1007/s00217-004-1109-9.
263. Recamales, Á.F.; Sayago, A.; González-Miret, M.L.; Hernanz, D. The Effect of Time and Storage Conditions on the Phenolic Composition and Colour of White Wine. *Food Res. Int.* **2006**, *39*, 220–229, doi:10.1016/j.foodres.2005.07.009.
264. Kallithraka, S.; Salacha, M.I.; Tzourou, I. Changes in Phenolic Composition and Antioxidant Activity of White Wine during Bottle Storage: Accelerated Browning Test

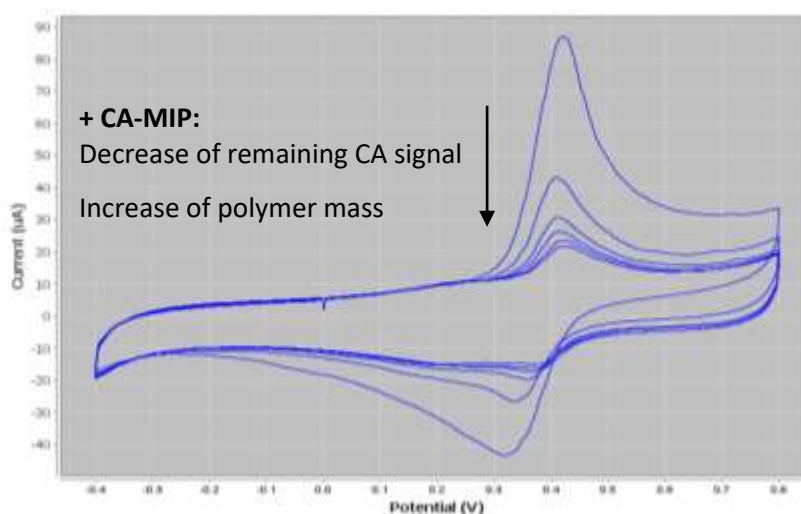
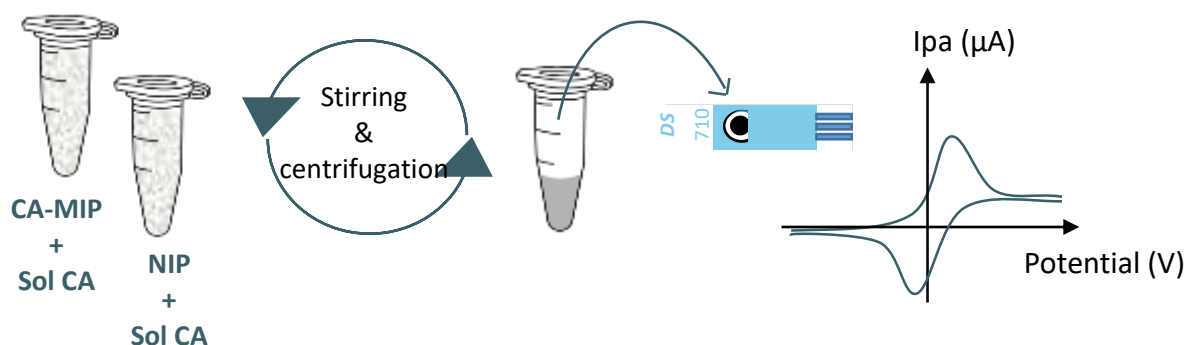
- versus Bottle Storage. *Food Chem.* **2009**, *113*, 500–505, doi:10.1016/j.foodchem.2008.07.083.
265. Espíndola, K.M.M.; Ferreira, R.G.; Narvaez, L.E.M.; Silva Rosario, A.C.R.; da Silva, A.H.M.; Silva, A.G.B.; Vieira, A.P.O.; Monteiro, M.C. Chemical and Pharmacological Aspects of Caffeic Acid and Its Activity in Hepatocarcinoma. *Front. Oncol.* **2019**, *9*, 541, doi:10.3389/fonc.2019.00541.
266. Mirzaei, S.; Gholami, M.H.; Zabolian, A.; Saleki, H.; Farahani, M.V.; Hamzehlou, S.; Far, F.B.; Sharifzadeh, S.O.; Samarghandian, S.; Khan, H.; et al. Caffeic Acid and Its Derivatives as Potential Modulators of Oncogenic Molecular Pathways: New Hope in the Fight against Cancer. *Pharmacol. Res.* **2021**, *171*, 105759, doi:10.1016/j.phrs.2021.105759.
267. Lamaoui, A.; García-Guzmán, J.J.; Amine, A.; Palacios-Santander, J.M.; Cubillana-Aguilera, L. Chapter 4 - Synthesis techniques of molecularly imprinted polymer composites. In *Woodhead Publishing Series in Composites Science and Engineering*; Sooraj, M.P., Nair, A.S., Mathew, B., Thomas, S.B.T.-M.I.P.C., Eds.; Woodhead Publishing, 2021; pp. 49–91 ISBN 978-0-12-819952-7.
268. Abraham, M.J.; Murtola, T.; Schulz, R.; Páll, S.; Smith, J.C.; Hess, B.; Lindahl, E. GROMACS: High Performance Molecular Simulations through Multi-Level Parallelism from Laptops to Supercomputers. *SoftwareX* **2015**, *1–2*, 19–25, doi:https://doi.org/10.1016/j.softx.2015.06.001.
269. Van Der Spoel, D.; Lindahl, E.; Hess, B.; Groenhof, G.; Mark, A.E.; Berendsen, H.J.C. GROMACS: Fast, Flexible, and Free. *J. Comput. Chem.* **2005**, *26*, 1701–1718, doi:10.1002/jcc.20291.
270. Dodda, L.S.; Vilseck, J.Z.; Tirado-rives, J.; Jorgensen, W.L. 1.14 \* CM1A-LBCC: Localized Bond-Charge Corrected CM1A Charges for Condensed-Phase Simulations. **2017**, doi:10.1021/acs.jpcc.7b00272.
271. Jorgensen, W.L.; Tirado-rives, J.; Fields, F. Potential Energy Functions for Atomic-Level Simulations of Water and Organic and Biomolecular Systems. **2005**, *102*, 6665–6670.
272. Dodda, L.S.; Vaca, I.C. De; Tirado-rives, J.; Jorgensen, W.L. LigParGen Web Server : An Automatic OPLS-AA Parameter Generator for Organic Ligands. **2017**, 1–6, doi:10.1093/nar/gkx312.
273. Abascal, J.L.F.; Vega, C. A General Purpose Model for the Condensed Phases of Water : TIP4P / 2005. **2005**, 1–12, doi:10.1063/1.2121687.
274. Hess, B. P-LINCS: A Parallel Linear Constraint Solver for Molecular Simulation. *J. Chem. Theory Comput.* **2008**, *4*, 116–122, doi:10.1021/ct700200b.
275. Essmann, U.; Perera, L.; Berkowitz, M.; Darden, T.; Lee, H.; Pedersen, L. A Smooth Particle Mesh Ewald Method. *J. Chem. Phys.* **1995**, *103*, 8577, doi:10.1063/1.470117.
276. Martínez, L.; Andrade, R.; Birgin, E.G.; Martínez, J.M. Software News and Update Packmol : A Package for Building Initial Configurations. **2009**, doi:10.1002/jcc.
277. BelBruno, J.J. Molecularly Imprinted Polymers. *Chem. Rev.* **2019**, *119*, 94–119, doi:10.1021/acs.chemrev.8b00171.

**Part III**  
**Results and discussion**

## **Chapter 1**

Combination of screen printed carbon electrode and  
molecularly imprinted polymers for the selective  
determination of caffeic acid in wine

## ❖ Graphical Abstract



## 1. Introduction

The aim of this chapter is to present a simple combination between *ex-situ* radical polymerization of a CA-MIP/NIP couple for the detection of caffeic acid in wine using screen printed carbon electrodes (SPCE).

Bulk polymerization was used for the preparation of the polymers with thermal initiation. The used ratio of CA/N-PAA/EGDMA was 1/4/20 and the solvent was composed of a mixture of acetonitrile and methanol. The application of the polymers was indirect in terms of contact with the SPCE so the detected concentration refers to the remaining caffeic acid that was not retained by the polymer.

**The main objectives** of this chapter are:

- Synthesis of a selective CA-MIP and evaluation of its rebinding properties.
- Application of the CA-MIP in wine.
- Application of the CA-MIP in wine using a conventional technique: HPLC-UV.

Rebinding properties were studied at pH 3 and pH 7 in hydro-alcoholic medium. The time of stirring of the samples when the polymers are added to CA solutions was chosen based on a kinetic study that showed the stability is reached after two hours of stirring. Selectivity studies were also applied in order to evaluate the response of the polymer towards other interferents with similar structures to CA. The rebinding to CA was 28.6 times higher than to *p*-coumaric acid.

Afterwards, the CA-MIP was applied in wine, where rebinding properties were also tested. In order to evaluate the results given by our method, this same experiment was done with HPLC-UV. Recovery values with CV method ranged between 79% and 89%, and with HPLC-UV they ranged between 82% and 84%. Compared to each other, the recovery ranged between 96% and 105%.

In wine, the anodic peak current was linear to CA concentration from 0.17 to 0.56 mM with a LOD of 0.06 mM and a LOQ of 0.11 mM. The anodic peak current was linear to CA concentration from 0.17 to 0.56 mM with a LOD of 0.06 mM and a LOQ of 0.11 mM.

Consequently, this indirect method is fast, selective, and requires simple instrumentation. It could facilitate the detection of polyphenols in food matrices and thus could be used in several industrial applications.

**The main results** obtained in this chapter are:

- The synthesis of a CA-MIP selective for caffeic acid capable of adsorbing CA to a greater extent than its interferents.
- Application of the CA-MIP in wine with a recovery ranging between 79% and 89%
- Validation of the CV method with HPLC-UV, with recovery values ranging between 96% and 106%.

## **2. Article 1: Combination of screen printed carbon electrode and molecularly imprinted polymers for the selective determination of caffeic acid in wine**

### **Abstract**

Caffeic acid (CA) is an efficient antioxidant found in wine, in plants and can be extracted from by-products of food industry. A molecularly imprinted polymer specific to caffeic acid (CA-MIP) was prepared by radical polymerization using N-phenylacrylamide as functional monomer, ethylene glycol dimethacrylate as cross-linker, and azobisisobutyronitrile as initiator, in the presence of CA as template molecule. Rebinding activities between the polymers and CA were promoted by an indirect method and characterized by cyclic voltammetry (CV) using a screen-printed carbon electrode (SPCE). It is a fast method, which requires simple and portable instrumentation. The polymer showed a high selectivity toward CA and a good repeatability. CA-MIP was then applied in wine samples spiked with CA, and the results were compared to those obtained by a chromatographic method. With a limit of detection of 0.06 mM in wine, the recovery values confirm that the method is suitable for further applications.

**Keywords:** Electrochemistry, Molecularly imprinted polymer, Screen-printed carbon electrode, Caffeic acid, Wine, Cyclic voltammetry

## 2.1. Introduction

Antioxidants (AO) are of great importance in our life, whether it is in biology (oxidative stress), medicine (damage by oxidation on RNA and DNA, Alzheimer's disease and cancer) [1,2], nutrition (loss of essential fatty acids, toxicological impact of lipid oxidation products, loss of amino acids such as Tryptophan) [3,4] and so in our personal health. Their main targets are reactive oxygen species (ROS), such as free radicals (superoxide ion  $O_2^{\bullet-}$ , peroxide  $ROO^{\bullet}$ , hydroxyl radical  $HO^{\bullet}$ , singlet dioxygen  $^1O_2$  or  $^{\bullet}O-O^{\bullet}$ ), mainly derived from oxidation reactions. The ROS target different structures (lipids and particularly unsaturated fatty acid residues, proteins with sensible side chains such as Met, Cys, Lys, Trp, Tyr, Phe, and carbohydrates) that can affect foods and health [5]. Antioxidants (AO-H) constitute a family of molecules that react preferentially and readily with radicals. They exchange a single electron and a hydrogen atom with the radical ( $R^{\bullet}$ ):  $R^{\bullet} + AO-H \rightarrow R-H + AO^{\bullet}$ . The radical antioxidant ( $AO^{\bullet}$ ) is stabilized by resonance (dissemination of the free electron on the structure). Sometimes, it polymerizes ( $AO^{\bullet} + AO^{\bullet} \rightarrow AO-AO$ ) or gives a non-radical product when it is a diradical ( $^{\bullet}AO^{\bullet} \rightarrow AO'$ ). Therefore, AO protect the oxidizable species commonly found in pharmaceuticals, paramedical products, cosmetics, and foods [6]. A particular consideration is given to natural antioxidants that can be easily found in our nutrition. Caffeic acid, for example, is a very common polyphenol, known for its antioxidant, anti-inflammatory, anti-AIDS and anticarcinogenic activity. It belongs to the class of phenolic acids, specifically hydroxycinnamic acids. It is widespread in plants and foods such as rosemary, fruits such wild blueberries, blackcurrant, artichokes, black beans, but also coproducts of already prepared plants and fruits such as potatoes peels or fruits peels that can be valorized by antioxidant extraction, and drinks such as ginkgo infusion, tea, wine etc. [7,8].

The importance of these natural antioxidants makes their determination essential especially in food products, in order to protect them from oxidation and to provide the consumer with a safe product and good organoleptic qualities. Several methods have been developed for assessing the total antioxidant capacity. Direct methods to measure the antioxidant capacity (AOC, named sometime antioxidant ability AOA or efficiency AOE) consist in a continuous record of the oxidation degree of a system during storage. They are based on a comparison between a control without AO and a system containing AO, under normal or accelerated conditions (for example RANCIMAT method). The degree of oxidation as a function of time is observed by different methods: concentration of peroxide (AOAC 965.33-Peroxide Value, conjugated diene at 233 nm AOCS Official Method Ti 1a-64), concentration of secondary products such as aldehyde (thiobarbituric acid value AOCS Official Method Cd 19-90), carbonyl (p-anisidine value AOCS

Official Method Cd 18-90). The direct evaluation of AOC is strongly time consuming and not fully adapted for the evaluation of AO yield of extraction from plants or peels of fruit and plant.

The indirect methods of AO capacity are based on evaluation of radical exchange capacity and are classified according to their mechanism of action: (1) hydrogen atom transfer (HAT) based assays such as total radical-trapping antioxidant parameter (TRAP), oxygen radical absorbance capacity (ORAC), and crocin-bleaching assays (CBAs) and (2) electron transfer (ET) based assays such as 2,2-diphenyl-1-picrylhydrazyl assay (DPPH), trolox equivalent antioxidant capacity (TEAC), ferric ion reducing antioxidant power (FRAP), cupric ion reducing antioxidant capacity (CUPRAC) and the Folin-Ciocalteu assays [9,10]. These indirect methods are not correlated with each other, or with direct evaluation methods of AOC. Other methods were used for antioxidant detection and quantification, the most common being liquid chromatography (HPLC) coupled to UV or mass spectrometer, and present as well several limitations. HPLC-MS devices are relatively expensive and the related methods are time consuming because they require a tedious sample preparation step. However, most of the above cited methods are relatively expensive, time consuming especially when they require sample preparation, and many of them present lack of specificity [11,12].

To overcome these obstacles, electrochemical methods can be used as an alternative to the conventional techniques. They are simple, fast, involve low-cost and easily accessible instrumentations, and do not require any complicated sample preparation. Electrochemical reduction mimics ET method (electron transfer) but offers a wider solvent range even apolar solvent using specific supporting electrolytes, allowing the analysis of non-polar antioxidants, contrary to ET which uses polar solvents (DPPH-acetone, ethanol, methanol; TEAC and FRAP, CUPRAC in water). Electroanalytical techniques, especially voltammetry (cyclic voltammetry, differential pulse voltammetry) is widely used to evaluate the antioxidant potential in several samples [13–15]. Moreover, the use of disposable screen-printed electrodes (SPE) instead of traditional electrodes implies a decrease of the sample volume used in each experiment and make the measurements faster and more accurate as the tedious cleaning processes of the electrode is eliminated. With a natural mix of antioxidants, the voltammogram obtained with a plant extracts for example is complex, without clear peaks of oxidation and reduction. Cyclic voltammetry is adapted to evaluate the content and antioxidant capacity of isolated antioxidant found in wine or to evaluate globally the AOC of a wine [16], but not specifically one antioxidant in a mixture.

The only issue with the electrochemistry-antioxidants combination is the lack of selectivity (very closed oxidation peaks), the instability of the antioxidants, their high reactivity and the structural

similarity between the compounds (for example, caffeic acid, ferulic acid or hydroxytyrosol). To this end, molecular imprinting is a possible solution, capable of improving the selectivity towards the studied compound. It is a technique which consists in creating synthetic polymers with binding sites complementary to the target molecule, in terms of shape, size and functional groups. The molecular imprinting technique uses two main strategies: radical polymerization of organic monomers giving MIP (molecular imprinting polymer) or hydrolysis and condensation of alkoxy silanes by acid or base catalysis giving MIS (molecular imprinting silica). The main reagents to synthesize MIP are template, which is most often the target molecule, functional monomer, cross-linker, initiator and the solvent. Their choices are based on the polymerization process used for the polymer synthesis. The majority of the imprinted polymers are acrylate based molecularly imprinted polymers (MIP), synthesized by radical polymerization commonly using methacrylic acid (MAA) as a functional monomer. On the other hand, molecularly imprinted silicas (MIS) are synthesized by sol-gel process, based on two steps hydrolysis and condensation. The main functional monomers are alkoxy silane molecules, such as (3-Aminopropyl)-triethoxysilane (APTES) and (3-Aminopropyl)-trimethoxysilane (PTMOS) [6,17].

Molecularly imprinted polymers were initially used as solid phase extraction material (MISPE) to replace immunosorbents [18,19] and aptamers because of their cheap and simple preparation, also for their high thermal and chemical stability [20,21]. They have been used for the analysis of several compounds, such as drugs [22,23], pesticides [24,25], industrial contaminants [25,28], etc., mostly coupled with high performance liquid chromatography (HPLC). Then, the application of MIPs and their designs have evolved, and they have been used for antioxidants detection in many sectors (drugs, foods, biological fluids, etc.) [6]. The combination of MIPs with electrochemical techniques, especially voltammetry, was applied for antioxidants detection, such as caffeic acid in wine, using different types of electrodes. For example, [26] modified a platinum electrode with (poly(3,4-ethylenedioxy) thiophene), [27] modified a screen-printed carbon electrode with graphene oxide by electrochemical reduction, [28] used a nitrogen-doped carbon modified glassy carbon electrode, for the determination of caffeic acid in wine samples. The voltammetry analysis of one antioxidant in wine is challenging due to the numerous antioxidants in wine, 365 molecules with AOC identified in white wine [29], maybe much more in red wine, for instance hydroxybenzoic acids such as caffeic acid, stilbenes such as resveratrol, polyphenols like, flavonols, flavonoids, anthocyanidins, anthocyanins, or tannins [30,31].

The main objective of this work was to combine cyclic voltammetry and MIP, in order to implement a new method for the specific detection of caffeic acid in hydroalcoholic medium

such as wine. This new method should be simpler and easier than those previously developed. It should not imply any interference with other antioxidants. For this reason, an MIP specific to CA was synthesized then characterized by FTIR, laser diffraction granulometry, nitrogen adsorption and scanning electron microscopy. Several parameters were studied during the development of this new CA-MIP/CV method: pH, polymer mass and selectivity. The final step was the utilisation and the validation of this new method in a Burgundy red wine.

## 2.2. Material and methods

### 2.2.1. Chemicals

Caffeic acid ( $\geq 98\%$ , CAS number 331-39-5), N-phenylacrylamide (N-PAA 99%, CAS number 2210-24-4), ethylene glycol dimethacrylate (EGDMA 98%, CAS number 97-90-5), azobisisobutyronitrile (AIBN 98%, CAS number 78-67-1), *p*-coumaric acid ( $\geq 98\%$ , CAS number 501-98-4), gallic acid (97.5-102.5 titration, CAS number 149-91-7), *trans*-ferulic acid ( $\geq 99\%$ , CAS number 537-98-4), sinapic acid ( $\geq 98\%$ , powder, 530-59-6), acetonitrile (ACN, gradient grade,  $\geq 99\%$ , CAS number 75-05-8), methanol (gradient grade,  $\geq 99\%$ , CAS number 67-56-1), phosphate buffered saline (PBS tablets), ethanol (EtOH, absolute, CAS number 64-17-5), acetic acid (glacial, CAS number 64-19-7) were purchased from Sigma Aldrich, France. Water used in all experiments was deionised and obtained from an Elga Ionic system PURELAB Option.

### 2.2.2. Instrumentation

All the voltammetric measurements were carried out using a portable and easy-to-handle  $\mu$ Stat-i 400 potentiostat, connected to a PC, and screen-printed carbon electrodes, all purchased from Metrohm, France. The analyses were performed with a scan rate of 50 mV/s, between -0.4 and + 0.8 V. The measured intensity (anodic peak intensity,  $I_{pa}$ ) is proportional to the concentration of the detected compound in the medium.

For the morphological characterization, Fourier transform infrared (FTIR) spectroscopy were recorded on a PerkinElmer spectrum 65 FT-IR spectrometer in the range 4000 – 500  $\text{cm}^{-1}$  using attenuated total reflectance sampling. 64 scans with a resolution of 4  $\text{cm}^{-1}$  were applied.

Brunauer–Emmett–Teller (BET) method was used for surface area analysis and was performed by nitrogen adsorption-desorption at a temperature of 77 K using an ASAP 2020 instrument. Prior to analysis, 50 mg of sample were outgassed for 14 h at room temperature.

Scanning Electron Microscopy (SEM) was applied for the surface morphological characterization using a Zeiss Gemini SEM 500 apparatus. A SE2 Everhart-Thornley was used as a detector.

### **2.2.3. Synthesis of the molecularly imprinted and non-imprinted polymers**

The molecularly imprinted polymer specific for caffeic acid (CA MIP) was prepared at room temperature and then synthesized under thermal conditions. The template molecule, caffeic acid (CA, 0.5 mmol) was solubilized in methanol, then acetonitrile was added (50 mL, 20/80 v/v, respectively). While stirring, the functional monomer (N-PAA, 2 mmol) was added, followed by the cross-linker (EGDMA, 10 mmol), and then the initiator (AIBN, 0.44 mmol). The mixture was degassed by nitrogen sparging. In parallel, non-imprinted polymer (NIP) was prepared under the same conditions as CA MIP, but without adding the template. The reaction mixtures were placed in an incubator under 60 °C for 24 hours. Afterwards, the polymer was separated from the solution by centrifugation at 10 000 g for 10 min at 20 °C and then washed with a 10 % (m/v) acetic acid solution with ethanol in order to eliminate the template from the polymer. Several washing steps were required until caffeic acid was no more detectable by HPLC. After washing, the polymers were dried for 6 h at 60 °C. They were stored at room temperature until use.

### **2.2.4. Effect of pH on electrochemical detection of CA in hydro-alcoholic medium**

Two calibration curves were constructed over the range of 0.06 mM to 2.78 mM of caffeic acid. Six standards were prepared in an aqueous ethanolic buffer, aqueous phosphate buffer (PBS 0.05 M) / ethanol (EtOH 90/10, v/v) solution, at pH 3 and pH 7, and voltammetric measurements were applied.

### **2.2.5. Rebinding experiments of CA using MIP and NIP in hydro-alcoholic medium: effect of pH and of the polymer mass**

Rebinding properties (steps represented in figure S2 of the supplementary material) were studied by adding the CA MIP to 1 mL of (PBS 0.05 M/EtOH) (90/10, v/v) solution, containing 1.11 mM of CA, varying the pH (pH 3 and pH 7) or varying the mass of the polymer CA MIP, ranging from 10 mg to 50 mg. The Eppendorf tubes were agitated for 2 hours at room temperature using a Stuart rotator SB2. The same procedure was performed with the NIP. After separating the polymer from the liquid by centrifugation at 10 000 g for 10 min at room temperature, the supernatant was deposited on the surface of a screen-printed carbon electrode attached to the

potentiostat and CV analyses were carried out. The obtained voltammograms were directly related to the amount of CA remaining in the solution and that was not sorbed by the CA-MIP. The concentration of CA retained by the CA-MIP polymer ( $C_{\text{ads}}$ , mM) was calculated by the difference between the initial amount of CA concentration ( $C_0$ , mM), initially added to the solution, and the remaining CA concentration ( $C$ , mM) in the supernatant. The amount of retained or adsorbed CA ( $N_{\text{ads}}$ ,  $\mu\text{mol}$ ) was calculated based on the concentration ( $C_{\text{ads}}$ ).

The time of contact between the polymers and the solution was determined based on a kinetic study in which nine samples were prepared in the same previous solution containing 1.11 mM of caffeic acid and 20 mg of polymer, CA MIP or NIP. The supernatants were evaluated at various times ranging from 1 min to 4 hours. The rebinding is so fast that even at one minute, the amount of retained caffeic acid reached about 0.78 mM, and by 4 h it was 0.83 mM (figure S3). The selected contact time was 2 h of stirring (0.80 mM), as it represents the time where the kinetics became stable.

#### **2.2.6. Selectivity studies**

10 mg of CA MIP or NIP were contacted, in Eppendorf tubes, with 1 mL of (PBS 0.05 M/ EtOH) (90/10, v/v, pH 3) solution containing 0.55 mM of caffeic acid, sinapic acid, p-coumaric acid, ferulic acid or gallic acid, separately. The tubes were then agitated for 2 h and finally centrifuged for 10 min at 10.000 g at room temperature. The supernatants were analyzed by cyclic voltammetry using the same method described in paragraph 2.5 in order to determine the amount of caffeic acid or its interferences retained by the polymers.

A calibration curve was constructed over the range 0.06 to 0.55 mM of each phenolic acid.

#### **2.2.7. Preparation and electrochemical analysis of CA in wine samples**

A sample of Burgundy red wine (Pinot Noir, 2018) was purchased at a local supermarket. The proposed method was tested to determine CA in wine using the same previously described procedure (paragraph 2.5). The wine was diluted 10 times in a (PBS 0.05 M/ EtOH) (90/10, v/v, pH 3), and 10 mg of CA-MIP or NIP were added to 1 mL of the diluted wine. Analytical recovery experiments were also performed after spiking four different samples with 0.17, 0.22, 0.28 and 0.42 mM of caffeic acid. Voltammograms were extracted in order to determine the rebinding properties and the efficiency of the method.

A calibration curve was constructed over the range 0.06 mM to 1.67 mM of caffeic acid in the diluted wine. The calibration curve equations and the correlation coefficients were  $y = 35.3x + 1.80$  and  $R^2 = 0.995$  ( $y$  is  $I_{pa}$  in  $\mu A$  and  $x$  is caffeic acid concentration in mM).

### **2.2.8. HPLC determination of CA in wine samples**

CA in wine samples was analyzed by an HPLC alternative method using a C18-column on a Shimadzu LC equipped with a UV visible absorbance detector. The determination was performed using a gradient of mobile phase: acetonitrile/water. Flow rate was  $1.0 \text{ mL}\cdot\text{min}^{-1}$  and detection was performed at 325 nm. The same samples prepared for the electrochemical analysis in 2.2.7 were also prepared for HPLC, then filtrated and injected.

A calibration curve was constructed over the range 0.06 mM to 1.67 mM of caffeic acid in the diluted wine. The calibration curve equations and the correlation coefficients were  $y = 114432.x + 60205$  and  $R^2 = 0.9964$ .

## **2.3. Results and discussion**

### **2.3.1. Synthesis of the molecularly imprinted CA-MIP and non-imprinted polymers NIP**

The synthesis of the polymers was based on radical polymerization, in which the functional monomer binds to the CA through its functional groups (dipole-dipole interactions and  $\pi$ - $\pi$  stacking), and to the cross-linker in order to constitute the polymer (Figure 23). The polymerization was initiated by the AIBN under thermal effect. The used ratio of template to functional monomer and cross-linker was 1:4:20 based on previous MIP synthesis done in our group [32]. For the solvent choice, several studies used a mixture of acetonitrile and toluene [33] for the synthesis of MIP specific to CA. Toluene allows the solubilisation of caffeic acid, but given its high toxicity, it was replaced by methanol in this study.

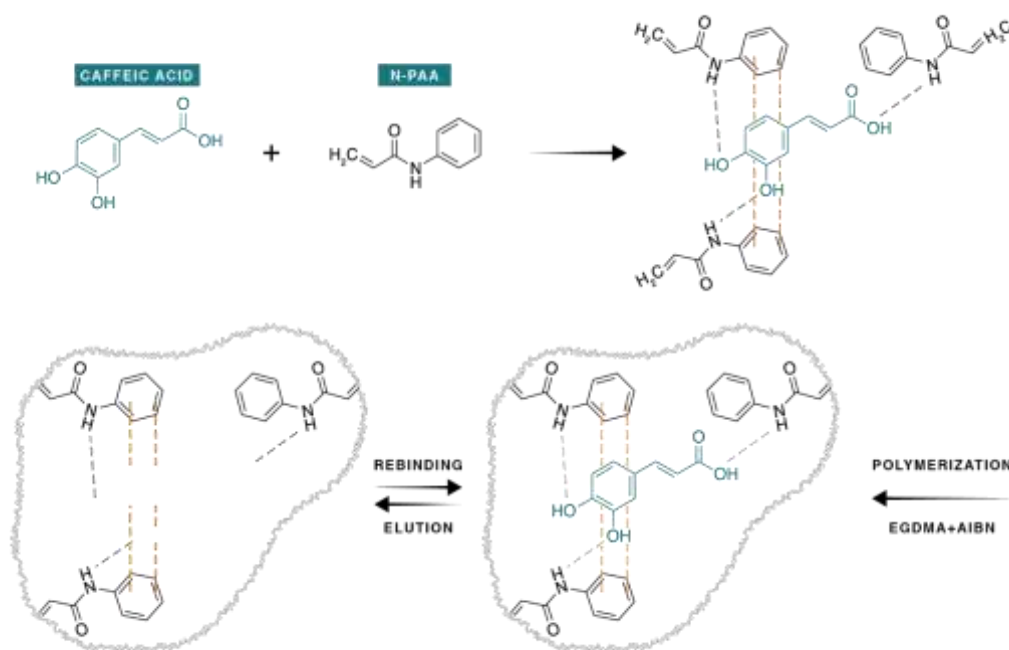


**Figure 23.** Proposed chemical reactions and interactions involved in the CA-MIP synthesis.

### 2.3.2. Morphological characterization

The CA-MIP and NIP were characterized by Fourier transform infrared (FTIR) spectroscopy, laser diffraction granulometry, Scanning Electron Microscopy and BET method. Results and figures are presented in Supplementary materials.

FTIR spectrum (figure S4) of both polymers showed that all the observed peaks are related to the absorption of the EGDMA cross-linker and the N-phenylacrylamide monomer after the radical polymerization. The main absorption bands were at:  $1740\text{ cm}^{-1}$  (C=O group in EGDMA and N-PAA),  $1461\text{ cm}^{-1}$  and  $1409\text{ cm}^{-1}$  (aromatic ring in N-PAA),  $1289\text{ cm}^{-1}$  and  $1180\text{ cm}^{-1}$  (C-O-C group in EGDMA).

BET analysis was applied to determine the specific surface area of the sample. For CA-MIP, it was  $9.9\text{ m}^2\cdot\text{g}^{-1}$ , and for NIP, it was  $8.3\text{ m}^2\cdot\text{g}^{-1}$ .

SEM micrographs (figure S5) showed bigger particle size for CA-MIP than NIP, that ranged from 381 to 427 nm.

### 2.3.3. Effect of pH on CA detection by voltammetry

The choice of pH is a major factor in caffeic acid detection. Figure 24 represents the calibration curves and their corresponding cyclic voltammograms (in inset), and shows that at pH 3, the intensity is greatly increased compared to pH 7. For example, at 2.78 mM of caffeic acid, the intensity was 153.5  $\mu\text{A}$  at pH 3 and 76.8  $\mu\text{A}$  at pH 7.

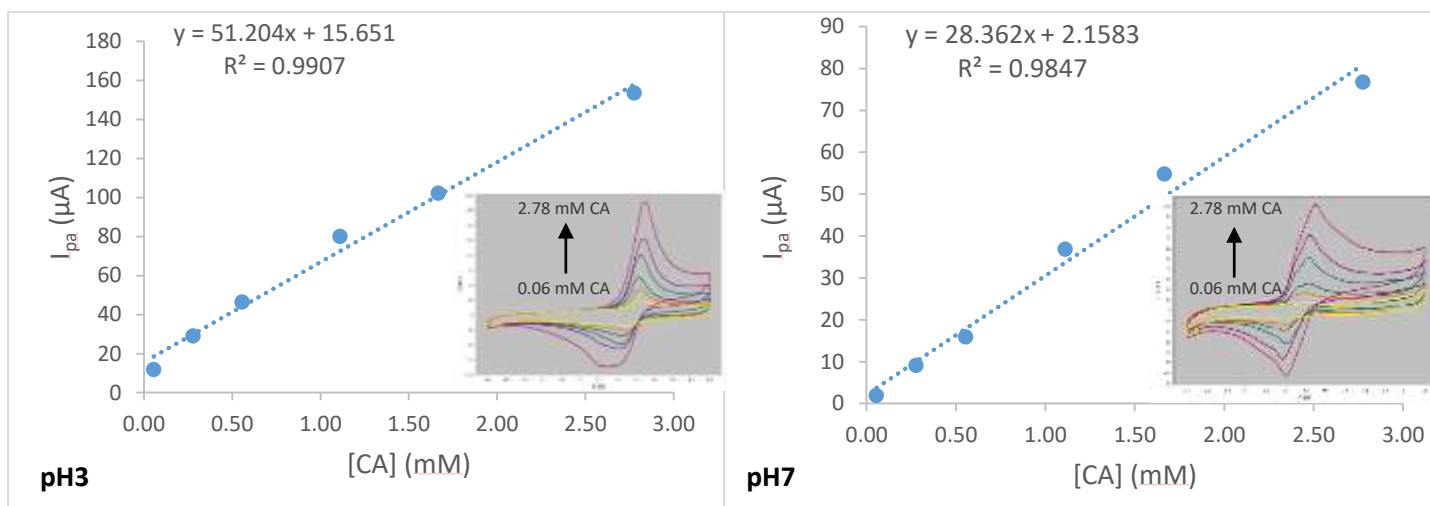


**Figure 24.** Calibration curves for caffeic acid (CA) in (PBS 0.05 M/ EtOH) (90/10, v/v) solution, at pH 3 (left) and pH 7 (right). Inset: CV for caffeic acid at different concentrations, ranging from 0.06 to 2.78 mM of CA. The critical value of the Pearson's correlation coefficient is 0.974 for 6 points (degree of freedom 4) and a level of significance for a two-tailed test of 0.1 %.

As explained by Genaro-Mattos et al. [34], this could be related to the structure of caffeic acid which has three ionizable hydroxyl groups: carboxyl group ( $\text{pK}_a = 4.8$ ), p-hydroxy group ( $\text{pK}_a = 8.6$ ) and m-hydroxy group ( $\text{pK}_a = 11.2$ ) (figure S6). The increase of pH in the medium results in the deprotonation of caffeic acid, which decreases its interaction with the functional monomer. At pH 7, where the pH is higher than the  $\text{pK}_a$  of the carboxylic group, the carboxylic ion is the major species present in the solution. The deprotonated species are less stable than the protonated ones.

### 2.3.4. Effect of pH on the rebinding properties of CA

Testing the effect of pH on caffeic acid by cyclic voltammetry in the presence of polymers CA-MIP is important, it helps understand if there is any matrix effect exerted by the polymer. The same measurement done with cyclic voltammetry as figure 24 were conducted in the presence of caffeic acid (CA) but this time in addition of imprinting polymers CA-MIP, and non-imprinting

polymer (NIP). The difference in intensity at the anodic peak ( $I_{pa}$ ) between CA alone and CA with CA-MIP or NIP allows the calculation of the absorption of CA by the CA-MIP and NIP.

At pH 3, the intensity of the signal is greatly increased, and so is the reuptake activity of the polymer. As shown in figure 25, the quantity of caffeic acid adsorbed at pH 3, in the presence of 10 mg or 50 mg of polymer, is more important than the quantity adsorbed at pH 7. This confirms the explanation proposed in paragraph 3.3, and that the structure of caffeic acid could be the reason for these differences.

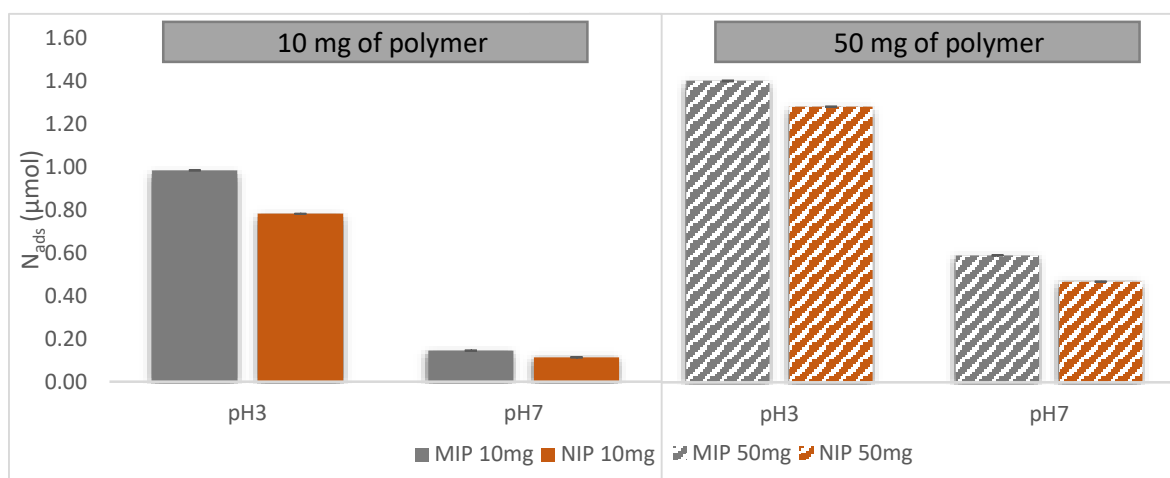


**Figure 25.** pH effect on the quantity of caffeic acid adsorbed ( $N_{ads}$ ) by CA-MIP using cyclic voltammetry in a (PBS 0.05 M/EtOH) (90/10, v/v) solution containing 1.11mM of CA, in the presence 10 mg (left) and 50 mg (right) of CA-MIPCA and NIP.

### 2.3.5. Effect of the polymer mass on the rebinding of CA

Figure 26 shows (a) the CV responses of the SPCE, after dropping on its surface 50 μL of the supernatant containing caffeic acid, with progressive addition of CA-MIP, at pH 3, and (b) the amount of caffeic acid retained by the polymer CA-MIP.

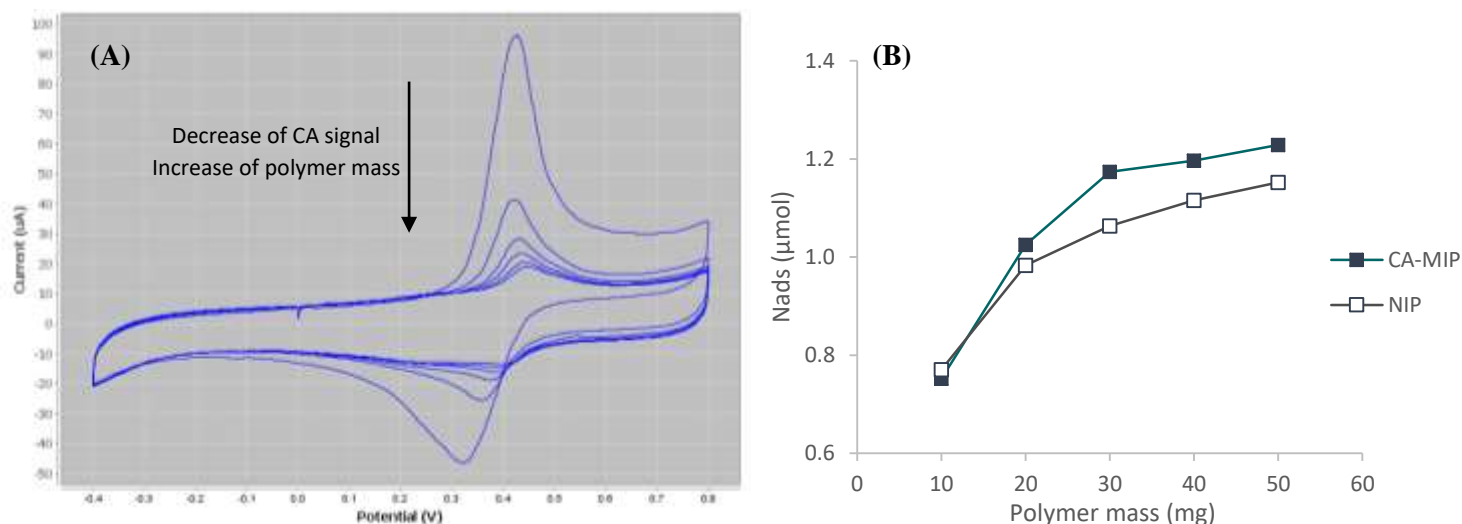


**Figure 26.** (A): CV of caffeic acid (CA) remaining in the medium after adding different quantities of CA-MIP (0, 10, 20, 30, 40 and 50 mg). Scan rate: 50 mV/s; the arrow shows the reduction of  $I_{pa}$  and the remaining caffeic acid with increasing the content of imprinting polymer CA-MIP. (B): effect of the polymer mass on the amount of adsorbed caffeic acid in a (PBS 0.05 M/EtOH) (90/10, v/v) solution containing 1.11 mM of caffeic acid. The error bar is of 0.15% for all samples

The decrease of the anodic peak current,  $I_{pa}$  (Figure 26), is a result of the increase of the added polymer mass. As shown in figure S3, reuptake activity is relatively fast. At 10 mg, 62.6 % of the added caffeic acid were already adsorbed. A slight difference can be observed between the imprinting CA-MIP and non-imprinting NIP responses. This could be explained by the fact that MIP has chemical and steric complementarity with the target molecule (CA). However, NIP has only chemical complementarity with CA. The chemical complementarity is due to the functional monomer which is present in both MIP and NIP. Steric interactions result from the template molecule which, after washing, leaves specific cavities into the polymers.

### 2.3.6. Selectivity studies

In order to study the selectivity of the CA-MIP, cyclic voltammograms were obtained after dropping 50 µL of each solution, containing different antioxidants with a very close structure of caffeic acid, named interferent. The selectivity coefficient  $\alpha$  was calculated for each interferent as follows:

$$\alpha = \frac{N_{adsCA}}{N_{ads\text{ interferent}}} \quad (1)$$

Where  $N_{ads\text{ CA}}$  is the amount of adsorbed caffeic acid, and  $N_{ads\text{ interferent}}$  is the amount of adsorbed interferent by the polymer. As showed in figure 27, CA-MIP has the highest selectivity for caffeic acid: 2.1 times greater than for ferulic acid and sinapic acid, 3.4 times than for gallic

acid and 28.6 times than for *p*-coumaric acid. This high selectivity can be explained by the arrangement of the functional groups matched with CA inside the polymer. The ortho-diphenol structure of CA could be behind this high selectivity.

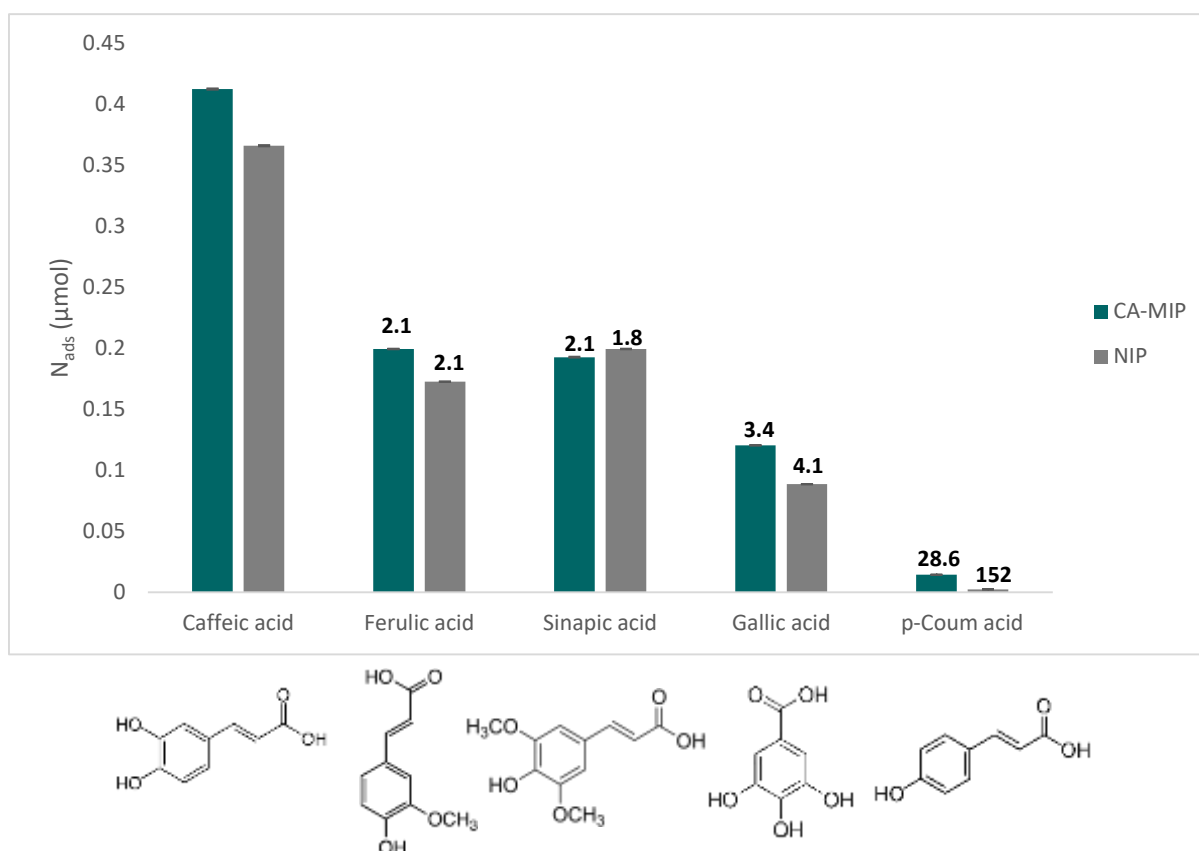


**Figure 27.** Relative amount of caffeic acid and its interferences adsorbed by the CA-MIP and NIP in a (PBS 0.05M/EtOH) (90/10, v/v) solution containing 0.55 mM of each compound, in the presence of 10 mg of MIP or NIP. The selectivity coefficient  $\alpha$  is represented in bold above every bar. Interferents: ferulic acid, sinapic acid, gallic acid and *p*-coumaric acid.

### 2.3.7. Application in wine, validation, recovery tests and limit of detection

Binding properties were studied in a Burgundy red wine, where CA-MIP was applied for CA determination using the new cyclic voltammetry (CV) method. Analytical recovery was calculated using the following equation and results are presented in Table 6:

$$Recovery = \frac{[CA]_{found}}{[CA]_{added}} \times 100 \quad (2)$$

The obtained percentages for the CV method ranged between 79 and 89%. These values imply that the matrix has little influence on the CA-MIP activity and are acceptable for trace analysis in real sample matrix. A limit of detection (LOD) of 0.06 mM and a limit of quantification (LOQ)

of 0.11 mM were respectively determined for the CV-MIP-CA method using the following formulas:

$$LOD = \frac{(intercept+3s)}{slope} \quad (3)$$

$$LOQ = \frac{(intercept+10s)}{slope} \quad (4)$$

Where the intercept and the slope were obtained from the calibration curve determined in wine and “s” corresponds to standard deviation of the intercept (Figure S7).

To validate the new developed cyclic voltammetry method using CA-MIP, an alternative HPLC-UV method was used to analyze the same wine samples. The concentrations of CA found in these same wine samples by HPLC-UV are presented in Table 6. Recovery percentages determined by HPLC were very close to those determined by the MIP-CA/CV method. A good correlation between the CA concentration measured by CA-MIP/CV and the CA concentration measured by HPLC-UV was obtained ( $R^2 = 0.9973$ ) (Figure S8).

**Table 6.** Added and recovered concentration of CA from wine samples using the MIP-CA/Cyclic voltammetry and the HPLC-UV methods.

Wine sample	Cyclic voltammetry			HPLC-UV	
	Added [CA] (mmol / L)	Found [CA] (mmol / L)	Recovery (%)	Found [CA] (mmol / L)	Recovery (%)
No CA added	0	0.009 ±0.004	-	0.010 ±0.002	-
1 <sup>st</sup> level	0.167	0.149 ±0.009	89	0.141 ±0.005	88
2 <sup>nd</sup> level	0.222	0.187 ±0.01	84	0.183 ±0.008	89
3 <sup>rd</sup> level	0.278	0.221 ±0.008	79	0.230 ±0.019	83
4 <sup>th</sup> level	0.416	0.337 ±0.014	81	0.343 ±0.013	81

## 2.4. Conclusion

Consequently, this indirect method applied with CA-MIP is a fast, simple, accurate and selective method for CA determination in wine samples. This method could facilitate the detection of polyphenols in food matrices and thus could be used in several industrial applications.

## References

1. Reuter, S.; Gupta, S.C.; Chaturvedi, M.M.; Aggarwal, B.B. Oxidative Stress, Inflammation, and Cancer: How Are They Linked? *Free Radic. Biol. Med.* 2010, 49, 1603–1616, doi:10.1016/j.freeradbiomed.2010.09.006.
2. Kong, Q.; Lin, C.-L.G. Oxidative Damage to RNA: Mechanisms, Consequences, and Diseases. *Cell. Mol. Life Sci.* 2010, 67, 1817–1829, doi:10.1007/s00018-010-0277-y.
3. Jacobitz, A.W.; Liu, Q.; Suravajjala, S.; Agrawal, N.J. Tryptophan Oxidation of a Monoclonal Antibody Under Diverse Oxidative Stress Conditions: Distinct Oxidative Pathways Favor Specific Tryptophan Residues. *J. Pharm. Sci.* 2021, 110, 719–726, doi:10.1016/j.xphs.2020.10.039.
4. Zhang, W.; Xiao, S.; Ahn, D.U. Protein Oxidation: Basic Principles and Implications for Meat Quality. *Crit. Rev. Food Sci. Nutr.* 2013, 53, 1191–1201, doi:10.1080/10408398.2011.577540.
5. Basli, A.; Soulet, S.; Chaher, N.; Mérillon, J.M.; Chibane, M.; Monti, J.P.; Richard, T. Wine Polyphenols: Potential Agents in Neuroprotection. *Oxid. Med. Cell. Longev.* 2012, 2012, doi:10.1155/2012/805762.
6. Elhachem, M.; Cayot, P.; Abboud, M.; Louka, N.; Maroun, R.G.; Bou-maroun, E. The Importance of Developing Electrochemical Sensors Based on Molecularly Imprinted Polymers for a Rapid Detection of Antioxidants; antioxidants, 2021; ISBN 3338077408.
7. Murilo, K.; Espíndola, M.; Ferreira, R.G.; Eduardo, L.; Narvaez, M.; Caroline, A.; Silva, R.; Hanna, A.; Gabrielle, A.; Silva, B.; et al. Chemical and Pharmacological Aspects of Caffeic Acid and Its Activity in Hepatocarcinoma. 2019, 9, 3–5, doi:10.3389/fonc.2019.00541.
8. Mirzaei, S.; Gholami, M.H.; Zabolian, A.; Saleki, H.; Farahani, M.V.; Hamzehlou, S.; Far, F.B.; Sharifzadeh, S.O.; Samarghandian, S.; Khan, H.; et al. Caffeic Acid and Its Derivatives as Potential Modulators of Oncogenic Molecular Pathways: New Hope in the Fight against Cancer. *Pharmacol. Res.* 2021, 171, 105759, doi:10.1016/j.phrs.2021.105759.
9. Balasaheb, S.; Pal, D. *RSC Advances*. 2015, 27986–28006, doi:10.1039/c4ra13315c.
10. Debelo, H.; Li, M.; Ferruzzi, M.G. Processing Influences on Food Polyphenol Profiles and Biological Activity. *Curr. Opin. Food Sci.* 2020, doi:10.1016/j.cofs.2020.03.001.
11. Apak, R.; Özyürek, M.; Güçlü, K.; Çapanoğlu, E. Antioxidant Activity/Capacity Measurement. 1. Classification, Physicochemical Principles, Mechanisms, and Electron Transfer (ET)-Based Assays. *J. Agric. Food Chem.* 2016, 64, 997–1027, doi:10.1021/acs.jafc.5b04739.
12. Apak, R.; Özyürek, M.; Güçlü, K.; Çapanoğlu, E. Antioxidant Activity/Capacity Measurement. 2. Hydrogen Atom Transfer (HAT)-Based, Mixed-Mode (Electron Transfer (ET)/HAT), and Lipid Peroxidation Assays. *J. Agric. Food Chem.* 2016, 64, 1028–1045, doi:10.1021/acs.jafc.5b04743.
13. Benbouguerra, N.; Richard, T.; Saucier, C.; Garcia, F. Voltammetric Behavior, Flavanol and Anthocyanin Contents, and Antioxidant Capacity of Grape Skins and Seeds during Ripening (*Vitis Vinifera* Var. Merlot, Tannat, and Syrah). *Antioxidants* 2020, 9.
14. Haque, M.A.; Morozova, K.; Lawrence, N.; Ferrentino, G.; Scampicchio, M. Radical Scavenging Activity of Antioxidants by Cyclic Voltammetry. *Electroanalysis* 2021, 33, 23–28, doi:https://doi.org/10.1002/elan.202060245.

15. Schaumlöffel, L. de S.; Dambros, J.W.V.; Bolognese Fernandes, P.R.; Gutterres, M.; Piatnicki, C.M.S. Direct and Simultaneous Determination of Four Phenolic Antioxidants in Biodiesel Using Differential Pulse Voltammetry Assisted by Artificial Neural Networks and Variable Selection by Decision Trees. *Fuel* 2019, 236, 803–810, doi:<https://doi.org/10.1016/j.fuel.2018.09.048>.
16. Kilmartin, P.A.; Zou, H.; Waterhouse, A.L. A Cyclic Voltammetry Method Suitable for Characterizing Antioxidant Properties of Wine and Wine Phenolics. *J. Agric. Food Chem.* 2001, 49, 1957–1965, doi:10.1021/jf001044u.
17. Lafarge, C.; Bitar, M.; El Hosry, L.; Cayot, P.; Bou-Maroun, E. Comparison of Molecularly Imprinted Polymers (MIP) and Sol–Gel Molecularly Imprinted Silica (MIS) for Fungicide in a Hydro Alcoholic Solution. *Mater. Today Commun.* 2020, 24, 101157, doi:10.1016/j.mtcomm.2020.101157.
18. Pichon, V. Selective Sample Treatment Using Molecularly Imprinted Polymers. *J. Chromatogr. A* 2007, 1152, 41–53, doi:10.1016/j.chroma.2007.02.109.
19. Turiel, E.; Martín-Esteban, A. Application of Molecularly Imprinted Polymers in Microextraction and Solventless Extraction Techniques; 1st ed.; Elsevier B.V., 2019; Vol. 86; ISBN 97804444642660.
20. Du, F.; Guo, L.; Qin, Q.; Zheng, X.; Ruan, G.; Li, J.; Li, G. Recent Advances in Aptamer-Functionalized Materials in Sample Preparation. *TrAC Trends Anal. Chem.* 2015, 67, 134–146, doi:<https://doi.org/10.1016/j.trac.2015.01.007>.
21. Pichon, V.; Delaunay, N.; Combès, A. Sample Preparation Using Molecularly Imprinted Polymers. *Anal. Chem.* 2019, doi:10.1021/acs.analchem.9b04816.
22. Kadhivel, P.; Combès, A.; Bordron, L.; Pichon, V. Development and Application of Water-Compatible Molecularly Imprinted Polymers for the Selective Extraction of Carbamazepine from Environmental Waters. *Anal. Bioanal. Chem.* 2019, 411, 1525–1536, doi:10.1007/s00216-019-01586-8.
23. Zhu, G.; Cheng, G.; Wang, P.; Li, W.; Wang, Y.; Fan, J. Water Compatible Imprinted Polymer Prepared in Water for Selective Solid Phase Extraction and Determination of Ciprofloxacin in Real Samples. *Talanta* 2019, 200, 307–315, doi:<https://doi.org/10.1016/j.talanta.2019.03.070>.
24. Li, Z.; Qian, Z.; Hu, S.; Gong, T.; Xian, Q. Molecularly Imprinted Solid Phase Extraction Coupled with Gas Chromatography-Mass Spectrometry for Determination of N-Nitrosodiphenylamine in Water Samples. *Chemosphere* 2018, 212, 872–880, doi:<https://doi.org/10.1016/j.chemosphere.2018.08.159>.
25. Sun, X.; Wang, M.; Peng, J.; Yang, L.; Wang, X.; Wang, F.; Zhang, X.; Wu, Q.; Chen, R.; Chen, J. Dummy Molecularly Imprinted Solid Phase Extraction of Climbazole from Environmental Water Samples. *Talanta* 2019, 196, 47–53, doi:<https://doi.org/10.1016/j.talanta.2018.12.017>.
26. Bianchini, C.; Curulli, A.; Pasquali, M.; Zane, D. Determination of Caffeic Acid in Wine Using PEDOT Film Modified Electrode. *Food Chem.* 2014, 156, 81–86, doi:10.1016/j.foodchem.2014.01.074.
27. Velmurugan, M.; Balasubramanian, P.; Chen, S.M. Determination of Caffeic Acid in Wine Samples Based on the Electrochemical Reduction of Graphene Oxide Modified Screen Printed Carbon Electrode. *Int. J. Electrochem. Sci.* 2017, 12, 4173–4182, doi:10.20964/2017.05.01.

28. Karikalan, N.; Karthik, R.; Chen, S.M.; Chen, H.A. A Voltammetric Determination of Caffeic Acid in Red Wines Based on the Nitrogen Doped Carbon Modified Glassy Carbon Electrode. *Sci. Rep.* 2017, 7, 1–10, doi:10.1038/srep45924.
29. Romanet, R.; Sarhane, Z.; Bahut, F.; Uhl, J.; Schmitt-Kopplin, P.; Nikolantonaki, M.; Gougeon, R.D. Exploring the Chemical Space of White Wine Antioxidant Capacity: A Combined DPPH, EPR and FT-ICR-MS Study. *Food Chem.* 2021, 355, 129566, doi:10.1016/j.foodchem.2021.129566.
30. Lingua, M.; Fabani, M.; Wunderlin, D.; Baroni, V. In Vivo Antioxidant Activity of Grape, Pomace and Wine from Three Red Varieties Grown in Argentina: Its Relationship to Phenolic Profile. *J. Funct. Foods* 2016, 20, 332–345, doi:10.1016/j.jff.2015.10.034.
31. Poklar Ulrih, N.; Opara, R.; Skrt, M.; Košmerl, T.; Wondra, M.; Abram, V. Part I. Polyphenols Composition and Antioxidant Potential during ‘Blaufränkisch’ Grape Maceration and Red Wine Maturation, and the Effects of Trans-Resveratrol Addition. *Food Chem. Toxicol.* 2020, 137, 111122, doi:https://doi.org/10.1016/j.fct.2020.111122.
32. Bitar, M.; Maalouly, J.; Chebib, H.; Lerbret, A.; Cayot, P.; Bou-maroun, E. Experimental Design Approach in the Synthesis of Molecularly Imprinted Polymers Specific for Iprodione Fungicide. *REACT* 2015, 94, 17–24, doi:10.1016/j.reactfunctpolym.2015.07.002.
33. Miura, C.; Matsunaga, H.; Haginaka, J. Molecularly Imprinted Polymer for Caffeic Acid by Precipitation Polymerization and Its Application to Extraction of Caffeic Acid and Chlorogenic Acid from *Eucommia Ulmodies* Leaves. *J. Pharm. Biomed. Anal.* 2016, 127, 32–38, doi:10.1016/j.jpba.2015.12.052.
34. Genaro-Mattos, T.; Maurício, Â.; Rettori, D.; Alonso, A.; Hermes-Lima, M. Antioxidant Activity of Caffeic Acid against Iron-Induced Free Radical Generation—A Chemical Approach. *PLoS One* 2015, 10, e0129963, doi:10.1371/journal.pone.0129963.

## **Chapter 2**

Optimization of a molecularly imprinted polymer  
synthesis for a specific and selective detection of caffeic  
acid in wine

In this chapter we extend the previous work (presented in article 1) by optimizing the synthesis parameters in order to improve the performance of the CA-MIP polymer.

## 1. Introduction

The CA-MIP prepared in chapter 1 showed good rebinding in hydro-alcoholic medium and selectivity towards caffeic acid regarding other interferents, and was successfully applied in wine. However, the specificity was weak, since the CA-MIP and NIP had close responses. The lack of specificity can indicate non-specific interactions established within the CA-MIP polymer that made it perform as the NIP.

This result led us to optimize the preparation conditions by considering the effect of several parameters: functional monomer, solvent(s), solubility of the template, and type of radical initiation.

**The main objectives** of this chapter are:

- Synthesis of 11 CA-MIP/NIP associations and evaluation of their rebinding properties
- Identification of the optimal couple
- Application of the optimal CA-MIP in wine

Eleven associations of CA-MIP/NIP were synthesized by varying one parameter at a time. For the functional monomer, N-phenylacrylamide (N-PAA) and methacrylic acid (MAA) were used. For the solvents, acetonitrile (ACN), toluene and mixtures of 80/20 v/v ACN/methanol and ACN/toluene were tested. For the radical initiation, thermal and UV polymerizations were undertaken.

Rebinding properties were tested with every association obtained after polymerization, washing and drying. The results showed that the functional monomer had a major effect on the performance of the polymer. As a first observation, MAA gave the best specificity. In addition, UV initiation was better than thermal initiation. This indicates that the type of radical initiation had also an important influence. Couple 6 prepared with MAA in ACN/MeOH mixture and UV initiation was the optimal choice. It was tested in a hydro-alcoholic medium where it showed a relevant selectivity towards caffeic acid regarding other interferents with similar structures to this phenolic compound, and good rebinding properties. The maximum number of sites was

determined using the x-intercept of the Scatchard plot with  $N1 = 29.8 \mu\text{mol.g}^{-1}$  for the CA-MIP6.

The couple was successfully applied in wine (spiked with CA) and two ways of analysis were tested: variation of CA concentration in the presence of 10 mg of polymer, and variation of the polymer mass in the presence of 0.056 mM of CA.

This method was validated with HPLC-UV where the same samples of spiked wine were injected and showed a recovery yield ranging between 104 and 111% with a limit of detection  $\text{LOD} = 0.13 \text{ mM}$  and a limit of quantification  $\text{LOQ} = 0.32 \text{ mM}$ .

This detection method is easy to use and could be improved when using electropolymerization as a direct method. In this case, the polymer is directly synthesized on the surface of the screen-printed carbon electrode and form an electrochemical sensor used for the direct detection of caffeic acid or any other structurally related compound in wine.

**The main results** obtained in this chapter are:

- Testing the synthesized polymers in hydro-alcoholic medium and CA-MIP6 showed the best performance in terms of selectivity and specificity.
- Application of the CA-MIP6 in wine with a  $\text{LOD} = 0.32 \text{ mM}$ .
- Validation of the CV method using HPLC-UV, with recovery values ranging between 104% and 111%.

## **2. Article 2: Optimization of a molecularly imprinted polymer synthesis for a specific and selective detection of caffeic acid in wine**

### **Abstract**

Molecular imprinting is a very simple strategy to make detection of compounds more specific and more selective. This targeted analytical strategy using molecularly imprinted polymer (MIP) synthesis needs to get the optimized conditions, several trials should be done by changing one parameter at a time: functional monomer, solvent, pH, type of polymerization, type of radical initiation (UV or thermal), etc. A selective molecularly imprinted polymer was prepared for caffeic acid detection. Caffeic acid is an efficient antioxidant present in wine. The synthesis of MIP presented a lack of specificity which is the difference between the imprinted (MIP) and non-imprinted (NIP) polymer response. This difference is not mandatory, but it enhances the specificity of the MIP. Therefore, a number of trials were done in order to obtain the most suitable conditions for the synthesis of a selective and specific CA-MIP. Morphological characterizations were also done for the optimal CA-MIP, and the electrochemical detection of CA was performed by cyclic voltammetry (CV). The polymer showed good specificity and selectivity in the presence of interferents (molecules structurally close to CA), and was successfully applied in wine in a linear range between 0 and 1.11 mM with a limit of detection (LOD) of 0.13 mM. The method was validated by HPLC-UV with recovery values ranging between 104 and 111 %.

**Keywords:** molecularly imprinted polymer, synthesis optimization, electrochemistry, wine, antioxidants.

## 2.1. Introduction

The presence of antioxidants in foods, beverages, cosmetics and pharmaceuticals has become of great importance to both the producer and the consumer, who is becoming increasingly aware of their health benefits [1–3]. This fact has made research much more focused on the valorization of these compounds, their extraction, detection, identification and monitoring, in order to provide the consumer with a safe product. Detection methods are numerous but the majority are expensive and time consuming, especially when they require sample preparation [4–9]. The most common are liquid chromatography coupled to UV or mass spectrometry.

Caffeic acid is an orthodiphenol that belongs to the subgroup of hydroxycinnamic acids, it was chosen for its antioxidant characteristics, and the fact that it is widespread in plants (rosemary), fruits (wild blueberries, blackcurrant), drinks (ginkgo infusion, tea, wine, coffee) and also coproducts of already prepared plants and fruits such as potatoes peels or fruits peels that can be valorized by antioxidant extraction [11–15].

A rapid method has been presented by Elhachem et al., 2022, for the electrochemical detection of caffeic acid using molecularly imprinted polymers (MIP) and screen printed electrodes, and has been applied in wine. This simple and rapid method showed important results of selectivity and was validated by a reference method, the HPLC-UV, except that it presented a lack of specificity concerning the difference between the printed and non-printed polymer. For this reason, it proved important to optimize the synthesis of this polymer couple in order to keep its selectivity and to improve its specificity.

The MIP synthesis is in general easy to perform, but requires a long procedure to optimize its conditions and reagents. A lot of parameters can influence the synthesis, starting with the reagents (template, functional monomer, cross-linker, initiator), the solvent, the radical initiation method (thermal and UV), the type of polymerization (precipitation, mass, bulk), the drying conditions and the washing method for the template extraction [16–18]. Once the important parameters are set up, the rebinding tests are applied to study the MIP performance.

In this work, several CA-MIP/NIP couples were synthesized by varying one parameter each time and the rebinding characteristics were studied in order to choose an optimal couple to apply in the detection of caffeic acid in hydro-alcoholic. In addition, morphological characterizations were done for the optimal polymer, and rebinding tests were applied in wine. Recovery tests were determined and HPLC-UV was used as a conventional technique for comparison and validation of the method.

## 2.2. Material & methods

### 2.2.1. Chemicals

Caffeic acid ( $\geq 98\%$ , CAS number 331-39-5), N-phenylacrylamide (N-PAA 99%, CAS number 2210-24-4), methacrylic acid (MAA 99% CAS number 79-41-4) ethylene glycol dimethacrylate (EGDMA 98%, CAS number 97-90-5), azobisisobutyronitrile (AIBN 98%, CAS number 78-67-1), 2,2-Dimethoxy-2-phenylacetophenone (DMPAP 99% CAS number 24650-42-8), p-coumaric acid ( $\geq 98\%$ , CAS number 501-98-4), gallic acid (97.5-102.5 titration, CAS number 149-91-7), trans-ferulic acid ( $\geq 99\%$ , CAS number 537-98-4), sinapic acid ( $\geq 98\%$ , powder, 530-59-6), acetonitrile (ACN, gradient grade,  $\geq 99\%$ , CAS number 75-05-8), methanol (gradient grade,  $\geq 99\%$ , CAS number 67-56-1), toluene (CAS number 108-88-3) phosphate buffered saline (PBS tablets), ethanol (EtOH, absolute, CAS number 64-17-5), acetic acid (glacial, CAS number 64-19-7) all the chemicals were purchased from Sigma Aldrich, France.

Water used in all experiments was deionised and obtained from an Elga Ionic system PURELAB Option.

### 2.2.2. Instrumentation

All the voltammetric measurements were carried out using a portable and easy-to-handle  $\mu$ Stat-i 400 potentiostat, connected to a PC, and screen-printed carbon electrodes, all purchased from Metrohm, France. The analyses were performed with a scan rate of 50 mV/s, between -0.4 and +0.8 V. The measured intensity (anodic peak intensity,  $I_{pa}$ ) is proportional to the concentration of the detected compound in the medium.

For the morphological characterization, Fourier transform infrared (FTIR) spectroscopy were recorded on a PerkinElmer spectrum 65 FT-IR spectrometer in the range 4000 – 500  $\text{cm}^{-1}$  using attenuated total reflectance sampling. 64 scans with a resolution of 4  $\text{cm}^{-1}$  were applied.

Scanning Electron Microscopy (SEM) was applied for the surface morphological characterization using a Zeiss Gemini SEM 500 apparatus. A SE2 Everhart-Thornley was used as a detector.

Brunauer–Emmett–Teller (BET) method was used for surface area analysis, and was performed by nitrogen adsorption-desorption at a temperature of 77 K using an ASAP 2020 instrument. Prior to analysis, 50 mg of sample were outgassed for 14 h at room temperature.

### 2.2.3. Synthesis of several couples of molecularly imprinted and non-imprinted polymers for caffeic acid

In order to obtain the optimal couple CA-MIP/NIP, eleven polymerizations were conducted by varying one of the following parameters: functional monomer, solvent or the method of polymerization. Table 7 shows the several synthesis trials, with one variation at a time.

**Table 7.** Synthesis of 11 couples of CA-MIP/NIP.

MIP: molecularly imprinted polymer, NIP: non imprinted polymer, T: template, FM: functional monomer, CL: cross-linker, I: initiator, S: solvent, CA: caffeic acid, N-PAA: N-phenylacrylamide, EGDMA: ethylene glycol dimethacrylate, AIBN: azobisisobutyronitrile, DMPAP: 2,2-dimethoxy-2-phenylacetophenone, ACN: acetonitrile. UV at 365 nm for 24 hours, thermal at 60°C for 24 hours.

CA-MIP/NIP	T	FM	CL	I	S (80/20)	Type of radical initiation
1	CA	N-PAA	EGDMA	AIBN	ACN/MeOH	Thermal
2	CA	N-PAA	EGDMA	DMPAP	ACN/MeOH	UV
3	CA	N-PAA	EGDMA	DMPAP	ACN/Toluene	UV
4	CA	N-PAA	EGDMA	AIBN	ACN/Toluene	Thermal
5	CA	MAA	EGDMA	AIBN	ACN/MeOH	Thermal
6	CA	MAA	EGDMA	DMPAP	ACN/MeOH	UV
7	CA	MAA	EGDMA	AIBN	ACN/Toluene	Thermal
8	CA	MAA	EGDMA	DMPAP	ACN/Toluene	UV
9	CA	N-PAA	EGDMA	AIBN	ACN	Thermal
10	CA	N-PAA	EGDMA	AIBN	Toluene	Thermal
11	CA	MAA	EGDMA	AIBN	Toluene	Thermal

The template molecule (T: CA) was added to the solvent. When methanol is used, CA was solubilized in it before adding acetonitrile. While stirring, the functional monomer (FM: N-PAA or MAA) was added, followed by the cross-linker (CL: EGDMA), and then the initiator. The mixture was degassed by nitrogen sparging for 20 min. A ratio of 1:4:20 was used for the T/FM/CL in both UV and thermal polymerizations.

In UV polymerization, 0.33 mmol of CA was added in a total volume of 33.3 mL of the solvents. The reaction mixtures were placed in tubes and fixed at 10 cm from a UV lamp (365 nm), for 24 hours.

In thermal polymerization, 0.5 mmol of CA was added in a total volume of 50 mL of the solvents. The reaction mixtures were placed in an incubator under 60 °C for 24 hours.

Afterwards, the polymer was separated from the solution by centrifugation at 11,872 g for 10 min at 20 °C and then washed with a 10 % (v/v) acetic acid solution with ethanol in order to extract the template from the polymer. Several washing steps were required until caffeic acid was no more detectable by HPLC. After washing, the polymers were dried overnight at 60 °C. They were stored at room temperature until use.

#### **2.2.4. Rebinding experiments of caffeic acid**

Rebinding experiment was performed on both CA-MIP and NIP of all the couples. The quantity of adsorbed CA by the polymer was determined after varying the polymer mass from 10 to 50 mg.

A certain mass of polymer was weighed in an Eppendorf tube. Afterward 1 mL of PBS/ethanol (PBS 0.05M pH3/EtOH, 90/10, v/v) containing 1.11 mM of CA was added.

The samples were placed on a rotator for 2 hours (the stirring time was chosen based on a kinetic study where the rebinding properties of one sample were tested at various times of stirring, ranging from 5 min to 4 hours) followed by centrifugation at 10,640 g for 10 minutes.

For electrochemical measurements, 50  $\mu$ L of the supernatant were deposited by drop casting on the surface of a screen printed carbon electrode. The analysis was performed at a scan rate of 50 mV/s, between -0.4 and +0.8 V.

The anodic peak current ( $I_{pa}$ ) is proportional to the caffeic acid concentration remaining in the sample, in other terms, the caffeic acid that was not retained by the polymer. The difference between the initial concentration of CA that was added in the sample ( $C_0$ , mM) and the

remaining concentration (C, mM) is calculated and used for the determination of the adsorbed amount ( $N_{ads}$ ,  $\mu\text{mol}$ ).

A calibration curve was constructed over the range of 0 to 2.78 mM of CA solution prepared in PBS/EtOH. Among all the CA-MIP/NIP, the couple number 6 showed the best performance and was chosen for the following applications.

### 2.2.5. Characterization of the CA-polymer using adsorption models

It is important to calculate the number of binding sites of a polymer for its template. Langmuir isotherms represent one of the distribution models that represent the kinetics of ligand binding to receptors. The binding equilibrium between CA [I] and the binding sites [S] is represented by the following equation:



The binding affinity constant (K) is given by:

$$K = \frac{[IS]}{[I][S]} \quad (2)$$

This constant is related to the number of binding sites ( $N_t$ ) by:

$$K = \frac{B}{F(N_t - B)} \quad (3);$$

$$\frac{B}{F} = KN_t - KB \quad (4)$$

where B is the concentration of bound CA and F the concentration of free CA, at equilibrium. They are calculated based on the rebinding properties experiment applied in the model wine spiked with CA. The parameters K and  $N_t$  were obtained by linear regression of the Langmuir model (equation 4) via Scatchard plots.

### 2.2.6. Selectivity tests

Selectivity tests were performed in order to test the response of the polymer towards CA and other interferents with similar structures.

10 mg of CA-MIP6/NIP6 were added to 1 mL of PBS/EtOH containing 0.55 mM of each of the following compounds: caffeic acid, sinapic acid, ferulic acid, p-coumaric acid and gallic

acid, separately. The samples were then stirred and centrifuged as described in paragraph 4, and the supernatants were deposited on the SPCE and CV measurements were applied.

### **2.2.7. Application of the polymer in Wine**

The rebinding properties were tested again, but this time in wine samples. A Burgundy red wine (Pinot Noir, 2020) was purchased from a local supermarket.

The wine was diluted 10 times in PBS/EtOH, and spiked with different concentrations of caffeic acid ranging between 0 and 1.11 mM of caffeic acid. The rebinding properties were tested using the same previous procedure described in paragraph 4, by adding 1 mL of the spiked wine in different Eppendorf tubes in the presence of 10 mg of polymer. In parallel, another test was applied by fixing the CA concentration at 0.056 mM (it represents an average concentration of CA present in red wine [19]) and varying the polymer mass: 10; 20; 30; 50; 60 and 80 mg. The variation of the polymer mass helps to estimate the amount of polymer required for the recapture of CA present in the medium. After stirring and centrifugation, the supernatants were deposited on the SPCE and voltammetric measurements were applied.

A calibration curve was constructed over the range of 0 to 1.665 mM of caffeic acid in diluted wine. The calibration curve equation and the correlation coefficient were  $y=0,1988x + 2,5632$  and  $R^2= 0,9989$  ( $y$  is the  $I_{pa}$  in  $\mu A$  and  $x$  is the caffeic acid concentration in mM).

### **2.2.8. Determination of CA in wine samples with HPLC**

HPLC is used as a conventional method to determine CA concentration in the same wine samples prepared in paragraph 6, in order to evaluate the efficiency of our method. A Restek column (Pinnacle II, C18 5  $\mu m$ , 150  $\times$  4.6 mm) and a Shimadzu LC (LC-20AT) equipped with a UV visible absorbance detector (SPD-20A) were used.

The chromatographic separation was achieved with a gradient of two solvents: (solvent A 0.1% v/v acetic acid in water, solvent B 0.1% v/v acetic acid in acetonitrile) 7.5 % of B from 0 to 8 min, 95 % from 8 to 10 min and 7.5 % from 10 to 12 min. Flow rate was 1.0 mL.min<sup>-1</sup> and detection of CA was performed at 325 nm.

## 2.3. Results and Discussion

### 2.3.1. Synthesis of imprinted and non-imprinted polymers

Two functional monomers were chosen for the synthesis. N-acrylamide was already used in the previous experiment (CA-MIP1/NIP1). Its chemical structure, having an aromatic ring and hydroxyl groups, allows it to form  $\pi$ - $\pi$  stacking and hydrogen bonds with the template. Methacrylic acid is a well-known functional monomer, commonly used in radical polymerization because of its high interaction with acid template.

As preliminary results, the solubility of CA in the solvent, the presence or absence of the polymerization, and the resulting polymer yield were noted before the rebinding experiments of the polymers. The results are shown in table 8, based on the conditions presented in table 7.

The solubility of the template in the solvent is essential, because it is the starting point of the polymerization that promotes template-monomer interactions. Table 8 shows that when the template was not soluble, no polymerization of CA-MIP was obtained (couples 4;7;8 and 9) or if it happened, it forms non-specific cavities that make MIP and NIP responses close to each other (couples 3;10;11). The obtained yield is not the most important factor, but it is still valuable because it avoids the need to make a new synthesis for additional applications. A synthesis is easy, but the washing step can be long. Finally, the result that matters the most is the specificity of the polymer that is represented in table 8 by  $\Delta N_{ads}$  and % of NIP adsorption in the presence of 10 mg of polymer.  $\Delta N_{ads}$  is the difference between the amount of CA retained by CA-MIP and the one retained by NIP. The increase of  $\Delta N_{ads}$  indicates an increase of the specificity. The % of NIP adsorption is defined by the amount of CA retained by the NIP regarding the CA-MIP. The lower the value, the higher the specificity. Couples 5 and 6 showed the best specificity with a low or no adsorption by the NIP6 regarding CA-MIP6. Although both couples had MAA as functional monomer, an additional factor helped determine the best couple and it is the type of radical initiation. In this case, couple 6 showed a better specificity due to UV polymerization that proved a better contribution in the formation of the cavities and the stability of the polymer than the thermal initiation.

**Table 8.** Resulting polymers characteristics before and after polymerization.  $\Delta N_{ads}$  ( $\mu\text{mol}$ ) represents the difference between the adsorbed amount of CA by CA-MIP and NIP in the presence of 10 mg of polymer and % of NIP adsorption represents the amount of caffeic acid retained by the NIP regarding the amount retained by CA-MIP in the presence of 10 mg of polymer.

CA-MIP/NIP	Solubility of CA	Polymerization	Yield	$\Delta N_{ads}$ ( $\mu\text{mol}$ )	% of NIP adsorption
<b>1</b>	YES	YES	CA-MIP1 43% NIP1 76%	0.04	94.2
<b>2</b>	YES	YES	CA-MIP2 12% NIP2 59%	0.06	94.3
<b>3</b>	NO	YES	CA-MIP3 33% NIP3 72%	0.02	97.9
<b>4</b>	NO	CA-MIP: NO NIP: YES	NIP4 80%	/	/
<b>5</b>	YES	YES	CA-MIP5 70% NIP5 93%	0.2	20
<b>6</b>	YES	YES	CA-MIP6 73% NIP6 88%	0.27	0
<b>7</b>	NO	NO	/	/	/
<b>8</b>	NO	NO	/	/	/
<b>9</b>	NO	CA-MIP: NO NIP: YES	NIP9 59%	/	/
<b>10</b>	NO	YES	CA-MIP10 53% NIP10 67%	0.08	92.2
<b>11</b>	NO	YES	CA-MIP11 87% NIP11 90%	-0.01	109

### 2.3.2. Optimization of the CA-MIP/NIP synthesis

As explained, eleven couples of CA-MIP/NIP were synthesized. The optimal polymer was chosen based on its performance in the presence of a caffeic acid solution, and especially the difference between CA-MIP and NIP. Compared to the CA-MIP1/NIP1, the couple CA-MIP6/NIP6 had the most important difference between the rebinding activity of the CA-MIP and NIP (Figure 28).  $N_{ads}$  represents the amount of caffeic acid adsorbed by the polymer.

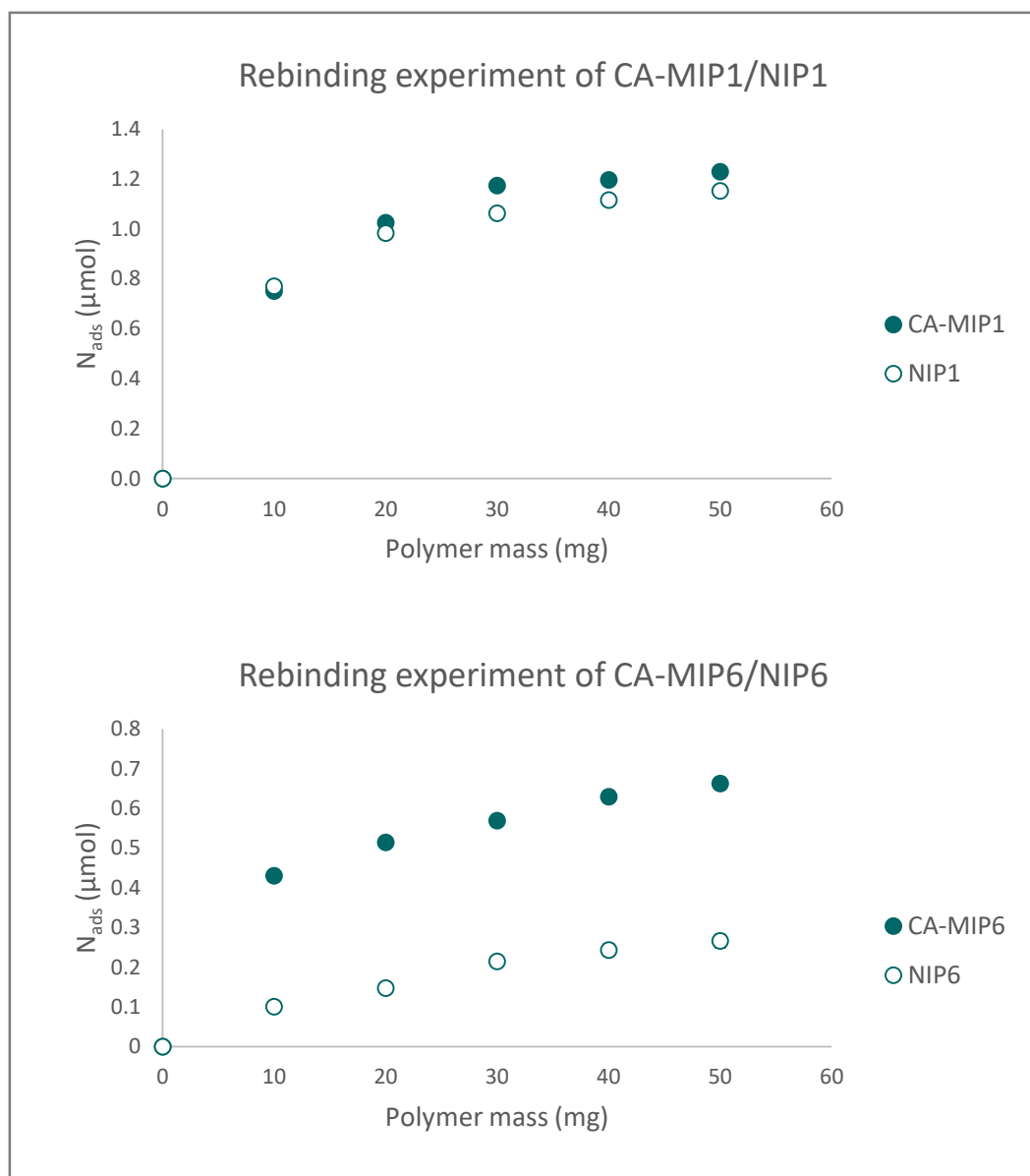


**Figure 28.** Comparison between the rebinding experiments performed by CA-MIP1/NIP1 and CA-MIP6/NIP6, showing the amount of adsorbed caffeic acid by each polymer.

The difference between the syntheses of CA-MIP6/NIP6 and the other polymers remains in the functional monomer (FM) and the type of radical initiation. The results presented in figure 28 show that MAA, used for the synthesis of the couple 6, improved the difference between the imprinted and non-imprinted polymers. MAA seems to be a better functional monomer than N-PAA due to the interaction between the acid function of MAA and the acid function of the template. The  $\pi$ - $\pi$  stacking contributes to a lesser extent in the difference between MIP and NIP. In MIP/NIP 6, a UV polymerization was used rather than a thermal polymerization. Thus, the difference CA-MIP6/NIP6 prepared at room temperature is better than that of the difference

CA-MIP1/NIP1 obtained at 60 °C. The specific cavities, which are at the origin of the difference between MIP and NIP, seem to be more structured and better formed at low temperature.

### 2.3.3. Morphological characterization

The CA-MIP6 and NIP6 were characterized by Fourier transform infrared (FTIR) spectroscopy, Scanning Electron Microscopy and BET method.

FTIR spectrum of both polymers (Figure 29) showed that all the observed peaks are related to the absorption of the EGDMA cross-linker and the MAA monomer after the radical polymerization, except one peak for CA-MIP6 at 881  $\text{cm}^{-1}$ , attributed to the C-H out-of-plane bending from phenyl rings which can be due to the presence of the template during the synthesis. The main absorption bands were at: 2976  $\text{cm}^{-1}$  (C-H stretching), 1720  $\text{cm}^{-1}$  (C=O stretching in EGDMA and MAA), 1056, 1085, 1153, 1270 and 1380  $\text{cm}^{-1}$  (C-O stretching).

SEM micrographs (Figure 30) showed aggregated particles for CA-MIP6 and CA-NIP6. The particle size for these 2 polymers is around 10-20 nm. These values are 20 to 40 times less than the size of MIP1/NIP1.

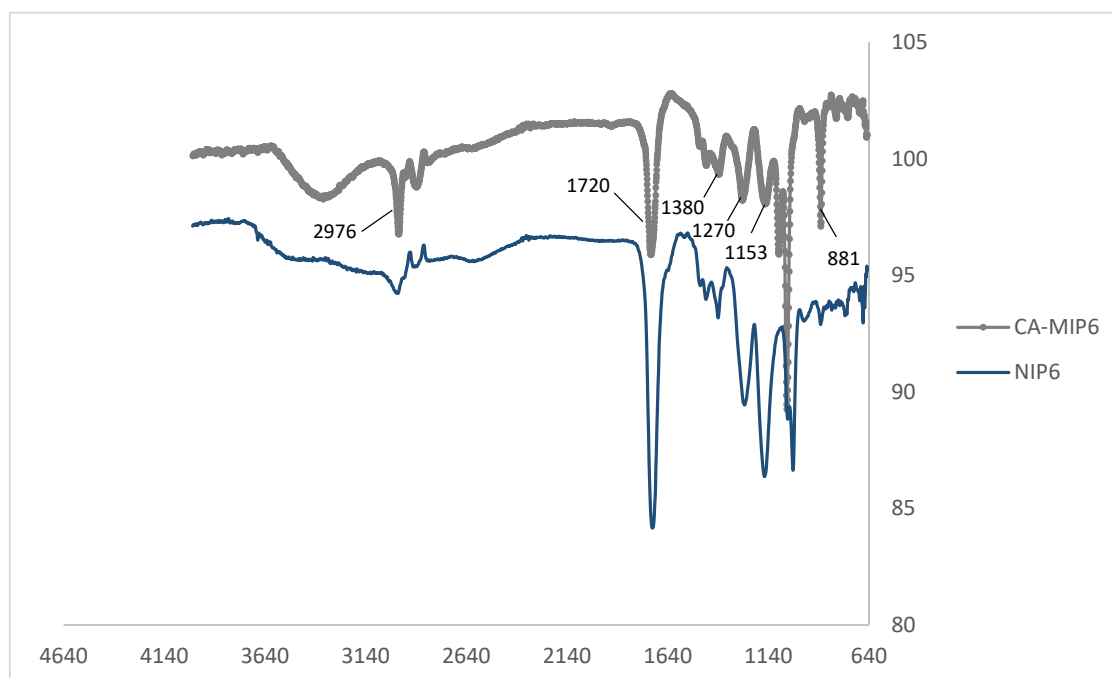


**Figure 29.** FTIR spectra of CA-MIP6 and NIP6.

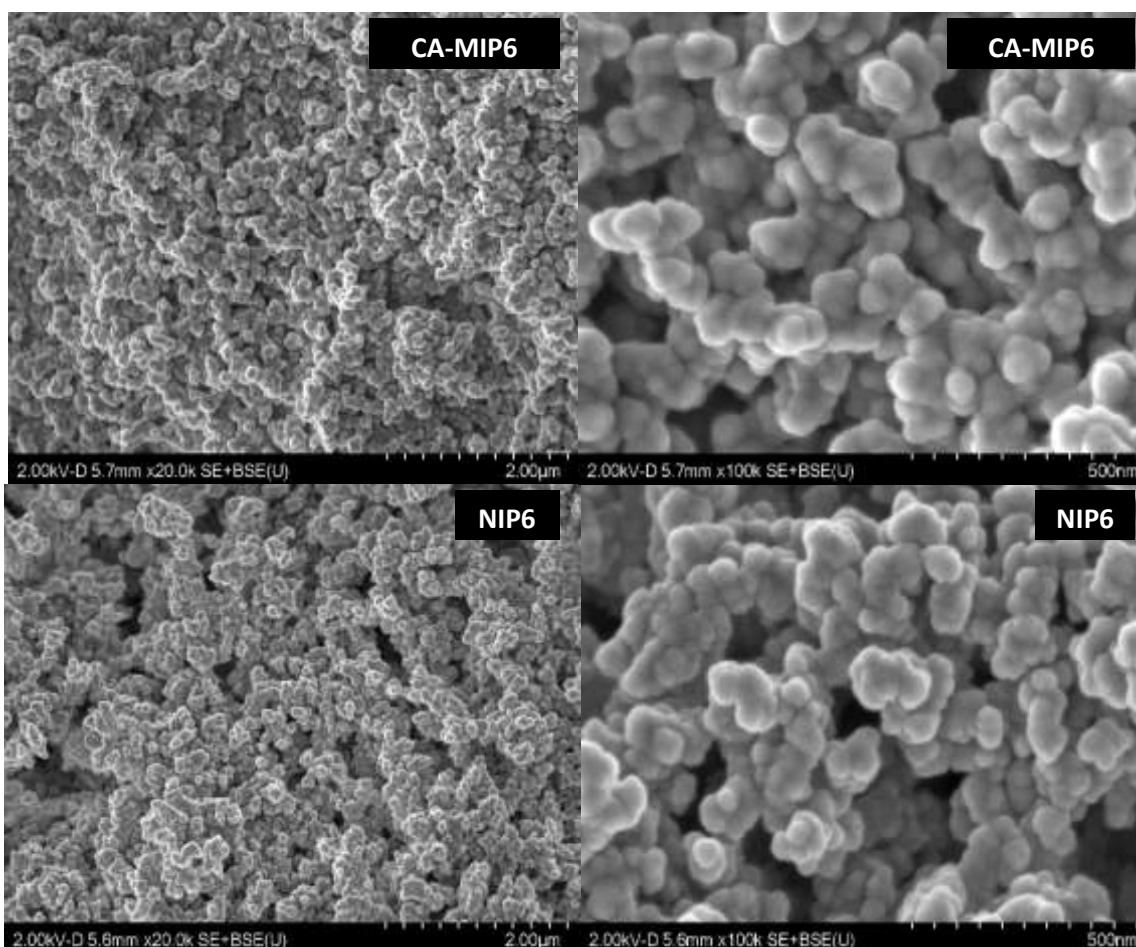


**Figure 30.** SEM images for CA-MIP6 and NIP6 at different scales

BET method was applied to determine the specific surface area of the sample. For CA-MIP1, it was  $9.9 \text{ m}^2 \cdot \text{g}^{-1}$ , and for NIP1, it was  $8.3 \text{ m}^2 \cdot \text{g}^{-1}$ . For CA-MIP6, it is  $82.4 \text{ m}^2 \cdot \text{g}^{-1}$ , and for NIP, it is  $89.0 \text{ m}^2 \cdot \text{g}^{-1}$ . The conditions of the optimal couple MIP/NIP have clearly increased the specific surface area of the sample which could be due the better formation of the specific cavities in MIP6 in comparison to MIP1.

#### **2.3.4. Analysis of binding properties: Langmuir isotherm**

The Scatchard plot shows that the recognition sites of the imprinted polymer are heterogeneous: one of high affinity (site 1) and the other of low affinity (site 2) (Figure 31). However, the non-imprinted polymer showed homogeneous sites.

The binding constant of the high affinity sites ( $K_1$ ) of the imprinted polymer CA-MIP6 is  $0.1298 \mu\text{mol/L}$  as determined by the slope of the Scatchard regression equation.  $K_1$  is about 7 times greater than the binding constant of the low affinity sites ( $K_2$ ).

CA-NIP6 presents only low affinity sites. This result could explain the difference of CA adsorption between MIP6 and NIP6.

The maximum number of interaction sites ( $N_1$ ) for the CA-MIP6 is  $29.8 \mu\text{mol.g}^{-1}$ . It was determined from the x-intercept of the Scatchard plot.

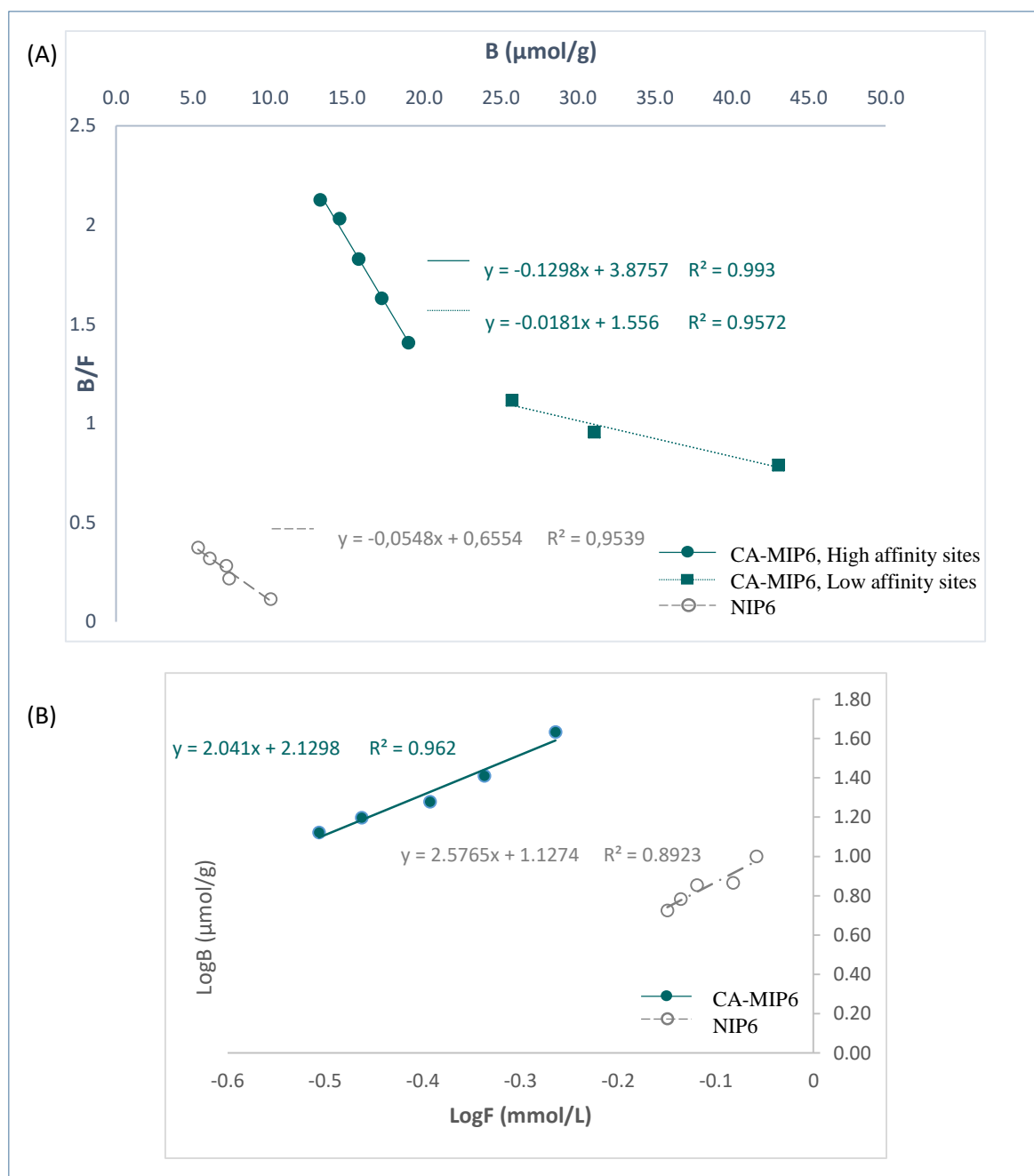


**Figure 31.** (A) Scatchard plots for CA-MIP6 and NIP6, and (B) affinity distributions plotted in log format

### 2.3.5. The behaviour of the polymer towards other interferents

In order to study the selectivity of the CA-MIP6 towards caffeic acid, cyclic voltammograms were obtained after dropping 50  $\mu\text{L}$  of each solution, containing different interferents with close structures to caffeic acid (Figure 32).

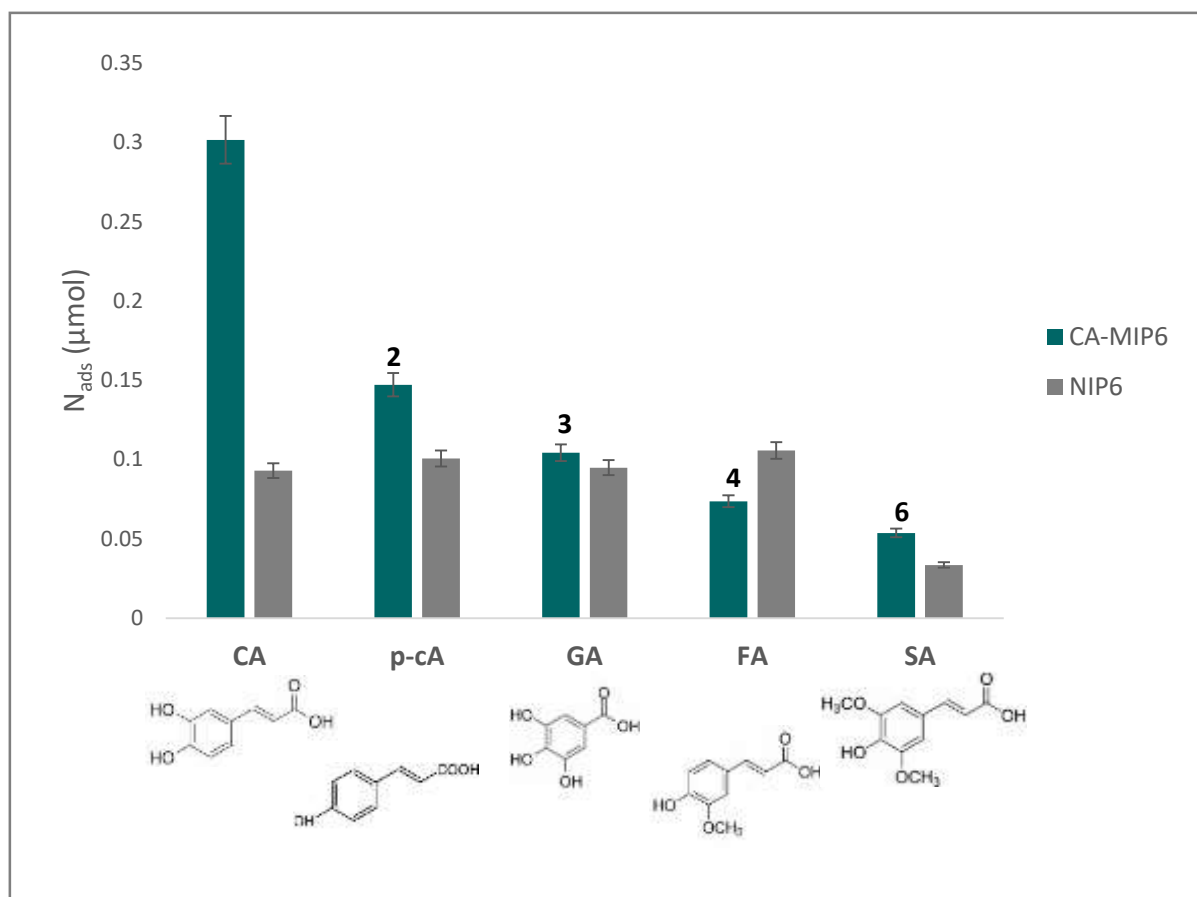


**Figure 32.** Relative amount of caffeic acid and its interferents adsorbed by the CA-MIP6 and NIP6, in a PBS/EtOH solution containing 0.55 mM of each compound, in the presence of 10mg of polymer. CA: caffeic acid, *p*-cA: *p*-coumaric acid, GA: gallic acid, FA: ferulic acid, SA: sinapic acid. The selectivity coefficient  $\alpha$  is calculated and given above MIP bars.

The selectivity coefficient  $\alpha$  was calculated for each interferent as follows:

$$\alpha = \frac{N_{ads\ CA}}{N_{ads\ interferent}}$$

where  $N_{ads\ CA}$  is the amount of adsorbed caffeic acid, and  $N_{ads\ interferent}$  is the amount of adsorbed interferent by the polymer. As showed in Figure 32, CA-MIP6 has the highest selectivity for caffeic acid: 2 times greater than for *p*-coumaric acid, 3 times than for gallic acid, 4 times than for ferulic acid and 6 times than for sinapic acid. This high selectivity can be explained by the arrangement of the functional groups and the cavities matched with CA inside the polymer. The ortho-diphenol structure of CA, bound to the MAA could be behind this matching, given that the difference between CA-MIP6 and NIP towards caffeic acid is maintained.

### 2.3.6. Application in wine, recovery tests and limit of detection

CA-MIP6 was applied in a Burgundy red wine, in order to evaluate the binding properties with caffeic acid. Figure 33.A represents the variation of CA concentration in the presence of 10 mg of polymer. The results show an increase of rebinding with an important difference CA-MIP6/NIP6. The NIP did not show any rebinding activity in the presence of concentrations ranging between 0 and 0.28 mM, which is the maximum of CA concentration found in wine. Meanwhile, Figure 33.B shows that starting 60 mg of polymer the rebinding reaches the maximum of adsorption.

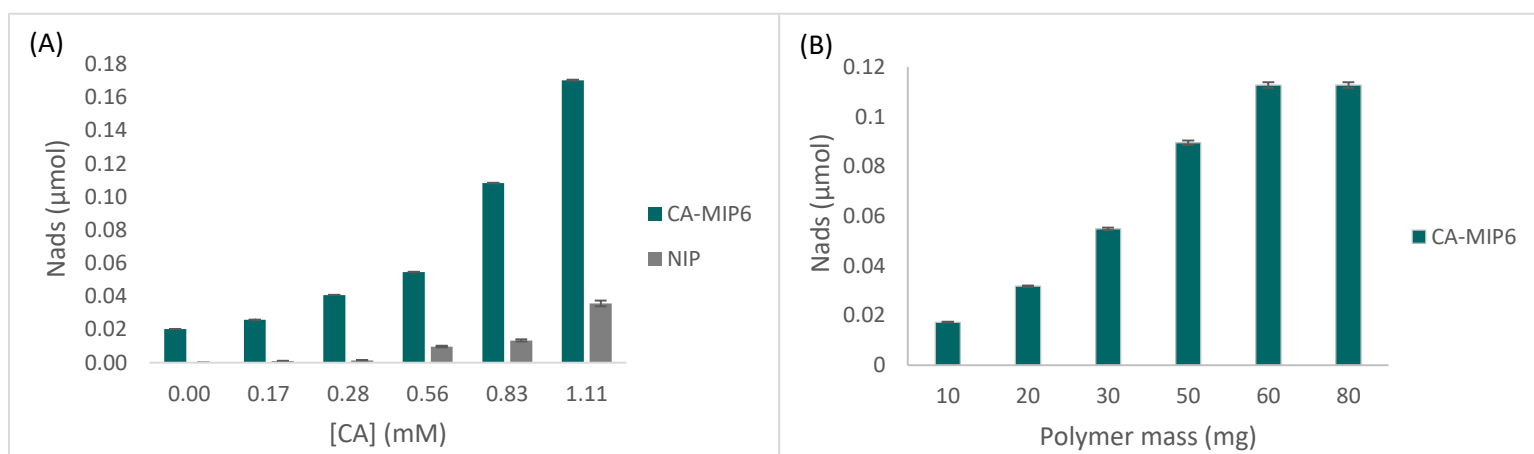


**Figure 33.** Rebinding properties of CA-MIP6 in spiked wine: (A) variation of the amount of CA in the presence of 10 mg of polymer; and (B) variation of polymer mass in the presence of 0.056 mM of caffeic acid in the solution.

The same samples prepared with different concentrations of CA were injected in HPLC-UV in order to validate the efficiency of our method.

Analytical recovery was calculated using the following equation, and results are presented in Table 9:

$$\text{Recovery (\%)} = \frac{[CA]_{\text{found in CV}}}{[CA]_{\text{found in HPLC}}} \times 100$$

The recovery values ranged between 104 and 111%. This indicates that the CV method is accurate and may be promising for future commercial applications. Recovery values higher than 100% could be explained by the fact that CA-MIP6, although it interacts mainly with caffeic acid, is able to adsorb structurally related interferents. However, the values for percentage recovery remain acceptable for analytical applications.

**Table 9.** Added and recovered concentration of CA from wine samples using the CA-MIP6/Cyclic voltammetry and the HPLC-UV methods. [CA] values are represented in % of rebinding.

Polymer mass (mg)	Found [CA] in CV (%)	Found [CA] in HPLC-UV (%)	Recovery (%)
10	23	22	104
20	35	32	109
30	41	37	111

A limit of detection (LOD) of 0.13 mM and a limit of quantification (LOQ) of 0.32 mM were respectively determined for the CV-CA-MIP6 method using the following formulas:

$$LOD = \frac{(intercept + 3s)}{slope}$$

$$LOQ = \frac{(intercept + 10s)}{slope}$$

Where the intercept and the slope were obtained from the calibration curve determined in wine and “s” corresponds to standard deviation of the intercept. These values are in accordance with the range of caffeic acid concentrations found in red wine.

## 2.4. Conclusion

The synthesis conditions of the CA-MIP/NIP couple were optimized and led to the preparation of a specific couple in terms of rebinding differences between CA-MIP and NIP towards the template, preserving its selectivity characteristics. The optimal polymer was successfully applied in wine and its performance was validated by a conventional chromatographic method, giving a recovery range between 104 and 111 % with a limit of detection LOD of 0.13 mM and a limit of quantification LOQ of 0.32 mM. This method is simple, fast and requires very simple instruments. It could be improved to lead to a direct method such as electropolymerization, where the polymer is directly synthesized on the surface of the screen-printed carbon electrode in order to develop a specific sensor for the direct detection of caffeic acid or any other compound in real matrices.

## References

1. Mitterer-Daltoé, M.; Bordim, J.; Lise, C.; Breda, L.; Casagrande, M.; Lima, V. Consumer Awareness of Food Antioxidants. Synthetic vs. Natural. *Food Sci. Technol.* **2021**, *41*, 208–212, doi:10.1590/fst.15120.
2. Zehiroglu, C.; Ozturk Sarikaya, S.B. The Importance of Antioxidants and Place in Today's Scientific and Technological Studies. *J. Food Sci. Technol.* **2019**, *56*, 4757–4774, doi:10.1007/s13197-019-03952-x.
3. Wilson, D.W.; Nash, P.; Singh, H.; Griffiths, K.; Singh, R.; De Meester, F.; Horiuchi, R.; Takahashi, T. The Role of Food Antioxidants, Benefits of Functional Foods, and Influence of Feeding Habits on the Health of the Older Person: An Overview. *Antioxidants* **2017**, *6*, 1–20, doi:10.3390/antiox6040081.
4. Mendonça, J. da S.; Guimarães, R. de C.A.; Zorgetto-Pinheiro, V.A.; Fernandes, C.D. Pietro; Marcelino, G.; Bogo, D.; Freitas, K. de C.; Hiane, P.A.; de Pádua Melo, E.S.; Vilela, M.L.B.; et al. Natural Antioxidant Evaluation: A Review of Detection Methods. *Molecules* **2022**, *27*, 3563, doi:10.3390/molecules27113563.
5. Apak, R.; Özyürek, M.; Güçlü, K.; Çapanoğlu, E. Antioxidant Activity/Capacity Measurement. 1. Classification, Physicochemical Principles, Mechanisms, and Electron Transfer (ET)-Based Assays. *J. Agric. Food Chem.* **2016**, *64*, 997–1027, doi:10.1021/acs.jafc.5b04739.
6. Amorati, R.; Valgimigli, L. Advantages and Limitations of Common Testing Methods for Antioxidants. *Free Radic. Res.* **2015**, *49*, 633–649, doi:10.3109/10715762.2014.996146.
7. Munteanu, I.G.; Apetrei, C. Analytical Methods Used in Determining Antioxidant Activity: A Review. *Int. J. Mol. Sci.* **2021**, *22*, doi:10.3390/ijms22073380.
8. Moharram, H.A.; Youssef, M.M. Methods for Determining the Antioxidant Activity : A Review. **2014**, *11*, 31–42.
9. Prior, R.L.; Wu, X.; Schaich, K. Standardized Methods for the Determination of Antioxidant Capacity and Phenolics in Foods and Dietary Supplements. *J. Agric. Food Chem.* **2005**, *53*, 4290–4302, doi:10.1021/jf0502698.
10. Elhachem, M.; Cayot, P.; Abboud, M.; Louka, N.; Maroun, R.G.; Bou-maroun, E. *The Importance of Developing Electrochemical Sensors Based on Molecularly Imprinted Polymers for a Rapid Detection of Antioxidants*; antioxidants, 2021; ISBN 3338077408.
11. Murilo, K.; Espíndola, M.; Ferreira, R.G.; Eduardo, L.; Narvaez, M.; Caroline, A.; Silva, R.; Hanna, A.; Gabrielle, A.; Silva, B.; et al. Chemical and Pharmacological Aspects of Caffeic Acid and Its Activity in Hepatocarcinoma. **2019**, *9*, 3–5, doi:10.3389/fonc.2019.00541.
12. Mirzaei, S.; Gholami, M.H.; Zabolian, A.; Saleki, H.; Farahani, M.V.; Hamzehlou, S.; Far, F.B.; Sharifzadeh, S.O.; Samarghandian, S.; Khan, H.; et al. Caffeic Acid and Its Derivatives as Potential Modulators of Oncogenic Molecular Pathways: New Hope in the Fight against Cancer. *Pharmacol. Res.* **2021**, *171*, 105759, doi:10.1016/j.phrs.2021.105759.
13. Cizmarova, B.; Hubkova, B.; Bolerazska, B.; Marekova, M.; Birkova, A. Caffeic Acid : A Brief Overview of Its Presence , Metabolism , and Bioactivity. **2020**, *3*, 74–81.
14. Richelle, M.; Tavazzi, I.; Offord, E. Comparison of the Antioxidant Activity of Commonly Consumed Polyphenolic Beverages (Coffee, Cocoa, and Tea) Prepared per Cup Serving. *J. Agric. Food Chem.* **2001**, *49*, 3438–3442, doi:10.1021/jf0101410.
15. Meinhart, A.D.; Caldeirão, L.; Damin, F.M.; Filho, J.T.; Godoy, H.T. Analysis of Chlorogenic Acids Isomers and Caffeic Acid in 89 Herbal Infusions (Tea). *J. Food Compos. Anal.* **2018**, *73*, 76–82, doi:https://doi.org/10.1016/j.jfca.2018.08.001.

16. Rostamizadeh, K.; Abdollahi, H.; Parsajoo, C. Synthesis, Optimization, and Characterization of Molecularly Imprinted Nanoparticles. *Int. Nano Lett.* **2013**, *3*, 1–9, doi:10.1186/2228-5326-3-20.
17. Karim, K.; Breton, F.; Rouillon, R.; Piletska, E. V; Guerreiro, A.; Chianella, I.; Piletsky, S.A. How to Find Effective Functional Monomers for Effective Molecularly Imprinted Polymers? *Adv. Drug Deliv. Rev.* **2005**, *57*, 1795–1808, doi:https://doi.org/10.1016/j.addr.2005.07.013.
18. Vasapollo, G.; Sole, R. Del; Mergola, L.; Lazzoi, M.R.; Scardino, A.; Scorrano, S.; Mele, G. Molecularly Imprinted Polymers: Present and Future Prospective. *Int. J. Mol. Sci.* **2011**, *12*, 5908–5945, doi:10.3390/ijms12095908.
19. Kekelidze, I.; Ebelashvili, N.; Japaridze, M.; Chankvetadze, B.; Chankvetadze, L. Phenolic Antioxidants in Red Dessert Wine Produced with Innovative Technology. *Ann. Agrar. Sci.* **2018**, *16*, 34–38, doi:https://doi.org/10.1016/j.aasci.2017.12.005.

## **Chapter 3**

Molecularly imprinted electrochemical sensor for a direct  
caffeic acid detection in wine

In the previous chapter, we have demonstrated that the addition of an optimized CA-MIP to a solution of phenolic acids allows an indirect but selective detection of CA. This chapter has the objective to demonstrate direct detection of CA using electropolymerization. In this technique, a MIP is directly polymerized on the surface of the screen-printed carbon electrode.

## 1. Introduction

Chapter 1 and 2 concerned the *ex-situ* approach where the polymerization of CA-MIP and NIP and their application were done apart the electrode. Chapter 3 is devoted to electropolymerization. The polymers are synthesized directly on the surface of the electrode to form a sensor specific to caffeic acid (CA) ready to be applied in the medium.

**The main objectives** of this chapter are:

- Preparation of a MIPCA-sensor by electropolymerization for the detection of CA in wine
- Optimization of polymerization conditions and parameters
- Development of the sensor and evaluation of its rebinding characteristics
- Evaluation of the repeatability and stability of the sensor
- Application of the sensor in wine and validation of the method by HPLC-UV

The preparation of the sensor needs optimization of the conditions and the parameters:

- Choice of a convenient functional monomer. We used molecular simulation to avoid wasting time and reagents
- Choice of the template ratio to functional monomer concentrations that gives the best rebinding
- Choice of the cycles number that controls the thickness of the polymer on the surface of the SPCE and affects the structure of the polymer and its performance
- Choice of the sensor immersion time in the rebinding solution after polymerization and washing in a way that yields a maximum quantity of caffeic acid that rebinds to the polymer

Morphological characterization, selectivity tests and application in wine were realized with the prepared sensor.

4-aminobenzoic acid (4-ABA) was chosen as a functional monomer for the CA-MIP sensor. After optimization, a ratio of 1:10 with 10 cycles and 20 min of immersion of the sensor in rebinding solution were selected as conditions of polymerization. Cyclic voltammetry (CV) was used for the polymerization and differential pulse voltammetry (DPV) was used for the detection.

The obtained sensor was firstly applied in a hydro-alcoholic medium and showed good rebinding characteristics with high specificity (in terms of MIP-NIP difference) and selectivity towards CA regarding other interferents. Repeatability and stability were also tested and indicated that the sensor can be used for at least 15 times with same levels of precision and it is stable when stored in 0.05M PBS solution at pH3.

The sensor was successfully applied in wine and the results were compared to HPLC-UV. The recovery values ranged between 95 and 116% with a limit of detection (LOD) of 0.68  $\mu\text{M}$  (nearly 1  $\text{mg}\cdot\text{L}^{-1}$ ).

The simplicity of this method and the obtained results indicate that the developed MIP-sensor could be a promising green technique for future commercial applications.

**The main results** of this chapter are:

- The functional monomer was chosen using molecular simulation and the polymerization conditions were optimized before the preparation of the sensor
- A specific and selective MIP-sensor was developed for the detection of CA with a LOD = 0.68  $\mu\text{M}$
- The sensor was successfully applied in wine and the results were validated by HPLC-UV with recovery values ranging between 95 and 106%.

## 2. Article 3: Molecularly imprinted electrochemical sensor for a direct caffeic acid detection in wine

### Abstract

Caffeic acid (CA) is a phenolic acid that belongs to the class of hydroxycinnamic acids. It is widespread throughout the plant kingdom. As an antioxidant, it is responsible for could participate in the protection of living organisms against several diseases as well as the food products against food deterioration. Therefore, the evaluation and the detection of these compounds have always been interesting since they could present several industrial applications. Among all the used techniques for antioxidants characterization, electropolymerization seems to be currently the most suitable and interesting. It consists of creating a sensor modified with a molecularly imprinted polymer (MIP-sensor) that enhances its specificity and selectivity. In our study, a MIP-sensor was developed for CA detection in a hydro-alcoholic medium and afterwards applied in wine samples. The selection of the functional monomer was performed by molecular simulation. Under the optimized conditions, the MIP was polymerized on the surface of a screen-printed carbon electrode (SPCE) using a hydro-alcoholic solution containing 4-aminobenzoic acid (4-ABA) as a functional monomer and CA as a template molecule. The polymerization was performed by cyclic voltammetry (CV), and the detection of CA by differential pulse voltammetry (DPV) in the linear range between 0 and 40  $\mu\text{M}$  ( $R^2=0.9992$ ), with a limit of detection (LOD) of 0.68  $\mu\text{M}$ . The MIP-sensor was found to be selective toward CA compared to other interferents, repeatable and stable. It was successfully applied in wine samples and the method was validated by HPLC-UV.

**Keywords:** electropolymerization; MIP-sensor; differential pulse voltammetry; molecular simulation; wine; Screen printed electrode; industrial applications

## 2.1. Introduction

Antioxidants are groups of compounds that neutralize free radicals and reactive oxygen species (ROS) in the cell, providing protection of the body against the development of chronic diseases caused by these ROS including cardiovascular diseases, gastrointestinal diseases, Alzheimer's disease, cancer, inflammation, etc. [1–5]. In food products and beverages, phenolic acids became one of the most interesting topics for researchers. Both natural and synthetic are important in the food industry, but a greater importance is given to the natural ones, these are widely spread throughout the plant kingdom.

Two classes of phenolic acids are abundant in foods, namely hydroxybenzoic acids and hydroxycinnamic acids. The hydroxycinnamic acids are relatively more common, e.g., *p*-coumaric acid, caffeic acid (CA), ferulic acid, chlorogenic acid and sinapic acid. CA is generally the most abundant phenolic acid and represents 75-100% of the total hydroxycinnamic acid content of most fruits (e.g., apple, plums, tomatoes and grapes) [4]. CA is also the most powerful antioxidant of the hydroxycinnamic acids (O-diphenol structure).

The importance of these compounds has pushed researchers to develop and explore more antioxidant evaluation and detection techniques. Chromatographic techniques such as high performance liquid chromatography and gas chromatography are commonly used as separation techniques, coupled to detection systems, including UV-Vis spectroscopy, mass spectrometry, electrochemical, and fluorometric detection. HPLC-UV, GC-MS and LC-MS are the most common tandem techniques [6]. One of the greater limitations presented by these techniques is the time and solvent consumption, as well as the sample preparation.

For antioxidant activity evaluation, several assays were developed and applied according to the chemical reaction that may be involved: electron transfer (ET) or hydrogen atom transfer (HAT). ET assays include the Cupric Reducing Antioxidant Power (CUPRAC) test, the Ferric Reducing Antioxidant Power (FRAP) test and the Folin–Ciocalteu test. HAT assays include the Oxygen Radical Absorption Capacity (ORAC) test, the Hydroxyl Radical Antioxidant Capacity (HORAC) test, the Total Peroxyl Radical Trapping Antioxidant Parameter (TRAP) test, DPPH test (2,2 diphenyl 1 picrylhydrazyl) and the Total Oxyradical Scavenging Capacity (TOSC) test. All these methods were successfully applied but the majority present several disadvantages (time consuming, expensive, they do not reflect the situation in an oxidant food or an in vivo situation, lack of specificity, etc. [5,7,8]).

In order to overcome all these limitations, researchers used electrochemistry as an easy and fast method with relatively low-cost instrumentations. Voltammetry techniques are mainly used for antioxidant detection that are known to be electroactive or redox active compounds [9]. Moreover, screen-printed electrodes (SPE) replaced traditional electrodes to avoid cleaning problems that affect the results. SPE are small, inexpensive, easy, single use and require small volumes of the samples. Electrochemical method is adapted to evaluate the quantity (quantity of current in C), but also the antioxidant capacity using the oxidation potential value (in mV). Nevertheless, this method works with single molecule in solution or two, but not with a complex mixture of several antioxidants. Given the instability of antioxidants and the similarity between their chemical structures when they belong to the same class, it is often difficult to report the results for a specific antioxidant that makes the selectivity of the technique weak. For this reason, molecular imprinting, a rapidly growing technique, is considered as a convenient option to improve the detection of antioxidants in a complex medium and enhance the selectivity [9].

Molecular imprinting is a technique that consists of creating complementary images in terms of structure and chemical functionalities of a target molecule (template) within a synthetic polymer. Those molecularly imprinted polymers (MIPs), and the non-imprinted polymers (NIPs), combined with the SPE, form a sensor specific to one antioxidant or a family of antioxidants with close chemical structures. In this case, several ways exist in order to prepare the sensor and to polymerize the MIP and NIP [10] on the surface of the electrode.

There is the ex-situ and the in-situ synthesis. Ex-situ synthesis consists of preparing the polymers separately (UV or thermal polymerization) and then deposit them on the electrode by spin coating or drop casting. And in-situ synthesis is the polymerization directly on the surface of the electrode by applying a range of potentials to a solution containing the pre-polymerization complex in presence of the template molecule, also known by electropolymerization.

Electropolymerization seems to be the most appealing procedure. When the most suitable conditions are found (functional monomer, ratio of the concentrations of the functional monomer and the template, solvent, number of cycles, etc.), this technique can easily control the thickness and the morphology of the resulting polymer on the surface of the electrode [11].

In this work, a simple and selective caffeic acid-MIP sensor was prepared by the electropolymerization of 4-aminobenzoic (4-ABA) acid in aqueous solutions directly on the surface of a screen-printed carbon electrode (SPCE). 4-ABA was selected among nine monomers using molecular simulation. Caffeic acid was detected firstly in a hydro-alcoholic

medium in the presence of other interferents with similar structures to caffeic acid, and then in wine. The same wine samples were injected in HPLC-UV in order to compare the results and validate the method. The recovery tests were accurate and the developed sensor could be suitable for application in commercial analytical solutions such as food products.

## 2.2. Material and methods

### 2.2.1. Reagents

Caffeic acid ( $\geq 98\%$ , CAS number 331-39-5), 4-aminobenzoic acid ( $\geq 99\%$ , CAS number 150-13-0), *p*-coumaric acid ( $\geq 98\%$ , CAS number 501-98-4), gallic acid (97.5-102.5 titration, CAS number 149-91-7), *trans*-ferulic acid ( $\geq 99\%$ , CAS number 537-98-4), sinapic acid ( $\geq 98\%$ , powder, 530-59-6), phosphate buffered saline (PBS tablets), ethanol (EtOH, absolute, CAS number 64-17-5), and acetic acid (glacial, CAS number 64-19-7) were purchased from Sigma Aldrich, France.

Water used in all experiments was deionised and obtained from an Elga Ionic system PURELAB Option.

### 2.2.2. Instrumentation

All the voltammetric measurements were carried out using a portable and easy-to-handle  $\mu$ Stat-i MultiX potentiostat, connected to a PC, and screen-printed carbon electrodes, all purchased from Metrohm, France. The analyses were performed with cyclic voltammetry for the polymerization and differential pulse voltammetry for the detection. The measured intensity (anodic peak intensity,  $I_{pa}$ ) is proportional to the concentration of the detected compound in the medium.

### 2.2.3. Molecular simulation

The choice of the functional monomer was made using molecular simulation. Nine monomers, 4-aminobenzoic acid (4-ABA), aniline (ANL), *o*-phenylenediamine (OPD), carbazole (CBZ), mercaptobenzimidazole (MBI), *m*-phenylenediamine (MPD), *m*-phenylenediamine (MPD), phenol (PHE), pyrrole (PYR) and thiophene (TPH) were studied as potential functional monomers for CA-MIP film formation. These 9 functional monomers were previously selected by examining their structure, which suggests that they are likely to interact favorably, non-

covalently, with caffeic acid. To conduct this study, the program GROMACS [12,13] was used with the OPLS-AA force field parameters [14,15] to represent caffeic acid, functional monomers, and ethanol. These parameters were automatically generated by the LigParGen server [16], available at <http://zarbi.chem.yale.edu/ligpargen/>. No further optimization of these parameters was performed. Water molecules were represented by the TIP4P/2005 model [17]. The LINCS algorithm [18] was used to fix the length of all bonds involving a hydrogen atom and the equations of motion were integrated with the Verlet leapfrog algorithm using a time step of 2 fs.

An ethanol/water mixture (10/90 v/v) was used as the solvent for the polymerization tests. The mixtures were prepared with the PACKMOL program [19] (<http://leandro.iqm.unicamp.br/m3g/packmol/home.shtml>). Each mixture consisted of 1 molecule of caffeic acid, 4 molecules of functional monomer, 113 molecules of ethanol, and 3327 molecules of water in a cubic simulation box with an initial side length of 48 Å, which corresponds to a caffeic acid concentration of approximately 15 mM. For each mixture, 3 independent random configurations were generated. The energy of these configurations was minimized using the steepest slope algorithm. A 200 ps molecular dynamics simulation in the canonical set (N, V, T) was then performed to heat the system from 10 K to 298 K. Finally, a 200 ns molecular dynamics simulation in the isothermal-isobaric ensemble (N, P, T) with T = 298 K and P = 1 atm was performed, recording atomic coordinates every 2 ps. The interactions between caffeic acid and functional monomers were analyzed over the second half of each simulation (t = [100 ns-200 ns]), determining the average values of the following three parameters: (i) the number of functional monomers in contact with caffeic acid (coordination number), (ii) the number of hydrogen bonds formed between caffeic acid and functional monomers, and (iii) the interaction energy between caffeic acid and functional monomers.

#### 2.2.4. MIP sensor development

Under the optimum conditions, the electropolymerization of the MIP-sensor was performed on the SPCE surface using cyclic voltammetry (CV) in the potential range from -0.2 to 1 V, at a scan rate of 100 mV/s for 20 consecutive cycles. A drop of 50 µL of the pre-polymerization mixture containing 0.05 mM caffeic acid and 0.5 mM 4-ABA as a functional monomer in a PBS 0.05M pH3/ethanol 90/10 v/v mixture was used as the polymerization medium. A non-imprinted polymer (NIP) electrode was prepared using the same experimental conditions, but

without adding CA into the polymerization solution. The electrodes were then rinsed with ultrapure water and immersed in the washing solution ethanol/acetic acid 90/10 v/v for 10 min, then in ethanol for 10 min. The electrodes were air dried and fixed on the potentiostat, 50  $\mu\text{L}$  of PBS 0.05M pH3 were dropped on the surface of the MIP-SPCE and a differential pulse voltammetry (DPV) signal was applied between 0.1 to 0.8 V,  $E_{\text{step}}$ : 0.004 V,  $E_{\text{pulse}}$ : 0.08 V,  $t_{\text{pulse}}$  : 200 ms and  $S_{\text{rate}}$  : 0.04 V for the detection. After the extraction of CA, the SPCE was dipped in a CA solutions ranging between 2  $\mu\text{M}$  and 40  $\mu\text{M}$  prepared in PBS 0.05M pH3/ethanol 90/10 v/v for 20 min. Then the SPCE was rinsed, dried and connected again, with 50  $\mu\text{L}$  of PBS on its surface, and a DPV is applied, for the rebinding evaluation.

Several important parameters for the performance of the MIP-sensor were optimized including the ratio of the template to functional monomer concentrations, the number of cycles and the rebinding time.

### **2.2.5. Selectivity tests**

The performance of the MIP-sensor was evaluated in the presence of interferents with similar chemical structures to caffeic acid: gallic acid (GA), trans-ferulic acid (FA), *p*-coumaric acid (*p*-CA) and sinapic acid (SA) by preparing 50  $\mu\text{M}$  of each solution separately, and using them as incubation solutions to the sensor. Rebinding tests were applied as described in paragraph 2.2.4.

### **2.2.6. Application of the sensor in wine and recovery tests**

Five samples of a red Burgundy wine (Pinot noir, 2017) were prepared. The wine was diluted 10 times and spiked with different concentrations of caffeic acid ranging between 11 and 167  $\mu\text{M}$ . The MIP-sensor was applied as described previously and the same samples were injected in HPLC-UV in order to compare the results and validate the DPV method.

## **2.3. Results and discussion**

### **2.3.1. Choice of the functional monomer based on molecular simulation**

The selection of a suitable functional monomer with strong interactions with the template before the polymerization may lead to a better imprinting effect. For this purpose, molecular

simulation was used as a valuable pre-screening strategy that enables the selection of the monomer with the best complementarity with the template in terms of coordination number (CN), total interaction energy ( $E_{\text{int}}$ , kJ/mol) and number of hydrogen bonds (nHB) (Table 10).

**Table 10.** Coordination number (CN), total interaction energy ( $E_{\text{int}}$ ) for the CA–monomer complexes, as well as the number of hydrogen bonds (nHB) responsible for their stabilization.

<b>Complex</b>	<b>CN</b>	<b><math>E_{\text{int}}</math> (kJ/mol)</b>	<b>nHB</b>
<b>CA-ABA</b>	0.48	-9.0	0.039
<b>CA-ANL</b>	0.17	-2.1	0.016
<b>CA-CBZ</b>	0.31	-5.6	0.009
<b>CA-MBI</b>	0.39	-7.5	0.022
<b>CA-MPD</b>	0.19	-2.7	0.032
<b>CA-OPD</b>	0.17	-2.4	0.023
<b>CA-PHE</b>	0.20	-2.5	0.007
<b>CA-PYR</b>	0.08	-0.7	0.005
<b>CA-TPH</b>	0.16	-1.6	0.000

These results indicate that 4-ABA is expected to present the highest affinity for CA ( $E_{\text{int}} = -9$  kJ/mol). The preferential stabilization of the CA-ABA complex can be associated with the strong hydrogen bonds established between the hydroxyl group or dialkylamine group in 4-ABA and the hydroxyl group in CA (Figure 34).

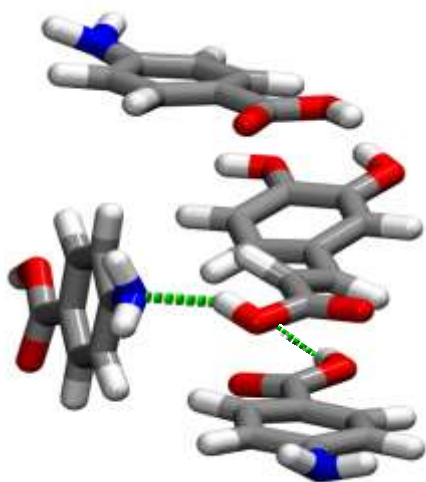


**Figure 34.** CA-ABA aggregation

According to these theoretical results, 4-ABA should present the highest selectivity for the CA template. Therefore, this monomer was selected to be used for molecular imprinting of CA.

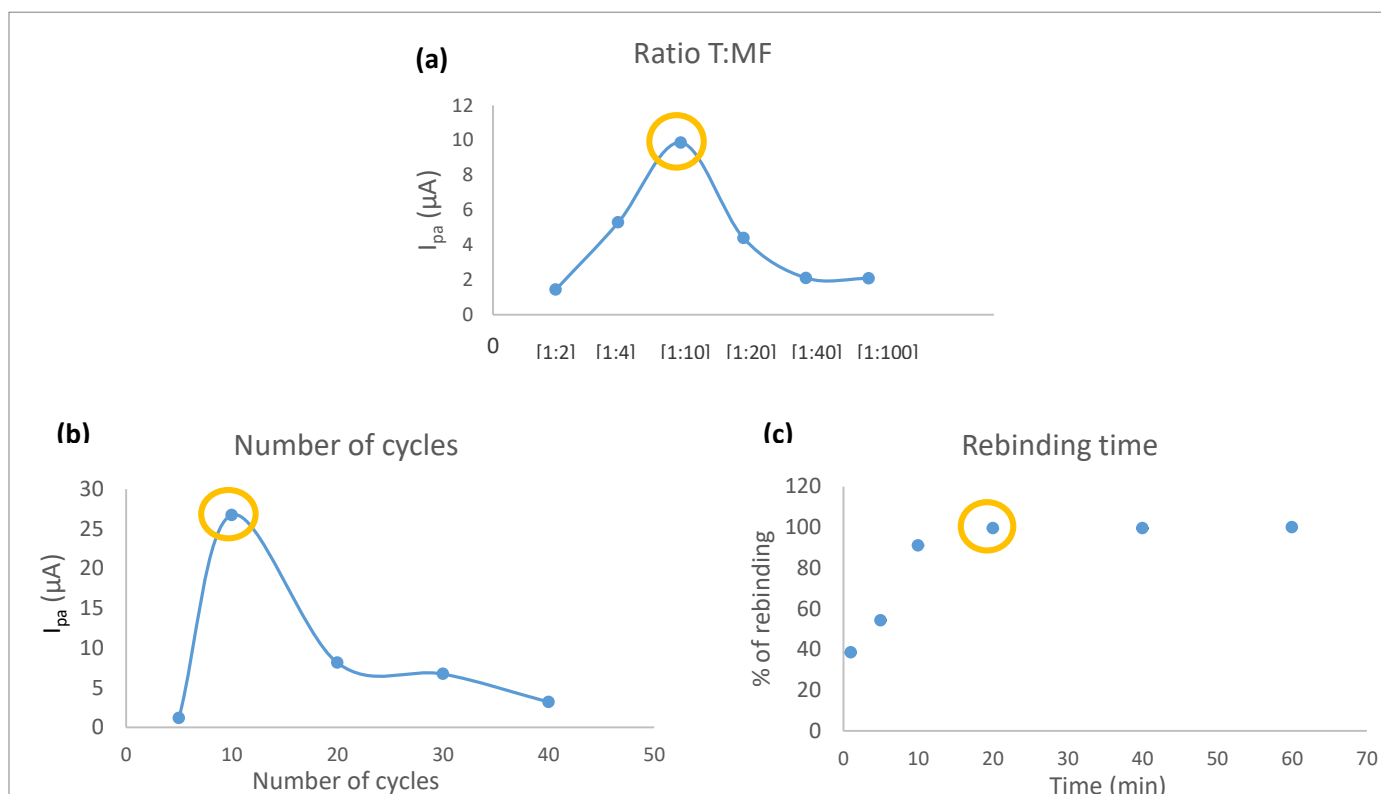
### 2.3.2. Optimization of the parameters

Figure 35 shows the results of the optimized parameters after the rebinding step. Several ratios of template to functional monomer concentrations were tested and it was observed that the electrochemical performance of the prepared MIP is strongly dependent on this parameter. The signal increased up to [1:10] ratio (9.865  $\mu\text{A}$ ) and decreased with higher concentrations of functional monomer (Figure 35a).

The main advantage of electropolymerization is the control of the polymer thickness can be achieved by adjusting the number of potential cycles. Different CV cycles were applied, ranging from 5 to 40. As shown in Figure 35b, the highest peak current intensity of the MIP-sensor was obtained with 10 cycles (26.7  $\mu\text{A}$ ) and then a continuous decrease was observed. This decrease can be explained by an increase in the thickness of the polymer, which makes it difficult to extract CA molecules imprinted close to the surface. For this reason, 10 cycles were used.

The rebinding time corresponds to the time of immersion of the MIP-sensor in the rebinding solution before DPV evaluation. Different rebinding times were tested, ranging from 1 to 60 min. The highest current was obtained after 20 min of immersion and then reached a plateau (Figure 35c). For this reason, 20 min was used as rebinding time.

Finally, we considered these trails as a first step of optimization, given the first optimal conditions: 10 cycles, 20 min of rebinding, ratio T/FM 1 :10. We have not used a regular Simplex plan for experimental research to perfect the optimization. It is time consuming and not fully necessary considering our results for CA detection.



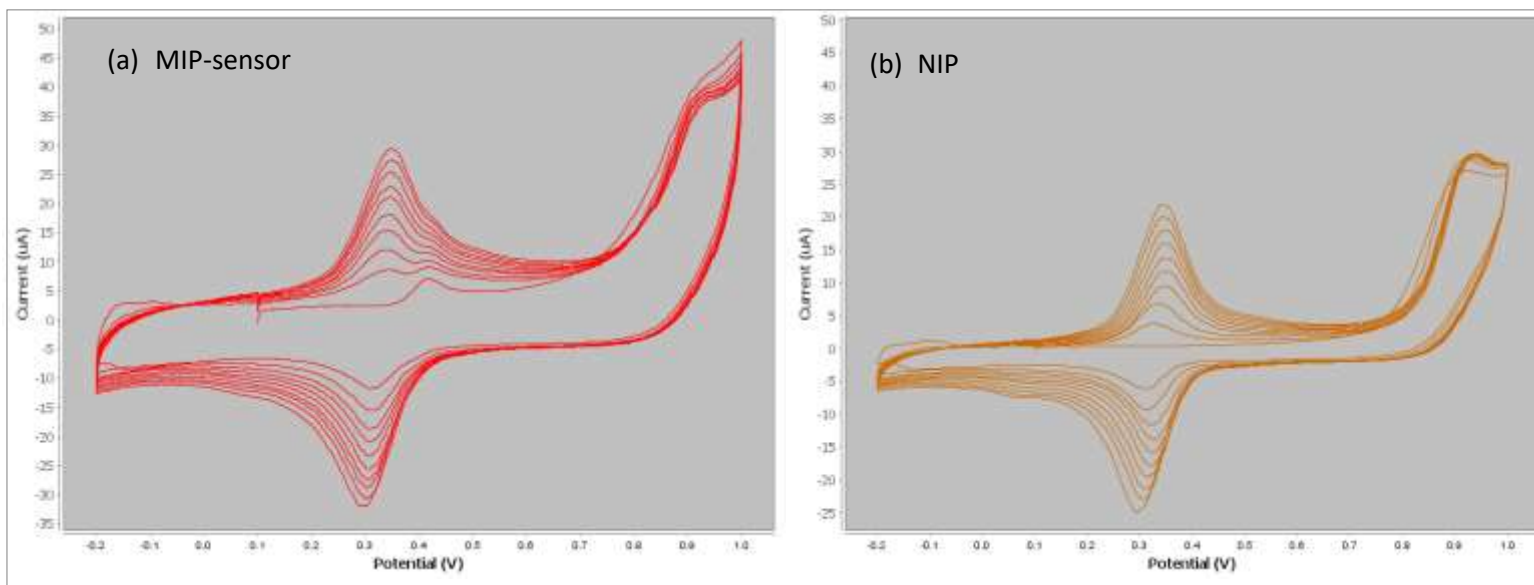
**Figure 35.** Optimization of the polymerization parameters: (a) ratio of the template (T) to functional monomer (FM) concentrations, (b) the number of cycles and (c) the rebinding time.

### 2.3.3. Analytical performance of the MIP sensor

Under the optimized experimental conditions described above, the determination of CA molecules at different concentrations was evaluated by DPV, as well as the performance of the MIP-sensor in the presence of interferents.

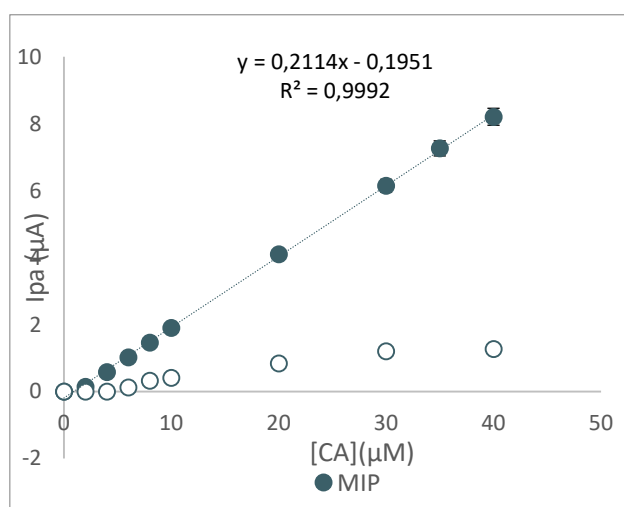
### 2.3.4. Application in hydro-alcoholic medium

Figure 36 represents the CV signals of the MIP-sensor and the corresponding NIP at the end of the polymerization, just before the extraction of the template. The CA peak is remarkable in the first polymerization cycles of the MIP-sensor.



**Figure 36.** CV signals representing the polymerization of the MIP(a) and the NIP(b) on the surface of the SPCE

Once the sensors were washed and the template extracted, they were immersed in CA solutions with different concentrations, prepared in PBS 0.05M pH 3/ethanol 90/10 v/v for 20 min. Figure 36 shows a linear relationship between the oxidation peak current of the MIP-sensor and the concentration of CA in the range between 0 and 40  $\mu\text{M}$  ( $R^2 = 0.9992$ ). The MIP-sensor gave a signal that is on average 5 times greater than that given by the NIP, indicating that it is a caffeic acid specific sensor. The limits of detection (LOD) and quantification (LOQ), given by the equations  $\text{LOD} = 3s/m$  and  $\text{LOQ} = 10s/m$  where “s” is the standard deviation of the intercept and “m” is the slope of the calibration plot, are found to be 0.68 and 2.05  $\mu\text{M}$ , respectively.



**Figure 37.** Rebinding activity of the MIP-sensor and the NIP in the presence of different concentrations of caffeic acid, prepared in a hydro-alcoholic solution

### 2.3.5. Repeatability and stability of the sensor

The repeatability (intra-day precision) and the stability of the MIP-sensor were also tested.

The repeatability was estimated over 23 consecutive repetitions, at 50  $\mu\text{M}$  of caffeic acid, and expressed as relative standard deviation (RSD) and percentage decrease of the peak current. The RSD was found to be 4.6% at the 15th trial with 2.6% of  $I_{\text{pa}}$  decrease. At the end, after 23 repetitions, the RSD increased to 10.4% with 37% of  $I_{\text{pa}}$  decrease. This means that the sensor can be safely used with satisfactory levels of precision up to at least 15 times consecutively.

Moreover, the stability of the MIP-sensor was also evaluated. Two types of storage were tried. One sensor was stored dry at room temperature (sensor A), and the second one (sensor B) was stored in 0.05M PBS solution at pH3 and their response were evaluated at day 7; 12 and 15. It was found that the peak current decreased 6; 10 and 26%, respectively, from the initial response of sensor A, and 2; 7 and 11%, respectively, for sensor B. These results show that the MIP-sensor is stable and better stored in 0.05M PBS solution at pH3.

### 2.3.6. Selectivity tests

The evaluation of the MIP-sensor performance in the presence of interferents was done. Four compounds with similar structures were selected, GA, FA, SA and *p*-CA, and prepared at a concentration of 30  $\mu\text{M}$ . Both MIP and NIP were used to analyze solutions of each individual compound, including CA. The results were expressed as % of the peak current or rebinding relative to the MIP-sensor peak current obtained in the presence of CA (Figure 37). As expected, the response of the MIP-sensor in the presence of CA was higher than those of other interferents, indicating the effective imprinting process and the greater selectivity for caffeic acid. FA and SA showed lower peaks corresponding to 23 and 33% of the CA peak, respectively. GA and *p*-CA did not show any response. This could be due to the affinity between CA and the imprinted cavities on the MIP created by 4-ABA. Therefore, the MIP-sensor showed a selective recognition toward CA.

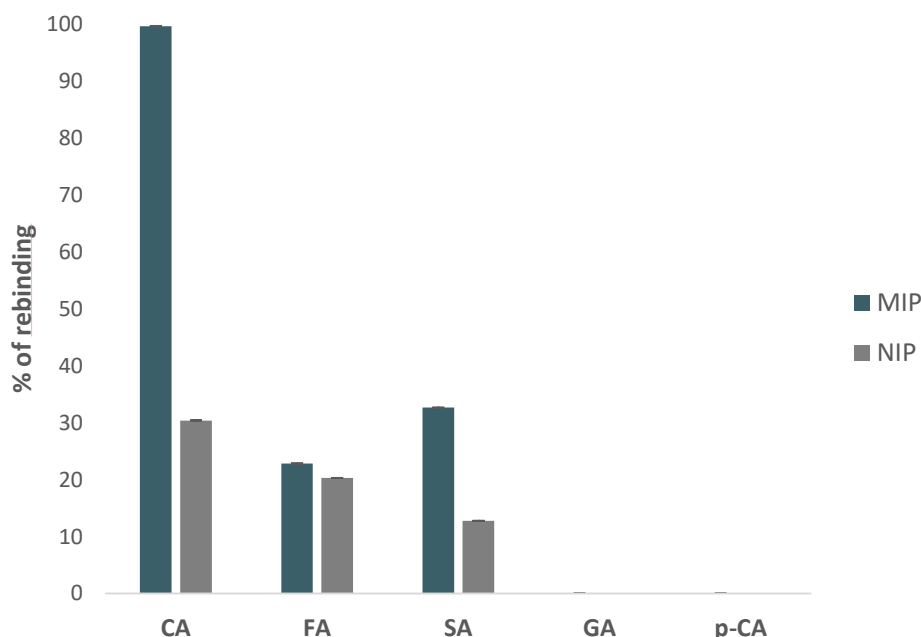


**Figure 38.** The MIP-sensor and NIP response represented by % of rebinding in the presence of CA and other interferents: trans-ferulic acid (FA), sinapic acid (SA) gallic acid (G), and p-coumaric acid (*p*-CA).

### 2.3.7. Detection of CA in wine samples and comparison between DPV and HPLC-UV

Finally, the detection of CA in wine was performed using the standard addition method, where the wine was spiked with five different concentrations of caffeic acid: 11; 33; 44; 56 and 167  $\mu\text{M}$ . 50  $\mu\text{L}$  were deposited on the surface of MIP-sensors and DPV signal was applied. In order to compare the results with a conventional method, the samples were injected in HPLC-UV for the validation of the DPV method using the MIP-sensor. Two types of recovery were calculated, recovery a (equation 1) and recovery b (equation 2). Recovery b compares the results found with DPV and HPLC, and they were in the range between 95 and 116% (Table 11).

$$\text{Recovery a} = \frac{[\text{CA}]_{\text{found in DPV}}}{[\text{CA}]_{\text{added}}} \quad (1)$$

$$\text{Recovery b} = \frac{[\text{CA}]_{\text{found in DPV}}}{[\text{CA}]_{\text{found in HPLC}}} \quad (2)$$

**Table 11.** Determination of CA concentration and recovery values in spiked wine samples with the developed MIP sensor with DPV and HPLC-UV methods.

Added CA $\mu\text{M}$	DPV		HPLC	
	Found CA $\mu\text{M}$	Recovery 1 (%)	Found CA ( $\mu\text{M}$ )	Recovery 2 (%)
11	$12.0 \pm 0.3$	106	$12.0 \pm 0.6$	95
33	$33.0 \pm 0.9$	100	$29.0 \pm 0.6$	116
44	$43.0 \pm 1.8$	98	$39.0 \pm 0.3$	110
56	$53 \pm 2.3$	95	$54.0 \pm 0.9$	98
167	$178 \pm 5$	107	$169 \pm 6$	106

These results show that the proposed MIP-sensor could be used as an accurate strategy for CA determination in wine samples without the need of sample pre-treatment or preparation.

## 2.4. Conclusions

In this work, a selective and specific MIP electrochemical sensor was developed for the determination of caffeic acid in hydro-alcoholic and wine samples. The functional monomer was chosen based on molecular simulation. The proposed sensor exhibited a relevant linear relationship ( $R^2=0.9992$ ) in the concentration range of 0 to 40  $\mu\text{M}$  with a LOD of 0.68  $\mu\text{M}$  (nearly 1  $\text{mg}\cdot\text{L}^{-1}$ ) showing that this method is sensitive enough to be applied in real samples, given that the limits were reached without any sample pre-treatment. The sensor showed a good selectivity toward CA compared to other interferents with close chemical structures. Moreover, the MIP-sensor was successfully applied in wine samples and the method was validated by HPLC-UV as it showed recovery values ranging between 95 and 116%. All these results, in addition to the simplicity and the rapidity of sensor preparation indicate that the developed MIP-sensor may be a promising green technique for future commercial applications, such as CA or any other individual or class of antioxidants detection in different food matrices.

## References

1. Luksiene, Z.; Brovko, L. Antibacterial Photosensitization-Based Treatment for Food Safety. 2013, 185–199, doi:10.1007/s12393-013-9070-7.
2. Roohinejad, S.; Koubaa, M.; Barba, F.J.; Saljoughian, S.; Amid, M.; Greiner, R. Application of Seaweeds to Develop New Food Products with Enhanced Shelf-Life, Quality and Health-Related Beneficial Properties. *Food Res. Int.* 2017, 99, 1066–1083, doi:https://doi.org/10.1016/j.foodres.2016.08.016.
3. Wilson, D.W.; Nash, P.; Buttar, H.S.; Griffiths, K.; Singh, R.; De Meester, F.; Horiuchi, R.; Takahashi, T. The Role of Food Antioxidants, Benefits of Functional Foods, and Influence of Feeding Habits on the Health of the Older Person: An Overview. *Antioxidants (Basel, Switzerland)* 2017, 6, doi:10.3390/antiox6040081.
4. Manach, C.; Scalbert, A.; Morand, C.; Rémésy, C.; Jiménez, L. Polyphenols: Food Sources and Bioavailability. *Am. J. Clin. Nutr.* 2004, 79, 727–747, doi:10.1093/ajcn/79.5.727.
5. Munteanu, I.G.; Apetrei, C. Analytical Methods Used in Determining Antioxidant Activity: A Review. *Int. J. Mol. Sci.* 2021, 22, doi:10.3390/ijms22073380.
6. Robbins, R.J. Phenolic Acids in Foods: An Overview of Analytical Methodology. *J. Agric. Food Chem.* 2003, 51, 2866–2887, doi:10.1021/jf026182t.
7. Apak, R.; Özyürek, M.; Güçlü, K.; Çapanoğlu, E. Antioxidant Activity/Capacity Measurement. 1. Classification, Physicochemical Principles, Mechanisms, and Electron Transfer (ET)-Based Assays. *J. Agric. Food Chem.* 2016, 64, 997–1027, doi:10.1021/acs.jafc.5b04739.
8. Apak, R.; Özyürek, M.; Güçlü, K.; Çapanoğlu, E. Antioxidant Activity/Capacity Measurement. 2. Hydrogen Atom Transfer (HAT)-Based, Mixed-Mode (Electron Transfer (ET)/HAT), and Lipid Peroxidation Assays. *J. Agric. Food Chem.* 2016, 64, 1028–1045, doi:10.1021/acs.jafc.5b04743.
9. Elhachem, M.; Cayot, P.; Abboud, M.; Louka, N.; Maroun, R.G.; Bou-maroun, E. The Importance of Developing Electrochemical Sensors Based on Molecularly Imprinted Polymers for a Rapid Detection of Antioxidants; antioxidants, 2021; ISBN 3338077408.
10. Ertürk, G.; Mattiasson, B. Molecular Imprinting Techniques Used for the Preparation of Biosensors. *Sensors (Basel)*. 2017, 17, doi:10.3390/s17020288.
11. Sharma, P.S.; Souza, F.D.Ö.; Kutner, W. Molecular Imprinting for Selective Chemical Sensing of Hazardous Compounds and Drugs of Abuse. *Trends Anal. Chem.* 2012, 34, 59–77, doi:10.1016/j.trac.2011.11.005.

12. Abraham, M.J.; Murtola, T.; Schulz, R.; Páll, S.; Smith, J.C.; Hess, B.; Lindahl, E. GROMACS: High Performance Molecular Simulations through Multi-Level Parallelism from Laptops to Supercomputers. *SoftwareX* 2015, 1–2, 19–25, doi:<https://doi.org/10.1016/j.softx.2015.06.001>.
13. Van Der Spoel, D.; Lindahl, E.; Hess, B.; Groenhof, G.; Mark, A.E.; Berendsen, H.J.C. GROMACS: Fast, Flexible, and Free. *J. Comput. Chem.* 2005, 26, 1701–1718, doi:[10.1002/jcc.20291](https://doi.org/10.1002/jcc.20291).
14. Dodda, L.S.; Vilseck, J.Z.; Tirado-rives, J.; Jorgensen, W.L. 1.14 \* CM1A-LBCC: Localized Bond-Charge Corrected CM1A Charges for Condensed-Phase Simulations. 2017, doi:[10.1021/acs.jpcc.7b00272](https://doi.org/10.1021/acs.jpcc.7b00272).
15. Jorgensen, W.L.; Tirado-rives, J.; Fields, F. Potential Energy Functions for Atomic-Level Simulations of Water and Organic and Biomolecular Systems. 2005, 102, 6665–6670.
16. Dodda, L.S.; Vaca, I.C. De; Tirado-rives, J.; Jorgensen, W.L. LigParGen Web Server : An Automatic OPLS-AA Parameter Generator for Organic Ligands. 2017, 1–6, doi:[10.1093/nar/gkx312](https://doi.org/10.1093/nar/gkx312).
17. Abascal, J.L.F.; Vega, C. A General Purpose Model for the Condensed Phases of Water : TIP4P / 2005. 2005, 1–12, doi:[10.1063/1.2121687](https://doi.org/10.1063/1.2121687).
18. Hess, B. P-LINCS: A Parallel Linear Constraint Solver for Molecular Simulation. *J. Chem. Theory Comput.* 2008, 4, 116–122, doi:[10.1021/ct700200b](https://doi.org/10.1021/ct700200b).
19. Martínez, L.; Andrade, R.; Birgin, E.G.; Martínez, J.M. Software News and Update Packmol : A Package for Building Initial Configurations. 2009, doi:[10.1002/jcc](https://doi.org/10.1002/jcc).

**Part IV**  
**Conclusion and perspectives**

## Conclusion and perspectives

The current needs of research, health and food all require rapid and cost effective research techniques. Compounds such as antioxidants are being actively monitored. Molecular imprinting coupled with electrochemistry can provide an answer to the challenge of detecting these compounds. This thesis contributes to the research of antioxidant detection, in our case caffeic acid, by developing a simple and rapid electrochemical method for the detection of caffeic acid in wine using molecularly imprinted polymers.

The methods developed were based on two approaches: *ex-situ* and *in-situ* polymerization.

This work started with the *ex-situ* method, where the polymer was prepared and applied in the rebinding solution apart from the electrode. In chapter 1, a molecularly imprinted polymer specific to caffeic acid (CA-MIP) was polymerized and applied in a hydro-alcoholic medium, then applied in wine. The only lack in its performance was the specificity. This concern was the subject of chapter 2 in which a work of optimization of the preparation was done to achieve a better specificity. Among couples, one was chosen (CA-MIP6/NIP6) for its characteristics of rebinding and difference between the response of the MIP and the NIP. This optimization showed that several parameters can influence the synthesis. Starting with solubility of the template in the solvent, followed by the type of the functional monomer and the type of radical initiation used. The polymer was successfully applied in wine and validated by HPLC-UV with recovery values ranging between 104 and 111% and with a limit of detection (LOD) of 0.13 mM.

A more advanced method with easier preparation and better precision was investigated in chapter 3. *In-situ* polymerization or electropolymerization is a more accurate technique where an electrochemical sensor is prepared by polymerizing the MIP directly on the surface of the electrode (SPCE). An important work was done for the optimization of the conditions starting with the choice of functional monomer that was done using molecular simulation to avoid time and reagents waste, the ratio of template to functional monomer concentrations, the number of cycles that control the thickness of the polymer and the time of immersion of the sensor in the rebinding solution. Once the optimal conditions were selected, the MIP-sensor was developed and applied in hydro-alcoholic medium where it showed a good specificity (MIP-sensor signal was 5 times greater than NIP) and selectivity toward caffeic acid with a linear relationship between the peak current ( $I_{pa}$ ) and the concentration of CA ranging between 0 and 40  $\mu\text{M}$  ( $R^2 = 0.9992$ ) and a limit of detection of 0.68  $\mu\text{M}$ , obviously lower than the one obtained with

the indirect method. The repeatability and stability were also tested and showed that the sensor can be used up to 15 times conserving its precision and it was better stored in 0.05M PBS at pH3. When applied in wine, the results were compared to HPLC-UV and gave recovery values ranging between 95 and 116%. These results showed that this method could potentially improve antioxidant detection in wine as well as in other matrices and in other industrial applications especially that it is close to the requirements of green chemistry since limited sample preparation and small volumes of samples are used.

As a next step, this method deserves to be improved to enhance the electrochemical signal; one suggestion could be the modification of the surfaces of the SPEs, with multi-walled carbon nanotubes (MWCNT), with electrochemically reduced graphene oxide (ERGO) or other nanoparticles. Several studies mentioned the modification of the electrode and helped obtaining better results. Moreover, this method could be applied beyond the detection of individual antioxidants to a family of antioxidants. What might also be interesting is the development of a method for the detection of antioxidants in non-aqueous media, such as oils.

To go further, this methodology might be applicable not only with antioxidants, but for the detection of other compounds in food matrices such as proteins, viruses and bacteria as well. The detection of these molecules by our method present some challenges that would be interesting to overcome such as the synthesis parameters of the MIPs for more complex templates, the choice of reagents and all the working conditions. The detection of these molecules would allow a better control and protection from food allergies and food intoxication. The optimization of this method may one day lead to the replacement of conventional methods by a simpler and faster one with accurate and satisfactory results.

Overall, this thesis combined several domains in science, several techniques and ideas that led to the development of methods used for the “rapid detection of food antioxidants using electrochemical sensors based on molecularly imprinted polymers”.

## Supplementary Material

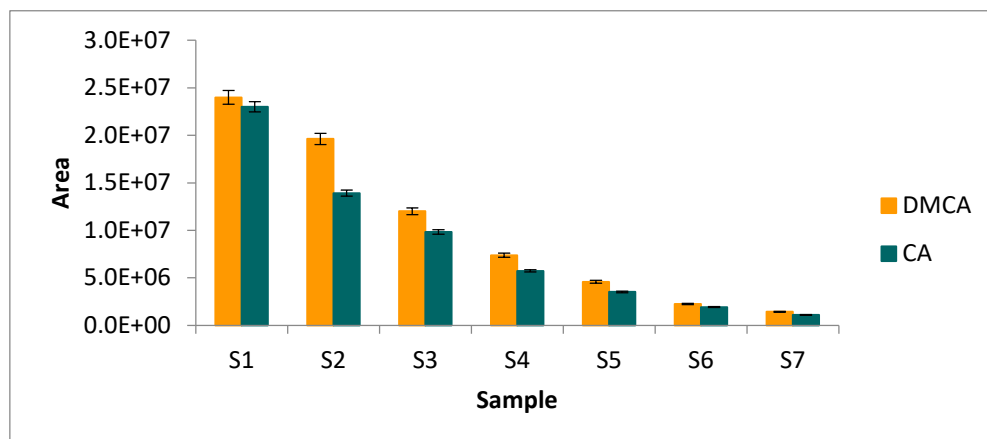


**Figure S1.** Remaining template (DMCA, CA) during the washing steps of the polymers.

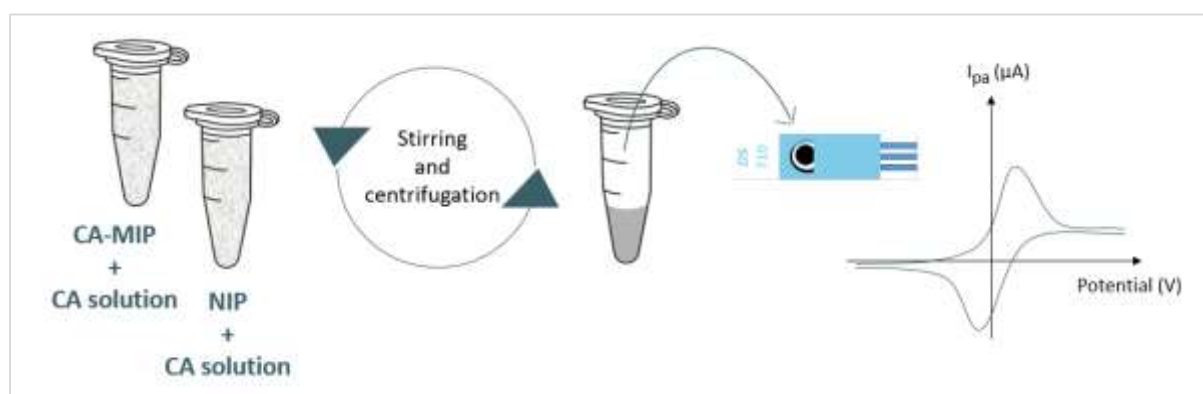


**Figure S2.** Preparation steps of rebinding experiments using CA-MIP/NIP and measured by CV.

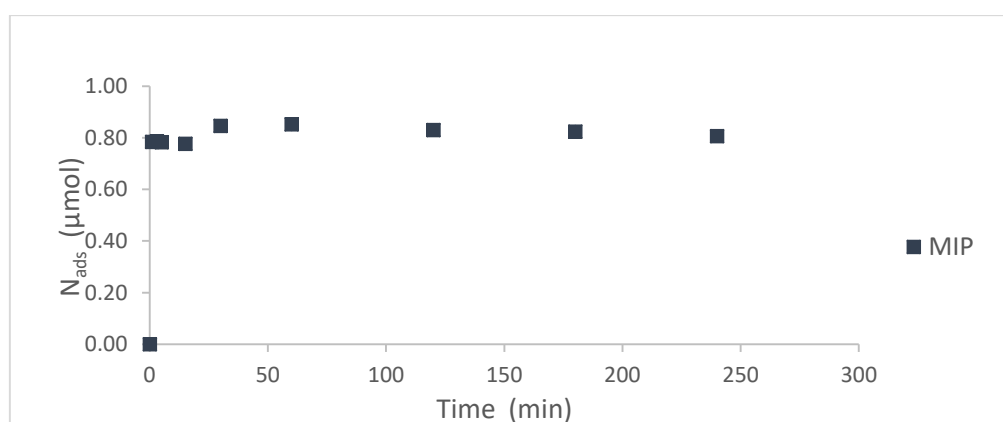


**Figure S3.** Kinetic study representing the amount of adsorbed caffeic acid from 1 min to 4 hours of stirring, applied with nine samples of 1 mL containing 1.11 mM of caffeic acid in the presence of 20 mg CA-MIP (error bars are smaller than the symbol).

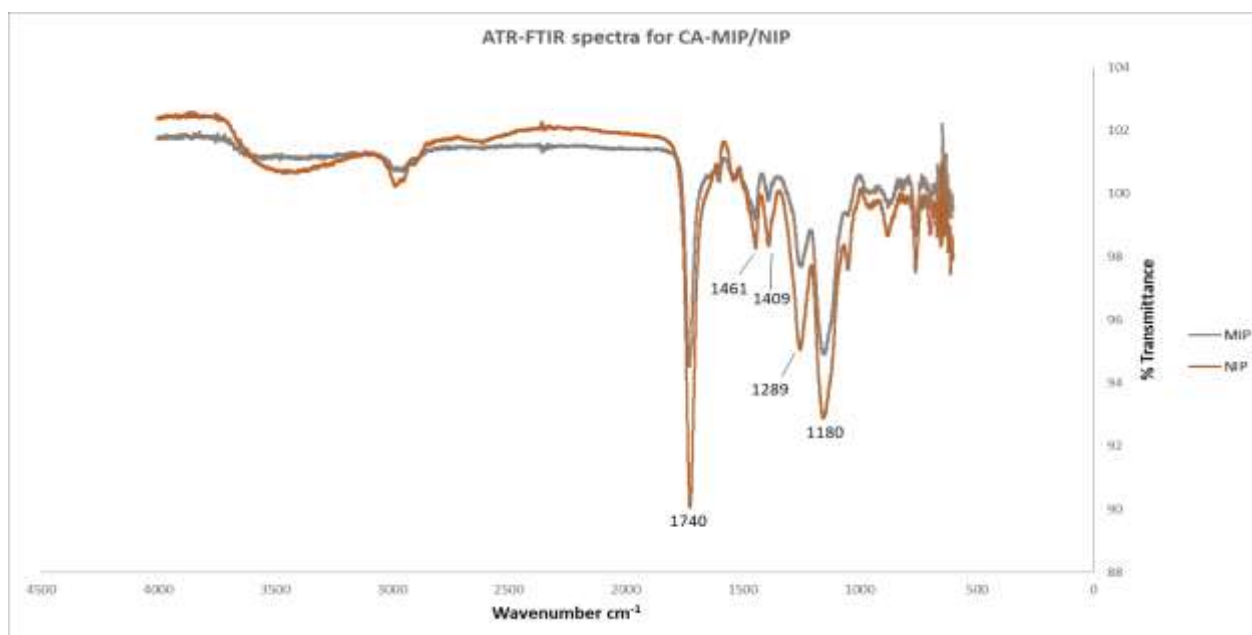


Figure S4. ATR-FTIR spectra for CA-MIP and NIP.

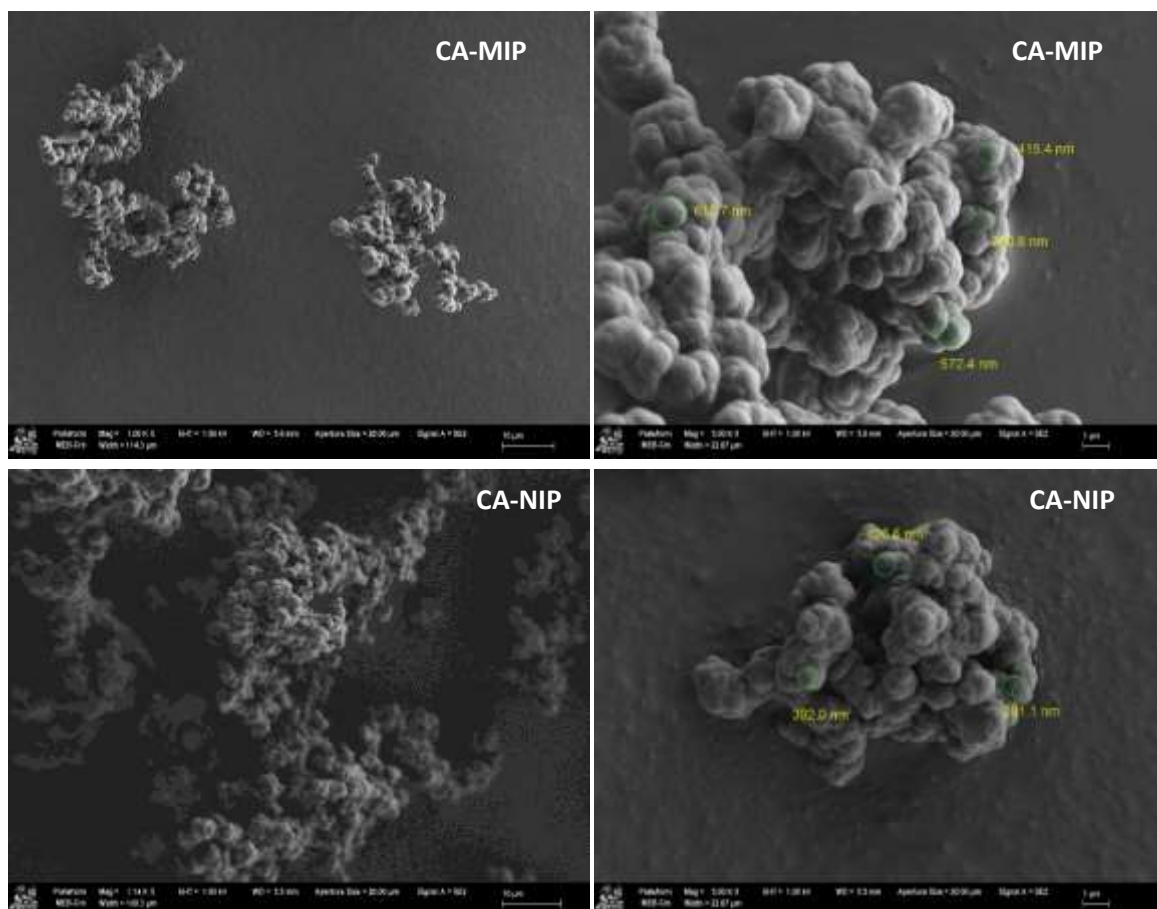
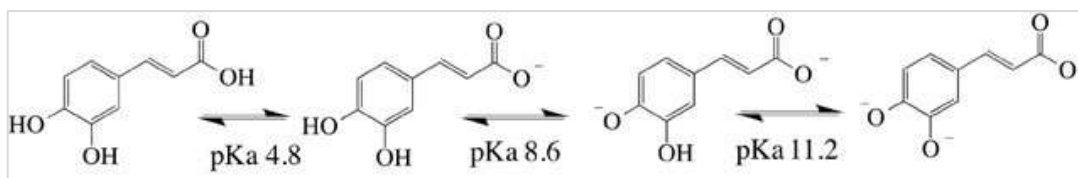
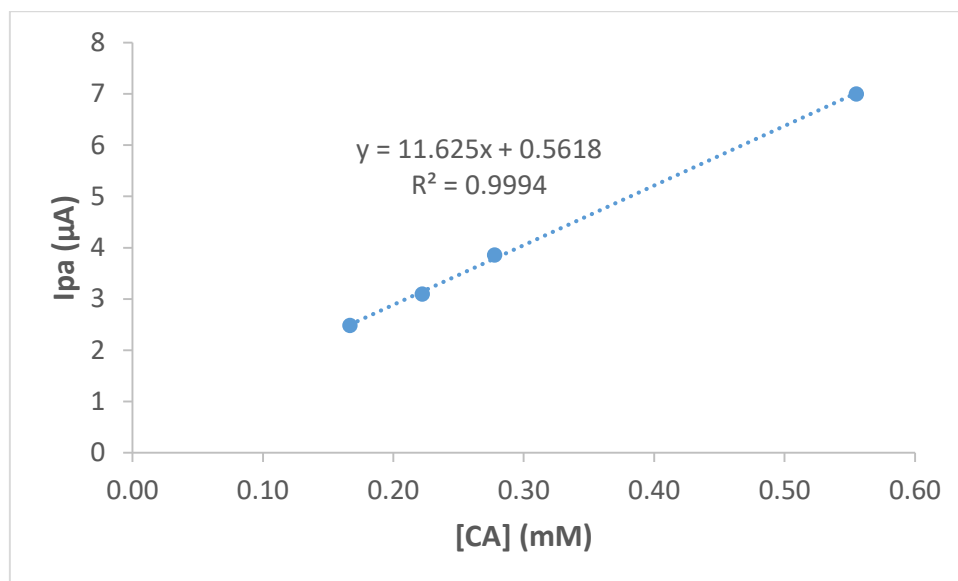


Figure S5. SEM images of CA-MIP and NIP at different scales.



**Figure S6.** Deprotonation of caffeic acid as a function of increasing pH and the respective pKa values. [34]



**Figure S7.** Calibration curve for the determination of CA in red wine using the MIP-CA/CV method. The wine was diluted 10 times in a (PBS 0.05 M/ EtOH) (90/10, v/v, pH 3), and 10 mg of CA-MIP were added to 1 mL of the diluted wine. Cyclic voltammetry parameters: voltage range of -0.4 to 0.8 V at a scan rate of 50 mV/s versus Ag/AgCl.

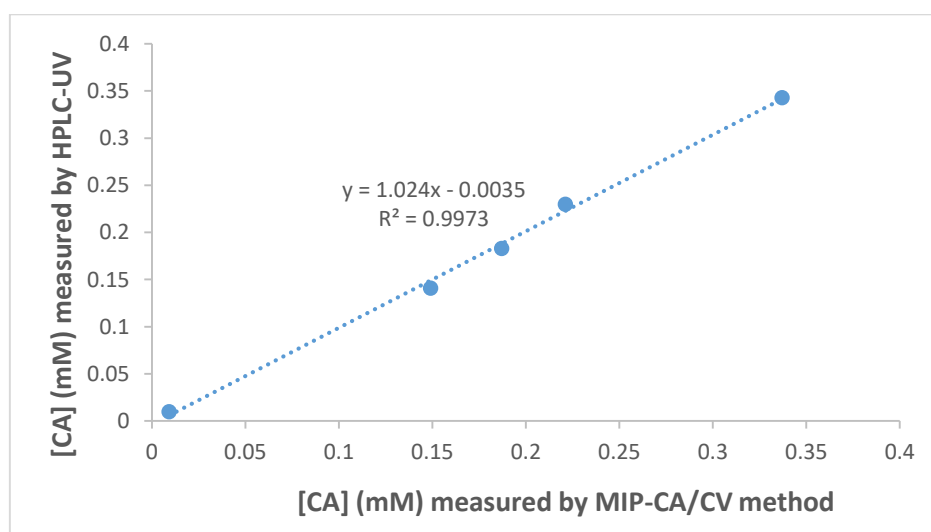


**Figure S8.** Correlation between MIP-CA/Cyclic voltammetry method and HPLC-UV method for the determination of CA in wine.